UNIVERSIDAD COMPLUTENSE DE MADRID

FACULTAD DE CIENCIAS BIOLÓGICAS

PRODUCCIÓN DE ETANOL DE SEGUNDA GENERACIÓN A PARTIR DE PAJA DE TRIGO:

HONGOS, ENZIMAS FÚNGICAS Y APLICACIONES

SECOND-GENERATION ETHANOL PRODUCTION FROM WHEAT STRAW:

FUNGI, FUNGAL ENZYMES, AND APPLICATIONS

TESIS DOCTORAL DE:

DAVINIA SALVACHÚA RODRÍGUEZ

BAJO LA DIRECCIÓN DE:

MARÍA JESÚS MARTÍNEZ HERNÁNDEZ
ALICIA PRIETO ORZANCO

Madrid, 2013

Producción de etanol de segunda generación a partir de paja de trigo: hongos, enzimas fúngicas y aplicaciones

Tesis Doctoral

Davinia Salvachúa Rodríguez

Portada y contraportada: Micrografías de microscopía electrónica de barrido de paja de trigo degradada por hongos basidiomicetos, realizadas en el Museo de Ciencias Naturales (CSIC) de Madrid.

Producción de etanol de segunda generación a partir de paja de trigo: hongos, enzimas fúngicas y aplicaciones

Tesis doctoral para optar al grado de

Doctora por la Universidad Complutense de Madrid

presentada por:

Davinia Salvachúa Rodríguez

DIRECTORAS:

Dra. Mª Jesús Martínez Hernández y Dra. Alicia Prieto Orzanco

Centro de Investigaciones Biológicas

Consejo Superior de Investigaciones Científicas

TUTORA:

Dra. Belén Patiño Álvarez

Facultad de Ciencias Biológicas

Universidad Complutense de Madrid

Madrid, 2013

Second-generation ethanol production from wheat straw: fungi, fungal enzymes, and applications

A dissertation for the degree of Doctor of Philosophy to be presented at the University Complutense of Madrid by:

Davinia Salvachúa Rodríguez

DIRECTORS:

Dr. Mª Jesús Martínez Hernández and Dr. Alicia Prieto Orzanco

Centro de Investigaciones Biológicas

Consejo Superior de Investigaciones Científicas

TUTOR:

Dr. Belén Patiño Álvarez

Facultad de Ciencias Biológicas

Universidad Complutense de Madrid

Madrid, 2013

Mª JESÚS MARTÍNEZ HERNÁNDEZ, INVESTIGADORA CIENTÍFICA DEL CSIC, DRA. EN CIENCIAS BIOLÓGICAS, Y ALICIA PRIETO ORZANCO, DRA. EN CIENCIAS BIOLÓGICAS, CIENTÍFICA TITULAR DEL CSIC,

CERTIFICAN:

Que el presente trabajo "Producción de etanol de segunda generación a partir de paja de trigo: hongos, enzimas fúngicas y aplicaciones", constituye la memoria que presenta la Licenciada en Ciencias Biológicas por la Universidad de Alcalá, Davinia Salvachúa Rodríguez para optar al grado de Doctora y ha sido realizada bajo su dirección en el Departamento de Biología Medioambiental del Centro de Investigaciones Biológicas del CSIC.

Y para que conste, firman el presente certificado en Madrid, a 10 de Mayo de 2013.

Dra. Mª Jesús Martínez

Dra. Alicia Prieto

LAS DIRECTORAS DE LA TESIS, DRA. Mª JESÚS MARTÍNEZ HERNÁNDEZ, INVESTIGADORA CIENTÍFICA DEL CSIC, Y DRA. ALICIA PRIETO ORZANCO, CIENTÍFICA TITULAR DEL CSIC, Y JUAN CARLOS GUTIERREZ FERNÁNDEZ, COORDINADOR DEL DOCTORADO EN MICROBIOLOGÍA Y PARASITOLOGÍA DE LA UNIVERSIDAD COMPLUTENSE DE MADRID,

CERTIFICAN:

Que Davinia Salvachúa Rodríguez, con DNI 72886844-M, a quien se autoriza para presentar la solicitud de "**Mención de Doctor Europeo**", ha realizado dos estancias fuera de España:

1) La primera de ellas en la Universidad Estatal de Pensilvania, en **Estados Unidos**, desde el 1 de Septiembre al 20 de Diciembre de 2012, bajo la supervisión del Dr. Ming Tien. Las principales actividades desarrolladas en esta estancia se relacionan con el Capítulo 3 de la presente Tesis.

2) Y la segunda en el Centro de Investigación Técnica- VTT, en **Finlandia**, desde el 2 de Septiembre al 11 de Diciembre de 2011, bajo la supervisión de la Dra. Kristiina Kruus. Las principales actividades desarrolladas en esta estancia se relacionan con el Capítulo 5 de la presente Tesis.

Adjunto a este documento se entregan los Certificados del Centro correspondiente a cada estancia.

Y para que conste, firman el presente certificado en Madrid, a 23 de Mayo de 2013.

Dra. Mª Jesús Martínez Dra. Alicia Prieto Dr. Juan Carlos Gutiérrez Lda. Davinia Salvachúa

A mis padres

A mi hermana

“Nos pasamos la vida esperando que pase algo… y lo único que pasa es la vida. No entendemos el valor de los momentos hasta que son convertidos en recuerdos. Por eso haz lo que quieras hacer, antes de que se convierta en lo que te gustaría haber hecho. No hagas de tu vida un borrador, tal vez no tengas tiempo de pasarlo a limpio... ”

Bob Marley

ÍNDICE DE CONTENIDOS

RESUMEN

En la actualidad, uno de los objetivos prioritarios de los países industrializados es la exploración de nuevos recursos energéticos para la producción de energías renovables, que aseguren el abastecimiento a la población y sean respetuosas con el medio ambiente. El bioetanol, principalmente obtenido a partir de los azúcares de caña de azúcar, remolacha y grano de cereales, es una de las alternativas más atractivas para sustituir, o al menos disminuir, el consumo de gasolina. Sin embargo, en los últimos años la investigación se ha focalizado en el empleo de otras materias primas, como los residuos lignocelulósicos, para evitar interferencias con aquellas implicadas en la cadena alimentaria, dando lugar a los denominados biocombustibles de segunda generación (2G). No obstante, para poder aprovechar los carbohidratos que contienen estos sustratos se requieren varias etapas: (1) pretratamiento de la biomasa lignocelulósica, para alterar la lignina y dejar accesibles los polisacáridos de la pared celular vegetal; (2) hidrólisis enzimática de estos polisacáridos (celulosa y hemicelulosa) y (3) fermentación alcohólica de los azúcares liberados, utilizando microorganismos capaces de fermentar tanto la glucosa como la xilosa, para lograr el máximo rendimiento.

En este contexto, uno de los objetivos del presente trabajo fue estudiar si el pretratamiento fúngico puede ser una alternativa a los tratamientos físico-químicos utilizados actualmente, como la explosión a vapor, para producir etanol 2G a partir de paja de trigo. Conocida la capacidad de los hongos de podredumbre blanca para degradar la lignocelulosa, se realizó un muestreo con 21 basidiomicetos en condiciones de fermentación en estado sólido, para comprobar su eficiencia en el pretratamiento de paja de trigo, complementándolo con un lavado alcalino suave que facilita la solubilización de la lignina y mejora el rendimiento de la hidrólisis enzimática. Se seleccionaron los hongos que produjeron un sustrato con mayor recuperación global de azúcares fermentables y se demostró que este pretratamiento combinado, a diferencia de la explosión a vapor, no produce compuestos indeseados que afecten negativamente a las etapas de hidrólisis y fermentación, pudiendo ser una alternativa a ciertos métodos físico-químicos.

De entre los hongos previamente muestreados, se seleccionó *Irpex lacteus* por producir los mejores rendimientos del proceso en el menor tiempo de incubación. Tras ensayar diferentes condiciones de cultivo durante la fermentación en estado sólido con este hongo, se comprobó que la adición de Mn^{2+} mejoraba significativamente la recuperación de glucosa. La búsqueda de marcadores de la eficiencia del biopretratamiento resultó infructuosa ya que no se logró correlacionar claramente la recuperación

final de azúcares con ciertos parámetros como la degradación de la lignina, la biomasa fúngica y/o las enzimas secretadas por este hongo.

Con el propósito de analizar si el sistema enzimático secretado por *I. lacteus* tiene un papel esencial en la alta recuperación de azúcares obtenida tras el biopretratamiento de la paja de trigo, se analizó su secretoma y se comparó con el de *Phanerochaete chrysosporium* y *Pleurotus ostreatus* ya que produjeron patrones de degradación diferentes. *I. lacteus* produce una amplia batería de celulasas y hemicelulasas pero no aquellas que hidrolizan completamente la celulosa o hemicelulosa, como β-glucosidasas o β-xilosidasas. Además posee un sistema potente de degradación de la lignina, principalmente compuesto de peroxidasas y enzimas productoras de H_2O_2. Este perfil enzimático justifica un enriquecimiento del sustrato en azúcares, puesto que el hongo no los consume durante su crecimiento y además los deja más accesibles para las enzimas hidrolíticas. El análisis del secretoma de *P. chrysosporium* y *P. ostreatus* fue también coherente con sus patrones de degradación preferente de polisacáridos y lignina, respectivamente, secretando el primero más celulasas y hemicelulasas y el segundo más oxidorreductasas.

Un estudio más en detalle de las peroxidasas secretadas por *I. lacteus*, puso de manifiesto que este tipo de enzimas se producen tanto en condiciones de fermentación en estado sólido como en medio líquido. Se detectaron peroxidasas que oxidan el manganeso (MnP) y un nuevo tipo de peroxidasa de alto potencial redox, que fue purificada y caracterizada como una peroxidasa decoloradora de tintes (DyP) muy estable a pH ácido, altas temperaturas y elevadas concentraciones de H_2O_2. Además, se ha comprobado que suplementando con DyP el cóctel empleado durante la hidrólisis enzimática de paja de trigo, se mejora significativamente la digestibilidad de la celulosa. Los resultados sugieren que esta nueva peroxidasa podría ser de gran interés para aumentar el rendimiento en la producción de etanol 2G a partir de este material lignocelulósico.

Finalmente, con el objetivo de buscar nuevas aplicaciones biotecnológicas para las peroxidasas fúngicas de alto potencial redox, se comprobó que tanto el crudo de *I. lacteus* (que contiene mayoritariamente MnP y DyP) como la peroxidasa versátil (VP) de *Pleurotus eryngii* son capaces de polimerizar lignanos, aunque esta última con mayor eficiencia. Tras este resultado, se seleccionó VP para catalizar la polimerización de otras moléculas como péptidos, proteínas y arabinoxilanos feruloilados, poniendo de manifiesto que es posible utilizar estas enzimas para generar productos con propiedades nuevas o diferentes.

SUMMARY

INTRODUCTION

Ethanol is one of main renewable fuels contributing to the reduction of the negative environmental impact generated by the worldwide utilization of fossil fuels. In particular, second-generation bioethanol production from lignocellulosic substrates offers a great potential since those feedstocks do not compete with feed and food resources. Moreover, lignocellulosic materials are the major component of biomass on earth (Lin and Tanaka, 2006). Among them, agricultural wastes are the most copious and cheapest, being wheat straw the foremost in Europe and the second worldwide (Kim and Dale, 2004). However, due to the complexity of its structure, obtaining high sugar release from this substrate is a challenge.

Bioethanol production from wheat straw includes three main steps: (i) pretreatment, to disrupt the lignocellulose structure, improving cellulose and hemicellulose accessibility, (ii) enzymatic hydrolysis of the previous polymers to release monosaccharides, and (iii) ethanol fermentation from those sugar monomers (Talebnia et al., 2010). Currently, the bottlenecks of this process are both pretreatment and enzymatic hydrolysis, mainly due to the fact that the complex technologies and efficient enzymes required to obtain high yields increase considerably the process costs. In addition, to make bioethanol competitive with other fuels, pentoses from hemicelluloses should also be fermented (Gírio et al., 2010).

Currently, the most common and effective tools for pretreatment are certain physicochemical technologies, such as steam explosion. However, they require high pressures, temperatures, and frequently an additional acid or alkali treatment, generating by-products such as weak acids, furan derivatives, and phenolic substances, that adversely affect subsequent steps (Alvira et al., 2010). Regarding enzymatic hydrolysis, one of the key factors is the availability of enzymes or enzyme complexes with new or upgraded activities to enhance biomass degradation (Couturier et al., 2012).

AIMS

In this context, the aims of the present Thesis are:

i) To perform a screening with different fungi, in order to assay the efficiency of a biological pretreatment compared to current physicochemical methods in second-generation ethanol production process from wheat straw.

ii) Once selected the most efficient species, to optimize culture conditions in order to get enhanced digestibility and sugar recoveries from wheat straw.

iii) To study the enzymatic system and characterize new enzymes with biotechnological potential from the selected fungus.

iv) To assess the relevance of those enzymes to be used in different steps of the ethanol-production process or in other biotechnological applications.

RESULTS AND DISCUSSION

1. Biological pretreatment of wheat straw: fungal screening

In the fungal kingdom, white-rot fungi (Basidiomycota *phylum*) are the only microorganisms capable of altering all plant components, including lignin, cellulose, and hemicellulose (Martínez et al., 2005). Consequently, they were considered adequate tools for disassembling lignocellulose from wheat straw during a biological pretreatment. First of all, a screening of twenty-one different basidiomycetes was performed to test their ability degrading wheat straw. The organisms selected for biopretreatment should consume few sugars for its own growth and produce high lignocellulose deconstruction, to render more accessible polysaccharides for enzymatic hydrolysis and increased fermentable sugar yields (Kuhar et al., 2008).

Biopretreatment assays were performed under solid-state fermentation (SSF) conditions, employing 100-mL Erlenmeyer flasks with 2 g of wheat straw and 6 mL of water. Changes in substrate composition (lignin, cellulose, and hemicellulose losses), secretion of ligninolytic enzymes, enzymatic hydrolysis efficiency, and ethanol yields were evaluated at 7, 14, and 21 days of incubation. One of the main disadvantages of the biological pretreatments is the long storage times required to achieve significant disorganization of the raw material (Galbe and Zacchi, 2007). Therefore, the effect of reinforcing fungal action with a mild NaOH-washing after biological pretreatments was tested, since alkali induces lignin solubilization (Kumar et al., 2009). In the current work, this treatment showed to be crucial to improve cellulose digestibility after biological pretreatment, although did not affect at all hemicellulose digestibility.

Most of the fungi colonized the substrate during biopretreatment. However, they produced very different lignocellulose degradation patterns. Some of them were not able to degrade lignin, showing a polysaccharide-preferential degradation (e.g. *Phanerochaete chrysosporium*). Others degraded both components simultaneously (e.g. *Irpex lacteus* and *Pleurotus ostreatus*) and other group was able to selectively remove lignin (e.g. *Pleurotus eryngii*). Every biopretreated substrate was further subjected

to enzymatic hydrolysis, and the conversion yield of polysaccharides into fermentable sugars (digestibility), was calculated. Treatment for 14 and 21 days with 8 of the fungal strains rendered a modified substrate with enhanced digestibility compared to non-biotreated wheat straw (36% for cellulose and 35% for hemicelluloses). Pretreatment with *I. lacteus* gave a cellulose digestibility of 82% and *Panus tigrinus* provided 78% of the hemicellulose digestible. These figures are better than those reported in previous studies (Capelari and Tomás-Pejó, 1997; Dias et al., 2010) and the incubation times, shorter. But in order to quantify the amount of potentially fermentable sugars, digestibility values are not the only relevant parameter to be taken into account. Carbohydrate losses during biopretreatment must also be considered to calculate the final sugar yields. Then, only 7 fungal treatments improved global sugar yields compared to non bio-treated straw, with maximum values of 69% glucose in 21-day cultures of *Poria subvermispora* and 62% xylose after 14-day *I. lacteus* treatment.

The conversion from glucose to ethanol by *Saccharomyces cerevisiae* was finally tested and most conversion yields were superior to 90%, giving maximum ethanol yields of 62% (in samples from *I. lacteus* and *P. subvermipora* treatments). These findings make clear that no significant inhibitors were produced during the combined biological and chemical pretreatment.

In view of these results, biological pretreatment could be proposed as an alternative to some physicochemical pretreatments. For example, some physical pretreatments, such as wheat straw pulverization, generate substrate digestibilities of 61% (Koullas et al., 1992), a value lower than the global sugar yields obtained in the present study. On the other hand, Chen et al. (2008) reported on a chemical pretreatment using acid and alkaline reagents which allowed a glucose recovery 10% higher than that attained in this study. However, due to the production of inhibitors, the final ethanol yield was only 3% better.

Our data demonstrate that very few fungi are suitable to increase sugar recoveries from wheat straw. Although similar ethanol yields were obtained from *I. lacteus* and *P. subversmispora* treated wheat straw, the former species was selected for generating the best yields at the shortest incubation time (14 days).

2. Biological pretreatment of wheat straw: optimization of culture conditions for SSF with *I. lacteus*

The encouraging results from *I. lacteus* biopretreatment can be improved introducing subtle modifications in the initial SSF conditions, since the extent and pattern of wheat straw degradation can be altered by changing

several nutritional or environmental culture parameters (Reid, 1989a; Reid, 1989b; Wan and Li, 2012). Among them, we have tested the effect of several factors on global sugar yields, namely the inoculum, the moisture content, substrate particle size, and the presence of some ions (e.g. Mn^{2+}, Fe^{2+}, Cu^{+2}) or organic compounds (e.g. peptone, wheat thin stillage). The results were compared to *I. lacteus* cultures grown under the conditions described for the screening, which were considered as the control for these experiments.

The increase of fungal biomass added for inoculation did not significantly affect the extent and degradation pattern of lignocellulose. Oppositely, particle size reduction brought significantly increased hemicellulose depletion compared to *I. lacteus* control cultures. This finding can be explained from an improved accessibility to hemicellulose and a preferential use of xylose for fungal growth (Xu et al., 2009). Consequently, although hemicellulose digestibility was better, less fermentable xylose was available, demonstrating that this change is not beneficial for the whole process. Neither maintaining the moisture content constant nor a two-fold humidity level changed the extent of lignin or cellulose degradation respect to control cultures, although produced negligible hemicellulose decay. It has previously been observed that xylanase production can be reduced by water excesses (Mohana et al., 2008), resulting in those low hemicellulose losses. Digestibility and sugar yields were unaffected by the moisture variations assayed.

Ion supplementation produced different wheat straw degradation patterns. Cu^{2+} and Fe^{2+} induced more cellulose and less hemicellulose consumption compared to controls, and Mn^{2+} showed just the opposite behavior. Neither Cu^{2+} nor Fe^{2+} addition improved digestibility nor global sugar yields but produced the highest lignin degradation. Cu^{2+} in cultures stimulates the production of ligninolytic enzymes such as laccases (Pedersen and Meyer, 2009), and Fe^{2+} favors the production of hydroxyl radicals, through Fenton reactions, which are implicated in lignin degradation (Evans et al., 1994; Gómez-Toribio et al., 2001). In contrast, Mn^{2+} addition did not produce significant increases in digestibility but improved final glucose yields in 6% compared to controls. This fact can be related to the induction of some ligninolytic enzymes such as manganese-dependent peroxidases (MnPs) (Camarero et al., 1996). Peptone and wheat thin stillage did not enhance sugar yields; in fact, peptone decreased significantly the values compared to controls. Enzyme production in SSF is dependent on the N source and the fungus and, in the case of the ligninolytic system, activation normally occurs at low nitrogen concentrations (Kachlishvili et al., 2006).

Only Mn^{2+} addition positively affected sugar yields, although it should be emphasized that in any case the values from these experiments were significantly higher than those reported in other studies pretreating wheat straw with other fungi or *I. lacteus* (Dias et al., 2010; Pinto et al., 2012; Wan and Li, 2011).

With the aim of searching indicators for *I. lacteus* biopretreatment efficiency, correlations of these parameters with cellulose, hemicellulose, and lignin losses, digestibility, sugar yields, ligninolytic enzymes secretion, and fungal biomass were calculated, but no significant associations were detected among any of the factors and sugar yields. All these results show the complexity of fungal lignocellulose degradation, since a single variation can produce remarkable differences in process efficiency and pattern degradation.

It is known that the lignin polymer is the main obstacle for the efficient utilization of lignocellulosic substrates, and then its disorganization would facilitate the access of hydrolytic enzymes to polysaccharides (Kuhar et al., 2008). However, both fungal screening and the different treatments assayed with *I. lacteus* evidenced that the highest delignification levels did not correspond to the highest fermentable sugar yields. Probably, after breaking this barrier during biopretreatment, sugars become more accessible and are consumed for fungal growth.

3. Proteins secreted by *I. lacteus* during wheat straw biopretreatment

The previous set of data demonstrated the efficiency of *I. lacteus* degrading wheat straw. Then, it became evident that the enzyme system involved in such an efficient process merit an in-depth study. Proteomic tools are a perfect choice to study the pool of extracellular proteins, also known as the secretome, released by an organism (Bouws et al., 2008). To do so, two methodologies were used. The first approach consisted of separating the proteins in two-dimensional gels, followed by in-gel digestion of each spot and MS/MS analysis of the tryptic peptides. This procedure was carried out to analyze secretomes of *I. lacteus* from 7, 14, and 21 SSF-incubation days, from 21-d Mn^{2+} supplemented cultures, and also from liquid cultures in a synthetic medium without wheat straw. The second, a shotgun procedure, was applied for comparison of the unfractionated 21-d extracellular pool of proteins from *I. lacteus* and two well-known lignocellulose degraders: *P. chrysosporium* and *P. ostreatus* with preferential polysaccharide and lignin degradation patterns, respectively. It involved the analysis of the tryptic digest from the entire secretome through nanoLC-MS/MS, and allowed the identification of minor proteins undetectable by the former technique.

Considering the evolution of the composition of *I. lacteus* secretome over the time growing on wheat straw (7, 14, and 21 days), its degradative mechanism can be proposed. From the first week of SSF, *I. lacteus* degraded cellulose using a large machinery of exocellulases and endoglucanases. Simultaneously, hemicellulose and pectins were mainly being broken down via acetyl xylan esterase and rhamnogalacturonan hydrolase, respectively. Due to the specific hydrolytic action of these enzymes, big polysaccharide fragments were mostly released. On the other hand, proteases and lignin-degrading oxidoreductases such as MnP and an homologous to the hypothetical peroxidase cpop21 (later characterized as a DyP) were released, as well as glyoxal oxidase and cellobiose dehydrogenase, which are involved in the production of H_2O_2 (Vanden Wymelenberg et al., 2005). These enzymes went ahead with wheat straw deconstruction, facilitating the action of the carbohydrate-degrading enzymes. This enzyme profile yielded easily hydrolysable products with high sugar content. The key of that sugar enrichment is that the extracellular enzymatic pool is deficient in the proteins that hydrolyze completely cellulose and hemicelluloses to monosaccharides, hampering extensive sugar consumption for fungal growth. As an example, β-glucosidases, β-xylosidases, and α-glucuronidases were not detected in the secretome of *I. lacteus* from SSF cultures or were detected only as minor proteins. Such an "enzyme cocktail" could be interesting to improve sugar yields during biopretreatment.

The positive effect on glucose yields prompted by Mn^{2+} supplementation to the cultures could be explained as a decrease in cellulose consumption since the release of several isoforms of cellulases was lower. Additionally, as suggested from the previous work, MnP was induced, improving sugar accessibility for enzymatic hydrolysis.

Analysis of *P. chrysosporium* and *P. ostreatus* secretomes, was coherent with their respective degradation patterns, the former secreting more cellulases and hemicelulases and the latter producing more oxidoreductases. To date, few reports on basidiomycete secretomes are available, since most of these studies have been performed with ascomycetes. The knowledge of the protein pools released under a specific set of conditions could be very interesting for improving industrial processes which require enzyme cocktails for hydrolysis of different substrates (Ravalason et al., 2012).

4. Production, isolation, and characterization of a novel DyP-type peroxidase from *I. lacteus*

As previously mentioned, one of the proteins from *I. lacteus* secretome showed high homology to cpop21, a hypothetical peroxidase from

Polyporaceae. This hypothetical protein seems to belong to a really interesting group of enzymes denominated dye-decolorizing peroxidases (DyPs). To date, only eight DyPs have been characterized and six of them are produced by fungi (Liers et al., 2012). DyPs are high-redox potential enzymes; however, its role in nature is still controversial. For all these reasons, a deeper study of this enzyme was considered. First of all, to ease its purification, the enzyme production was followed in liquid medium through the oxidation of DyP-specific substrates, such as anthraquinone dyes, in the presence of H_2O_2. The maximum activity was detected at 21 incubation days. The enzyme was purified after several chromatographic steps, and then its physicochemical, spectroscopic, and catalytic properties, were studied and described. According to its N-terminal sequence, peptide mass fingerprinting, and MS/MS analysis, *I. lacteus* DyP showed a high homology (>95%) with the hypothetical protein cpop21. The enzyme had low optimal pH (2-4), was very stable to acid pH and temperature after long periods of time, and showed better activity and stability to high H_2O_2 concentrations than other DyPs (García-Ruiz et al., 2012; Ogola et al., 2010). Other attractive features of *I. lacteus* DyP were its high catalytic efficiency oxidizing the recalcitrant anthraquinone and azo dyes assayed, and its ability oxidizing non-phenolic aromatic compounds like veratryl alcohol. These results disclosed a promising biotechnological potential for this enzyme.

5. Application of *I. lacteus* DyP during the enzymatic hydrolysis of wheat straw

The effect of incorporating *I. lacteus* DyP to complement cellulases and hemicellulases during the enzymatic hydrolysis of wheat straw was checked. The lignocellulosic substrate was first subjected or not to biological pretreatment and/or mild alkali washing. In non-biopretreated alkali-washed wheat straw, cellulose digestibility values lifted from 27 to 38% after DyP addition and from 24 to 30% when the substrate was not alkali-treated. The effect of DyP was more evident on biopretreated wheat straw, where cellulose digestibility rose from 71 to 89% in NaOH-treated samples but only from 43 to 50% in samples not exposed to alkali. Nevertheless, no significant increases or even some decreases were observed for hemicellulose digestibility. These results suggest that *I. lacteus* DyP displayed a synergistic action with cellulases during the hydrolysis of wheat straw, significantly increasing fermentable glucose recoveries from this substrate. Similar results have been described in a patent (Zorn et al., 2009) after treating non starch-carbohydrates with a peroxidase of *Marasmius scorodonius*, which seems to be a DyP-type peroxidase. However, very few investigations include peroxidases in this type of application, what stresses the novelty of these results.

6. New applications for high-redox potential peroxidases

Plant peroxidases, which are involved in lignin biosynthesis (Adler, 1977), have been the main type of enzymes used for *in vitro* biopolymerization reactions (Hollmann and Arends, 2012; Kobayashi et al., 2001). In contrast, the role of fungal peroxidases as biocatalyzers of cross-linking reactions has been poorly studied.

As previously shown, the secretome of *I. lacteus* growing in liquid medium contained low- and high-redox potential peroxidases as MnP and DyP, respectively. The former is able to oxidize Mn^{2+} to Mn^{3+} (Martínez et al., 1996) and the latter acts on many different molecules but not on Mn^{2+} (Liers et al., 2012). Thus, the efficiency of the *I. lacteus* crude for lignan polymerization was evaluated, and compared with that from a pure preparation of the versatile peroxidase (VP) from *Pleurotus eryngii* catalyzing the same reaction. VP was selected for being a fungal enzyme combining MnP and lignin peroxidase (LiP) activities, and then able to oxidize low and high-redox potential compounds (Martínez et al., 1996). Lignans are diphenolic compounds found in the cell wall of higher plants, formed by β-β coupling of two cinnamyl precursors (Saleem et al., 2005). Polymerization was carried out in ethanol, as required to dissolve the lignans, and in the presence and absence of Mn^{2+}, and the reaction products were analyzed by MALDI-TOF. Both catalysts were able to induce lignans polymerization, although VP produced higher molecular mass species, indicating that this enzyme was more efficient than the *I. lacteus* crude, especially in reactions with Mn^{2+}. Moreover, Mn^{2+} seemed to increase VP catalytic efficiency and stability when the enzyme was in organic co-solvents, reaching higher polymerization degrees than those reported for other fungal enzymes (Buchert et al., 2002).

Once the efficiency of VP was demonstrated polymerizing lignans, this enzyme was also used, in the presence of Mn^{2+}, to catalyse the cross-linking of other low molecular mass compounds, such as peptides, as well as larger macromolecules, like proteins (β-casein) and feruloylated arabinoxylans (FAX). These cross-linking reactions resulted also successful, and even some hetero-condensation reactions took place, generating new molecules. The polymerization of lignans into larger molecules could be relevant from an industrial point of view, since it constitutes a possible mechanism to eliminate deleterious compounds that appear in side-streams from industrial processing of lignocellulosic biomass (Buchert et al., 2002) or to produce value-added polymers or materials with improved functional properties (Mattinen et al., 2009). The other molecules tested for cross-linking, such as peptides, proteins, and FAX, are known to have functional properties (Arihara, 2006; Niño-

Medina et al., 2010; Saleem et al., 2005; Stanic et al., 2010), so their modification *via* polymerization can be tailored to prepare products with enhanced or modified organoleptic or functional properties such as reduced fat content, texture, mouth feel, digestibility, etc.

CONCLUSIONS

The work presented in this Thesis allows going a step forward in the understanding of how lignocellulose is being degraded by different fungi in nature. Among the diversity of fungal degradation patterns, few fungi showed to be adequate for biopretreatment processes facing second-generation bioethanol production. *I. lacteus* was the best fungus degrading wheat straw, generating substrates with high sugar content and easily hydrolysable. Secretome studies by using proteomic tools were a perfect option to get insight into all the enzymatic mechanisms implicated in that biological process and to understand the reasons for its efficiency. A novel DyP, detected from that secretome, was produced, purified, and characterized showing high biotechnological potential. Moreover, it was further used for enzymatic hydrolysis of wheat straw together with cellulases and hemicellulases, improving significantly cellulose breakdown. A survey of other potential applications of fungal high-redox potential peroxidases, revealed the efficiency of VP polymerizing different types of phenolic molecules, illustrating the unavoidable coexistence of degradation and polymerization processes in nature.

REFERENCES

Adler, E., 1977. Lignin chemistry - Past, present and future. Wood Sci. Technol. 11, 169-218.

Alvira, P., Tomás-Pejó, E., Ballesteros, M., Negro, M.J., 2010. Pretreatment technologies for an efficient bioethanol production process based on enzymatic hydrolysis: A review. Bioresour. Technol. 101, 4851-4861.

Arihara, K., 2006. Functional properties of bioactive peptides derived from meat proteins, in: Nollet, L.M.L., Toldrá, F. (Eds.), Advanced technologies for meat processing. CRC Press, Boca Raton, FL, pp. 254-273.

Bouws, H., Wattenberg, A., Zorn, H., 2008. Fungal secretomes - nature's toolbox for white biotechnology. Appl. Microbiol. Biotechnol. 80, 381-388.

Buchert, J., Mustranta, A., Tamminen, T., Spetz, P., Holmbom, B., 2002. Modification of spruce lignans with *Trametes hirsuta* laccase. Holzforschung 56, 579-584.

Camarero, S., Böckle, B., Martínez, M.J., Martínez, A.T., 1996. Manganese-mediated lignin degradation by *Pleurotus pulmonarius*. Appl. Environ. Microbiol. 62, 1070-1072.

Capelari, M. Tomás-Pejó, E., 1997. Lignin degradation and in vitro digestibility of wheat straw treated with brazilian tropical species of white-rot fungi. Folia Microbiologica 42, 481-487.

Chen, H., Han, Y., Xu, J., 2008. Simultaneous saccharification and fermentation of steam exploded wheat straw pretreated with alkaline peroxide. Process Biochem. 43, 1462-1466.

Couturier, M., Navarro, D., Olive, C., Chevret, D., Haon, M., Favel, A., Lesage-Meessen, L., Henrissat, B. et al., 2012. Post-genomic analyses of fungal lignocellulosic biomass degradation reveal the unexpected potential of the plant pathogen *Ustilago maydis*. BMC Genomics 13.

Dias, A.A., Freitas, G.S., Marques, G.S.M., Sampaio, A., Fraga, I.S., Rodrigues, M.A.M., Evtuguin, D.V., Bezerra, R.M.F., 2010. Enzymatic saccharification of biologically pre-treated wheat straw with white-rot fungi. Bioresour. Technol. 101, 6045-6050.

Evans, C.S., Dutton, M.V., Guillén, F., Veness, R.G., 1994. Enzymes and small molecular mass agents involved with lignocellulose degradation. FEMS Microbiol. Rev. 13, 235-240.

Galbe, M. Zacchi, G., 2007. Pretreatment of lignocellulosic materials for efficient bioethanol production. Adv. Biochem. Eng. Biotechnol. 108, 41-65.

García-Ruiz, E., Gonzalez-Perez, D., Ruiz-Dueñas, F.J., Martinez, A.T., Alcalde, M., 2012. Directed evolution of a temperature-, peroxide- and alkaline pH-tolerant versatile peroxidase. Biochem. J. 441, 487-498.

Gírio, F.M., Fonseca, C., Carvalheiro, F., Duarte, L.C., Marques, S., Bogel-Lukasik, R., 2010. Hemicelluloses for fuel ethanol: A review. Bioresour. Technol. 101, 4775-4800.

Gómez-Toribio, V., Martínez, A.T., Martínez, M.J., Guillén, F., 2001. Oxidation of hydroquinones by the versatile ligninolytic peroxidase from *Pleurotus eryngii*: H_2O_2 generation and the influence of Mn^{2+}. Eur. J. Biochem. 268, 4787-4793.

Hollmann, F. Arends, I.W., 2012. Enzyme initiated radical polymerizations. Polymers 4, 759-793.

Kachlishvili, E., Penninckx, M., Tsiklauri, N., Elisashvili, V., 2006. Effect of nitrogen source on lignocellulolytic enzyme production by white-rot basidiomycetes under solid-state cultivation. World J. Microbiol. Biotechnol. 22, 391-397.

Kim, S. Dale, B.E., 2004. Global potential bioethanol production from wasted crops and crop residues. Biomass Bioenerg. 26, 361-375.

Kobayashi, S., Uyama, H., Kimura, S., 2001. Enzymatic polymerization. Chem. Rev. 101, 3793-3818.

Koullas, D.P., Christakopoulos, P., Kekos, D., Macris, B.J., Koukios, E.G., 1992. Correlating the effect of pretreatment on the enzymatic-hydrolysis of straw. Biotechnol. Bioeng. 39, 113-116.

Kuhar, S., Nair, L.M., Kuhad, R.C., 2008. Pretreatment of lignocellulosic material with fungi capable of higher lignin degradation and lower carbohydrate degradation improves substrate acid hydrolysis and the eventual conversion to ethanol. Can. J. Microbiol. 54, 305-313.

Kumar, P., Barrett, D., Delwiche, M., Stroeve, P., 2009. Methods for pretreatment of lignocellulosic biomass for efficient hydrolysis and biofuel production. Ind. Eng. Chem. Res. 48, 3713-3729.

Liers, C., Pecyna, M.J., Kellner, H., Worrich, A., Zorn, H., Steffen, K.T., Hofrichter, M., Ullrich, R., 2012. Substrate oxidation by dye-decolorizing peroxidases (DyPs) from wood- and litter-degrading agaricomycetes compared to other fungal and plant heme-peroxidases. Appl. Microbiol. Biotechnol. doi:10.1007/s00253-012-4521-2.

Lin, Y., Tanaka, S., 2006. Ethanol fermentation from biomass resources: current state and prospects. Appl. Microbiol. Biotechnol. 69, 627-642.

Martínez, A.T., Speranza, M., Ruiz-Dueñas, F.J., Ferreira, P., Camarero, S., Guillén, F., Martínez, M.J., Gutiérrez, A. et al., 2005. Biodegradation of lignocellulosics: Microbiological, chemical and enzymatic aspects of fungal attack to lignin. Intern. Microbiol. 8, 195-204.

Martínez, M.J., Ruiz-Dueñas, F.J., Guillén, F., Martínez, A.T., 1996. Purification and catalytic properties of two manganese-peroxidase isoenzymes from *Pleurotus eryngii*. Eur. J. Biochem. 237, 424-432.

Mattinen, M.L., Struijs, K., Suortti, T., Mattila, I., Kruus, K., Willför, S., Tamminen, T., Vincken, J.P., 2009. Modification of lignans by *Trametes hirsuta* laccase. Bioresources 4, 482-496.

Mohana, S., Shah, A., Divecha, J., Madamwar, D., 2008. Xylanase production by *Burkholderia* sp. DMAX strain under solid state fermentation using distillery spent wash. Bioresour. Technol. 99, 7553-7564.

Niño-Medina, G., Carvajal-Millan, E., Rascón-Chu, A., Marquez-Escalante, J.A., Guerrero, V., Salas-Munoz, E., 2010. Feruloylated arabinoxylans and arabinoxylan gels: structure, sources and applications. Phytochem. Rev. 9, 111-120.

Ogola, H.J., Hashimoto, N., Miyabe, S., Ashida, H., Ishikawa, T., Shibata, H., Sawa, Y., 2010. Enhancement of hydrogen peroxide stability of a novel *Anabaena* sp. DyP-type peroxidase by site-directed mutagenesis of methionine residues. Appl. Microbiol. Biotechnol. 87, 1727-1736.

Pedersen, M., Meyer, A.S., 2009. Influence of substrate particle size and wet oxidation on physical surface structures and enzymatic hydrolysis of wheat straw. Biotechnol. Progr. 25, 399-408.

Pinto, P.A., Dias, A.A., Fraga, I., Marques, G., Rodrigues, M.A.M., Colaco, J., Sampaio, A., Bezerra, R.M.F., 2012. Influence of ligninolytic enzymes on straw saccharification during fungal pretreatment. Bioresour. Technol. 111, 261-267.

Ravalason, H., Grisel, S., Chevret, D., Favel, A., Berrin, J.G., Sigoillot, J.C., Herpoel-Gimbert, I., 2012. *Fusarium verticillioides* secretome as a source of auxiliary

enzymes to enhance saccharification of wheat straw. Bioresour. Technol. 114, 589-596.

Reid, I.D., 1989a. Optimization of solid-state fermentation for selective delignification of aspen wood with *Phlebia tremellosa*. Enzyme Microb. Technol. 11, 804-809.

Reid, I.D., 1989b. Solid-state fermentations for biological delignification. Enzyme Microb. Technol. 11, 786-803.

Saleem, M., Kim, H.J., Ali, M.S., Lee, Y.S., 2005. An update on bioactive plant lignans. Nat. Prod. Rep. 22, 696-716.

Stanic, D., Monogioudi, E., Dilek, E., Radosavljevic, J., Atanaskovic-Markovic, M., Vuckovic, O., Raija, L., Mattinen, M. et al., 2010. Digestibility and allergenicity assessment of enzymatically crosslinked beta-casein. Mol. Nutr. Food Res. 54, 1273-1284.

Talebnia, F., Karakashev, D., Angelidaki, I., 2010. Production of bioethanol from wheat straw: An overview on pretreatment, hydrolysis and fermentation. Bioresour. Technol. 101, 4744-4753.

Vanden Wymelenberg, A., Sabat, G., Martínez, D., Rajangam, A.S., Teeri, T.T., Gaskell, J., Kersten, P.J., Cullen, D., 2005. The *Phanerochaete chrysosporium* secretome: Database predictions and initial mass spectrometry peptide identifications in cellulose-grown medium. J. Biotechnol. 118, 17-34.

Wan, C., Li, Y., 2011. Effectiveness of microbial pretreatment by *Ceriporiopsis subvermispora* on different biomass feedstocks. Bioresour. Technol. 102, 7507-7512.

Wan, C., Li, Y., 2012. Fungal pretreatment of lignocellulosic biomass. Biotechnol. Advances doi:.10.1016/j.biotechadv.2012.03.003.

Xu, C., Ma, F., Zhang, X., 2009. Lignocellulose degradation and enzyme production by *Irpex lacteus* CD2 during solid-state fermentation of corn stover. J. Biosci. Bioeng. 108, 372-375.

Zorn, H., Szweda, R., Kumar, M., Wilms, J., 2009. Method for modifying non-starch carbohydrate material using peroxidase enzyme. Patent [US200913054178].

ESTRUCTURA DE LA TESIS

El presente trabajo, para obtener el Título de Doctor, se estructura en cinco grandes capítulos, que se corresponden con cuatro artículos científicos ya publicados y uno más en preparación (Capítulo 3). El contenido de los trabajos publicados se ha mantenido íntegramente y el material suplementario ha sido incluido en el texto principal o al final del capítulo. Todos los capítulos han sido formateados para que este trabajo mantenga una estructura homogénea y todos ellos contienen su propia introducción, material y métodos, resultados, discusión y bibliografía. También se incluye una introducción y discusión general que relacionan todos ellos y que contienen su propia bibliografía.

Lista de publicaciones

A continuación se muestran las publicaciones que forman parte de la presente Tesis Doctoral:

Capítulo 1. Salvachúa, D., Prieto, A., López-Abelairas, M., Lu-Chau, T., Martínez, A.T., Martínez, M.J. 2011. Fungal pretreatment: An alternative in second-generation ethanol from wheat straw. Bioresour. Technol. 102, 7500-7506.

Capítulo 2. Salvachúa, D., Prieto, A., Vaquero, M.E., Martínez, A.T., Martínez, M.J. 2013. Sugar recoveries from wheat straw following treatments with the fungus *Irpex lacteus*. Bioresour. Technol. 131, 218-225.

Capítulo 3. Salvachúa, D., Tien, M., Fernández, M., García-Tabares, F., de los Ríos, V., Martínez, A.T., Martínez, M.J., Prieto, A. 2013. Differential proteomic analysis of the secretome of *Irpex lacteus* and other white-rot fungi growing on wheat straw. *Manuscript in preparation*.

Capítulo 4. Salvachúa, D., Prieto, A., Martínez, A.T., Martínez, M.J. 2013. Characterization of a novel DyP-type peroxidase from *Irpex lacteus* and its application in the enzymatic hydrolysis of wheat straw. Appl. Environm. Microbiol. doi: 10.1128/AEM.00699-13.

Capítulo 5. Salvachúa, D., Prieto, A., Mattinen, M.L., Tamminen, T., Liitiä, T., Lille, M., Willför, S., Martínez, A.T., Martínez, M.J. and Faulds, C.B. 2013. Versatile peroxidase as a valuable tool for generating new biomolecules by homogeneous and heterogeneous cross-linking. Enzyme Microb. Technol. 52, 303-311.

Introducción general



1. EL BIOETANOL

1.1. Situación actual

Uno de los mayores retos del siglo XXI es encontrar nuevas fuentes de energía que sean renovables, respetuosas con el medio ambiente, seguras, efectivas y capaces de asegurar el abastecimiento de combustible a la población. Los biocombustibles podrían ser una de las vías de solución ya que se consideran una alternativa para sustituir a los combustibles fósiles. Aunque, al menos a corto plazo, no van a reemplazarlos totalmente, sí que pueden contribuir, de forma significativa, a reducir nuestra dependencia del petróleo y disminuir la producción de gases invernadero, de acuerdo con los criterios establecidos en el Protocolo de Kyoto (http://europa.eu/legislation_summaries/environment/tackling_climate_change/ l28060_es.htm).

La Unión Europea (UE) se ha implicado activamente en el objetivo de reducir las emisiones de CO_2 a través de varias líneas de actuación. Concretamente, las recogidas en la Directiva 2009/28/CE, destinadas a conseguir una mejora de la eficiencia energética, señalan como objetivo obligatorio alcanzar una cuota del 20% de energía procedente de fuentes renovables en el consumo total para el año 2020. Pero además, esta Directiva marca expresamente como objetivo vinculante para todos los Estados miembros que, al menos, el 10% de la energía utilizada en el sector transporte proceda de fuentes renovables. La legislación para conseguir este objetivo varía en cada país, dependiendo, principalmente, de sus políticas agrarias, motivaciones ambientales y de las materias primas disponibles. Sin embargo, en todos los países de la UE la producción de biocombustibles juega un papel importante.

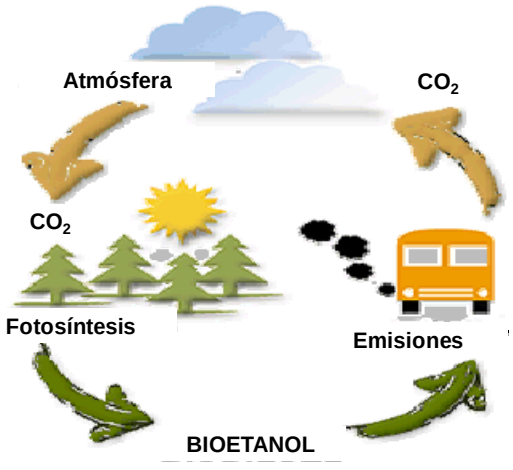

Fig. 1. Sistema de reciclado del CO_2 usando bioetanol como combustible.

Entre los biocombustibles se encuentra el bioetanol, un carburante obtenido como resultado de la fermentación de materia orgánica vegetal rica en carbohidratos. Debido al carácter renovable de estas materias primas, el uso de este y otros biocarburantes contribuye a la reducción de las emisiones de CO_2 (Fig. 1), puesto que evita la liberación de C derivada de la movilización de fuentes de carbono secuestradas de la atmósfera hace miles de años (combustibles fósiles).

Según la Agencia Internacional de la Energía (IEA), EEUU es el primer productor de bioetanol seguido de Brasil, la UE y Asia (http//:www.iea.org). En concreto, la UE produjo 3.700 millones de litros de bioetanol en el año 2009 (Fig. 2), 10 veces menos que EEUU (http//:www.biofuels-plattform.ch/en/infos/eu-bioethanol.php). En el año 2012, los principales productores europeos de este combustible fueron Francia y Alemania, ocupando España el tercer lugar. Entre las empresas del sector destaca Abengoa, una empresa española cuya actividad se ha expandido en Europa y EEUU. Esta compañía utiliza y comercializa, desde hace años, bioetanol obtenido a partir de grano de cereal (cebada, trigo o maíz), dependiendo la materia prima concreta de los recursos disponibles en los países en los que está establecida. En el año 2003, Abengoa además creó la División de "Bioenergía" para desarrollar procesos innovadores en este campo.

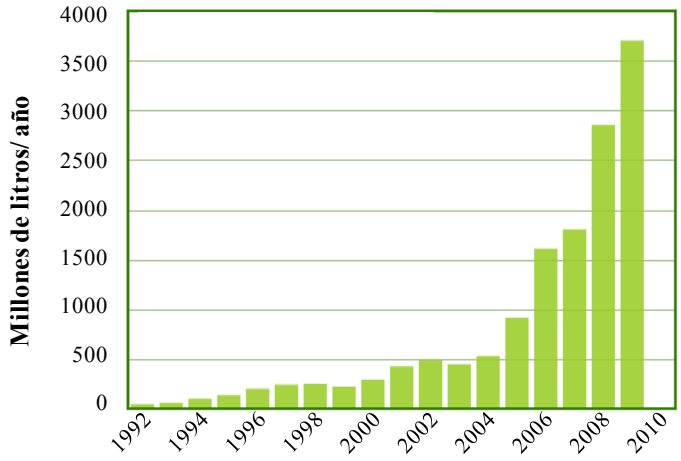

Fig. 2. Producción de bioetanol en Europa desde el año 1992 hasta el año 2009.

El etanol puede utilizarse como combustible único, mezclado en diferentes proporciones con la gasolina o como aditivo de la misma. En la UE, las mezclas más habituales y autorizadas, que pueden utilizarse sin modificar los motores, contienen un 5%, 10% o 15% de bioetanol (denominadas E5, E10 y E15, respectivamente). En otros países, como EEUU y Brasil, se comercializan carburantes con una riqueza de etanol comprendida entre el 85 y el 100%, aptas solo para vehículos flexifuel, con motores adaptados para su combustión.

Actualmente la mayor parte del bioetanol comercializado para biocarburantes se obtiene a partir de biomasa vegetal, definida por la Real Academia Española como "materia orgánica originada en un proceso biológico, espontáneo o provocado, utilizable como fuente de energía". El origen de esta biomasa es muy heterogéneo (caña de azúcar, remolacha,

cereales, etc.) y dependiendo de si los azúcares fermentables se encuentran libres o en forma de polisacáridos, los tratamientos para su conversión en etanol son muy diversos. En muchos casos es necesaria una etapa de hidrólisis que libere la glucosa para poder fermentarla hasta etanol. Una vez producido el alcohol es preciso concentrarlo, y para comercializarlo como aditivo de la gasolina, debe de estar deshidratado y poco oxigenado (Nigam y Singh, 2011). La complejidad de este proceso y los costes asociados hace que en muchos casos el precio del bioetanol no pueda competir con el de la gasolina. Esta es una de las razones por las que el empleo de etanol no acaba de afianzarse en la UE, pero otro factor a tener en cuenta es que también es más barato producir otros carburantes, como el biodiésel, a partir de derivados del aceite. De hecho, en 2011 el consumo de biodiésel en la UE fue mucho mayor que el de etanol, 77% frente al 23%, respectivamente (http//:www.iea.org).

Un problema añadido es que, en la actualidad, la producción de etanol a partir de biomasa vegetal se basa en el empleo de materias primas aptas para la alimentación. Este hecho llevó a plantear cuestiones tales como el porcentaje de alimentos o tierras cultivables dedicadas a la producción de cereales para fabricación de combustibles o para el consumo humano, generando una gran controversia. Muchas voces se alzaban contra el uso de recursos naturales que podían entrar en competencia con los recursos alimentarios y por eso en Diciembre de 2012 se propuso una enmienda a la Directiva 2009/28/CE para limitar la producción de biocarburantes a partir de cultivos alimentarios. Por estas razones y porque la disponibilidad de biocombustibles es insuficiente para cubrir las demandas programadas por la UE para el año 2020, la producción de bioetanol a partir de materias primas alternativas y el desarrollo de tecnologías más efectivas y menos costosas es una prioridad para muchos países (Sun y Cheng, 2002).

1.2. Clasificación del bioetanol

Según la materia prima utilizada para su producción se diferencian 3 tipos de bioetanol, denominados de 1ª, 2ª o 3ª generación.

1.2.1. Bioetanol de primera generación (1G)

El etanol 1G procede de materias primas con alto contenido en azúcares fermentables. La producción más eficiente se obtiene utilizando caña de azúcar, sorgo o remolacha, plantas con un alto contenido en sacarosa. Para la fermentación de dicho glúcido no se necesita ningún pretratamiento, ya que levaduras como *Saccharomyces cerevisiae* pueden metabolizar dímeros azucarados (Cardona et al., 2010). Este tipo de materias primas se utiliza en Brasil y otros países tropicales o subtropicales.

La otra fuente de la que se nutre la producción de etanol 1G son los sustratos ricos en almidón. En este caso, para liberar la glucosa y dejarla disponible para ser fermentada por las levaduras, se necesita un tratamiento previo que consiste en la hidrólisis con α-amilasas. Actualmente, el almidón contenido en los granos de cereales es el más usado para producir etanol 1G en EEUU y en Europa (Cardona y Sánchez, 2007).

1.2.2. Bioetanol de segunda generación (2G)

La materia prima utilizada para producir etanol 2G es la lignocelulosa, cuyo empleo presenta varias ventajas. Por una parte, el material lignocelulósico no compite con el sector alimentario, ya que se obtiene a partir de productos tales como madera, astillas, residuos agrícolas e incluso desperdicios domésticos, representando el recurso renovable más abundante en todo el mundo (Lin y Tanaka, 2006). Además, el empleo de nuevos cultivos energéticos posibilita una mayor producción de biomasa por unidad de superficie y una mayor cantidad de materia prima para ser utilizada en la producción de bioetanol. Por otra parte, se plantea la consolidación de estos cultivos en terrenos no explotados para cultivos alimentarios, lo que redundaría en una mejora de la eficiencia del uso del suelo. La utilización de otros materiales, como la paja de cereales, es muy interesante ya que proporciona un valor añadido a un residuo lignocelulósico muy abundante en los países productores de cereales (http://www.abengoabioenergy.com/web/es/nuevas_tecnologias). En cuanto al potencial de abastecimiento de bioetanol 2G, algunos estudios sugieren que con este tipo de materia prima se podrían alcanzar niveles de producción hasta 16 veces superiores a los actualmente obtenidos a partir de grano de cereales (Balat et al., 2008).

Sin embargo, la conversión de lignocelulosa a etanol a escala comercial es todavía un reto, ya que se requieren pretratamientos específicos para desestructurar este material, procesamientos de producción más sofisticados, más inversión por unidad de producción e instalaciones de mayor envergadura que las de 1G (Nigam y Singh, 2011). El proceso de producción de etanol 2G se detalla en la Sección 2.

1.2.3. Bioetanol de tercera generación (3G)

La última generación de biocombustibles dirige su atención a la explotación de ciertos organismos como levaduras, hongos y microalgas. Algunos de estos organismos son considerados como fuentes potenciales para la producción de bioetanol y biodiésel ya que pueden sintetizar y almacenar grandes cantidades lípidos, proteínas e hidratos de carbono durante períodos cortos de tiempo (Nigam y Singh, 2011; Xiong et al.,

2008). Además, también pueden utilizarse para producir otros compuestos con alto valor añadido para el sector alimentario, químico o farmacéutico.

2. BIOETANOL DE SEGUNDA GENERACIÓN A PARTIR DE PAJA DE TRIGO

Como se ha mencionado anteriormente, el bioetanol 2G se obtiene a partir de material lignocelulósico y se considera una de las alternativas más viables para sustituir o disminuir el uso de gasolina por dos razones principales: no compite con el sector alimentario y la lignocelulosa es el recurso renovable más abundante en el planeta. Entre los residuos agrícolas, la paja de trigo ocupa un lugar destacado como materia prima para la producción de etanol 2G ya que se prevé que en 2013 la producción mundial de este cereal alcance una producción de 690 millones de toneladas, produciendo Europa más de 130 millones de toneladas (http://www.fao.org/worldfoodsituation/wfs-home/csdb/es/). Sin embargo, para realizar con éxito este proceso es necesario liberar los azúcares de la lignocelulosa para que las levaduras puedan fermentarlos, algo realmente difícil, tal y como veremos a continuación al analizar en detalle la estructura de la pared celular vegetal.

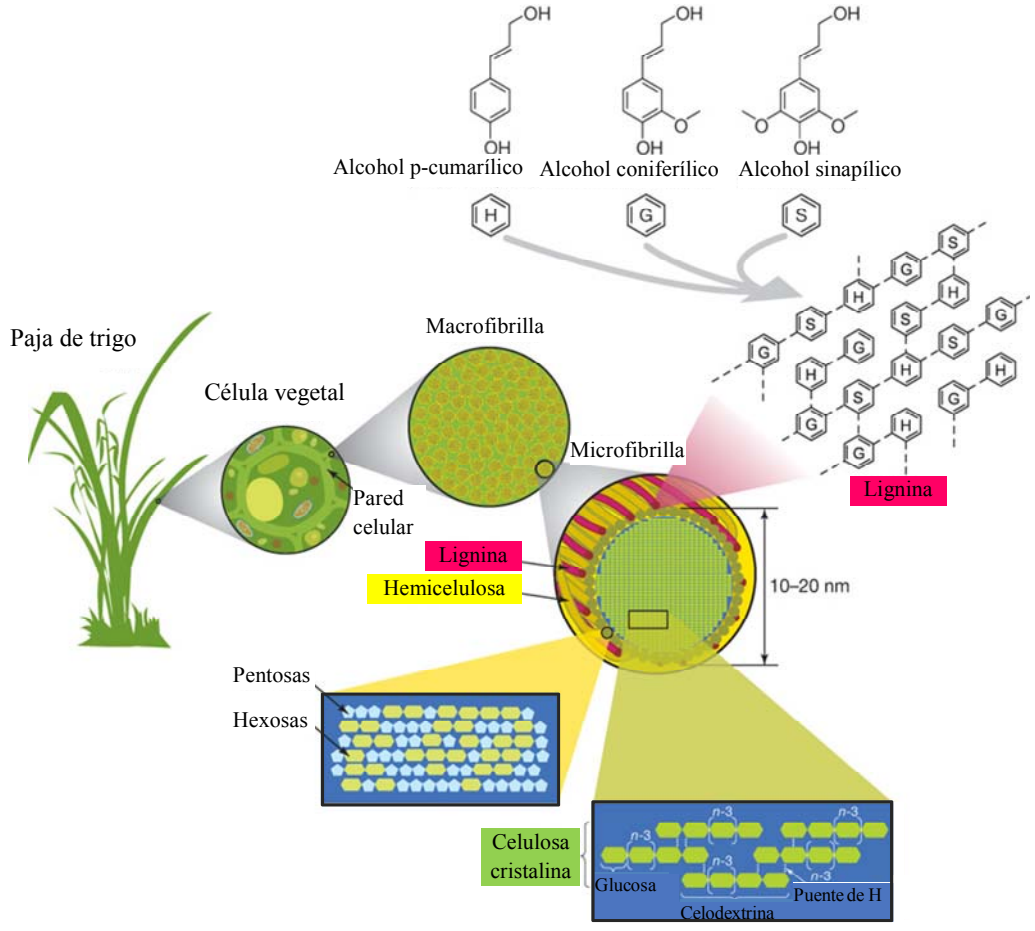

Fig. 3. Estructura de la lignocelulosa. Imagen adaptada de Rubin et al. (2008).

2.1. Estructura de la lignocelulosa

La paja de trigo, como otros residuos lignocelulósicos, contiene tres componentes principales (% peso/peso): celulosa (33-40%), hemicelulosa (20-25%) y lignina (15-20%) (Fig. 3). Los porcentajes de estos componentes pueden variar significativamente dependiendo de la especie, del suelo y de las condiciones climáticas (Prasad et al., 2007).

2.1.1. La celulosa

La celulosa no solo es el principal componente de la pared celular vegetal, sino que es el polisacárido más abundante sobre la superficie terrestre. Su estructura tiene como base polímeros lineales constituidos por monómeros de D-glucosa (Fig. 4), unidos por enlaces glicosídicos β-(1,4) y dispuestos en paquetes de largas cadenas unidas por puentes de hidrógeno, que forman las fibrillas elementales (Baldrian y Valaskova, 2008). Éstas se agrupan formando microfibrillas, que se encuentran cubiertas de hemicelulosa y lignina, y se orientan de forma diferente en cada nivel de la pared secundaria para darle resistencia. Y estas microfibrillas se agrupan a su vez formando macrofibrillas (Fujita y Harada, 1991).

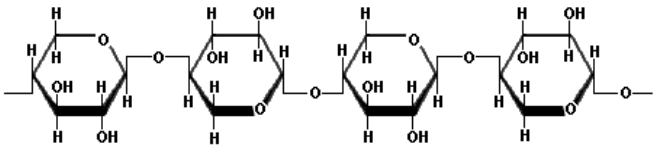

Fig. 4. Detalle de la estructura molecular de la celulosa.

2.1.2. La hemicelulosa

La hemicelulosa (Fig. 5) está formada por polisacáridos muy heterogéneos e incluye diversos azúcares como pentosas (β-D-xilosa y α-L-arabinosa), hexosas (β-D-glucosa, β-D-manosa, α-D-galactosa), y/o ácidos urónicos (ácido α-D-glucurónico, α-D-4-O-metilgalacturónico y α-D-galacturónico). Otros azúcares como α-L-ramnosa y α-L-fucosa pueden representar también una pequeña fracción de la hemicelulosa (Gírio et al., 2010). En la hemicelulosa de la paja de trigo, el xilano es el polímero más abundante, constituyendo alrededor de un 18% del peso total. Este xilano está formado por residuos de xilopiranosa (acetilados en su mayoría), unidos entre sí por enlaces glicosídicos β-(1,4).

En general, las unidades de la hemicelulosa varían dependiendo del tipo de planta. Por ejemplo, en las maderas duras (frondosas), el principal componente es un xilano altamente acetilado, en las maderas blandas

(coníferas) los galactomananos son más abundantes que el xilano y en las plantas herbáceas, el xilano, siendo también el polímero más abundante, tiene menos residuos acetilados que en las maderas duras (Camarero, 1995).

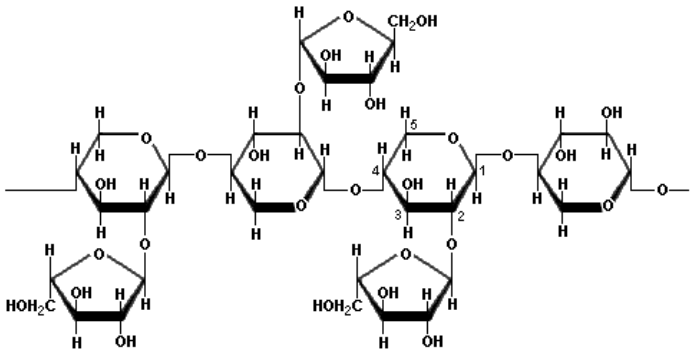

Fig. 5. Detalle de la estructura molecular de la hemicelulosa.

2.1.3. La lignina

La lignina es un heteropolímero aromático tridimensional formado por tres tipos de precursores fenilpropano, denominados hidroxipropil (H), guayacil (G) y siringil (S) (Fig. 3), aunque recientemente se han descrito otros diferentes a partir de paja de trigo (del Río, 2012). Estos alcoholes *p*-hidroxicinamílicos (monolignoles), se acoplan entre sí después de sufrir una deshidrogenación enzimática mediante enlaces éter y C-C entre los carbonos del anillo y de las cadenas laterales (Fig. 6). La deshidrogenación consiste en una reacción de transferencia de un electrón catalizada por peroxidasas o lacasas de la planta en presencia de peróxido de hidrógeno u oxígeno, respectivamente (Adler, 1977), de manera que se forman radicales libres de tipo fenoxilo estabilizados en diversas formas resonantes (Fig. 7) y que son los que se unen entre sí. El enlace más generado, y favorecido por cuestiones energéticas, es aquel producido entre la posición β del monolignol radical y el radical fenoxilo del polímero de lignina creciente dando lugar a la formación de un enlace tipo β-*O*-4´.

Inicialmente el polímero de lignina se deposita en la lámina media y la pared primaria y finalmente cementa las diferentes capas de la pared secundaria, formado una matriz sobre la celulosa y la hemicelulosa. La lignina, por su naturaleza hidrofóbica y su estructura recalcitrante, es el componente de la pared vegetal que confiere a la planta rigidez y protección frente a los patógenos y a la desecación (Buranov y Mazza, 2008).

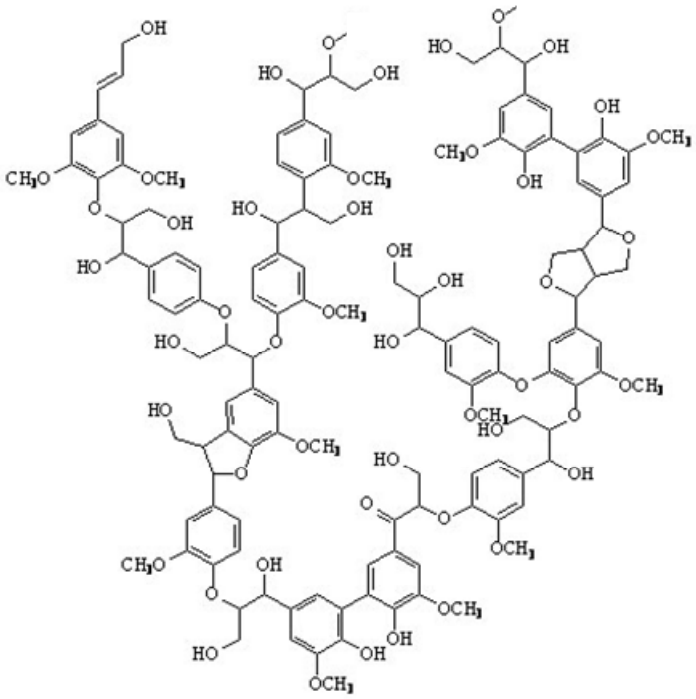

Fig. 6. Detalle de la estructura molecular de la lignina.

2.1.4. Otros componentes de la lignocelulosa

Aparte de todos estos elementos, en la pared vegetal hay también ácidos cinámicos, como el ácido *p*-cumárico, que contribuyen a la unión de la lignina con las hemicelulosas mediante enlaces covalentes, o el ácido ferúlico, que es el principal responsable de las uniones entre la lignina y los polisacáridos. Por último, y como componentes minoritarios de la paja de trigo, también cabe mencionar la presencia de pectinas, proteínas, lípidos y minerales (Fengel y Wegener, 1984).

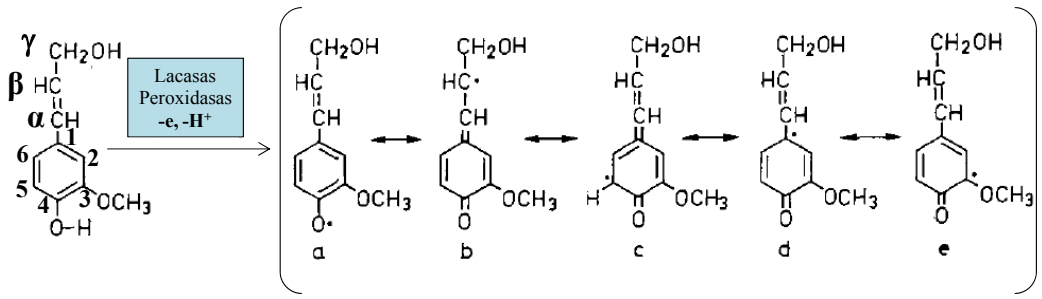

Fig. 7. Deshidrogenación del alcohol coniferílico. La molécula "e" no está implicada en la biosíntesis de la lignina ya que no se encuentra termodinámicamente favorecida. Figura adaptada de Adler et al. (1977).

2.2. Etapas de producción de bioetanol a partir de paja de trigo

Debido a la complejidad estructural de la paja de trigo, se requieren al menos tres grandes pasos operacionales para hacer accesibles los azúcares de la pared celular vegetal y producir, a partir de ellos, etanol u otros productos de interés para el sector alimentario o químico: pretratamiento, hidrólisis enzimática y fermentación (Fig. 8).

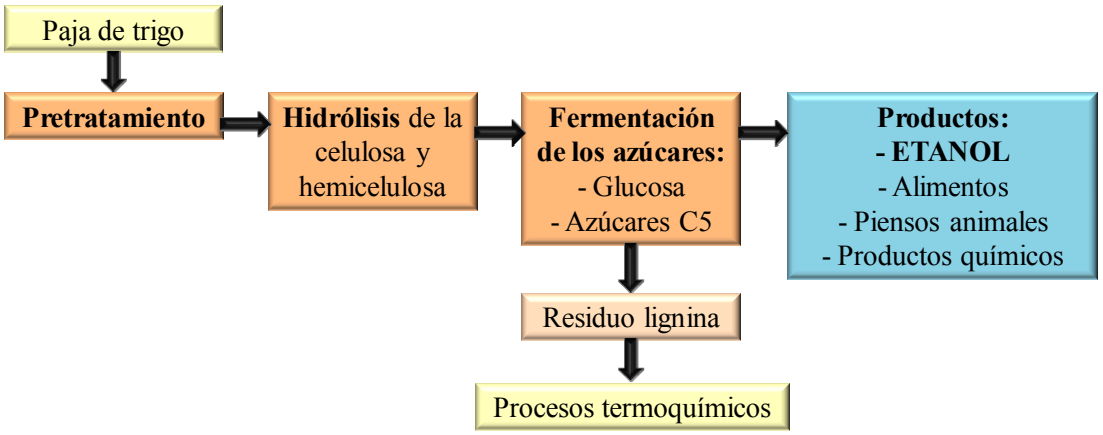

Fig. 8. Esquema del proceso de producción de etanol y otros productos de interés a partir de paja de trigo. Esquema adaptado de Gray et al. (2006).

2.2.1. Pretratamiento

El objetivo de esta etapa es convertir la biomasa lignocelulósica, altamente resistente a la acción de las enzimas hidrolíticas, en un material mucho más accesible, a partir del cual sea posible la despolimerización eficiente de los polisacáridos. Esto se logra rompiendo las uniones entre celulosa, hemicelulosa y lignina, y/o produciendo la modificación estructural de estos componentes. La eficiencia del pretratamiento se correlaciona directamente con la producción de un sustrato altamente digerible y en el que no haya inhibidores que perjudiquen las subsecuentes etapas del proceso (Talebnia et al., 2010). Se han ensayado diversos métodos para pretratar paja de trigo pero ninguno de ellos resulta completamente eficaz y las empresas seleccionan el que les parece más adecuado, en función de las materias primas y las instalaciones de las que disponen. Los métodos de pretratamiento se clasifican principalmente en cuatro tipos principales: físicos, físico-químicos, químicos y biológicos.

2.2.1.1. Métodos físicos

Estos pretratamientos se basan principalmente en la reducción del tamaño de partícula de la materia prima a través de procesos de molienda, triturado, astillado y pulverización. La disminución del tamaño de partícula conlleva una mayor digestibilidad, pero también un incremento en el consumo de

energía (Talebnia et al., 2010). En los últimos años se están ensayando, y con buenos resultados, técnicas de extrusión, en las que la materia prima es sometida simultáneamente a un tratamiento térmico, de cizallamiento y de mezcla a su paso por el extrusor, lo que favorece su transformación (Karunanithy y Muthukumarappan, 2010).

2.2.1.2. Métodos químicos

En estos procesos se emplean ácidos, bases y agentes oxidantes (ej. peróxido y ozono), generando cada uno resultados muy diferentes. Por ejemplo, los agentes alcalinos y oxidantes facilitan la eliminación de la lignina, mientras que un tratamiento ácido facilitaría la solubilización de la hemicelulosa (Talebnia et al., 2010). Un inconveniente de estas tecnologías es que durante los tratamientos se generan subproductos que pueden inhibir etapas posteriores y afectar negativamente el rendimiento global del proceso. Además, el uso de ácidos, aunque sean muy diluidos, incrementa la corrosión de los equipos y, como consecuencia, los costes de mantenimiento.

2.2.1.3. Métodos físico-químicos

El objetivo de este tipo de pretratamientos es solubilizar los diferentes componentes de la lignocelulosa, variando la temperatura, presión, pH y contenido en humedad de la materia prima. Dentro de este grupo existen varias modalidades, como la explosión por vapor o *steam explosion* (EV), el pretratamiento con agua caliente en fase líquida (ACL), la explosión por vapor con amoniaco (AFEX) y, más recientemente, la extrusión en presencia de agentes químicos.

El pretratamiento por EV, en el que la paja se somete a cambios muy bruscos de temperatura y presión en tiempos muy cortos, es uno de los métodos más eficaces hasta el momento (Ballesteros et al., 2006b). En ocasiones el procedimiento se hace en presencia de H_2SO_4 o SO_2, diluidos, para incrementar los rendimientos del proceso ya que contribuyen a solubilizar eficazmente las hemicelulosas. Sin embargo, este tipo de pretratamiento, además de ser muy caro, produce compuestos derivados de la descomposición de los azúcares (furfural, 5-hidroximetilfurfural, ácido acético, ácido fórmico, etc) y de la degradación de la lignina (fenoles), que afectan negativamente tanto a la etapa de hidrólisis enzimática como a la de fermentación (Ballesteros et al., 2006a; Kabel et al., 2007).

El método ACL consiste en humedecer la paja con agua caliente y someterla a presión durante tiempos de tratamiento mucho más largos que los usados en la EV (Petersen et al., 2009).

La tecnología AFEX se basa en tratamientos alcalinos, utilizando amoniaco y cambios de temperatura y presión (Mosier et al., 2005). Este tratamiento es efectivo con material herbáceo ya que parece que no genera inhibidores, sin embargo todavía hay muy pocos estudios y es necesario comprobar su eficiencia (Talebnia et al., 2010).

Y por último, la extrusión puede ser combinada durante el tratamiento con agua caliente, ácidos, bases o surfactantes ya sea en procesos discontinuos o continuos (Duque et al., 2013).

2.2.1.4. Métodos biológicos

El biopretratamiento, que será descrito con más detalle en la sección 3, se basa en la capacidad de algunos organismos para degradar la lignina y así facilitar la accesibilidad a la celulosa y hemicelulosa. Es un procedimiento respetuoso con el medio ambiente y no produce compuestos inhibidores que afecten negativamente al resto del proceso.

2.2.2. Hidrólisis enzimática

El objetivo de esta etapa consiste la degradación de los polisacáridos de la pared celular vegetal, la celulosa y hemicelulosa, hasta sus correspondientes monosacáridos, azúcares potencialmente fermentables.

Para este proceso se emplean diversas enzimas hidrolíticas, principalmente celulasas y xilanasas, producidas por hongos o bacterias. Sin embargo, a veces se requieren otras enzimas, especialmente en el caso de la hemicelulosa ya que, dependiendo de su origen, puede presentar alta heterogeneidad (Gírio, 2010). Para facilitar la hidrólisis de un material tan complejo, dependiendo de la materia prima utilizada, se pueden añadir proteasas, expansinas, o incluso enzimas ligninolíticas (Talebnia et al., 2010). Un análisis más detallado de las enzimas utilizadas para la hidrólisis de la celulosa y la hemicelulosa se abordará en la sección 4.

2.2.3. Fermentación alcohólica

La fermentación alcohólica consiste en la producción de etanol a partir de los azúcares liberados tras la hidrólisis enzimática. A nivel industrial, la fermentación de la glucosa se realiza eficientemente utilizando la levadura *S. cerevisiae*. Estequiométricamente, la conversión de glucosa a etanol es de 0.51 gramos de etanol por gramo de azúcar pero en la práctica, obtener el 100% de conversión es muy difícil ya que aproximadamente el 5% de los azúcares se utilizan para el crecimiento y el metabolismo celular de la levadura.

Sin embargo, para que la producción de etanol 2G se consolide y el proceso pueda ser rentable, es necesario también fermentar las pentosas derivadas de la hidrólisis de la hemicelulosa de la pared vegetal, principalmente la xilosa en el caso de la paja de trigo. Este proceso está menos estudiado y, hasta el momento, son muy pocos los organismos capaces de fermentar eficazmente la xilosa en medios complejos. Entre los organismos que podrían fermentar la xilosa se encuentran las levaduras *Candida shehatae, Pachysolen tannophylus* y *Pichia stipitis*. Hasta el momento, ninguna de estas levaduras tolera altas concentraciones de etanol y además son muy sensibles a los inhibidores que se producen durante el pretratamiento del material lignocelulósico (Hahn-Hagerdal et al., 2007).

2.3. Retos en la producción de etanol 2G

Además de conseguir métodos eficaces para el pretratamiento de la lignocelulosa, los principales retos para la viabilidad del proceso de producción de etanol 2G están relacionados con la búsqueda de enzimas más eficientes para la hidrólisis enzimática y la integración de las diferentes etapas (pretratamiento, hidrólisis enzimática y fermentación) para abaratar los costes de procesamiento.

2.3.1. Búsqueda de enzimas eficaces

Actualmente existen muchos grupos de investigación y empresas tratando de obtener cócteles enzimáticos que aumenten la eficiencia del proceso. A continuación se describen diferentes métodos/herramientas para este propósito (Fig. 9).

2.3.1.1. Screening de microorganismos productores de enzimas

A partir de muestras naturales (material lignocelulósico principalmente) se seleccionan los organismos con mayor capacidad para hidrolizar los sustratos seleccionados. Los mejores candidatos (generalmente hongos o bacterias) son aislados, identificados y cultivados, buscando inductores adecuados para incrementar la secreción de las actividades de interés. Después se purifican las enzimas y se estudian sus propiedades catalíticas para compararlas con otras enzimas, previamente caracterizadas, relacionadas con el proceso de producción de bioetanol 2G.

2.3.1.2. Estudios de secretómica

El análisis del conjunto de las proteínas extracelulares secretadas por un organismo se realiza utilizando técnicas proteómicas. A través de estos métodos, se pueden comparar además patrones de secreción en diferentes condiciones de cultivo. Estos estudios implican el análisis, por espectrometría de masas, de los péptidos trípticos generados a partir

proteínas individuales, separadas en geles bidimensionales, o incluso del conjunto de proteínas secretadas sin fraccionamiento previo (nano-HPLC-MS/MS). Con estas metodologías se pueden detectar e identificar, con diferente sensibilidad según la técnica empleada, muchas de las enzimas del secretoma, así como identificar péptidos internos (siempre que haya proteínas similares en las bases de datos) que aporten información sobre las proteínas desconocidas. En caso de encontrar enzimas que se sobreexpresan o se producen exclusivamente en presencia de sustratos lignocelulósicos, estas podrían tener un papel importante durante la hidrólisis de la celulosa, hemicelulosa o lignina.

2.3.1.3. Genómica y metagenómica

La finalidad de estos estudios, en el proceso de producción de etanol 2G, es la búsqueda de genes relacionados con enzimas que sean de especial interés, sobre todo para la etapa de hidrólisis enzimática. En el caso de la genómica, el enorme desarrollo y abaratamiento de las técnicas de secuenciación masiva está permitiendo conocer el genoma de numerosos microorganismos de interés. En el caso de la metagenómica la búsqueda de estos genes se amplía a microorganismos no cultivables. En ambos casos el objetivo final es la producción de enzimas con nuevas o mejores propiedades catalíticas, que permitan aumentar el rendimiento del proceso o disminuir los costes de producción.

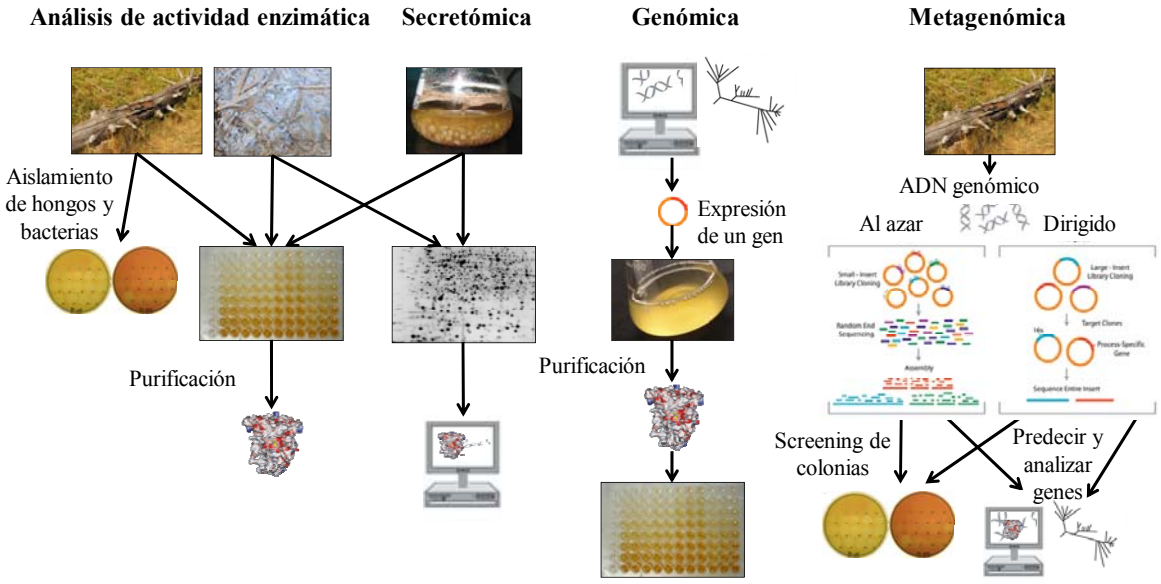

Fig. 9. Métodos comúnmente usados para la búsqueda de nuevas enzimas.

2.3.2. Integración de diferentes etapas del proceso de producción

A continuación se describen algunos procesos integrados que se están ensayando en la actualidad.

2.3.2.1. Co-fermentación de hexosas y pentosas

El empleo de cultivos mixtos de microorganismos compatibles capaces de fermentar hexosas y pentosas ha sido una de las propuestas iniciales encaminadas a la integración de las diferentes etapas, aunque plantea algunas dificultades técnicas. Las levaduras que fermentan hexosas crecen más rápido que las que metabolizan los azúcares C5 y además estas últimas se inhiben muy fácilmente por el etanol. Por ello, es interesante potenciar el crecimiento de las levaduras fermentadoras de pentosas en los co-cultivos durante las fases iniciales de la fermentación. Una de las estrategias para lograrlo es emplear mutantes de *S. cerevisiae* con una capacidad respiratoria reducida, y por tanto, ralentizar su crecimiento y la fermentación de las hexosas. Otras aproximaciones a este objetivo se basan en el diseño de organismos recombinantes capaces de fermentar ambos azúcares, como cepas de *Escherichia coli*, *Zymomonas* sp. (Cardona y Sánchez, 2007) o *S. cerevisiae* (Cardona y Sánchez, 2007; Wahlbom et al., 2008).

2.3.2.2. Sacarificación (hidrólisis enzimática) y fermentación/co-fermentación simultáneas

El principal problema de la integración de estos dos procesos es que la elevada concentración de azúcares que se obtiene al final de la fase de hidrólisis puede inhibir más a la levadura que el propio etanol que es capaz de producir. La clave para resolverlo estaría en la capacidad de los organismos fermentadores para convertir los azúcares en etanol tan pronto como sean liberados en la hidrólisis enzimática. Sin embargo, existen otras trabas, como por ejemplo que la temperatura y el pH requerido para ambos procesos suele ser muy diferente (Cardona y Sánchez, 2007). Por esta razón, está ganando particular interés el diseño de organismos sintéticos, con las rutas metabólicas necesarias para hidrolizar eficazmente los polisacáridos y fermentar eficientemente tanto la glucosa como la xilosa. Este tipo de organismos, aún en fase de desarrollo muy preliminar, constituirían una herramienta perfecta para integrar todas las etapas del proceso en una sola (Connor y Atsumi, 2010).

3. EL PRETRATAMIENTO BIOLÓGICO

Como se ha comentado previamente, la eliminación o desestructuración de la lignina es imprescindible para que la celulosa y la hemicelulosa queden accesibles a las enzimas hidrolíticas. El biopretratamiento se basa en la

degradación de esta barrera biológica por organismos vivos. Normalmente, el grado de deslignificación de la materia prima se correlaciona positivamente con su digestibilidad, es decir, con la cantidad de azúcares simples liberados partir de la celulosa y la hemicelulosa tras la etapa de hidrólisis enzimática (Bak et al., 2009; Taniguchi et al., 2005; Valmaseda et al., 1991; Zhang et al., 2007). En cualquier caso, la selección de un microorganismo para realizar el pretratamiento debe ser cuidadosamente evaluada teniendo en cuenta otros datos, como la pérdida de peso de la materia prima, ya que un aumento de digestibilidad no va necesariamente ligado a un mayor rendimiento global de azúcares fermentables.

3.1. Organismos degradadores de la lignocelulosa

En la naturaleza existen numerosos organismos capaces de degradar la lignocelulosa, pero sin duda los principales descomponedores de la biomasa son los hongos, y más concretamente, los basidiomicetos. La evolución de estos hongos ha discurrido en paralelo a la de las plantas vasculares, lo que ha propiciado que estos organismos desarrollaran mecanismos, muy inespecíficos, para poder colonizar sustratos inicialmente inaccesibles (Floudas et al., 2012). En función del patrón de degradación que producen sobre la lignocelulosa, se han dividido en dos grupos: los basidiomicetos de podredumbre parda y los de podredumbre blanca. Los primeros han desarrollado mecanismos oxidativos para metabolizar la celulosa, sin degradar la lignina, de manera que el material sobre el que crecen adquiere una tonalidad parda. Los segundos degradan la lignina, de manera preferente o simultánea a los polisacáridos, originando un residuo blanquecino (Guillén et al., 2000a; Valmaseda et al., 1991).

Además de los basidiomicetos, existen otros microorganismos descomponedores de lignina entre los que podemos citar actinomicetos del género *Streptomyces* (Berrocal et al., 2004), bacterias como *Pseudomonas* y *Xanthomonas* (Odier et al., 1981), hongos ascomicetos como *Chrysonilia sitophyla* (Rodríguez et al., 1997) o deuteromicetos como *Fusarium concolor* (Kuhar et al., 2008) y *Fusarium proliferatum* (Anderson et al., 2005). Sin embargo, para comenzar la degradación del material lignocelulósico, especialmente cuando su contenido en lignina es alto, los basidiomicetos parecen ser los mejores candidatos y, por esta razón, son los más estudiados para el pretratamiento biológico de la biomasa lignocelulósica.

3.2. Fermentación en estado sólido

Técnicamente, el biopretratamiento del material lignocelulósico con basidiomicetos de podredumbre blanca se realiza en condiciones de "fermentación en estado sólido" (Fig. 10). Esta denominación hace

referencia a las condiciones de cultivo de los microorganismos sobre sustratos sólidos, en ausencia de agua libre. En estas condiciones el contenido líquido se corresponde con la actividad de agua necesaria para el crecimiento y metabolismo celular, sin exceder la capacidad máxima de retención de agua del sustrato (Paredes-López y Alpuche-Solís, 1991).

Sin embargo, para optimizar y controlar los rendimientos del proceso es preciso evaluar cuidadosamente ciertos parámetros tales como la concentración de biomasa fúngica en el inóculo, el contenido en humedad y el tamaño de partícula del sustrato, la presencia de iones que faciliten la degradación y/o la temperatura y aireación de los cultivos (Reid, 1989; Wan y Li, 2012).

Fig. 10. Ensayos de biopretratamiento a pequeña escala en condiciones de fermentación en estado sólido.

3.3. Escalado del biopretratamiento

El escalado del biopretratamiento en condiciones de fermentación en estado sólido es complicado teniendo en cuenta la gran diversidad de parámetros implicados en este proceso. Debido a la baja actividad de agua y baja conductividad de las partículas sólidas, el propio organismo produce calor causando diferentes gradientes de temperatura dentro del mismo sustrato y, por tanto, generando patrones de degradación distintos. La optimización de los controles de temperatura y la disipación de ese calor es una de las mayores consideraciones en el diseño de biorreactores para cultivos de fermentación en estado sólido. Mitchel et al. (2006) han diseñado varios modelos de biorreactores: lechos empacados, reactores en bandeja, tambores giratorios o biorreactores en agitación. Aunque estos últimos pueden disipar muy bien el calor no son del todo válidos ya que la mayoría de los hongos se unen al sustrato mediante hifas y, con la agitación, muchas de ellas se romperían, perjudicando la colonización fúngica. Hasta el momento, los lechos empacados parecen la opción más adecuada.

3.4. Ventajas y desventajas

El pretratamiento biológico es un proceso respetuoso con el medio ambiente, no requiere costes energéticos elevados y no genera inhibidores que puedan afectar negativamente a la etapa de hidrólisis o fermentación. Sin embargo, antes de poder aplicar eficazmente un biopretratamiento fúngico, quedan por resolver algunos aspectos como el lento crecimiento de los hongos sobre la materia prima y el consumo de los polisacáridos de la paja de trigo para su propio crecimiento, que disminuiría el rendimiento de recuperación de azúcares fermentables.

4. ENZIMAS FÚNGICAS IMPLICADAS EN LA DEGRADACIÓN DE LA LIGNOCELULOSA

La degradación de la lignocelulosa es un proceso extracelular. Los hongos, para llevar a cabo este proceso, tienen dos tipos de sistemas enzimáticos: un sistema hidrolítico, en el que participan las enzimas responsables de la biodegradación de la celulosa y hemicelulosa, y un sistema oxidativo, en el que participan las enzimas que degradan la lignina.

4.1. Biodegradación de la celulosa

Los microorganismos que degradan la celulosa secretan una batería de enzimas muy amplia, con especificidades diferentes y que actúan conjuntamente. Las celulasas se dividen en tres grandes categorías (Baldrian y Valaskova, 2008):

(i) Endo-1,4-β-glucanasas, que inician un ataque al azar en múltiples sitios de la fibra de celulosa.

(ii) Exocelulasas o celobiohidrolasas, que liberan dímeros o monómeros desde los extremos terminales de las cadenas de glucosa.

(iii) β-glucosidasas, que hidrolizan la celobiosa (dímeros de glucosa) y otros oligosacáridos liberando monosacáridos.

4.2. Biodegradación de la hemicelulosa

La degradación de la hemicelulosa es más complicada debido a su heterogeneidad estructural y molecular, siendo los productos finales de hidrólisis monosacáridos y ácido acético (Gírio et al., 2010).

El xilano, que es el principal polímero de la hemicelulosa de la paja de trigo, requiere de la acción de endo y exo-1,4-β-xilanasas y 1,4-β-xilosidasas para liberar la xilosa. Además, dependiendo de la complejidad de las hemicelulosas, otras enzimas como las xilan-esterasas, mananasas, feruloil-esterasas, *p*-cumárico esterasas, α-1-arabinofuranosidasas, α-4-*O*-

metilglucuronidasas o α-glucuronidasas pueden ser necesarias para hidrolizar completamente este polisacárido.

4.3. Biodegradación de la lignina

La lignina posee una estructura compleja y altamente irregular, por lo que su biodegradación consiste en un proceso oxidativo (Fig. 11), muy inespecífico, en el que intervienen oxidorreductasas extracelulares (peroxidasas, lacasas y oxidasas productoras de H_2O_2) e intracelulares, metabolitos y especies activas de oxígeno (Guillén et al., 1994; Kirk y Farrell, 1987; Valmaseda et al., 1991).

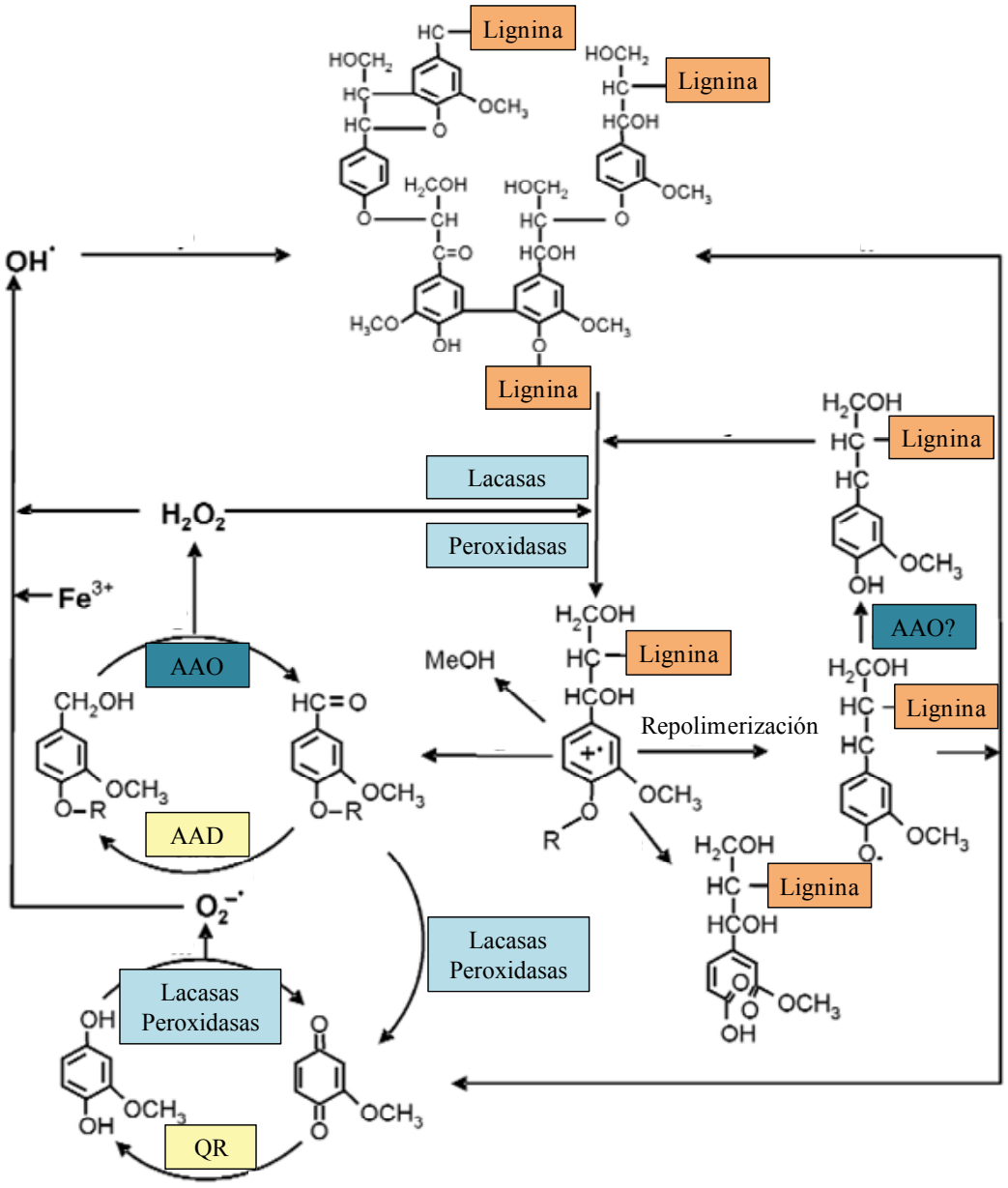

Fig. 11. Biodegradación de la lignina incluyendo reacciones enzimáticas y oxidantes. Esquema adaptado de Martínez et al. (2005). AAO= aril-alcohol oxidasa, AAD= aril-alcohol deshidrogenasa, QR= quinona reductasa.

4.3.1. Peroxidasas ligninolíticas

Este grupo de enzimas ha sido el más estudiado desde el descubrimiento de la lignina peroxidasa (LiP) y la manganeso peroxidasa (MnP) en *Phanerochaete chrysosporium* (Kuwahara et al., 1984; Tien y Kirk, 1983) aunque en la última década se han descrito también otras peroxidasas ligninolíticas, de alto potencial redox, como las peroxidasas versátiles (VP) y las peroxidasas decoloradoras de tintes (DyP). Todas las peroxidasas tienen en común que requieren ser activadas por hidroperóxido para después llevar a cabo dos oxidaciones monovalentes sucesivas de una gran variedad de compuestos.

Las LiP tienen un alto potencial de oxidorredución y preferentemente oxidan las unidades no fenólicas de la lignina mediante la sustracción de un electrón del anillo aromático, dando lugar a radicales catiónicos aromáticos, muy inestables, que evolucionan dando lugar a diferentes reacciones como la ruptura de enlaces carbono-carbono, desmetoxilaciones, descarboxilaciones, formación de quinonas, etc (Tien y Kirk, 1988).

Las MnP requieren Mn^{2+} para cerrar su ciclo catalítico y oxidan fundamentalmente compuestos fenólicos. El Mn^{3+} se genera en la reacción, y una vez estabilizado por compuestos quelantes, actúa como un agente oxidante difusible y altamente reactivo, pero también puede oxidar compuestos no fenólicos a través de otros intermediarios (tioles o lípidos insaturados) (Wariishi et al., 1989; 1992).

La VP fue descrita inicialmente en *P. eryngii* como una MnP capaz de oxidar sustratos no fenólicos típicos de la LiP (Martínez et al., 1996) pero después se describió como un nuevo tipo de peroxidasa que compartía propiedades catalíticas con las dos enzimas (Camarero et al., 1999).

Por último, recientemente se han descrito las DyP, enzimas que generalmente no oxidan Mn^{2+} pero que pueden degradar compuestos fenólicos y no fenólicos y sustratos específicos, como algunos colorantes de tipo antraquinona, que no son degradados por la LiP ni la VP (Liers et al., 2012).

4.3.2. Lacasas

Las lacasas son oxidasas multicobre que tienen como aceptor final el oxígeno. Catalizan la oxidación monoelectrónica de difenoles y aminas aromáticas, eliminando un electrón y un protón del grupo hidroxilo o amino para dar lugar a radicales fenoxilo o amino, respectivamente (Leonowicz et al., 2001). Su potencial de oxidación también puede expandirse a compuestos de naturaleza no fenólica, utilizando metabolitos de bajo peso molecular que son oxidados por estas enzimas y actúan como

agentes mediadores, dando lugar a lo que se conoce como sistema lacasa-mediador (Bourbonnais y Paice, 1990).

4.3.3. Oxidasas productoras de H_2O_2

Este grupo de enzimas participa en la producción de H_2O_2, que además de ser utilizado como cosustrato por las peroxidasas, puede generar radicales hidroxilo (OH·) a través de la reacción de Fenton. Dichos radicales son agentes oxidantes muy potentes, capaces de llevar a cabo la degradación de la lignocelulosa (Guillén et al., 2000a). Entre las enzimas extracelulares incluidas en este grupo destacan las aril-alcohol oxidasas (AAO), que oxidan alcoholes primarios α-insaturados y alcoholes alifáticos insaturados (Guillén et al., 1992), y la glioxal oxidasa que oxida aldehídos alifáticos secretados por el propio hongo, como el glioxal (Kersten y Cullen, 2007).

4.3.4. Sistemas reductores y especies activas de oxígeno

Entre las enzimas que participan en la degradación de la lignina se han descrito aril-alcohol deshidrogenasas (AAD) y quinona reductasas (QR), cuya acción es reducir los productos de oxidación que generan la AAO, las lacasas y las peroxidasas (Guillén et al., 1994; 2000a; 2000b). A través de ciclos de oxido-reducción de los sustratos que derivan de la degradación de la lignina o de metabolitos producidos por el propio hongo (Evans et al., 1994; Gutiérrez et al., 1994), todas estas enzimas participan en la generación de especies activas de oxígeno que conducen, en presencia de hierro, a la producción de radical hidroxilo (OH·) a través de la reacción de Fenton. La Figura 11 representa esquemáticamente la degradación de la lignina a través de los mecanismos previamente explicados.

Las enzimas y agentes oxidantes que acabamos de enumerar rompen y desestructuran el polímero de lignina, liberando fenoles, ácidos y alcoholes aromáticos. Una parte de ellos se mineralizan a CO_2 y agua, pero algunos intermediarios pueden repolimerizar (Fig. 11), mediante reacciones espontáneas catalizadas por el mismo sistema enzimático. La capacidad sintética de algunas de estas enzimas también puede ser aprovechada con fines biotecnológicos, tanto en síntesis de productos de alto valor añadido como para la destoxificación de compuestos que producen problemas medioambientales.

BIBLIOGRAFÍA

Adler, E., 1977. Lignin chemistry - Past, present and future. Wood Sci. Technol. 11, 169-218.

Anderson, A.J., Kwon, S.I., Carnicero, A., Falcón, M.A., 2005. Two isolates of *Fusarium proliferatum* from different habitats and global locations have similar abilities to degrade lignin. FEMS Microbiol. Lett. 249, 149-155.

Bak, J.S., Ko, J.K., Choi, I.G., Park, Y.C., Seo, J.H., Kim, K.H., 2009. Fungal pretreatment of lignocellulose by *Phanerochaete chrysosporium* to produce ethanol from rice straw. Biotechnol. Bioeng. 104, 471-482.

Baldrian, P. Valaskova, V., 2008. Degradation of cellulose by basidiomycetous fungi. FEMS Microbiol. Rev. 32, 501-521.

Ballesteros, I., Negro, M.J., Manzaneres, P., Oliva, J.M., Sáez, F., Ballesteros, M., 2006a. Steam explosion pretreatment for cereal conversion to ethanol. Appl. Biochem. Biotechnol. 129-132, 496-508.

Ballesteros, I., Negro, M.J., Oliva, J.M., Cabanas, A., Manzanares, P., Ballesteros, M., 2006b. Ethanol production from steam-explosion pretreated wheat straw. Appl. Biochem. Biotechnol. 129-132, 496-508.

Berrocal, M.M., Rodríguez, J., Hernández, M., Pérez, M.I., Roncero, M.B., Vidal, T., Ball, A.S., Arias, M.E., 2004. The analysis of handsheets from wheat straw following solid substrate fermentation by *Streptomyces cyaneus* and soda cooking treatment. Bioresour. Technol. 94, 27-31.

Bourbonnais, R., Paice, M.G., 1990. Oxidation of non-phenolic substrates. An expanded role for laccase in lignin biodegradation. FEBS Lett. 267, 99-102.

Buranov, A.U., Mazza, G., 2008. Lignin in straw of herbaceous crops. Ind. Crops Prod. 28, 237-259.

Camarero, S., 1995. Estudio de la deslignificación de la paja de trigo con *Pleurotus* para la fabricación de papel. Tesis, Universidad Complutense, Madrid.

Camarero, S., Sarkar, S., Ruiz-Dueñas, F.J., Martínez, M.J., Martínez, A.T., 1999. Description of a versatile peroxidase involved in natural degradation of lignin that has both Mn-peroxidase and lignin-peroxidase substrate binding sites. J. Biol. Chem. 274, 10324-10330.

Cardona, C., Quintero, J., Paz, I., 2010. Production of bioethanol from sugarcane bagasse: Status and perspectives. Bioresour. Technol. 101, 4754-4766.

Cardona, C.A., Sánchez, O.J., 2007. Fuel ethanol production: Process design trends and integration opportunities. Bioresour. Technol. 98, 2415-2457.

Connor, M.R., Atsumi, S., 2010. Synthetic biology guides biofuel production. J. Biomedic. Biotechnol. doi: 10.1155/2010/541698

del Río, J.C., Rencoret, J., Prinsen, P., Martínez, A.T., Ralph, J., Gutiérrez, A., 2012. Structural characterization of wheat straw lignin as revealed by analytical pyrolysis, 2D-NMR, and reductive cleavage methods. J. Agric. Food Chem. 60, 5922−5935.

Evans, C.S., Dutton, M.V., Guillén, F., Veness, R.G., 1994. Enzymes and small molecular mass agents involved with lignocellulose degradation. FEMS Microbiol. Rev. 13, 235-240.

Fengel,D. and Wegener,G., (1984) Wood: Chemistry, ultrastructure, reactions. Berlin: De Gruyter.

Floudas, D., Binder, M., Riley, R., Barry, K., Blanchette, R.A., Henrissat, B., Martinez, A.T., Otillar, R. et al., 2012. The paleozoic origin of enzymatic lignin decomposition reconstructed from 31 fungal genomes. Science 336, 1715-1719.

Fujita, M. Harada, H., 1991. Ultrastructure and formation of wood cell wall, in: David N.-S.Hon, Nobuo Shirashi (Eds.), Wood and cellulosic chemistry. Marcel Dekker Inc., New York, pp. 3-57.

Gírio, F.M., Fonseca, C., Carvalheiro, F., Duarte, L.C., Marques, S., Bogel-Lukasik, R., 2010. Hemicelluloses for fuel ethanol: A review. Bioresour. Technol. 101, 4775-4800.

Gray, K.A., Zhao, L.S., Emptage, M., 2006. Bioethanol. Curr. Op. Chem. Biol. 10, 141-146.

Guillén, F., Gómez-Toribio, V., Martínez, M.J., Martínez, A.T., 2000a. Production of hydroxyl radical by the synergistic action of fungal laccase and aryl alcohol oxidase. Arch. Biochem. Biophys. 383, 142-147.

Guillén, F., Martínez, A.T., Martínez, M.J., 1992. Substrate specificity and properties of the aryl-alcohol oxidase from the ligninolytic fungus *Pleurotus eryngii*. Eur. J. Biochem. 209, 603-611.

Guillén, F., Martínez, A.T., Martínez, M.J., Evans, C.S., 1994. Hydrogen peroxide-producing system of *Pleurotus eryngii* involving the extracellular enzyme aryl-alcohol oxidase. Appl. Microbiol. Biotechnol. 41, 465-470.

Guillén, F., Muñoz, C., Gómez-Toribio, V., Martínez, A.T., Martínez, M.J., 2000b. Oxygen activation during the oxidation of methoxyhydroquinones by laccase from *Pleurotus eryngii*. Appl. Environ. Microbiol. 66, 170-175.

Gutiérrez, A., Caramelo, L., Prieto, A., Martínez, M.J., Martínez, A.T., 1994. Anisaldehyde production and aryl-alcohol oxidase and dehydrogenase activities in ligninolytic fungi from the genus *Pleurotus*. Appl. Environ. Microbiol. 60, 1783-1788.

Hahn-Hagerdal, B., Karhumaa, K., Fonseca, C., Spencer-Martins, I., Gorwa-Grauslund, M.F., 2007. Towards industrial pentose-fermenting yeast strains. Appl. Microbiol. Biotechnol. 74, 937-953.

Kabel, M.A., Bos, G., Zeevalkin, J., Voragen, A.G.J., Schols, H.A., 2007. Effect of pretreatment severity on xylan solubility and enzymatic breakdown of the remaining cellulose from wheat straw. Bioresour. Technol. 98, 2032-2034.

Karunanithy, C. Muthukumarappan, K., 2010. Effect of extruder parameters and moisture content of switchgrass, prairie cord grass on sugar recovery from enzymatic hydrolysis. Appl. Biochem. Biotechnol. 162, 1785-1803.

Kersten, P. Cullen, D., 2007. Extracellular oxidative systems of the lignin-degrading basidiomycete *Phanerochaete chrysosporium*. Fungal Genet. Biol. 44, 77-87.

Kirk, T.K. Farrell, R.L., 1987. Enzymatic "combustion": The microbial degradation of lignin. Annu. Rev. Microbiol. 41, 465-505.

Kuhar, S., Nair, L.M., Kuhad, R.C., 2008. Pretreatment of lignocellulosic material with fungi capable of higher lignin degradation and lower carbohydrate degradation improves substrate acid hydrolysis and the eventual conversion to ethanol. Can. J. Microbiol. 54, 305-313.

Kuwahara, M., Glenn, J.K., Morgan, M.A., Gold, M.H., 1984. Separation and characterization of two extracellular H_2O_2-dependent oxidases from ligninolytic cultures of *Phanerochaete chrysosporium*. FEBS Lett. 169, 247-250.

Leonowicz, A., Cho, N.S., Luterek, J., Wilkolazka, A., Wojtás-Wasilewska, M., Matuszewska, A., Hofrichter, M., Wesenberg, D. et al., 2001. Fungal laccase: properties and activity on lignin. J. Basic Microb. 41, 185-227.

Liers, C., Pecyna, M.J., Kellner, H., Worrich, A., Zorn, H., Steffen, K.T., Hofrichter, M., Ullrich, R., 2012. Substrate oxidation by dye-decolorizing peroxidases (DyPs) from wood- and litter-degrading agaricomycetes compared to other fungal and plant heme-peroxidases. Appl. Microbiol. Biotechnol. doi:10.1007/s00253-012-4521-2.

Lin, Y., Tanaka, S., 2006. Ethanol fermentation from biomass resources: current state and prospects. Appl. Microbiol. Biotechnol. 69, 627-642.

Martínez, A.T., Speranza, M., Ruiz-Dueñas, F.J., Ferreira, P., Camarero, S., Guillén, F., Martínez, M.J., Gutiérrez, A. et al., 2005. Biodegradation of lignocellulosics: Microbiological, chemical and enzymatic aspects of fungal attack to lignin. Intern. Microbiol. 8, 195-204.

Martínez, M.J., Ruiz-Dueñas, F.J., Guillén, F., Martínez, A.T., 1996. Purification and catalytic properties of two manganese-peroxidase isoenzymes from *Pleurotus eryngii*. Eur. J. Biochem. 237, 424-432.

Mitchell,A.D., Krieger,N., Berovic,M., 2006. Solid-state fermentation bioreactors: fundamental of design and operations. Springer-Verlag Berlin Heidelberg: Springer.

Mosier, N., Wyman, C., Dale, B., Elander, R., Lee, Y.Y., Holtzapple, M., Ladisch, M., 2005. Features of promising technologies for pretreatment of lignocellulosic biomass. Bioresour. Technol. 96, 673-686.

Nigam, P.S., Singh, A., 2011. Production of liquid biofuels from renewable resources. Prog. Energy Combust. Sci. 37, 52-68.

Odier, E., Janin, G., Monties, B., 1981. Poplar lignin decomposition by Gram-negative aerobic bacteria. Appl. Environ. Microbiol. 41, 337-341.

Paredes-López, O., Alpuche-Solís, A., 1991. Solid substrate fermentation, a biotechnological approach to bioconversion of wastes, in: Martin, A.M. (Ed.), Bioconversion of waste materials to industrial products. Elsevier Applied Science, London, pp. 117-145.

Petersen, M.O., Larsen, J., Thomsen, M.H., 2009. Optimization of hydrothermal pretreatment of wheat straw for production of bioethanol at low water consumption without addition of chemicals. Biomass & Bioenergy 33, 834-840.

Prasad, S., Singh, A., Joshi, H., 2007. Ethanol as an alternative fuel from agricultural, industrial and urban residues. Res. Conserv. Recycl. 50, 1-39.

Reid, I.D., 1989. Solid-state fermentations for biological delignification. Enzyme Microb. Technol. 11, 786-803.

Rodríguez, J., Ferraz, A., Nogueira, R.F.P., Ferrer, I., Esposito, E., Durán, N., 1997. Lignin biodegradation by the ascomycete *Chrysonilia sitophila*. Appl. Biochem. Biotechnol. 62, 233-242.

Rubin, E.M., 2008. Genomics of cellulosic biofuels. Nature 454, 841-845.

Sun, Y., Cheng, J.Y., 2002. Hydrolysis of lignocellulosic materials for ethanol production: a review. Bioresour. Technol. 83, 1-11.

Talebnia, F., Karakashev, D., Angelidaki, I., 2010. Production of bioethanol from wheat straw: An overview on pretreatment, hydrolysis and fermentation. Bioresour. Technol. 101, 4744-4753.

Taniguchi, M., Suzuki, H., Watanabe, D., Sakai, K., Hoshino, K., Tanaka, T., 2005. Evaluation of pretreatment with *Pleurotus ostreatus* for enzymatic hydrolysis of rice straw. J. Biosci. Bioeng. 100, 637-643.

Tien, M., Kirk, T.K., 1983. Lignin-degrading enzyme from the hymenomycete *Phanerochaete chrysosporium* Burds. Science 221, 661-663.

Tien, M., Kirk, T.K., 1988. Lignin peroxidase of *Phanerochaete chrysosporium*. Meth. Enzymol. 161, 238-248.

Valmaseda, M., Martínez, M.J., Martínez, A.T., 1991. Kinetics of wheat straw solid-state fermentation with *Trametes versicolor* and *Pleurotus ostreatus* - Lignin and polysaccharide alteration and production of related enzymatic activities. Appl. Microbiol. Biotechnol. 35, 817-823.

Wahlbom, F., Hanh-Hägerdal,B., Jönsson,L., 2008. *Saccharomyces cerevisiae* mutant. Patent [US10946654]. United States.

Wan, C., Li, Y., 2012. Fungal pretreatment of lignocellulosic biomass. Biotechnol. Advances. doi.10.1016/j.biotechadv.2012.03.003.

Wariishi, H., Valli, K., Gold, M.H., 1992. Manganese(II) oxidation by manganese peroxidase from the basidiomycete *Phanerochaete chrysosporium*. Kinetic mechanism and role of chelators. J. Biol. Chem. 267, 23688-23695.

Wariishi, H., Valli, K., Renganathan, V., Gold, M.H., 1989. Thiol-mediated oxidation of nonphenolic lignin model compounds by manganese peroxidase of *Phanerochaete chrysosporium*. J. Biol. Chem. 264, 14185-14191.

Xiong, W., Li, X., Xiang, J., Wu, Q., 2008. High-density fermentation of microalga *Chlorella protothecoides* in bioreactor for microbio-diesel production. Appl. Microbiol. Biotechnol. 78, 29-36.

Zhang, S.P., Yan, Y.J., Ren, Z.W., Li, T.C., 2007. Fuel ethanol production from lignocellulosic biomass. Progr. Chem. 19, 1129-1133.

Objetivos

Los **Objetivos** de la presente Tesis Doctoral fueron los siguientes:

i) Realizar un muestreo con hongos basidiomicetos para estudiar si el biopretratamiento fúngico puede ser una alternativa a los pretratamientos físico-químicos utilizados actualmente para producir etanol de segunda generación a partir de paja de trigo.

ii) Optimizar las condiciones de cultivo con el hongo seleccionado a partir del muestreo para mejorar la recuperación de azúcares potencialmente fermentables durante el biopretratamiento fúngico de la paja de trigo.

iii) Estudiar el sistema enzimático del organismo seleccionado y caracterizar las enzimas de mayor interés.

iv) Comprobar el papel de estas enzimas en el proceso de producción de etanol de segunda generación y en otras aplicaciones biotecnológicas.

Chapter 1

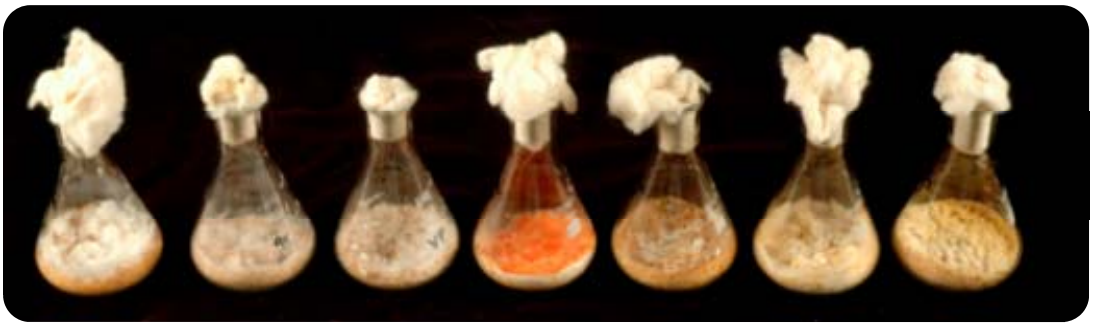

Fungal pretreatment: An alternative in second-generation ethanol from wheat straw.

Davinia Salvachúa, Alicia Prieto, María López-Abelairas, Thelmo Lu-Chau, Ángel T. Martínez, María Jesús Martínez

Bioresource Technology (2011) 102, 7500–7506.

ABSTRACT

The potential of a fungal pretreatment combined with a mild alkali treatment to replace or complement current physico-chemical methods for ethanol production from wheat straw has been investigated. Changes in substrate composition, secretion of ligninolytic enzymes, enzymatic hydrolysis efficiency and ethanol yield after 7, 14 and 21 days of solid-state fermentation were evaluated. Most fungi degraded lignin with variable selectivity degrees, although only eight of them improved sugar recovery compared to untreated samples. Glucose yield after 21 days of pretreatment with *Poria subvermispora* and *Irpex lacteus* reached 69% and 66% of cellulose available in the wheat straw, respectively, with an ethanol yield of 62% in both cases. Conversions from glucose to ethanol reached around 90%, showing that no inhibitors were generated during this pretreatment. No close correlations were found between ligninolytic enzymes production and sugar yields.

Keywords: Wheat straw, pretreatment, basidiomycetes, enzymatic hydrolysis, bioethanol.

1. INTRODUCTION

Lignocellulosic materials are the major component of biomass and represent the most abundant renewable energy resource available on earth (Lin and Tanaka, 2006). Among them, agricultural wastes are the most extended and the cheapest, especially wheat straw which is the most plentiful in Europe and the second one worldwide after rice straw (Kim and Dale, 2004). Moreover, wheat straw is a residue that does not compete with human food resources constituting an auspicious alternative to generate renewable biofuels.

Second-generation bioethanol production from wheat straw includes three main steps: (i) pretreatment, (ii) enzymatic hydrolysis of cellulose and hemicellulose, and (iii) ethanol fermentation (Talebnia et al., 2010). The aim of the pretreatment is the disruption of the lignocellulose structure, improving cellulose and hemicellulose accessibility. Nowadays, steam explosion, which requires high pressures and temperatures, is the most common and effective pretreatment for this purpose, although the severity of this process generates by-products that affect adversely subsequent steps (Alvira et al., 2010; Jurado et al., 2009). An alternative to avoid these problems is the use of biological pretreatments, which present additional advantages as being cheaper, safer, less energy consuming, and more environmentally friendly.

Biopretreatment is based on the capacity of some organisms of degrading lignin to gain access to cellulose and hemicellulose. Nevertheless, the literature shows a big controversial about this topic, since the largest lignin degradations not always correspond with the best sugar recoveries (Capelari and Tomás-Pejó, 1997; Shi et al., 2008). Biological degradation of lignocellulose is a complex process where many factors, as fungal strain, culture conditions, fungal enzymatic secretion, and oxidative mechanisms, are implicated (Guillén et al., 2000; Wan and Li, 2010). Therefore, analysis of the whole process is relevant to understand the mechanisms of fungal degradation and to get the best fungi and optimum growth conditions for obtaining the maximum amount of fermentable sugars.

The pretreatment of wheat straw by using basidiomycetes to produce ethanol has been barely studied. Moreover, the rates of this type of pretreatment are still far from industrial purposes besides of presenting disadvantages, as long storage times or extended cellulose and hemicellulose consumptions (Galbe and Zacchi, 2007). Nevertheless, it could be used alone or combined with other pretreatments to result more effective. Alkali pretreatments are well known to improve sugar recovery because they cause lignin solubilisation (Kumar et al., 2009; Talebnia et al.,

2010) but only a few investigations have complemented it with a biological pretreatment (Hatakka, 1983; Yu et al., 2010). In the present study, a fungal screening using 21 basidiomycetes has been carried out, combined with a very mild alkali washing, to select the best fungal strains to be included in the pretreatment step for second generation bioethanol production from wheat straw. The relationship among different variables, such as lignin degradation, cellulose and hemicellulose digestibility, and ethanol production was analysed, and the role of the ligninolytic enzymes in the process is discussed.

2. MATERIALS AND METHODS

2.1. Fungal strains and culture media

The strains of basidiomycetes used in the present study were obtained from different fungal collections: Centraalbureau voor Schimmelcultures (CBS; Baarn, The Netherlands), Instituto Jaime Ferrán de Microbiología (IJFM; Centro Investigaciones Biológicas, Madrid, Spain) and Colección Española de Cultivos Tipo (CECT; Burjassot, Valencia, Spain). Most of the fungi used in this study were white-rot fungi: *Bjerkandera anamorph* IJFM A757, *Bjerkandera adusta* CBS 595.78, *Coriolopsis rigida* CECT 20449, *Fomes fasciatus* IJFM A772, *Fomes fomentarius* IJFM A166, *Ganoderma austral* IJFM A130, *Irpex lacteus* IJFM A792, *Lentinus tigrinus* IJFM A790, *Panus tigrinus* (a synonym of *L. tigrinus*) IJFM A768, *Phanerochaete chrysosporium* CBS 481.73, *Phellinus robustus* IJFM A788, *Phlebia radiata* CBS 184.83, *Phlebiopsis gigantea* CBS 935.7, *Pleurotus eryngii* CBS 613.91, *Pleurotus ostreatus* CBS 411.71, *Polyporus alveolaris* IJFM A794, *Poria subvermispora* (a synonym of *Ceriporiopsis subvermispora*) IJFM A718, *Pycnoporus coccineus* IJFM A780, *Stereum hirsutum* IJFM A793, and *Trametes versicolor* IJFM A136. In addition one brown-rot fungus was used, *Postia placenta* IJFM A781. Strains were maintained on 2% malt extract agar (w/v) and preserved at 4 ºC.

Fungal strains were individually cultured at 28 ºC for 7 days on MEA plates. Four agar plugs of about 1 cm^2 were cut from actively growing mycelium and inoculated into 250 mL Erlenmeyer flasks with 30 mL of growth medium (pH 5.6) and incubated at 28 ºC, and 180 rpm for 7 days. The growth medium contained (L^{-1}): glucose, 40 g; $FeSO_4$ x $7H_2O$, 0.4 g; $(NH_4)_2SO_4$, 9 g; KH_2PO_4, 4 g; corn steep solids, 26.3 g; $CaCO_3$, 7 g; soybean oil, 2.8 mL. Each culture was aseptically homogenised (Omnimixer, Sorvall), and 2.5 mL were used to inoculate second generation cultures, which were incubated for 5 days as described above. These cultures will be used as inocula for solid state fermentation (SSF) experiments.

2.2. Pretreatment of wheat straw

2.2.1. Fungal screening

Wheat (*Triticum aestivum*) straw was harvested from Galicia fields (Spain) and chopped (<1 cm). Two grams of dry grinded wheat straw plus 6 mL of distilled water were autoclaved at 121 ºC for 15 min into 100 mL Erlenmeyer flasks capped with hydrophobic cotton. These flasks were inoculated with 5-day-old mycelia (2 mL) and incubated at 28 ºC. Triplicate flasks of each fungal culture were sampled after 7, 14 and 21 days. Samples were washed with distilled water (15 mL) at 28 ºC and 180 rpm for 1 h, and filtered under vacuum to remove most of the water-soluble components, which were stored at 4 ºC. The solid fractions from biopretreated wheat straw were dried in an aeration oven at 65 ºC and weighted. This value was used to calculate weight loss of the samples. Non-inoculated samples were incubated and treated under the same conditions, being used as control.

2.2.2. Mild alkali treatment

Solid fractions (300 mg, dry weight) were subjected to a mild alkali treatment with a final concentration of 0.1% sodium hydroxide (5% w/v), at 50 ºC and 165 rpm for 1 h. The alkali-treated material was filtered and washed, until neutrality, with distilled water at 50 ºC. Total reducing sugars were measured (Somogyi, 1945) in the filtrates, and the solid residue was dried at 60 ºC and weighted. The effect of the alkali treatment on subsequent enzymatic hydrolysis was investigated by comparison of different samples with and without alkali washing.

2.3. Enzymatic hydrolysis and sugar yield estimation

Solid residues or solid fractions, with or without alkali treatment respectively, were hydrolyzed in duplicate at 5% (w/v) by enzyme complexes (Novozymes Bagsvaerd, Denmark) as 15 FPU g^{-1} of cellulases (Celluclast and NS50010) and 30 U g^{-1} of xylanases (NS50013 and NS50030) in 100 mM sodium citrate buffer (pH 4.8) at 50 ºC, and 165 rpm for 60 hours. Tetracycline (200 μg mL^{-1}) was also added to avoid bacterial growth during enzymatic treatments. After hydrolysis, 0.5 mL of treated material were centrifuged at 5000 rpm for 5 minutes, and glucose and xylose content were measured in the supernatants. The ‘‘Glucose-TR’’ kit (Spinreact) was used to quantify glucose. Xylose content was calculated as the difference between total reducing sugars (Somogyi, 1945) and glucose. A set of samples was chosen to quantify glucose and xylose also by gas chromatography (GC) (Prieto et al., 2008), to compare both methodologies.

To probe enzymatic hydrolysis efficiency, cellulose (D_c) and hemicellulose (D_h) digestibilities were evaluated and expressed, according to Eq. (1), as the quotient between the percentage of glucose (G_r) and xylose (X_r) released from either the solid fraction or the solid residue from alkali washing and the theoretical maximum amount of glucose (G_s) and xylose (X_s) in the solid fraction, respectively.

Eq (1): $D_c \text{ or } D_h\ (\%) = (g\ G_r \text{ or } X_r\ /\ g\ G_s \text{ or } X_s) \times 100$

To calculate sugar yields, glucose (G_i) and xylose (X_i) per gram of dry wheat straw, glucose (G_f) and xylose (X_f) remaining in pretreated wheat straw, and cellulose (D_g) and hemicellulose (D_h) digestibilities were taken into account as shown in Eq. (2). Thus, this yield considers both, the sugar digestibility (D_c or D_h) and the percentage of sugar loss during the biological pretreatment (G_f/G_i or X_f/X_i).

Eq (2): $\text{Sugar yield } (\%) = [(G_f \times D_g) + (X_f \times D_h)] / (G_i + X_i)$

Glucose and xylose recovery yields were separately estimated applying Equations (3) and (4), respectively.

Eq (3): $\text{Glucose yield } (\%) = (G_f \times D_c) / G_i$

Eq (4): $\text{Xylose yield } (\%) = (X_f \times D_h) / X_i$

2.4. Fermentation to ethanol

To evaluate the potential inhibitory effect of fungal pretreatment and alkali washing on yeast growth, solid fractions or solid residues, hydrolysed with cellulases and xylanases as previously indicated, were subsequently fermented with *Saccharomyces cerevisiae* (Fermentis LPA 3035). The yeast (0.5 g L^{-1} inoculum) was grown at 32 ºC and 200 rpm for 24 h in 250 mL Erlenmeyer flasks containing 50 mL of a liquid medium. The medium was composed of (L^{-1}) glucose (20 g), yeast extract (3 g), peptone (5 g), and tetracycline (200 mg). Seven millilitres of hydrolysed wheat straw samples were inoculated with 350 µL of a yeast suspension (OD 625 nm = 2) in 10 mL glass tubes. Tubes were sealed with rubber plugs and incubated at 32 ºC and 200 rpm for 72 h. Then, tubes were centrifuged for 2 min at 7000 rpm and 5 mL of the supernatant were extracted with ethanol-free chloroform (0.5 mL) to determine the ethanol content in the organic phase by gas chromatography (GC). Methanol (1%) was added in the samples before chloroform extraction, as internal standard. GC analyses were performed on an Agilent 7890A instrument equipped with a flame ionisation detector (FID), using a HP5-MS capillary column (30 m x 0.25 mm, 0.25 µL film thickness) and helium (25 psi) as the carrier gas. Separation was carried out isothermically at 28 ºC, and injector and

detector were maintained at 100 ºC. Peaks were identified on the basis of sample coincidence with retention times of commercial standards, and quantified using peak areas and the corresponding response factors. All the experiments were carried out by triplicate. Finally, the ethanol conversion yield was calculated as shown in Eq. (5) taking into account the glucose recovery after enzymatic hydrolysis. The value 0.511 corresponds to the conversion factor from glucose to ethanol (Maiorella et al.,1981).

Eq (5): Glucose conversion (%) = [g L^{-1} ethanol produced in fermentation broth / (g L^{-1} initial glucose in fermentation broth x 0.511)] x 100

2.5. Substrate characterisation and analysis methods

Weight loss was calculated as the percentage of total solids lost after each biopretreatment. Klason lignin content and polysaccharide composition of untreated and biopretreated wheat straw were determined on hydrolysates according to standard Tappi methods (Tappi, 1974, 1975). Glucose and xylose were also measured as described in Section 2.3. The content of cellulose was calculated from glucose while hemicellulose was calculated from xylose, using an anhydro correction of 0.90 and 0.88 for both sugars, respectively. Total reducing sugars in the water-soluble extracts were determined using the Somogyi method (Somogyi, 1945).

2.6. Estimation of ligninolytic activities

Enzymatic activities were evaluated in water-soluble extracts of biopretreated wheat straw (Section 2.2.1). Laccase activity was assayed using 5 mM 2,6-dimethoxyphenol (DMP) in 100 mM sodium citrate buffer (pH 5.0; ε_{469} = 27,500 M^{-1} cm^{-1}, referred to DMP concentration). Mn^{2+}-oxidizing peroxidase was estimated by measuring the formation of Mn^{+3}-tartrate complex (ε_{238} = 6,500 M^{-1} cm^{-1}) during the oxidation of 0.1 mM $MnSO_4$ in 100 mM sodium tartrate buffer (pH 5.0) in the presence of 0.1 mM H_2O_2. Lignin peroxidase was assayed by veratraldehyde formation from 2 mM veratryl alcohol (3,4-dimethoxybenzyl alcohol) in 100 mM sodium tartrate buffer (pH 3), in the presence of 0.4 mM H_2O_2. International enzymatic units (µmoles per minute) were used.

3. RESULTS AND DISCUSSION

3.1. Fungal pretreatment of wheat straw

3.1.1. Cell wall components degradation

The objective of this study was to select fungal species, in a wide screening, to produce second generation bioethanol from biopretreated wheat straw. The selected strain should be the one giving the highest

amount of fermentable sugars from wheat straw in the shortest period of time. A screening of fungi was carried out to evaluate lignin and polysaccharides degradation from wheat straw after 7, 14 and 21 days of SSF. Most fungi colonised the substrate appropriately, except *F. fasciatus* which presented a poor evolution.

Polysaccharide content was first estimated from GC analysis. Untreated wheat straw used as control (0 and 21 days of incubation), was composed of 36.9% cellulose and 23% hemicellulose (18% xylan, 3.4% arabinan, 1.1% mannan, and 0.5% galactan). Cellulose and hemicellulose content were also evaluated by colorimetric methods. Glucose, assayed by the ‘‘Glucose-TR’’ kit (Spinreact), and xylose, determined by difference between total sugars and glucose, gave values not significantly different to those detected by GC. In the case of xylose this result could be explained because it is the major hemicellulose component in wheat straw (as shown by GC). In addition, this lignocellulosic material contained 24% lignin (22.8% acid-insoluble lignin and 1.2% acid-soluble lignin).

Weight loss of the cultures gives an estimation of the extent of substrate degradation. The greatest weight losses, after 21 days of SSF, were caused by *B. adusta*, *F. fomentarius* and *P. coccineus* (up to 35%), and the lowest by *P. eryngii*, *P. gigantea* and *P. placenta* (down to 6%). Composition of wheat straw after fungal treatment was analysed (Table 1) and different degradation patterns were appreciated among the studied basidiomycetes. Some fungi, as *P. chrysosporium* and *P. gigantea*, as well as the brown-rot *P. placenta*, were not able to degrade lignin under the assayed culture conditions, showing a polysaccharidic preferential degradation. Other fungi, as *P. tigrinus* and *P. radiata*, degraded lignin and sugars simultaneously. Finally, basidiomycetes as *P. eryngii* and *P. robustus* were able to remove lignin selectively and faster than the carbohydrate components in wheat straw.

On the other hand, sugar degradation can be balanced or preferential from cellulose or hemicellulose. *B. adusta* degraded both polymers equitably (54% and 43% respectively). *S. hirsutum* only altered cellulose (43%) and *P. coccineus* degraded almost all hemicellulose (98%) but less cellulose (31%). These data give information about the amount of glucose and xylose (from cellulose and hemicellulose, respectively) available for alcohol fermentation, since largest degradations should imply a performance decrease.

3.1.2. Water-soluble fraction analysis

To evaluate the total sugar recovery, water-soluble sugars from the hydrosoluble fraction were also analysed, since they could also be

potentially fermented. The greatest recovery reached only 6% after 21 days of pretreatment with *P. radiata*. Significantly less water-soluble sugars were quantified at 7 or 14 days with this fungus, and even at 21 days with the remaining fungi screened (data not shown). These results are in agreement with previous studies which showed that the two first weeks of incubation correspond to an early delignification stage with low water-soluble sugars content because fungi consume monosaccharides and disaccharides to grow (Valmaseda et al., 1991). Because of its low amount of sugars, the water-soluble fraction was not enzymatically hydrolysed for further ethanol production by yeasts. Consequently, this fraction was not taken into account in the final process yield.

Table 1. Degradation of wheat straw components (% of the initial content) produced by 21 basidiomycetes after incubation periods of 7, 14, and 21 days. Data are means of triplicates (±SD). CEL, cellulose; HEM, hemicellulose; LIG, lignin. *Bjerkandera**= *Bjerkandera* anamorph.

Fungi	Loss (%)								
	7 d			14 d			21 d		
	CEL	HEM	LIG	CEL	HEM	LIG	CEL	HEM	LIG
***Bjerkandera* ***	14 ± 0	7 ± 1	4 ± 3	16 ± 0	14 ± 3	1 ± 0	21 ± 1	12 ± 1	6 ± 0
B. adusta	27 ± 0	0 ± 0	9 ± 0	42 ± 2	16 ± 2	28 ± 1	54 ± 6	43 ± 5	37 ± 0
C. rigida	18 ± 0	28 ± 6	15 ± 0	22 ± 1	52 ± 10	24 ± 1	36 ± 2	42 ± 12	34 ± 1
F. fasciatus	0 ± 0	0 ± 1	0 ± 0	0 ± 0	0 ± 3	0 ± 0	0 ± 0	0 ± 1	0 ± 0
F. fomentarius	17 ± 1	2 ± 0	0 ± 0	30 ± 1	28 ± 4	17 ± 0	45 ± 1	51 ± 27	35 ± 1
G. australe	4 ± 0	13 ± 0	0 ± 0	4 ± 0	16 ± 1	9 ± 0	15 ± 0	23 ± 3	25 ± 1
I. lacteus	9 ± 0	13 ± 7	11 ± 0	17 ± 1	13 ± 4	27 ± 1	17 ± 0	26 ± 7	34 ± 2
L. tigrinus	24 ± 1	46 ± 10	0 ± 0	28 ± 1	68 ± 12	15 ± 1	40 ± 1	58 ± 9	23 ± 1
P. tigrinus	12 ± 0	24 ± 7	17 ± 1	20 ± 1	41 ± 7	32 ± 1	24 ± 1	60 ± 26	47 ± 4
P. chrysosporium	23 ± 0	36 ± 8	0 ± 0	31 ± 2	22 ± 2	0 ± 0	35 ± 0	70 ± 24	0 ± 0
P. robustus	4 ± 0	0 ± 1	0 ± 0	6 ± 0	0 ± 0	21 ± 1	8 ± 1	3 ± 0	25 ± 2
P. radiata	13 ± 1	36 ± 11	8 ± 0	20 ± 2	40 ± 10	29 ± 1	24 ± 3	41 ± 5	40 ± 2
P. gigantea	8 ± 0	0 ± 0	0 ± 0	9 ± 1	0 ± 0	0 ± 0	7 ± 0	9 ± 1	0 ± 0
P. eryngii	0 ± 0	0 ± 0	2 ± 0	0 ± 0	4 ± 0	14 ± 0	0 ± 0	8 ± 1	17 ± 1
P. ostreatus	10 ± 1	14 ± 1	2 ± 0	14 ± 1	38 ± 9	18 ± 0	22 ± 1	52 ± 13	27 ± 1
P. alveolaris	14 ± 1	8 ± 1	18 ± 1	18 ± 0	28 ± 9	34 ± 1	28 ± 2	42 ± 8	43 ± 2
P. subvermispora	1 ± 0	33 ± 10	8 ± 0	4 ± 0	35 ± 6	25 ± 1	13 ± 0	36 ± 6	30 ± 1
P. placenta	3 ± 0	11 ± 2	0 ± 0	0 ± 0	15 ± 3	0 ±0	2 ± 0	9 ± 3	1 ± 0
P. coccineus	12 ± 0	74 ± 43	11 ± 0	26 ± 2	77 ± 20	26 ± 1	31 ± 1	98 ± 1	36 ± 1
S. hirsutum	24 ± 0	0 ± 1	15 ± 1	37 ± 4	1 ± 0	30 ± 1	43 ± 2	2 ± 0	37 ± 2
T. versicolor	12 ± 0	5 ± 1	24 ± 1	18 ± 1	23 ± 3	33 ± 0	23 ± 1	21 ± 6	46 ± 1

3.2. Enzymatic hydrolysis

3.2.1. Digestibility

Digestibility represents the yield of conversion of the raw material into fermentable sugars. To increase this value in biopretreated wheat straw, samples are subjected to a very mild alkali treatment before enzymatic hydrolysis with cellulases and xylanases (Kumar et al., 2009; Yu et al., 2010, 2009). Preliminary studies in our laboratory showed that alkali

treatment with only 0.1% NaOH at 50 ºC during 1 h does not affect xylose recovery, probably because hemicellulose does not form packed crystalline structures like cellulose, becoming a substrate more accessible to fungi and enzymatic hydrolysis (Xu et al., 2009). However, this step is crucial to improve glucose release from cellulose, since digestibility at 21 days increased more than twice in several biopretreated samples (data not shown). Recently the use of a combined biological and mild chemical pretreatment of cornstalks has been reported (Yu et al., 2010). They obtained values of glucan digestibility comparable to those found in the present study, using similar temperatures and incubation times but with a NaOH concentration tenfold higher. There are several advantages of using low amounts of alkali for the chemical treatment. First of all, the effect of the biological pretreatment can be clearly observed, since it is not masked as a result of more aggressive alkali pretreatments. In addition, the process is cheaper and the generation of inhibitors for downstream steps of the process is diminished or even avoided.

Cellulose and hemicellulose conversion to fermentable sugars from biopretreated wheat straw is depicted in Fig. 1. No differences were found between controls analysed at the beginning (0 days) and at the end of the incubation time (21 days). In both cases, the conversion of cell wall polysaccharides to glucose and xylose was around 36% and 35%, respectively. Only eight of the fungal strains studied increased digestibilities at 14 and 21 days of biopretreatment with respect to the controls, and only one of them, *P. tigrinus*, was able to improve them after 7 days of SSF. The greatest values for glucose and xylose recovery were 82% and 78% in samples pretreated for 21 days with *I. lacteus* and *P. tigrinus*, respectively. Our results show higher increases in wheat straw digestibility in shorter incubation times than those reported in previous studies (Capelari and Tomás-Pejó, 1997; Dias et al., 2010; Valmaseda et al., 1991).

Lignin polymers are the main obstacle to the efficient utilization of lignocellulosic materials. Consequently, a preferential delignification would improve the process performance because it would facilitate the access of hydrolytic enzymes to polysaccharides (Camarero et al., 1994; Kuhar et al., 2008; Valmaseda et al., 1991) maintaining at the same time a good level of fermentable sugars, which would be only slightly consumed for fungal growth. With the aim to correlate both variables, lignin degradation and digestibility were compared. The two fungi that generated the highest lignin degradation, *T. versicolor* (46%) and *P. tigrinus* (47%), gave pretreated wheat straw with significant differences in cellulose and hemicelluloses digestibilities. After treatment with *T. versicolor*, cellulose digestibility was 25% less than after pretreating with *P. tigrinus*.

Otherwise, hemicellulose digestibility was not improved by *T. versicolor* treatment as compared with untreated wheat straw while, after growing of *P. tigrinus*, a 78% of conversion was reached. In contrast, fungi such as *P. eryngii* and *P. robustus*, which did not produce high lignin losses, were able to raise cellulose and hemicellulose digestibility of the substrate. According to these data, although lignin attack is essential to the efficiency of the enzymatic hydrolysis of cell wall polysaccharides, the highest lignin degradation is not always positively correlated with the highest levels of cellulose and hemicellulose digestibility. These results agree with previous reports (Capelari and Tomás-Pejó, 1997; Müller and Trösch, 1986), which remark that the level of delignification cannot be considered as the only parameter to assess if a microorganism is a valid candidate for biological pretreatment.

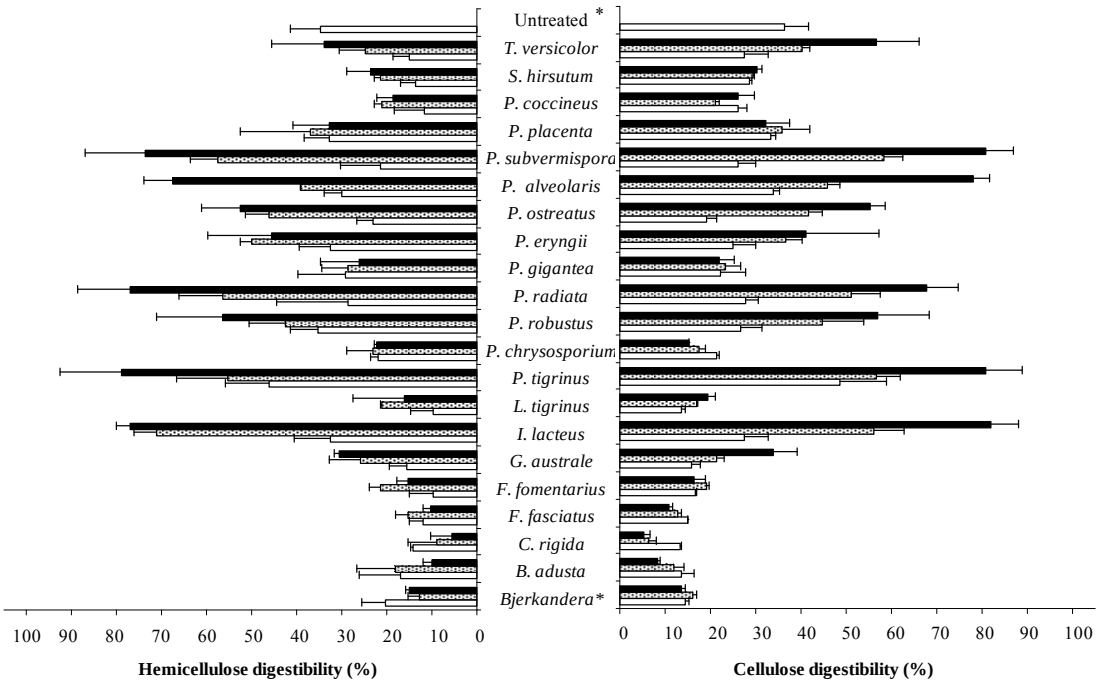

Fig. 1. Cellulose and hemicellulose digestibility (%) from pretreated wheat straw. White, dotted and black bars correspond to 7, 14, and 21 day cultures respectively. Control corresponds to non-inoculated wheat straw. Data are means of triplicates. *Bjerkandera** = *Bjerkandera* anamorph.

3.2.2. Fermentable sugar yields

Digestibility values and carbohydrate losses during biopretreatment were essential to quantify the amount of potentially fermentable sugars. Sugars were not found in the liquid fraction after alkali washing what indicates that only lignin was removed in this step.

The treatments which improved the recovery of fermentable sugars, compared to untreated wheat straw, are presented in Fig. 2. Glucose yields

increased in most cases after 21 days of fungal treatment, especially with *P. subvermispora* (69%) and *I. lacteus* (66%). In addition, only these two fungi led to a significant increase in glucose yield in samples pretreated for 14 days. During the first 2 weeks of incubation, fungi consume a huge amount of glucose and energy for their own growth. After this time, they continue on wheat straw degradation consuming less sugars, which increases the final sugar recovery (Valmaseda et al., 1991). In the present work we have obtained the highest yields reported so far from wheat straw combining a 21 days-biological pretreatment with a very mild chemical reagent. Recent studies described similar glucose recoveries by using corn stover treated with *C. subvermispora* during 35 days (Wan and Li, 2010) and rice straw treated with *P. chrysosporium* for 15 days (Bak et al., 2009) although in this case the raw material was autoclaved twice, before and after biopretreatment.

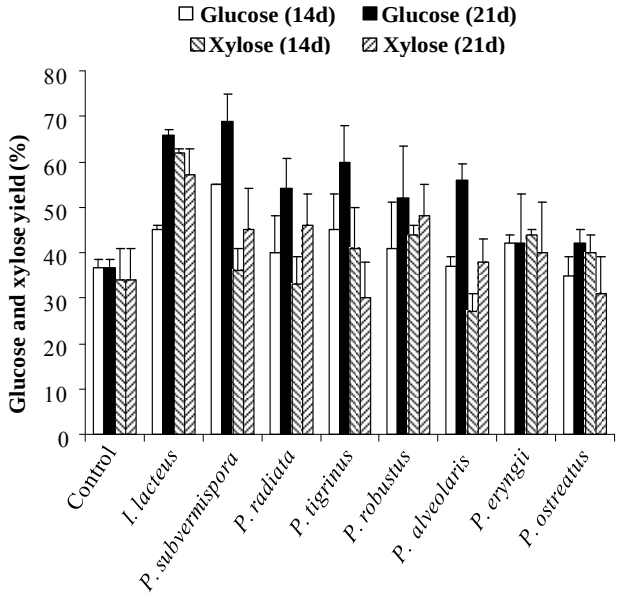

Fig. 2. Glucose and xylose yield (%) from 14 and 21 days pretreated wheat straw. Fungi are listed in order of the best sugar yields (left to right). Control corresponds to non-inoculated wheat straw. Data are means of triplicates.

Concerning xylose yields, the differences between untreated and pretreated samples were not very significant, excluding *I. lacteus* pretreatment which reached 62% and 47% at 14 and 21 days, respectively. This finding set out that, among the studied basidiomycetes, this fungus would be the best candidate to recover xylose from biological pretreatment. At the present time, xylose cannot be fermented at industrial scale; however it is important to know the extent of hemicellulose conversion to xylose to be taken into account to improve process yields in the future.

Considering the total sugar yield (data not shown), the best results were obtained after 21 days of incubation with *I. lacteus* (62%) and *P.*

subvermispora (61%). On the contrary, treatment with *P. ostreatus* did not increase significantly this yield and was not included in further ethanol fermentation experiments.

3.2.3. Relationship between fungal enzymes and sugar yield

Differences in wheat straw degradation have been related to variations in the pattern and levels of ligninolytic enzymes (Camarero et al., 1996; Manubens et al., 2007; Pedersen and Meyer, 2009). Consequently, those enzymes could be used as markers of the process yield. In this study, Mn^{2+}-oxidising peroxidases, laccase and LiP activities, as models of enzymes closely related to lignin degradation, were analysed in the water-soluble extracts from the 21 fungal strains during the 3 weeks of incubation (Fig. 3).

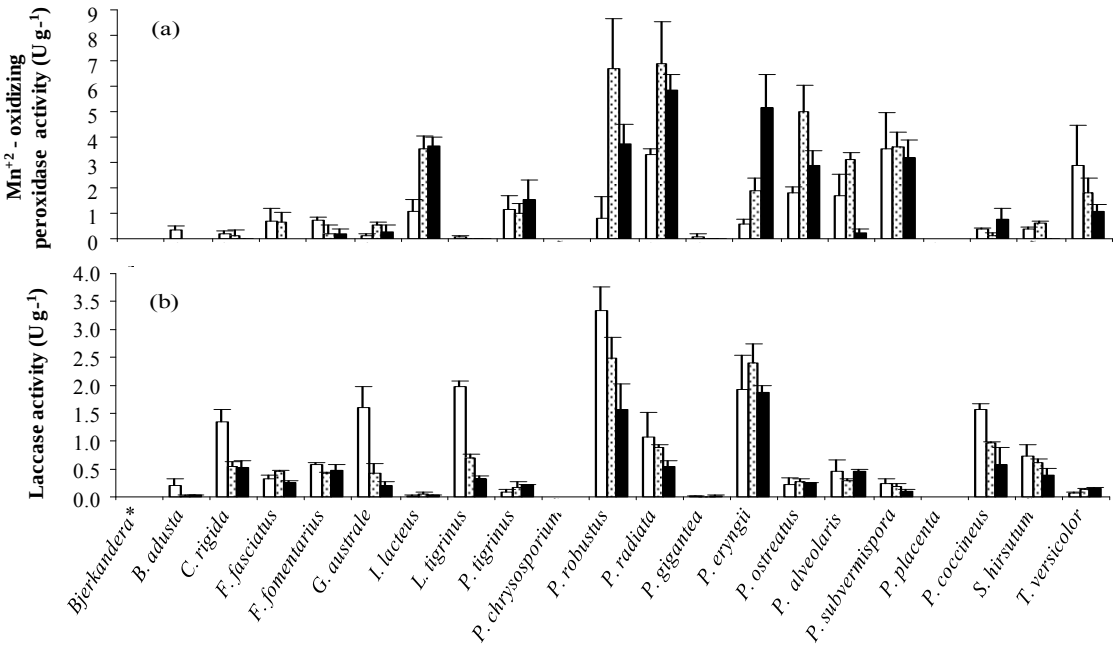

Fig. 3. Ligninolytic enzymes secreted by fungi during wheat straw biopretreatment: (a) Mn^{2+}-oxidising peroxidase and (b) laccase. White, dotted and black bars correspond to 7, 14, and 21 day cultures, respectively. Data are means of triplicates. *Bjerkandera* = Bjerkandera anamorph*.

LiP was not detected in any case. The largest Mn^{2+}-oxidising peroxidase activities (per gram of dry wheat straw) were detected in the seven cultures that gave an improved sugar recovery, with the maximum values in 14-days cultures of *P. radiata* (6.9 U g^{-1}) and *P. robustus* (6.7 U g^{-1}). In any case, these high activities were not correlated with the best sugar recoveries. On the other hand, the highest laccase activities were found in *P. robustus* (3.3 U g^{-1}) and P. *eryngii* (2.4 U g^{-1}) at 7 and 14 days, respectively. Both fungi displayed a preferential degradation of lignin,

which could be related to the high laccase secretion detected in these fungi. Fungi as *I. lacteus* and P. *subvermispora*, which showed low laccase activity (<0.25 U g^{-1}) and not very high Mn^{2+}-oxidising peroxidase activity (<3.6 U g^{-1}), gave the best sugar yields after wheat straw biopretreatment. These species showed a simultaneous degradation of all lignocellulosic components. Alternatively, other fungi which produced high lignin degradation presented very low ligninolytic activities (as *B. adusta* and *C. rigida*).

These results corroborate again that it is not easy to find a direct correlation among enzyme production, lignin degradation, and sugar yield in biopretreated wheat straw. As previously stated, lignin degradation is an oxidative and rather nonspecific process where extracellular ligninolytic enzymes participate, but also low molecular- weight extracellular oxidant compounds (e.g. Mn^{3+} and oxygen free radicals), which can be generated during the process, having a very important role (Guillén et al., 2000; Hammel et al., 2002).

3.3. Ethanol production

Evaluation of ethanol production is necessary to quantify the process final performance. At industrial level, only glucose is being fermented with high ethanol production yields while xylose fermentation, which is also essential for the economical success of lignocellulosic ethanol, continues being investigated to raise the low yields obtained so far (Gírio et al., 2010; Lee, 1997).

Glucose fermentations by *S. cerevisiae* were carried out on the seven enzymatic hydrolysates which gave significantly improved sugar recoveries as compared to control samples. Most conversion yields from available glucose to ethanol were superior to 90% except those coming from pretreatments with *P. tigrinus*, *P. eryngii* and *P. robustus*, which showed conversions of 84%, 81% and 79%, respectively. These results indicate that the fungal plus alkali washing pretreatment of wheat straw does not generate significant inhibitors of yeast growth. Based on the dry weight of wheat straw (1 g), the glucose availability (0.41 g per gram of dry wheat straw) and the stoichiometry of the reaction (1 glucose→2 ethanol + 2 CO_2), and estimating that 5% of glucose is used for yeast metabolism, the theoretical maximum ethanol production is approximately 0.2 g per gram of dry wheat straw (Eq. (5)). In this study, after checking total glucose consumption for yeast growth, the largest ethanol production found, which corresponds to the highest process yield, was around 62% of the theoretical maximum in samples pretreated with *I. lacteus* and *P. subvermispora* for 21 days (Table 2). These results were slightly higher than those reported for 35 day-pretreated corn stover with *P. subvermispora* (Wan and Li, 2010)

and similar to those obtained from rice straw, autoclaved twice and pretreated for 15 days with *P. chrysosporium* (62.7%) (Bak et al., 2009). In contrast, much lower ethanol production has been obtained from 14 days pretreated cotton stalks with *P. chrysosporium* (13%) (Shi et al., 2009).

The complete process from wheat straw to ethanol with the fungi which improved sugar recoveries, as compared to biologically untreated wheat straw is summarised in Table 2. It has been previously stated that to increase the final sugar yields it would be desirable to have a low consumption of sugars during biopretreatment. However, it can be highlighted that this is not the most important variable. It can be observed that although *P. eryngii* and *P. robustus* (fungi which degraded selectively the lignin) consumed less glucose for their growth than the other fungi, enzymatic hydrolysis after biopretreatments released the lowest amounts of glucose. On the other hand *P. alveolaris*, which consumed the highest amount of glucose from wheat straw, gave a glucose recovery after enzymatic hydrolysis slightly higher than those found in the above mentioned species. Finally, *I. lacteus* and *P. subvermispora*, showed intermediate levels of glucose consumption but gave the best glucose recoveries after enzymatic hydrolysis and also the best yields of ethanol production.

Then, they can be considered as the best species to be potentially used for wheat straw biopretreatment. Since conversions from glucose to ethanol were high in all cases, it can be guessed that the main differences in the whole process should arise from biopretreatment. Lignocellulose degradation mechanisms are very difficult to predict because of their complexity and variety, and influence the subsequent enzymatic hydrolysis step. Then, a complete study of the process is required for each fungal treatment, in order to analyse the efficiency of the biological pretreatment on ethanol production.

Chen et al. (2007) reported on a chemical pretreatment of wheat straw using acid and alkaline reagents, which allowed the recovery of more glucose (>10%) but with an ethanol production only 3% higher than the maximum reached in this study. Probably this is because, as stated above, biopretreatment does not generate toxic by-products affecting yeast growth, while steam explosion does (Alvira et al., 2010). Our results are still far from the high yields obtained using combined steam explosion and alkaline peroxide pretreatments (Chen et al., 2008), but suggest that the biological pretreatment with *I. lacteus* or *P. subvermispora*, complemented with a very mild alkali washing, could be an alternative to replace certain current chemical pretreatments without generating inhibitors of the fermentation step.

Table 2. Monitoring of glucose content (GLC) and ethanol production per gram of dry wheat straw (g WS). Wheat straw samples were biopretreated (B) during 21 days. A mild alkali washing (AW) was done after biopretreatment. Data are means of triplicates (±SD). EH = enzymatic hydrolysis.

Process step / Treatment	Initial WS	Pretreatment (B+AW)	EH	GLC fermentation	Process yield
	GLC (mg/g WS)	GLC (mg/g WS)	GLC (mg/g WS)	Ethanol (mg/g WS)	(%)
Theoretical maximum	410	410	410	199	100
Control[a]	410 ± 9	410 ± 9	133 ± 7	68 ± 2	35
I. lacteus	410 ± 9	340 ± 2	254 ± 8	123 ± 5	62
P. subvermispora	410 ± 9	357 ± 1	260 ± 14	122 ± 8	62
P. radiata	410 ± 9	311 ± 13	202 ± 13	97 ± 9	49
P. tigrinus	410 ± 9	311 ± 3	227 ± 18	97 ± 4	49
P. alveolaris	410 ± 9	295 ± 10	207 ± 7	94 ± 8	47
P. robustus	410 ± 9	377 ± 5	193 ± 21	78 ± 0	39
P. eryngii	410 ± 9	410 ± 0	151 ± 22	62 ± 9	31

[a] Control is a biologically untreated sample, only subjected to alkali washing.

4. CONCLUSIONS

Our data showed that very few fungi are suitable to increase sugar recoveries from wheat straw. The combination of a biological pretreatment by *I. lacteus* or *P. subvermispora* with a mild alkali pretreatment did not produce inhibitors for downstream processes, improving significantly ethanol production. These results turn both methods into possible and environmentally friendly alternatives in the production of second-generation ethanol. At the present time, pretreatments of wheat straw with the selected fungi are being carried out to scale up the process and check its viability at industrial level.

ACKNOWLEDGEMENTS

This work was supported mainly by the CENIT I+DEA project (funded by CDTI, Spain) and carried out in collaboration with Abengoa Bionergía Nuevas Tecnologías. Authors thank also the Galician government (I. Barreto program), DEMO-2 and Lignodeco EU projects for additional supports, and Novozymes for providing commercial enzymes. D.S. thanks a FPU fellowship from the MICINN.

REFERENCES

Alvira, P., Tomás-Pejó, E., Ballesteros, M., Negro, M.J., 2010. Pretreatment technologies for an efficient bioethanol production process based on enzymatic hydrolysis: a review. Bioresour. Technol. 101, 4851–4861.

Bak, J.S., Ko, J.K., Choi, I.G., Park, Y.C., Seo, J.H., Kim, K.H., 2009. Fungal pretreatment of lignocellulose by *Phanerochaete chrysosporium* to produce ethanol from rice straw. Biotechnol. Bioeng. 104, 471–482.

Camarero, S., Galletti, G.C., Martínez, A.T., 1994. Preferential degradation of phenolic lignin units by two white rot fungi. Appl. Environ. Microbiol. 60, 4509–4516.

Camarero, S., Bockle, B., Martínez, M.J., Martínez, A.T., 1996. Manganese-mediated lignin degradation by *Pleurotus pulmonarius*. Appl. Environ. Microbiol. 62, 1070–1072.

Capelari, M., Tomás-Pejó, E., 1997. Lignin degradation and in vitro digestibility of wheat straw treated with Brazilian Tropical species of white-rot fungi. Folia Microbiol. 42, 481–487.

Chen, Y., Sharma-Shivappa, R., Keshwani, D., Chen, C., 2007. Potential of agricultural residues and hay for bioethanol production. Appl. Biochem. Biotechnol. 142, 276–290.

Chen, H., Han, Y., Xu, J., 2008. Simultaneous saccharification and fermentation of steam exploded wheat straw pretreated with alkaline peroxide. Process Biochem. 43, 1462–1466.

Dias, A.A., Freitas, G.S., Marques, G.S.M., Sampaio, A., Fraga, I.S., Rodrigues, M.A.M., Evtuguin, D.V., Bezerra, R.M.F., 2010. Enzymatic saccharification of biologically pre-treated wheat straw with white-rot fungi. Bioresour. Technol. 101, 6045– 6050.

Galbe, M., Zacchi, G., 2007. Pretreatment of lignocellulosic materials for efficient bioethanol production. Adv. Biochem. Eng./Biotechnol. 108, 41–65.

Gírio, F.M., Fonseca, C., Carvalheiro, F., Duarte, L.C., Marques, S., Bogel-Lukasik, R., 2010. Hemicelluloses for fuel ethanol: a review. Bioresour. Technol. 101, 4775–4800.

Guillén, F., Muñoz, C., Gomez-Toribio, V., Martínez, A.T., Martínez, M.J., 2000. Oxygen activation during oxidation of methoxyhydroquinones by laccase from *Pleurotus eryngii*. Appl. Environ. Microbiol. 66, 170–175.

Hammel, K.E., Kapich, A.N., Jensen Jr., K.A., Ryan, Z.C., 2002. Reactive oxygen species as agents of wood decay by fungi. Enzyme Microb. Technol. 30, 445–453.

Hatakka, A.I., 1983. Pretreatment of wheat straw by white-rot fungi for enzymic saccharification of cellulose. Appl. Microbiol. Biotechnol. 18, 350–357.

Jurado, M., Prieto, A., Martínez-Alcalá, A., Martínez, A.T., Martínez, M.J., 2009. Laccase detoxification of steam-exploded wheat straw for second generation bioethanol. Bioresour. Technol. 100, 6378–6384.

Kim, S., Dale, B.E., 2004. Global potential bioethanol production from wasted crops and crop residues. Biomass Bioenerg. 26, 361–375.

Kuhar, S., Nair, L.M., Kuhad, R.C., 2008. Pretreatment of lignocellulosic material with fungi capable of higher lignin degradation and lower carbohydrate degradation

improves substrate acid hydrolysis and the eventual conversion to ethanol. Can. J. Microbiol. 54, 305–313.

Kumar, P., Barrett, D., Delwiche, M., Stroeve, P., 2009. Methods for pretreatment of lignocellulosic biomass for efficient hydrolysis and biofuel production. Ind. Eng. Chem. Res. 48, 3713–3729.

Lee, J., 1997. Biological conversion of lignocellulosic biomass to ethanol. J. Biotechnol. 56, 1–24.

Lin, Y., Tanaka, S., 2006. Ethanol fermentation from biomass resources: current state and prospects. Appl. Microbiol. Biotechnol. 69, 627–642.

Maiorella, B., Wilke, Ch.R., Blanch, H.W., 1981. Alcohol production and recovery. Adv. Biochem. Eng. Biotechnol. 20, 43–92.

Manubens, A., Canessa, P., Folch, C., Avila, M., Salas, L., Vicuña, R., 2007. Manganese affects the production of laccase in the basidiomycete *Ceriporiopsis subvermispora*. FEMS Microbiol. Lett. 275, 139–145.

Müller, H.W., Trösch, W., 1986. Screening of white-rot fungi for biological pretreatment of wheat straw for biogas production. Appl. Microbiol. Biotechnol. 24, 180–185.

Pedersen, M., Meyer, A.S., 2009. Influence of substrate particle size and wet oxidation on physical surface structures and enzymatic hydrolysis of wheat straw. Biotechnol. Prog. 25, 399–408.

Prieto, A., Leal, J.A., Bernabé, M., Hawksworth, D.L., 2008. A polysaccharide from *Lichina pygmaea* and *L. confinis* supports the recognition of Lichinomycetes. Mycol. Res. 112, 381–388.

Shi, J., Chinn, M.S., Sharma-Shivappa, R.R., 2008. Microbial pretreatment of cotton stalks by solid state cultivation of *Phanerochaete chrysosporium*. Bioresour. Technol. 99, 6556–6564.

Shi, J., Sharma-Shivappa, R.R., Chinn, M., Howell, N., 2009. Effect of microbial pretreatment on enzymatic hydrolysis and fermentation of cotton stalks for ethanol production. Biomass Bioenerg. 33, 88–96.

Somogyi, M., 1945. A new reagent for the determination of sugars. J. Biol. Chem. 160, 61–73.

Talebnia, F., Karakashev, D., Angelidaki, I., 2010. Production of bioethanol from wheat straw: an overview on pretreatment, hydrolysis and fermentation. Bioresour. Technol. 101, 4744–4753.

Tappi, 1974. Acid-insoluble lignin in wood and pulp. Tappi Rule. T 222-os, -74.

Tappi, 1975. Carbohydrate composition of extractive-free wood and wood pulp by gas–liquid chromatography. Tappi Rule. T 249-pm, -75.

Valmaseda, M., Martínez, M.J., Martínez, A.T., 1991. Kinetics of wheat straw solid state fermentation with *Trametes versicolor* and *Pleurotus ostreatus*: lignin and

polysaccharide alteration and production of related enzymatic activities. Appl. Microbiol. Biotechnol. 35, 817–823.

Wan, C., Li, Y., 2010. Microbial pretreatment of corn stover with *Ceriporiopsis subvermispora* for enzymatic hydrolysis and ethanol production. Bioresour. Technol. 101, 6398–6403.

Xu, C., Ma, F., Zhang, X., 2009. Lignocellulose degradation and enzyme production by *Irpex lacteus* CD2 during solid-state fermentation of corn stover. J. Biosci. Bioeng. 108, 372–375.

Yu, J., Zhang, J., He, J., Liu, Z., Yu, Z., 2009. Combinations of mild physical or chemical pretreatment with biological pretreatment for enzymatic hydrolysis of rice hull. Bioresour. Technol. 100, 903–908.

Yu, H., Du, W., Zhang, J., Ma, F., Zhang, X., Zhong, W., 2010. Fungal treatment of cornstalks enhances the delignification and xylan loss during mild alkaline pretreatment and enzymatic digestibility of glucan. Bioresour. Technol. 101, 6728–6734.

Chapter 2

Sugar recoveries from wheat straw following treatments with the fungus *Irpex lacteus*

Davinia Salvachúa, Alicia Prieto, María Eugenia Vaquero, Ángel T. Martínez, María Jesús Martínez

Bioresource Technology (2013) 131, 218–225.

ABSTRACT

Irpex lacteus is a white-rot fungus capable of increasing sugar recovery from wheat straw; however, in order to incorporate biopretreatment in bioethanol production, some process specifications need to be optimized. With this objective, *I. lacteus* was grown on different liquid culture media for use as inoculums. Additionally, the effect of wheat straw particle size, moisture content, organic and inorganic supplementations, and mild alkali washing during solid-state fermentation (SSF) on sugar yield were investigated. Wheat thin stillage was the best medium for producing inoculums. Supplementation of wheat straw with 0.3 mM Mn(II) during SSF resulted in glucose yields of 68% as compared to yields of 62% and 33% for cultures grown without supplementation or on untreated raw material, respectively after 21 days. Lignin loss, wheat straw digestibility, peroxidase activity, and fungal biomass were also correlated with sugar yields in the search for biopretreatment efficiency indicators.

Keywords:

Lignocellulose, wheat thin stillage, optimization, ergosterol, bioethanol

Abbreviations:

LiP, lignin peroxidase; MnP, manganese peroxidase; SSF, solid-state fermentation

1. INTRODUCTION

Wheat straw, the most abundant agricultural residue in Europe and the second worldwide, presents great potential for ethanol production (Talebnia et al., 2010); however, due to the complexity of its structure, especially the lignin framework, it is a challenge to obtain high sugar release from this substrate.

Steam explosion, one of the most used physico-chemical pretreatment methods to disrupt the lignocellulosic biomass, produces undesirable compounds such as weak acids, furan derivatives, and phenolic and inorganic substances which negatively affect the fermentation step (Hahn-Hägerdal et al., 2006). Biological pretreatments could be an alternative, since some organisms, like white-rot fungi, are able to degrade lignocellulose selectively and produce fewer yeast inhibitors than steam explosion (Salvachúa et al., 2011). One disadvantage of these treatments is the long incubation time necessary to reach yields similar to those obtained with current physico-chemical pretreatments. For this reason, combinations of biopretreatment with mild physical (Yamagishietal.,2011), alkali (Salvachúaetal.,2011; Sarithaetal.,2012; Zhongetal.,2011), organosolv (Canam et al., 2011), or hot water (Wang et al., 2012) treatments have been investigated.

The basidiomycete *Irpex lacteus*, has emerged as a fungus with great biodegradation potential (Novotny et al., 2009). The fungus has an exceptional ability to degrade corn stover (Xu et al.,2010), corn stalks (Du et al., 2011; Zhong et al., 2011), and wheat straw (Pinto et al., 2012; Salvachúa et al., 2011) under SSF conditions and thus to considerably increase sugar yields from these feedstock.

The present study focused on optimizing the production of *I. lacteus* inoculums for use in SSF of wheat straw by studying fungal biomass production. In addition, SSF cultural and nutritional parameters, such as nitrogen and mineral salt supplementation, wheat straw particle size, and moisture were analyzed as well as ergosterol and enzymes secretion during SSF. The efficiency of fungal treatment complemented with mild-alkali washing was determined by sugar yield estimations at 7, 14, and 21 days.

2. METHODS

2.1. Microorganism

The white-rot fungus *I. lacteus* (IJFM A792), deposited in the Fungal Culture Collection of the Centro de Investigaciones Biológicas (Madrid, Spain), was maintained on 2% malt extract agar (w/v) at 4 ºC and cultured

on plates containing the same medium at 28 ºC for one week before being used.

2.2. Pre-inoculum production

2.2.1. Culture media screening

Four 1-cm^2 agar plugs were cut from actively growing mycelium on agar plates and used to inoculate 250-mL Erlenmeyer flasks with 30 mL of growth medium (CSS) (Salvachúa et al.,2011) that were incubated at 28 ºC and 180 rpm for 7 days. These cultures were aseptically homogenized (Omnimixer, Sorvall), and 2.5 mL were used to inoculate 30 mL of different liquid culture media in 250-mL flasks. The screened media were: (i) CSS medium, (ii) K medium pH 5.5 (glucose, 20 g L^{-1}; $MgSO_4$ x $7H_2O$, 0.5 g L^{-1}; KH_2PO_4 g L^{-1}; yeast extract, 2 g L^{-1}; peptone, 5 g L^{-1}), (iii) wheat mush pH 5.5 diluted until the glucose concentration was 40 g L^{-1}, (iv) wheat thin stillage pH 4 (glucose, 4 g L^{-1}), (v) wheat thin stillage pH 4 supplemented with glucose to a final concentration of 40 g L^{-1}, (vi) wheat thin stillage pH 4 supplemented with nitrogen (0.3 g L^{-1}) from ammonium tartrate, and (vii) wheat thin stillage pH 4 with both glucose and nitrogen at the concentrations listed under (v) and (vi). Wheat mush and wheat thin stillage were obtained from first-generation bioethanol production at Bioetanol Galicia S.A. (Abengoa Bioenergy, Spain).

Cultures were collected at 3, 5, 7, and 10 days of incubation and vacuum-filtered through filter paper to separate the solids to measure biomass, and to determine total reducing sugars in the filtrate. The pH influence on biomass values was studied in wheat thin stillage medium, adjusted to pH 4, 4.5, 5, 5.5, and 6 with NaOH. These cultures were analyzed at 24, 48, and 72 h. All cultures were grown in triplicate and incubated at 28 ºC and180 rpm.

2.2.2. Inoculums for solid-state fermentation (SSF) experiments

Pre-inoculums were grown in wheat thin stillage medium pH 5 as described in Section 2.2.1 and 2.5 mL of an aseptically homogenized culture was used to inoculate the stillage. The cultures were incubated at 28 ºC and 180 rpm, and 2 mL of 1-day-old mycelium was used as inoculums for SSF experiments.

2.3. Wheat straw pretreatment

Wheat straw was harvested from Galician fields (Spain), dried, and chopped (<1 cm). *I. lacteus* basal cultures (ILC) with 2 g of wheat straw and 6 mL of water were prepared and cultured under SSF conditions as previously described (Salvachúa et al., 2011). These basal conditions were

modified in other *I. lacteus* cultures to test the effect of: (i) wheat straw particle size by using milled straw (MWS, <0.5 mm), (ii) maintaining moisture content at 75%, either by replacing lost water daily or by increasing the initial moisture content to 86%, and (iii) the addition of 0.3 mM $MnSO_4$, $CuSO_4$ and $FeSO_4$, peptone (20 g L^{-1}), and wheat thin stillage (diluted so as to reach 2 g L^{-1} of glucose). To maintain the original moisture content, the lost weight in control cultures was attributed to water evaporation and this amount was added to all treatments. Additives (salts and others) were dissolved in distilled water (6 mL) before autoclaving. Untreated wheat straw of both particle sizes was incubated under the same conditions as the treatments and used as controls. Assays were performed in triplicate.

Biopretreated and untreated wheat straw collected after 7, 14, and 21 days of incubation were washed with distilled water (15 mL) for 1 h, at 28 ºC and 180 rpm, and vacuum-filtered to extract water-soluble compounds. Solid fractions were dried in an aeration oven at 65 ºC and weighed. After calculating weight loss and analyzing the main remaining components in the wheat straw (see Section 2.6.), solid fractions were subjected to mild alkali treatments with 0.1% sodium hydroxide (5% w/v), at 50 ºC and 165 rpm for 1 h. This alkali mixture was then filtered, washed until neutral with distilled water at 50 ºC, dried at 65 ºC, and total reducing sugars were analyzed in the alkali filtrates.

2.4. Enzymatic hydrolysis, digestibility and sugar yield estimations

Pretreated fractions were hydrolyzed in duplicate at 5% (w/v) by commercial enzyme cocktails (from Novozymes, Denmark) as 15 FPU g1 of cellulases (Celluclast and NS50010) and 30 U g1 of xylanases (NS50013 and NS50030) in 100 mM sodium citrate buffer (pH 4.8) at 50 ºC, and 165 rpm for 60 h and analyzed for fermentable sugar release (Salvachúa et al., 2011). The digestibility of cellulose (D_c) and hemicellulose (D_h) was calculated according to Eq. (1), as the ratio between the percentage of glucose (G_r) or xylose (X_r) released from pretreated fractions and the estimated glucose (G_p) or xylose (X_p) in the fraction prior to enzymatic hydrolysis, respectively. Glucose (G_y) and xylose (X_y) yields were determined by taking into account glucose (G_i) and xylose (X_i) content per gram of dry wheat straw, glucose (G_f) and xylose (X_f) remaining after wheat straw pretreatment, and the digestibility of cellulose (D_c) and hemicellulose (D_h), respectively, as shown in Eq. (2).

Eq (1): $D_c \text{ or } D_h\ (\%) = (g\ G_r \text{ or } X_r / g\ G_p \text{ or } X_p) \times 100$

Eq (2): $G_y \text{ or } X_y\ (\%) = (G_f \text{ or } X_f \times D_c \text{ or } D_h) / G_i \text{ or } X_i$

2.5. Substrate characterization

Wheat straw weight loss for each fungal pretreatment was calculated as the percentage of total solids lost after water washing. Total hydrolysis of wheat straw was performed to determine Klason lignin (Tappi, 1974) and sugar composition.

2.6. Sugar and protein determination

Sugars from wheat mush and wheat thin stillage were analyzed by gas chromatography (GC) as previously reported (Prieto et al., 2008). Total reducing sugars were estimated by the Somogyi–Nelson method (Somogyi, 1945), using glucose as standard. Glucose, xylose, cellulose, and hemicelluloses estimations were calculated as described elsewhere (Salvachúa et al., 2011). Protein concentrations from wheat mush and wheat thin stillage were determined using the Bradford reagent (Bio-Rad), with bovine serum albumin as standard.

2.7. Enzyme assays

Enzymes were evaluated in the water-soluble fractions from SSF experiments and expressed in international enzyme units (micro moles per minute) per gram of wheat straw. Lignin peroxidase (LiP), laccase, and Mn(II)-oxidizing peroxidase (MnP) were analyzed in all treatments as previously described (Salvachúa et al.,2011). In addition, Mn(II)-independent peroxidase (MiP) activity was measured using 5 mM 2,6-dimethoxyphenol (DMP) in 100 mM sodium tartrate buffer (pH 5;ε_{469} = 27,500 $M^{-1}cm^{-1}$ referred to DMP concentration) in the presence of 0.1 mM H_2O_2.

2.8. Estimation of fungal growth

Liquid cultures were vacuum-filtered and the mycelia dried in an aeration oven at 65 ºC for 24 h and weighted.

During SSF experiments, fungal growth was estimated by measuring ergosterol content. First, the percentage of ergosterol in fungal cell walls was determined in lyophilized 5-day old mycelium obtained from CSS medium. Pulverized mycelium (5, 10, 20, 40, and 80 mg) was extracted as described below to calculate ergosterol content as micro gram per milli gram of fungal mycelium, which was taken as the reference value. To evaluate fungal growth in SSF cultures, 100 mg of untreated and biopretreated wheat straw samples were extracted according to the method of Seitz et al. (1979) with some modifications. Samples were placed in glass tubes with petroleum ether (1 mL) and 10% KOH in methanol (4 mL), and sonicated for 15 min. The mixture was left to settle for 45 min

and then samples were incubated at 70 ºC for 90 min. Milli- Q water (1 mL) and petroleum ether (2 mL) were added to the cooled samples and stirred for 30 s. Tubes were centrifuged at 470 g for 5 min and the organic phase was removed and allowed to dry at room temperature. Samples were resuspended in methanol and analyzed by HPLC-MS/MS. The system was equipped with a Surveyor HPLC with a Spheri-5 PTH column (Applied Biosystems; 220 mm x 2.1 mm x 5µm) coupled to a Finnigan TM LXQTM Linear Ion Trap Mass Spectrometer (Thermo). Samples were analyzed isocratically using methanol (100%) as mobile phase, with a flow of 300 µL min^{-1}. Ergosterol was identified and quantified by comparing the retention time and response factor with those of ergosterol standards analyzed under the same conditions. Fungal growth was estimated by comparing the ergosterol detected in each SSF culture (ED) with its percentage in pulverized mycelium (EP), according to Eq. (3).

Eq (3):

I. lacteus biomass (µg/g wheat straw) = (ED (µg/g wheat straw)/ EP) x 100

3. RESULTS AND DISCUSSION

3.1. Medium selection for inoculums production

Prior to media screening, characterization was carried out on the wheat mush and wheat thin stillage from the first-generation bioethanol production processes. The wheat mush contained glucose (240 g L^{-1}), xylose (6 g L^{-1}), and protein (3.6 g L^{-1}), and the wheat thin stillage included glucose (4 g L^{-1}), xylose (1 g L^{-1}), galactose (0.5 g L^{-1}), mannose (0.6 g L^{-1}), and protein (0.2 g L^{-1}). Taking into account these values, dilutions or glucose supplementations were carried out on wheat mush or wheat thin stillage-containing media, respectively, to reach a glucose content similar to that in the other media (maximum 40 g L^{-1}).

Biomass of *I. lacteus* was monitored in different liquid media over 10 d of incubation (Fig. 1). Wheat mush and K media had the lowest fungal biomass content (610 mg mL^{-1}) while the highest values (30 mg mL^{-1}) were found in media containing wheat thin stillage. Wheat thin stillage, the main by-product of ethanol-producing industries, is rich in organic matter and macronutrients (Bustamante et al., 2008), but its glucose content is low. In spite of the low glucose content, the initial growth of *I. lacteus* was significantly faster than that attained when wheat thin stillage was supplemented with glucose, which suggests that the glucose concentration was not the only crucial component for triggering fungal growth. Nitrogen supplementation of wheat thin stillage medium (by adding peptone) did not

improve *I. lacteus* growth, but the addition of both glucose and nitrogen to the medium did produce a slow increase in biomass, reaching a maximum ratio at 10 d of incubation instead of at 3 or 5 days.

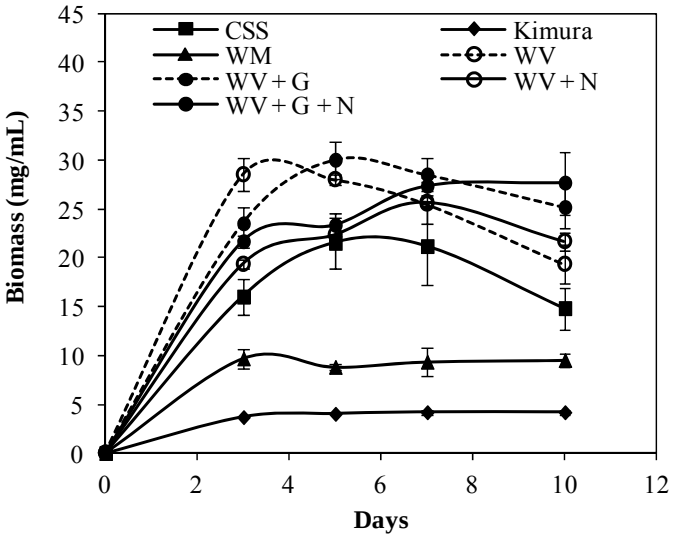

Fig. 1. *I. lacteus* biomass in different aqueous media for 10 days of incubation. CSS medium (CSS); WM = wheat mush; WV = wheat thin stillage; G = glucose; N = nitrogen.

To test the effect of pH on *I. lacteus* growth, the pH of wheat thin stillage medium was adjusted to different values. Fungal growth rate increased when the initial pH was 5, reaching similar biomass levels in one day as those obtained in the previous experiment, at pH 4, in 3 days (data not shown). Therefore, it can be concluded that growth is more dependent on specific medium components than on its initial pH, although the optimal pH value should be experimentally adjusted for a given medium. Considering the convenience of short process times and decreased costs, wheat thin stillage (pH 5) was selected for producing 1-day old inoculums. Wheat thin stillage contains polyphenols with potential phytotoxic and antimicrobial effects (Bustamante et al.,2008), as well as high levels of recalcitrant organic matter. The ability of *I. lacteus* to grow quickly and efficiently in this medium has been demonstrated in the present work, confirming the resistance of this species to toxic compounds (Novotny et al., 2009). Thus, a suitable cheap medium has been found for producing *I. lacteus* pre-inocula with high fungal biomass content and reduced process costs.

3.2. *I. lacteus* biopretreatment in different SSF conditions

3.2.1. Effect on wheat straw degradation

I. lacteus is a basidiomycete capable of improving sugar recovery from wheat straw without promoting significant changes in its microstructure and structural integrity (Fig. S1). Initial wheat straw consisted of cellulose

(37%), hemicelluloses (23%), and lignin (24%). As xylan was the principal component in hemicelluloses (18%) it was included in all subsequent estimations.

During SSF, the main weight losses occurred during the first 2 weeks, with similar results from 14 to 21 days in most treatments. High moisture content and peptone supplementation produced the lowest and highest weight losses, respectively, corresponding to approximately 20% and 38% at 21-d biopretreatment (data not shown).

Hemicellulose degradation increased by a factor of two after 14 and 21 days of fungal growth when straw with a particle size of 6 0.5 mm was used, although cellulose loss and lignin degradation diminished under these conditions (Table 1). These findings can be explained by the reduction in the ordered structure of smaller particles, especially of hemicellulose, which is not as well-packed as cellulose (Xu et al., 2009). Due to the accessibility of this component the fungus makes preferential use of xylose and hardly consumes or degrades other wheat straw components, like cellulose or lignin.

Regardless of the tested moisture contents maintained during the 3-week SSF period, cellulose and lignin losses were similar to those from control cultures (Table 1). In contrast, hemicelluloses degradation was either negligible with increased moisture or delayed under constant wetness. It has previously been observed that xylanase production can be reduced by water excesses (Mohana et al., 2008), resulting in those low hemicellulose losses. Those results could be explained by too much water possibly obstructing inter-particle spaces, thereby inhibiting gas circulation, compacting the substrate and making fungus action difficult (Reid, 1989), thus changing the degradation pattern relative to ILC.

While Cu(II) and Fe(II) supplementation resulted in low hemicellulose degradation (>11%) and fast cellulose consumption at 14 days (29%), less cellulose (17%) and more hemicelluloses (30%) degradation was observed with Mn(II) (Table 1). During the third week, cellulose content did not change significantly relative to previous weeks, but parallel increases in lignin and hemicellulose degradation were detected in all cases, with lignin reaching the highest degradation (45.9%) with Fe(II). Fe(II) favors the production of hydroxyl radicals, strong oxidants formed in Fenton reactions, which are considered to be one of the low-molecular weight agents implicated in the initial lignocellulose attack (Evans et al., 1994).

Lignin degradation was higher when peptone and wheat stillage was added compared to ILC at 14 and 21 days (Table 1). Therefore, peptone addition resulted in elevated cellulose (34%) and hemicellulose (50%)

consumption at 21 days. In contrast, wheat thin stillage supplementation provoked significantly less hemicelluloses loss. Enzyme production in SSF is dependent on the N source and the fungus and, in the case of the ligninolytic system, activation normally occurs at low nitrogen concentrations (Kachlishvili et al., 2006). Nevertheless, considering that this high lignin loss was accompanied by substantial differences in the composition of the wheat straw recovered after these SSF treatments, the action of other lignin degradation mechanisms, based on alternative oxidative processes (Tanaka et al., 1999), should be considered.

By comparing all treatments (Fig. 2), a positive correlation (r= 0.721) was found between lignin and cellulose loss during the 21-d biopretreatment.

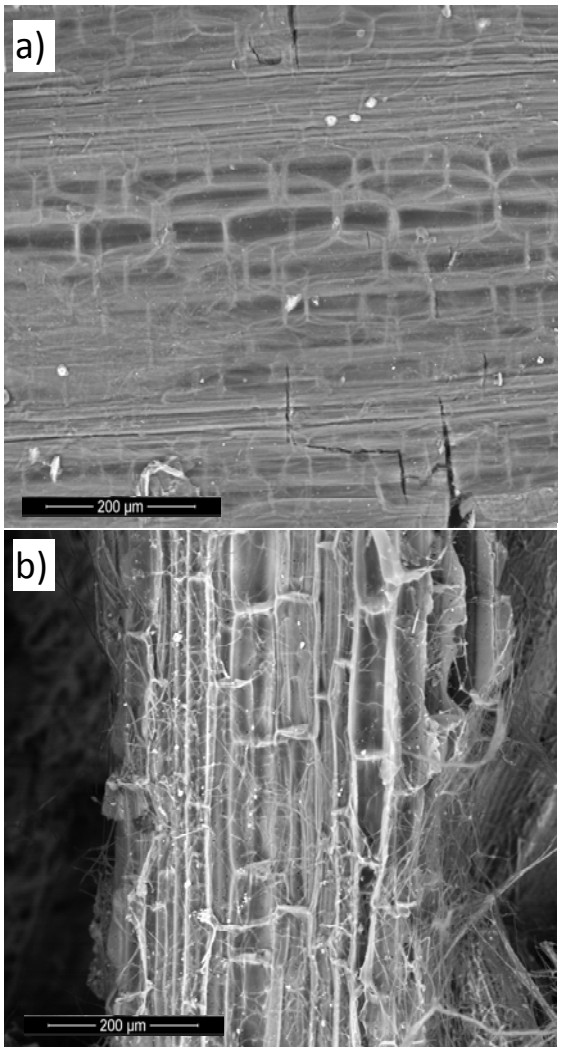

Supplemental Fig. S1. Scanning Electron Microscopy (SEM) of WS (a) non-biopretreated and (b) 21-d biopretreated with *I. lacteus*. Samples were directly dried from SSF cultures at 60ºC for 4 hours. The images were obtained with an ESEM XL30, at the Museo Nacional de Ciencias Naturales (MNCN, CSIC, Madrid, Spain), operating with secondary electrons and backscattering detectors (LFD-large field and BSED-backscattering electron, respectively). Arrow is signaling fungal mycelium.

It seems that as lignin is being degraded, accessibility to cellulose increases and consequently, *I. lacteus* consumes this component more extensively, resulting in a decrease in glucose yields. In contrast, hemicellulose losses were not dependent on cellulose (r= 0.141) or lignin (r= 0.385) degradation.

Table 1. Loss of wheat straw components after biopretreatment with *I. lacteus* after 7, 14, and 21 days of incubation under different SSF conditions. Values are calculated taking into account the initial content of each component in WS. Data are means of triplicates and standard deviations are provided. CEL = cellulose; HEM; hemicellulose; LIG = lignin; ILC =*I. lacteus* basal cultures; MWS = milled wheat straw; CM = constant moisture; HM = high moisture; WTS = wheat thin stillage.

	Loss (%)								
	7 days			14 days			21 days		
	CEL	HEM	LIG	CEL	HEM	LIG	CEL	HEM	LIG
ILC	13 ± 1	17 ± 1	19 ± 1	17 ± 0	19 ± 1	28 ± 1	21 ± 2	23 ± 2	36 ± 1
MWS	12 ± 0	26 ± 5	10 ± 0	13 ± 1	43 ± 11	23 ± 0	12 ± 1	49 ± 6	26 ± 0
CM	15± 1	2 ± 0	19 ± 1	23 ± 0	16 ± 3	24 ± 1	26 ± 0	39 ± 9	38 ± 1
HM	16 ± 0	0 ± 1	15 ± 0	22 ± 1	0 ± 0	27 ± 1	27 ± 1	2 ± 0	30 ± 1
Mn (II)	15 ± 1	0 ± 0	22 ± 1	17 ± 1	30 ± 3	32 ± 1	18 ± 1	45 ± 6	38 ± 1
Cu (II)	12 ± 0	4 ± 0	13 ± 1	28 ± 2	11 ± 1	29 ± 1	26 ± 1	11 ± 0	43 ± 2
Fe (II)	10 ± 0	6 ± 0	15 ± 0	30 ± 2	9 ± 0	30 ± 2	27 ± 1	24 ± 1	46 ± 0
Peptone	11 ± 0	16± 0	19 ± 1	23 ± 1	21 ± 2	32 ± 1	34 ± 1	50 ± 0	42 ± 0
WTS	13 ± 0	2 ± 2	18 ± 0	17 ± 1	3 ± 0	33 ± 1	19 ± 1	14 ± 1	40 ± 1

3.2.2. Effect on water-soluble sugars recovery

The sugar content of the water-soluble fraction was less than 1% in all cases, with the exception of the treatment with peptone where slightly higher values of 1.4 and 1.1% were detected at 14 and 21 days respectively (data not shown). This result parallels the highest sugar losses observed in treatments with peptone. Since most of the sugars released by fungal action are being consumed by the fungus itself for its own growth and survival and because of their low content the soluble sugars were not included in the final sugar yield calculations.

3.2.3. Effect on digestibility and sugar yields

To evaluate enzymatic hydrolysis efficiency, cellulose and hemicellulose digestibility were calculated after the wheat straw had been subjected to mild alkali treatment to improve digestibility (Salvachúa et al., 2011; Zhong et al., 2011) and sugar losses were not detected after alkali-washing and major increases were quantified in cellulose (around 20–30%) but not in hemicellulose digestibility (data not shown).

Neither an initial content of 86% nor maintaining 75% wetness was satisfactory, so this parameter merits further optimization for the SSF of

wheat straw by *I. lacteus*. Particle size reduction (MWS), boosted hemicellulose digestibility in all samples (Fig. 3). A slight increase in cellulose digestibility at 7 days of biopretreatment was observed only with MWS (5% more than non-milled wheat straw), but sugar yields after this short period were poor, suggesting a need for longer biopretreatments to enhance fermentable sugar recoveries relative to untreated straw, as reported by Pedersen and Meyer (2009).

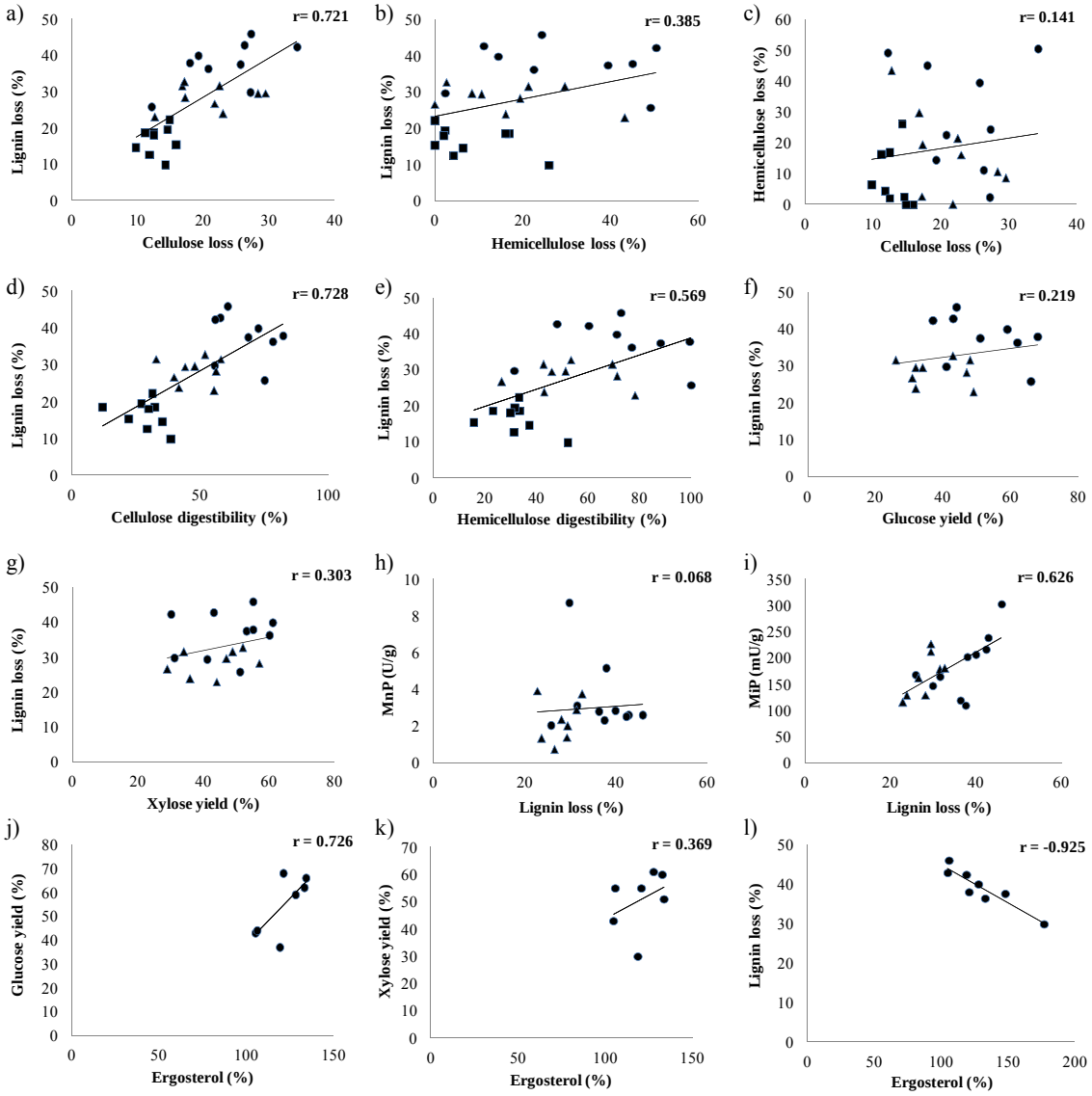

Fig. 2. Scatter plots comparing several variables analyzed under different SSF conditions during *I. lacteus* biopretreatment: (a–c) wheat straw components loss at 7, 14 and 21 days; (d–e) lignin loss with digestibility at 7, 14 and 21 days; (f–g) lignin loss with sugar yields at 14 and 21 days; (h i) lignin loss with peroxidas e activities at 14 and 21 days; and (j–k) ergosterol with both sugar yields and lignin loss at 21 days. Squares, triangles, and circles represent samples from 7, 14, and 21 days respectively.

After 14 days of fungal treatment, cellulose digestibility improved in most cases compared with untreated samples, except in the case of cultures with moisture variations, Cu(II), and peptone supplementations. In contrast, better hemicellulose digestibility was only found in ILC, cultures with MWS, and cultures with added Mn(II). Fermentable sugar yields were generally similar to those of untreated wheat straw cultures, although glucose recovery reached 47% in ILC, 49% using MWS as the substrate, and 48% with Mn(II) supplementation. Xylose recovery (Fig. 4) was higher in ILC (57%) and wheat thin stillage (52%) than in non-biopretreated samples.

At 21 days all treatments improved digestibility compared with non-biopretreated samples, with the exception of hemicelluloses digestibility from samples with added peptone. In fact, significant differences in hemicellulose digestibility were found between both MWS and Mn(II) supplemented treatments and control cultures, the hemicellulose being completely digested after enzymatic hydrolysis. Nevertheless, despite these significant improvements, hemicellulose was extensively degraded during fungal growth, decreasing the final xylose yield.

Only ILC, and Mn(II) and wheat thin stillage-supplemented treatments increased xylose yields up to 55–61%, while untreated samples gave 33% and 45% for wheat straw and MWS, respectively, with no significant differences among them (Fig. 4). These xylose recoveries are very high as compared with the 20% reported by Wan and Li (2011) after wheat straw biopretreatment with *Ceriporiopsis subvermispora* for 35 days. Concerning glucose (Fig. 4), five treatments (ILC, MWS, maintained moisture, Mn(II), and wheat thin stillage) improved recovery compared with untreated samples (33% and 37% for wheat straw and MWS, respectively), but only the Mn(II) treatment gave a better yield (68%) than ILC (62%). In view of these results, Mn(II) supplementation seems to be appropriate to significantly enhance glucose yields from 21-d SSF cultures of *I. lacteus* on wheat straw. As previously reported, Mn(II) addition to SSF cultures probably affects the induction of MnP thus increasing the efficiency of the process (Camarero et al., 1996).

According to the present data, Mn(II) supplementation produced total sugar recoveries 91% higher than those from untreated wheat straw. In comparison, a 62% increase in total reducing sugar recoveries was recently reported with *I. lacteus* in 21-d SSF cultures on wheat straw (Pinto et al., 2012). Moreover, significantly lower recoveries than those presented in this study were reached after wheat straw pretreatments using other fungi, such as *C. subvermispora* (Wan and Li, 2011) and Euc-1 (Dias et al., 2010).

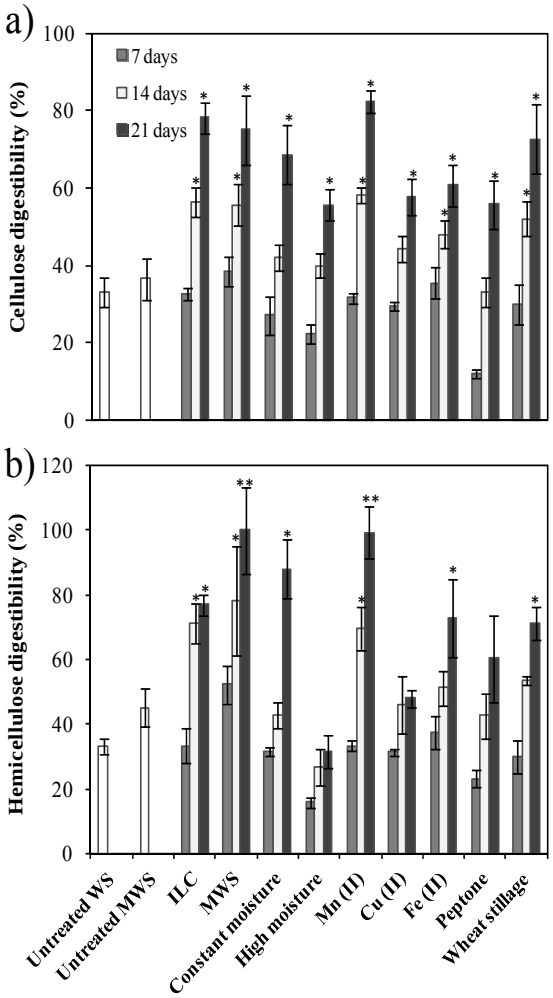

Fig. 3. Percentage of (a) cellulose and (b) hemicellulose digestibility from pretreated wheat straw (WS) during 7, 14 and 21 days of SSF. Untreated samples (white bars) correspond to non-biopretreated WS. Data are means of triplicates and standard deviations are provided. Asterisks over the bars represent samples with significantly higher values than non-biopretreated WS (*) and *I. lacteus* basal cultures (ILC) (**). MWS = milled wheat straw.

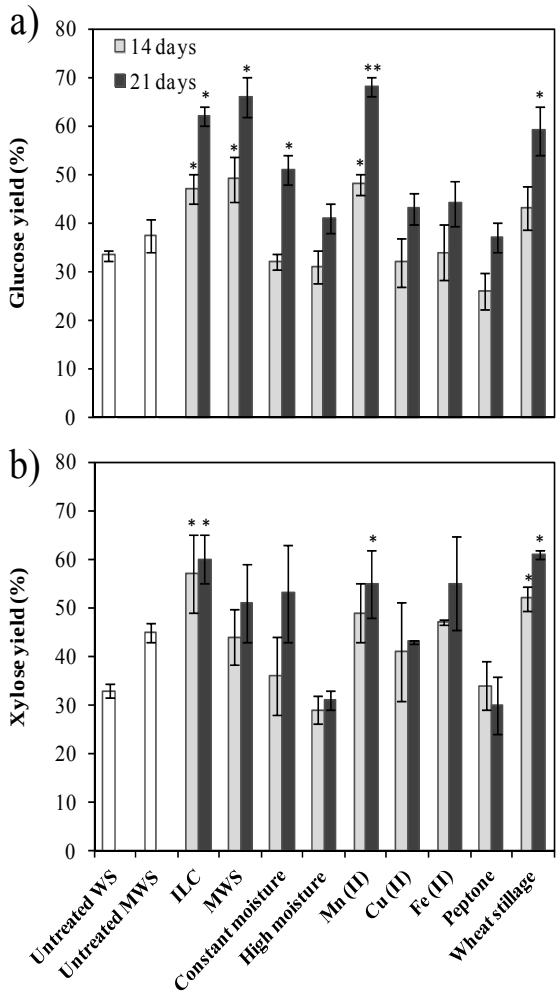

Fig. 4. Percentage of (a) glucose and (b) xylose yield from pretreated wheat straw (WS) after 14 and 21 days of SSF. Untreated samples (white bars) correspond to non-biopretreated WS. Data are means of triplicates and standard deviations are provided. Asterisks on bars represent samples with significantly higher values than non-biopretreated WS (*) and *I. lacteus* basal cultures (ILC) (**). MWS = milled wheat straw.

The efficiency of *I. lacteus* for biopretreating lignocellulosic material has already been demonstrated on other substrates. Zhong et al. (2011) described 50% yields after 15-d of SSF using corn stalks and Xu et al. (2010) obtained a 66.7% glucose yield from corn stover in 25-d treatments. Better glucose recoveries (82%) have also been reported by Du et al. (2011) with a 28-d biopretreatment of corn stalks with *I. lacteus*, after supplementing the enzymatic hydrolysis broth with by-products secreted by the same fungus.

3.3. Search for efficiency indicators of *I. lacteus* biopretreatment

3.3.1. Relationship between lignin degradation, digestibility, and sugar yields

A moderate positive correlation was found between lignin loss and digestibility of cellulose (r= 0.728) and hemicelluloses (r= 0.569), but no such correlation was found between lignin loss and glucose (r= 0.219) or xylose (r= 0.303) yields (Fig. 2). These results confirm that lignin is the main barrier preventing efficient enzymatic hydrolysis; however, lignin degradation is not directly correlated with the final yields of fermentable sugars since better sugar availability can also lead to their use as a carbon source for fungal growth.

3.3.2. Relationship between extracellular ligninolytic enzymes and sugar yields

Although the search for ligninolytic activities revealed the ab- sence of LiP and laccase activity under the assayed conditions, their activity was found in *I. lacteus* cultures growing on different substrates such as wheat straw and corn stalks (Dias et al., 2010; Du et al., 2011; Gupte et al., 2007). Conversely, peroxidase activity whether dependent on or independent of Mn(II) was considerable (Fig. 5) even though it was not found by Gupte et al. (2007) with the same fungus growing on wheat straw. According to the current data, the release of peroxidases seemed to play an important role during the first weeks of incubation. The levels of MnP were significantly higher, compared to ILC, only after 7 days of SSF on MWS, and after 21 days with either high moisture content or Mn(II) supplementation. On the other hand, MiP activity was, in general, notably superior when organic or inorganic compounds were added as supplements. As an exception, in 21-d cultures only the addition of Cu(II) and Fe(II) produced enhanced activities compared with ILC. Both minerals can induce the production of ligninolytic enzymes (Manubens et al., 2007).

No relationship was found between peroxidase activities and sugar yields, and no correlation (r= 0.068) was found between MnP activity and lignin loss, even so a moderate positive correlation (r= 0.626) was established between MiP and lignin loss (Fig. 2). This result suggests that MiP is probably more implicated in lignin degradation than MnP under the assayed conditions.

3.3.3. Relationship between fungal biomass, sugar yields, and lignin degradation

Ergosterol, an exclusive component of fungal cellular membranes (Pitt and Hocking, 2009), was selected as a fungal growth indicator. This sterol

was analyzed in freeze-dried fungal mycelium to calculate its approximate percentage in the fungal cells (0.46% ± 0.06). With this value, *I. lacteus* biomass estimations were carried out in wheat straw cultures. Basal amounts of ergosterol were detected in untreated samples, probably because of the presence of endogenous fungi on wheat straw taken from the field, so *I. lacteus* biomass estimations were not done in these samples (Table S1).

ILC experienced an increase in fungal biomass throughout the incubation period, though this biomass did not grow significantly from 14 to 21 days reaching 29.2 ± 2.1 mg g^{-1} wheat straw at 21 days. Since the best sugar yields were obtained at 21-d of SSF, ergosterol was analyzed only at that time. The lowest fungal growth was found in media supplemented with Cu(II), Fe(II) and peptone (23.2 ± 2.4, 23.3 ± 2.3, and 26.2 ± 0.8 mg g^{-1} wheat straw, respectively) (Table S1). Furthermore, those three treatments also gave the lowest glucose yields, thus a moderate correlation (r= 0.726) was found between both variables but not with respect to xylose yield (r= 0.369) (Fig. 2).

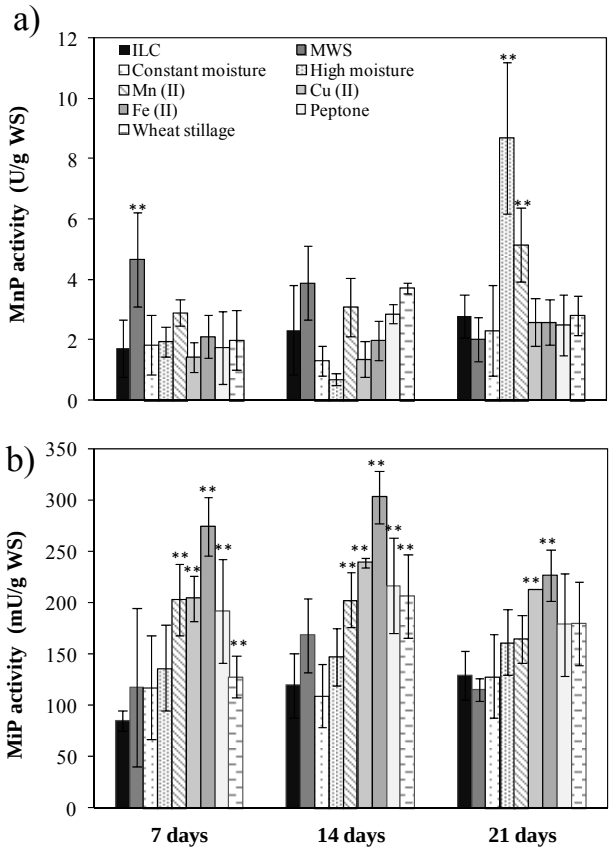

Fig. 5. (a) Mn(II)-oxidizing peroxidase (MnP) activity and (b) Mn(II) independent peroxidase (MiP) activity (U g^{-1} WS) detected in fungal cultures after 7, 14 and 21 days of SSF. Data are means of triplicates and standard deviations are provided. Asterisks on bars represent samples with significantly higher values than *I. lacteus* basal cultures (ILC) (**). WS = wheat straw; MWS = milled wheat straw.

Supplemental Table S1. Ergosterol (µg g^{-1} WS), estimated fungal biomass (mg g^{-1} WS), Mn(II) independent peroxidase (MiP), and Mn(II)-oxidizing peroxidase (MnP) production per mg of fungal biomass (mU mg^{-1}) from samples of *I. lacteus* biopretreated WS for 21-d. Untreated samples correspond to non-biopretreated WS. Data are means of triplicates. ILC = *I. lacteus* basal cultures; WS= wheat straw; MWS= milled wheat straw; NA: Unanalysed sample.

	Ergosterol (µg g^{-1} WS)	F. Biomass* (mg g^{-1} WS)	MiP (mU mg^{-1})	MnP (mU mg^{-1})
Untreated WS	24.3 ± 7.8	**	-	-
Untreated MWS	NA	**	-	-
ILC	133.1 ± 9.8	29.2 ± 6.2	4.4	95.1
MWS	134.1 ± 10.2	29.4 ± 2.2	3.9	68.6
Constant moisture	148.4 ± 25.0	32.6 ± 5.5	3.9	70.4
High moisture	177.2 ± 38.2	38.9 ± 8.4	4.1	223.6
Mn (II)	121.7 ± 12.0	26.7 ± 2.6	6.2	192.5
Cu (II)	105.7 ± 10.8	23.2 ± 2.4	9.1	111.2
Fe (II)	106.0 ± 10.5	23.3 ± 2.3	9.7	110.7
Peptone	119.5 ± 3.8	26.2 ± 0.8	6.8	95.4
Wheat thin stillage	128.6 ± 6.2	28.2 ± 1.4	6.4	100.0

* Fungal biomass was estimated by determining the ergosterol content in *I. lacteus* cell-wall and 21-d *I. lacteus* SSF cultures.
** Fungal biomass estimation was not done in untreated samples.

Lignin degradation and fungal biomass were also correlated, and a tight negative correlation was found between both variables (r= -0.925) (Fig. 2). Cultures with Cu(II) or Fe(II) had the lowest fungal biomass content but the highest levels of lignin degradation, which could be attributed to an overproduction of free radicals and/or to increased enzyme-releasing activity of the mycelium. When peroxidase production was expressed per mg of fungal biomass (Table S1) to determine if the increase in enzyme secretion could be correlated with the extent of fungal growth as previously reported (Kachlishvili et al., 2006), for MiP, the most active mycelia were found in treatments with Cu(II) and Fe(II), while MnP production was not linked to fungal growth.

Few ligninolytic activities were detected in *I. lacteus* SSF cultures on wheat straw, suggesting that with this fungus, lignin degradation could be mostly driven by oxidation mechanisms where the enzymes secreted play an important role in its production, according to data previously reported (Gómez-Toribio et al., 2001). Consequently, future studies will focus on the search for and characterization of potential oxidative species that could be strongly correlated with the efficiency of the process, such as hydroxyl radicals or low-molecular-weight substances released by *I. lacteus*.

4. CONCLUSIONS

Irpex lacteus is capable of modifying wheat straw to produce enhanced sugar yields at 14 and 21 days of SSF. Results obtained in this work demonstrate the high complexity of the fungal wheat straw degradation process, since a single modification of culture conditions can produce noteworthy differences in its efficiency. Digestibility was significantly improved by particle size reduction and Mn(II) supplementation in the cultures, the latter yielding the highest glucose recoveries. To gain an insight into lignocellulose breakdown mechanisms and optimize approaches for sugar exploitation, a proteomic study of the *I. lacteus* enzyme system is currently in progress.

ACKNOWLEDGEMENTS

This work was supported mainly by the CENIT I+DEA project (funded by CDTI, Spain) and carried out in collaboration with Abengoa Bionergía Nuevas Tecnologías. The authors also wish to thank DEMO-2 and Lignodeco EU projects for their additional support, Novozymes for providing commercial enzymes, A.J. García from the MNCN (CSIC), for his help in SEM experiments, and Mr. R. Chiverton for English corrections. D. Salvachúa gratefully acknowledges an FPU fellowship from the MICINN.

REFERENCES

Bustamante, M., Moral, R., Paredes, C., Perez-Espinosa, A., Moreno-Caselles, J., Perez-Murcia, M., 2008. Agrochemical characterisation of the solid by-products and residues from the winery and distillery industry. Waste Manage. 28, 372–380.

Camarero, S., Bockle, B., Martínez, M.J., Martínez, A.T., 1996. Manganese-mediated lignin degradation by *Pleurotus pulmonarius*. Appl. Environ. Microbiol. 62, 1070–1072.

Canam, T., Town, J.R., Tsang, A., McAllister, T.A., Dumonceaux, T.J., 2011. Biological pretreatment with a cellobiose dehydrogenase-deficient strain of *Trametes versicolor* enhances the biofuel potential of canola straw. Bioresour. Technol. 102, 10020–10027.

Dias, A.A., Freitas, G.S., Marques, G.S.M., Sampaio, A., Fraga, I.S., Rodrigues, M.A.M., Evtuguin, D.V., Bezerra, R.M.F., 2010. Enzymatic saccharification of biologically pre-treated wheat straw with white-rot fungi. Bioresour. Technol. 101, 6045–6050.

Du, W., Yu, H., Song, L., Zhang, J., Weng, C., Ma, F., Zhang, X., 2011. The promoting effect of byproducts from *Irpex lacteus* on subsequent enzymatic hydrolysis of bio-pretreated cornstalks. Biotech. Biofuels 4, 37.

Evans, C.S., Dutton, M.V., Guillén, F., Veness, R.G., 1994. Enzymes and small molecular mass agents involved with lignocellulose degradation. FEMS Microbiol. Rev. 13, 235–240.

Gómez-Toribio, V., Martínez, A.T., Martínez, M.J., Guillén, F., 2001. Oxidation of hydroquinones by the versatile ligninolytic peroxidase from *Pleurotus eryngii* :H_2O_2generation and the influence of Mn^{2+}. Eur. J. Biochem. 268,4787–4793.

Gupte, A., Gupte, S., Patel, H., 2007. Ligninolytic enzyme production under solid-state fermentation by white-rot fungi. J. Sci. Ind. Res. 66, 611–614.

Hahn-Hägerdal, B., Galbe, M., Gorwa-Grauslund, M.F., Liden, G., Zacchi, G., 2006. Bio-ethanol – the fuel of tomorrow from the residues of today. Trends Biotechnol. 24, 549–556.

Kachlishvili, E., Penninckx, M., Tsiklauri, N., Elisashvili, V., 2006. Effect of nitrogen source on lignocellulolytic enzyme production by white-rot basidiomycetes under solid-state cultivation. World J. Microbiol. Biotechnol. 22, 391–397.

Manubens, A., Canessa, P., Folch, C., Avila, M., Salas, L., Vicuña, R., 2007. Manganese affects the production of laccase in the basidiomycete *Ceriporiopsis subvermispora* . FEMS Microbiol. Lett. 275, 139–145.

Mohana, S., Shah, A., Divecha, J., Madamwar, D., 2008. Xylanase production by *Burkholderia* sp DMAX strain under solid state fermentation using distillery spent wash. Bioresour. Technol. 99, 7553–7564.

Novotny, C., Cajthaml, T., Svobodova, K., Susla, M., Sasek, V., 2009. *Irpex lacteus* ,a white-rot fungus with biotechnological potential - review. Folia Microbiol. 54, 375–390.

Pedersen, M., Meyer, A.S., 2009. Influence of substrate particle size and wet oxidation on physical surface structures and enzymatic hydrolysis of wheat straw. Biotechnol. Progr. 25, 399–408.

Pinto, P.A., Dias, A.A., Fraga, I., Marques, G., Rodrigues, M.A.M., Colaco, J., Sampaio, A., Bezerra, R.M.F., 2012. Influence of ligninolytic enzymes on straw saccharification during fungal pretreatment. Bioresour. Technol. 111, 261–267.

Pitt, J.I., Hocking, A.D., 2009. Methods for isolation, enumeration and identification. In: Pitt, J.I., Hocking, A.D. (Eds.), Fungi and Food Spoilage. Springer, New York, USA, pp. 19–52.

Prieto, A., Leal, J.A., Bernabé, M., Hawksworth, D.L., 2008. A polysaccharide from *Lichina pygmaea* and *L. confinis* supports the recognition of Lichinomycetes. Mycol. Res. 112, 381–388.

Reid, I.D., 1989. Solid-state fermentations for biological delignification. Enzyme Microb. Technol. 11, 786–803.

Salvachúa, D., Prieto, A., López-Abelairas, M., Lu-Chau, T., Martínez, A.T., Martínez, M.J., 2011. Fungal pretreatment: an alternative in second-generation ethanol from wheat straw. Bioresour. Technol. 102, 7500–7506.

Saritha, M., Arora, A., Nain, L., 2012. Pretreatment of paddy straw with *Trametes hirsuta* for improved enzymatic saccharification. Bioresour. Technol. 104, 459– 465.

Seitz, L.M., Shuer, D.B., Burroughs, R., Mohr, H.E., Hubbard, J.D., 1979. Ergosterol as a measure of fungal growth. Phytopathology 69, 1202–1203.

Somogyi, M., 1945. A new reagent for the determination of sugars. J. Biol. Chem. 160, 61–73.

Talebnia, F., Karakashev, D., Angelidaki, I., 2010. Production of bioethanol from wheat straw: an overview on pretreatment, hydrolysis and fermentation. Bioresour. Technol. 101, 4744–4753.

Tanaka, H., Itakura, S., Enoki, A., 1999. Hydroxyl radical generation and phenol oxidase activity in wood degradation by the white-rot basidiomycete *Irpex lacteus*. Mater. Org. 33, 91–105.

Tappi 1974. Acid-insoluble lignin in wood and pulp. Tappi Rule T 222-os.

Wan, C., Li, Y., 2011. Effectiveness of microbial pretreatment by *Ceriporiopsis subvermispora* on different biomass feedstocks. Bioresour. Technol. 102, 7507–7512.

Wang, W., Yuan, T., Wang, K., Cui, B., Dai, Y., 2012. Combination of biological pretreatment with liquid hot water pretreatment to enhance enzymatic hydrolysis of *Populus tomentosa* . Bioresour. Technol. 107, 282–286.

Xu, C., Ma, F., Zhang, X., 2009. Lignocellulose degradation and enzyme production by *Irpex lacteus* CD2 during solid-state fermentation of corn stover. J. Biosci. Bioeng. 108, 372–375.

Xu, C., Ma, F., Zhang, X., Chen, S., 2010. Biological pretreatment of corn stover by *Irpex lacteus* for enzymatic hydrolysis. J. Agric. Food Chem. 58, 10893–10898.

Yamagishi, K., Kimura, T., Watanabe, T., 2011. Treatment of rice straw with selected *Cyathus stercoreus* strains to improve enzymatic saccharification. Bioresour. Technol. 102, 6937–6943.

Zhong, W., Yu, H., Song, L., Zhang, X., 2011. Combined pretreatment with white-rot fungus and alkali at near room-temperature for improving saccharification of corn stalks. Bioresources 6, 3440–3451.

Chapter 3

Differential proteomic analysis of the secretome of *Irpex lacteus* and other white-rot fungi growing on wheat straw

Davinia Salvachúa, Ming Tien, María Fernández, Francisco García-Tabares, Vivian de los Ríos, Ángel T. Martínez, María Jesús Martínez, Alicia Prieto.

(Manuscript in preparation)

ABSTRACT

Identifying new high-performance enzymes or enzyme complexes to enhance biomass degradation is the key for the development of cost-effective processes for ethanol production. Previous works pointed to the basidiomycete *Irpex lacteus* as an efficient microorganism for wheat straw pretreatment, yielding easily hydrolysable products with high sugar content. Given this background, this fungus was selected to investigate the enzymatic system involved in lignocellulose decay, and its secretome was analyzed through 2D-PAGE, nanoLC/MS-MS, and homology searches against public databases. *I. lacteus* secreted a battery of cellulases and xylanases, but lacked those implicated in the final degradation of cellulose and hemicellulose to their monosaccharides, making these sugars poorly available for fungal consumption. A significant production of proteases, DyP, MnP, and H_2O_2 producing-enzymes, led to an improved deconstruction of wheat straw. The proteins secreted by this fungus in submerged cultures, as well as the secretomes from *Phanerochaete chrysosporium* and *Pleurotus ostreatus* growing on wheat straw, which produce different degradation pattern on this substrate, are also reported.

Keywords: Enzymatic hydrolysis, ethanol, DyP, *Pleurotus ostreatus*, *Phanerochaete chrysosporium*.

Abbreviations: CBH= Cellobiohydrolases; CDH= Cellobiose dehydrogenases; DyP= dye-decolorizing peroxidase; EPP= extracellular pool of proteins; GH= glycoside hydrolase; JGI= Joint Genome Institute; MM= molecular mass; MnP= manganese peroxidase; nanoLC-MS/MS= nano-high performance liquid chromatography-tandem mass spectrometry; pI= isoelectric point; SmF= submerged state fermentation; SSF= solid state fermentation.

1. INTRODUCTION

In the fungal kingdom, white-rot fungi (phylum Basidiomycota) are the only microorganisms known to be able to alter all plant components, including lignin, cellulose, and hemicellulose (Martínez et al., 2005). The applicability of this potential for a number of biotechnological processes, for instance, as a tool for lignocellulose pretreatment in second-generation ethanol production processes, has been suggested (Lee, 1997). However, for this purpose, the degrading microorganisms should display some desirable features, such as consuming low sugar for its own growth and promoting a high lignocellulose deconstruction, to render more accessible polysaccharides for enzymatic hydrolysis and thus increase fermentable sugar yields (Kuhar et al., 2008). To date, considering these fundamentals, very few fungi have been shown to be adequate for biological pretreatment of lignocellulosic material in this kind of processes (Salvachúa et al., 2011).

The white-rot fungus *I. lacteus* can degrade different lignocellulosic substrates (e.g. corn stover, wheat straw) yielding high sugar recoveries compared to other fungal treatments (Du et al., 2011; Pinto et al., 2012; Salvachúa et al., 2011; Xu et al., 2010). This extraordinary capacity is mainly the result of a high metabolic versatility and secretory potential. While different sets of hydrolytic enzymes are implicated in this process, the proteins secreted by *I. lacteus* during the biopretreatment of a lignocellulosic substrate remains unknown.

Secretomic analysis, apart from being an excellent method to understand the biological mechanisms of lignocellulose degradation, is a valuable tool in the search for new enzymes or interesting enzyme complexes in the biofuels field (Bouws et al., 2008; Couturier et al., 2012). For this reason, publications documenting fungal secretomes have increased in recent years. Most of them have been performed with ascomycetes, and are focused on enhancing the enzymatic hydrolysis of lignocelluloses more than on the pretreatment step (Ravalason et al., 2012; Ribeiro et al., 2012; Saykhedkar et al., 2012). Among the few reports concerning basidiomycetes, nearly all have dealt with the secretome of *P. chrysosporium* grown under several culture conditions (Abbas et al., 2005; Adav et al., 2012; Sato et al., 2007; Vanden Wymelenberg et al., 2005), since the genome of this organism is available from 2004 (Martínez et al., 2004). However, due to the rapid growth of genome sequencing and the associated ability to perform protein homology searches, the secretosome database of basidiomycetes is currently enlarging. To cite some examples, the secretomes from *Pleurotus sapidus* growing in submerged cultures either on peanut shells or on glass wool (Zorn et al., 2005), *Phanerochaete*

carnosa on spruce (Mahajan and Master, 2010), *Ganoderma lucidum* on sugarcane bagasse (Manavalan et al., 2012), and *Trametes trogii* on *Populus* wood (Ji et al., 2012) have been reported.

The aim of the current work is to get a deeper understanding on the dynamics of wheat straw degradation by *I. lacteus* over the time. In addition, the secretome´s composition after 21 days of solid state fermentation (SSF) on wheat straw will be compared to that released either in liquid cultures of the same fungus or in SSF cultures of two white-rot fungi, *P. chrysosporium* and *P. ostreatus,* grown on the same substrate. These fungi were selected because data from previous studies disclosed that the wheat straw degradation patterns induced by these species, when cultured under SSF conditions, were different to those described for *I. lacteus* (Salvachúa et al., 2011). Furthermore, the secreted protein/enzyme by these two fungi when growing on wheat straw has never been analyzed before, offering the additional advantage of having their genome sequences available. Advanced proteomic technologies, such as high-throughput nano-high performance liquid chromatography-tandem mass spectrometry (nanoLC-MS/MS), have been used to provide information on the physiology, diversity, enzyme interactions, and even kinetics of the expression profiles over the time, either from whole secretomes and from proteins isolated from two dimensional (2D)-gels. Two different databases were used for protein identification. At last, some interesting enzymes and enzyme complexes for biopreatment and enzymatic hydrolysis processes can be revealed from these results.

2. MATERIALS AND METHODS

2.1. Fungal strains and culture media

The white-rot fungi used in the present study were obtained from different fungal collections. *I. lacteus* Fr. 238 617/93 was provided from the Culture Collection of Basidiomycetes from the Academy of Sciences of the Czech Republic (CCBAS, Prague). *P. chrysosporium* CBS 481.73 and *P. ostreatus* CBS 411.71 were obtained from the Centraalbureau voor Schimmelcultures (CBS, Baarn, The Netherlands). The fungal species were maintained on 2% malt extract agar (MEA) tubes at 4 ºC. Prior to the experiments, the three fungi were grown at 28 ºC during 7 days on MEA plates. Four agar plugs of 1-cm^2 were excised, inoculated into 250 mL Erlenmeyer flasks with 30 mL of growth medium (pH 5.6) and incubated at 28 ºC, and 180 rpm for 7 days. The growth medium (CSS) contained (L^{-1}): corn steep solids, 26.3 g; glucose, 40 g; $FeSO_4x7H_2O$, 0.4 g; $(NH_4)_2SO_4$, 9 g; KH_2PO_4, 4 g; $CaCO_3$, 7 g. Each culture was aseptically homogenized (Omnimixer, Sorvall), and 2.5 mL were added to 250 mL flasks with 30 mL of CSS, incubating for 5 days as described above. These cultures were

used as inocula for (1) solid state fermentation cultures (SSF) of the three fungal species and (2) submerged fermentation (SmF) cultures of *I. lacteus.*

2.2. Solid-state fermentation (SSF) cultures and secretome extraction

Wheat (*Triticum aestivum*) straw, harvested from Galicia fields (Spain) and composed of 36.9% cellulose and 23% hemicellulose (18% xylan, 3.4% arabinan, 1.1% mannan, and 0.5% galactan), was chopped into fragments smaller than 1 cm. 100 mL Erlenmeyer flasks containing two grams of this substrate and distilled water (6 mL) were autoclaved at 121 ºC for 15 min, inoculated with 5-day-old mycelium from the different fungi (2 mL) and incubated at 28 ºC as previously described (Salvachúa et al., 2011). Non-inoculated samples were kept under the same conditions to be used as controls. The cultures of *P. ostreatus* and *P. chrysosporium* were collected after 21-d incubation. *I. lacteus* cultures were sampled after 7, 14 and 21 days. Since the positive effect of Mn^{2+} addition on wheat straw biopretreatment with *I. lacteus* has been reported (Salvachúa et al., 2013b), the secretome of this fungus in the presence of this cation was also studied. $MnSO_4$ (0.3 mM) was added to wheat straw before autoclaving and then the flasks were incubated for 21-d as detailed above. All cultures were performed in duplicate. After SSF, the cultures were washed with distilled water (15 mL) at 4 ºC and 180 rpm for 2 h, and filtered under vacuum to separate the solid fraction from the water-soluble components. Liquid samples were dialyzed by centrifugation with 30 volumes of Milli-Q water using 3-kDa cutoff Amicon Ultra centrifugal filter units (Millipore Corporation) and then freeze-dried for further protein precipitation.

2.3. Submerged fermentation (SmF) cultures of *I. lacteus* and secretome extraction

Submerged cultures were performed in triplicate in 250 mL flasks with 30 mL CSS. 21-d cultures were harvested and filtered to separate the mycelium. Then the culture broth was vacuum-filtered through 0.22 μm membranes (Millipore Corporation), dialyzed against water under continuous stirring at 4 ºC in a tangential ultra-filtration system (Amicon, Millipore Corporation) using a 3-kDa cutoff membrane and freeze-dried for further protein precipitation.

2.4. Preparation of protein extracts from SSF and SmF cultures

Freeze-dried samples from SSF and SmF samples were resuspended in water and precipitated using the methanol/chloroform protocol to remove salts, sugars and other impurities (Wessel and Flugge, 1984). Briefly, cold methanol and chloroform were added to the sample tubes and centrifuged (13,000 g at 4 ºC for 15 min). The protein-interphase was washed and

centrifuged twice with methanol. Pellets were dried and resuspended in different solutions depending on the subsequent analysis method, as described below. Protein concentration was estimated using the RC DC Protein Assay kit from Bio-Rad.

2.5. Secretome analysis

Two different approaches were followed to study the fungal secretomes: (1) Two dimensional-polyacrilamide gel electrophoresis (2D-PAGE), followed by tryptic digestion of each spot and nanoLC-MS/MS analysis of the peptides and (2) shotgun analysis of the extracellular pool of proteins (EPP), consisting on the tryptic digestion of the unfractionated EPP and nanoLC-MS/MS analysis of the peptides released.

2.5.1. 2D-electrophoresis

Samples from SSF and SmF cultures were individually analyzed in 2D-gels. The instruments and products detailed in this section were purchased from Bio-Rad unless otherwise stated. Protein pellets were resuspended in a sample solution containing 7 M urea, 2 M thiourea, 4% (w/v) CHAPS, and 0.0003% (w/v) bromophenol blue. For isoelectrofocusing (IEF), 140 µL of sample solution containing around 30 µg total protein, 18.2 mM dithiotreitol (DTT), and 0.5% immobilized pH gradient (IPG) buffer solution were loaded into 7 cm non linear pH 3-10 IPG strips.

The first dimension was run in a Protean IEF Cell system as recommended by the manufacturer, using a 7-steps program (50 V for 12 h, 250 V for 1 h, 500 V for 1 h, 1000 V for 1 h, 2000 V for 1 h, 8000 V for 1 h (linear ramp) and 8000 V until 3500 V·h were reached in this step). Samples were focused for a total of 12000 V·h.

After IEF, the strips were equilibrated, and the focused proteins reduced and alkylated, by immersion for 15 min in 2 mL equilibration buffer (50 mM Tris-HCl pH 8.8, 2% [w/v] SDS, 6 M urea, 30% [v/v] glycerol) containing 52 mM dithiothreitol (DTT), and then for 15 min the same buffer containing 130 mM iodoacetamide. The strips were applied on 12% SDS-gels and the second dimension was run in a cooled Mini-Protean 3 Dodeca Cell at 0.5 watts/gel for 30 min and then at 1.5 watts/gel until the die-front reached the bottom edge (approximately 1 h). As molecular mass markers, 2 µL Precision Plus Protein Unstained Standards were used.

Gels were stained with SYPRO Ruby protein gel stain as recommended by the manufacturer. Protein identification from 2D-gels was conducted only in *I. lacteus* samples. An EXQuest Spot Cutter was used for image acquisition and spots picking. Gel pieces (1 mm^2) from 2D-spots of the 21-d SSF *I. lacteus* secretome (Fig. 1c) and the differential spots from

Mn^{2+}-supplemented cultures (Fig. 1d) and submerged cultures (Fig. 1e) were excised. Fragments were rehydrated for 45 min at 4º C with a solution containing 12.5 ng/µL sequencing grade modified trypsin (Promega) in 50 mM ammonium bicarbonate, and then incubated overnight at 30 ºC in the same solution. The supernatant was removed and kept, and the fragments washed for 20 min at room temperature with 100% acetonitrile and then with 0.5% TFA. All supernatants were pooled together, dried by vacuum centrifugation.

2.5.2. Analysis of the whole extracellular pool of proteins (EPP)

The secretomes from *I. lacteus*, *P. ostreatus*, and *P. chrysosporium* 21-d SSF cultures and from submerged cultures of *I. lacteus* contained variable amounts of pigmented substances that could interfere with the LC-MS/MS analysis of the EPP. To clean the samples, the protein pellets were dissolved in sample buffer (37.5 mM Tris-HCl pH 8, 1.5% [w/v] SDS, 1 mM EDTA, 1.96 mM DTT, 0.005% [w/v] bromophenol blue and 12.5% [v/v] glycerol). Aliquots containing around 5 µg of protein in a total volume of 15 µL were denatured at 100 ºC for 15 min and run into a 12% SDS-gel. Prestained molecular mass markers were run in parallel. All markers were individually visualized after a short run of approximately 10 min at 25 mA in the stacking gel and 7 min at 20 mA in the resolving gel, and then the electrophoresis was stopped and the gel stained with Colloidal Blue Stain (Invitrogen). The protein gel fragment was horizontally cut into 3 similar fragments, which were excised into small pieces (1 mm^2), destained, and reduced and alkylated as previously described. After washing and drying, the three samples were separately digested with trypsin as explained before, and then pooled again to analyze the tryptic peptides mixture. Prior to identification, samples were purified with C18-ZipTips (Millipore Corporation), eluting with 70% acetonitrile in 50 mM ammonium bicarbonate, and dried by vacuum centrifugation.

2.5.3. Peptides analysis by nanoLC-MS/MS

Peptide mixtures from enzymatic digestions were dissolved in 5 µL buffer A (0.1% formic acid, 2% acetonitrile), and analyzed by nanoLC-MS/MS in a nanoEasy-HPLC (Proxeon) coupled to a nanoelectrospay ion source (Proxeon). Peptides were loaded onto a C18-A1 2 cm-precolumn (Thermo Scientific EASY-Column) and then eluted onto a Biosphere C18 capillary column (inner diameter 75 µm, 16 cm long, 3 µm particle size, Nanoseparations) at a flow-rate of 250 nL/min. Spots from 2D-gels were separated using a 60 min gradient using Buffer B (0.1% formic acid in ACN): 40 min from 0-35% Buffer B, 5 min from 35-45% Buffer B. For shotgun analysis, the peptides from EPP digestions were eluted with a 100

min gradient (55 min from 0-35% Buffer B, 16 min from 35-45% Buffer B). Mass spectra were acquired on an LTQ-Orbitrap Velos (ThermoScientific) in the positive ion mode. Full-scan MS spectra (m/z 300-1700) were acquired with a target value of 1,000,000 ions at a resolution of 60,000 at m/z 400. The 15 most intense ions were selected for collision induced dissociation (CID) fragmentation in the LTQ Velos with a target value of 10,000 and normalized collision energy of 38%. Precursor ion charge state screening and monoisotopic precursor selection were enabled. Singly charged ions and unassigned charge states were rejected. Dynamic exclusion of 30 s duration with a repeat count of 1 was enabled. Mass spectra files were searched against databases from Uniprot (http://www.uniprot.org/) and the Joint Genome Institute (JGI) (http://genome.jgi.doe.gov/programs/fungi/index.jsf) using the SEQUEST and MASCOT search engines through Thermo Proteome Discoverer (VERSION 1.3.0.339, Thermo). Search parameters included a maximum of two missed cleavages allowed, carbamidomethylation of cysteines as a fixed modification and oxidation of methionine as a variable modification. Precursor and fragment mass tolerance were set to 10 ppm and 0.8 Da, respectively. The peptides were validated through the algorithm Percolator (FDR 0.05) and only those with high and medium confidence were admitted. Unless otherwise specified, protein identifications were accepted if they contained at least two identified peptides.

Basidiomycota databases from Uniprot and JGI were used for *I. lacteus* homology queries since there is not a complete database of this fungus. Only 16 protein entries from *I. lacteus* are included in Uniprot, and none in JGI, which contains information from whole genomes of 74 basidiomycetes. In contrast, specific databases of *P. chrysosporium* and *P. ostreatus* from JGI and Uniprot were used for further peptide identification.

3. RESULTS AND DISCUSSION

The most significant hits from the proteins isolated from the 2D-gels, in terms of score and sequence coverage from both databases, are gathered in Supplementary Table S1. Protein identities provided on the basis of a single matching peptide, were considered as tentative. The functional classifications of the proteins identified from EPP analyses, from JGI and Uniprot databases, are collected in Supplementary Tables S2-S9.

Before discussing the experimental results, some general considerations should be laid down. In the case of 2D-gels, MS/MS analyses showed that a protein can be identified in several independent spots. In some cases this observation may be the result of the coexistence of different isoenzymes or closely related gene products (Yang et al., 2012), but the presence of protein fragments from proteolytic cleavage

(Vinzant et al., 2001) cannot be ruled out. In fact, some extracellular proteases, which may have digested susceptible proteins either in cultures or during sample preparation, have been identified in the present work. In addition, some spots contain more than one molecular species. A probably cause is co-migration of protein fragments with other full length proteins. It is also possible due to streaking of proteins observed in certain areas of the gels, presumably due to the impossibility of getting completely rid of a pigmented material contained in the extracts produced under SSF conditions. Additionally, it is worth mention that the correlation of the predicted molecular mass (MM) and/or pI of the hits with the values deduced from gels for each spot is not always accurate. This can be due to (1) a differential pattern of post-translational modifications, such as glycosylation, and (2) a match with a homologous protein from a different species.

3.1. Secretome of *I. lacteus* growing on wheat straw

3.1.1. Comparative analysis of the proteins secreted over the time

I. lacteus is a fungus which degrades simultaneously all components of wheat straw (Table 1). The biopretreated product keeps high sugar concentration with improved accessibility for further enzymatic hydrolysis aimed to second-generation ethanol production (Salvachúa et al., 2011). In order to study the major enzymes involved in the degradation of wheat straw and to investigate their variations over the time, the secretome of *I. lacteus* after 7, 14, and 21-d SSF was isolated and a comparative analysis, using 2D-PAGE, was performed.

The spot pattern proved to be highly reproducible in replicate cultures. Strips spanning a pH range of 3-10 were chosen for the first dimension (IEF) to view the entire picture of the secretome over the three weeks of incubation (Fig. 1a-c). Gels from control cultures (without fungi) did not show any spot (data not shown). Most proteins focused in a pH range of 3-6 and had molecular masses from 37 to 100 kDa, a profile similar to those reported for other basidiomycetes (Sato et al., 2007).

The evolution of enzymes release, concerning both the number of different molecular species and the amount of the proteins detected at different growth stages (7, 14 and 21-d), can be observed by simple visual inspection of the gels images (Fig. 1a-c). The one from the 21-d secretome did not only display the maximum spots number, but also contained all spots detected in the gels of samples from 7-d and 14-d SSF. Then, the spots from the 21-d gel (Fig. 1c), were chosen to be excised, in-gel digested, and subjected to MS/MS analysis for protein identification.

Table 1. Summary of cellulose (CEL), hemicellulose (HEM), and lignin (LIG) losses from wheat straw caused by fungal biopretreatments (SSF) during different incubation periods. Digestibility and sugar recoveries from biopretreated wheat straw are also shown. GLU= Glucose; XYL= Xylose; IL= *I. lacteus*; PC= *P. chrysosporium*; PO = *P. ostreatus.*

Fungus	Day	Loss (%)			Digestibility (%)		Sugar yields (%)		References
		CEL	HEM	LIG	CEL	HEM	GLU	XYL	
IL	7	9±0	13±7	11±0	28±4	32±8	24±2*	28±7*	(Salvachúa et al, 2011)
IL	14	17±1	13±4	27±1	56±6	71±5	46±1	61±1	(Salvachúa et al, 2011)
IL	21	21±2	23±2	36±1	78±4	78±2	62±2	61±4	(Salvachúa et al, 2013b)
IL + Mn^{2+}	21	18±1	45±6	38±1	82±3	99±8	68±2	55±6	(Salvachúa et al, 2013b)
PC	21	35±0	70±24	0±0	15±0	22±0	9±0*	7±6*	(Salvachúa et al, 2011)
PO	21	22±1	52±13	27±1	55±3	52±8	42±3	30±9	(Salvachúa et al, 2011)

*These values were below those obtained from non-biopretreated wheat straw.

Most of the hits that allowed the identification of *I. lacteus* proteins were from Uniprot except spot 27, which was not identified in this database, although the Basidiomycota database from JGI indicated homology with a serine-type peptidase (Table 2). Concerning the secretome composition over the time, 70% of the spots were already produced during the first week of incubation (Fig. 1a). The major enzymes at this stage (Table 2) were involved in cellulose (endoglucanases and exocellulases), hemicellulose (acetyl xylan esterases and endo-1,4-β-xylanase), and protein degradation (proteases), and their functions are explained below. It is worth pointing out that for complete cellulose degradation, the concerted action of three cellulolytic activities is required: endoglucanases, which hydrolyze internal 1,4-β-bonds, cellobiohydrolases, which act on chain ends of poly- or oligosaccharides releasing cellobiose, and β-glucosidases, that finally break cellobiose into two glucose monomers (Abbas et al., 2005). The latter enzyme was not detected in these 2D-gels. This may possibly explain the relatively lower extent of sugar consumption of *I. lacteus* during its growth on wheat straw. Cellobiohydrolases I and II (CBHI and CBHII) act, in a synergistic way, as exo-cellulases (Barr et al., 1996) from the reducing and the non-reducing end of the glucidic chain, respectively (Vanden Wymelenberg et al., 2005). The acetyl xylan esterase cleaves acetyl side groups from the hetero-xylan backbone and endo-1,4-β-xylanase hydrolyzes internal 1,4-β bonds of xylan (Sánchez, 2009). As occurred with cellulose, these enzymes cannot degrade hemicellulose or xylan polymers completely since β-xylosidases, arabinofuranosidases, or α-glucuronidases, which are also required (van den Brink and de Vries, 2011), were not produced by the fungus. Finally, proteases, as polyporopepsin, have been implicated in the activation of

cellulases, in the cleavage of functional domains of cellobiose dehydrogenases (CHD) (Kersten and Cullen, 2007), and also in trapping nitrogen in lignocellulose under nitrogen-starvation conditions (Sato et al., 2007). Most extracellular fungal enzymes are relatively resistant to proteases, and several activities have been detected even after 1-month incubation in the extracellular fungal protein mixture (Sato et al., 2007).

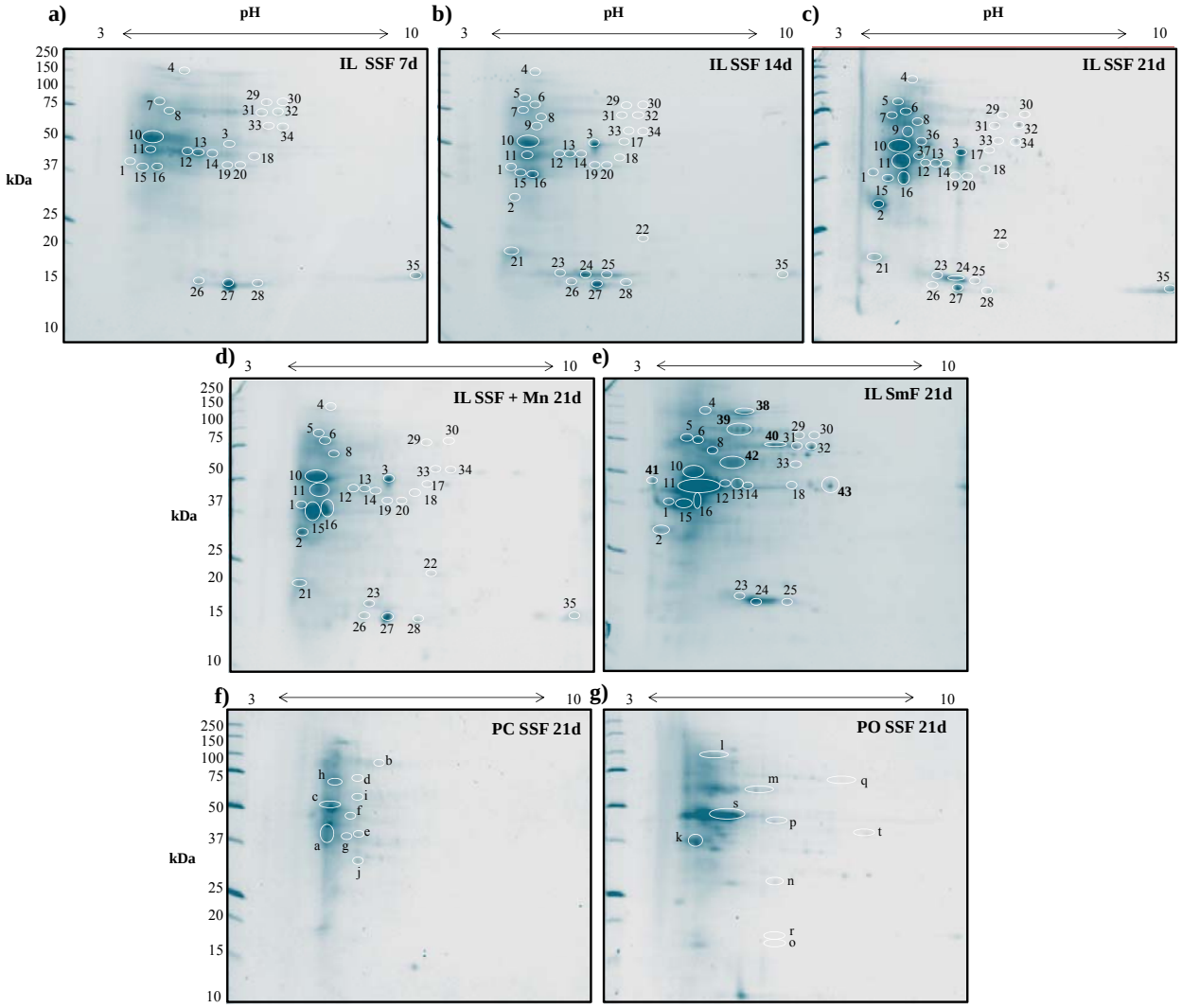

Fig. 1. 2D-gel images from *I. lacteus* secretomes released under SSF conditions on wheat straw for (a) 7-d, (b) 14-d, (c) 21-d, (d) 21-d with Mn^{+2} supplementation. (e) 2D-gel images of *I. lacteus* secretomes from 21-d submerged cultures. 2D-gel images from (h) *P. chrysosporium* and (i) *P. ostreatus* secretomes produced in SSF on wheat straw at 21-d. The spots analyzed are numbered on the gels and the proteins identified, detailed in Table 2. Alphabetic characters in gels (f) and (g) correspond to the proteins listed in Table 3. SSF= solid state fermentation on wheat straw; SmF= submerged cultures in CSS.

Table 2. Protein identification from 2D-gel spots (Fig. 1) of the secretomes from *I. lacteus* in SSF and SmF cultures. Only the hits with maximal score from Uniprot database are shown. UP= Unique peptides.

Spot	Day[1]	SmF[2]	Mn[3]	Predicted protein function	Species	Protein ID	MM (kDa)	pI	Score	UP
1	7			Cellobiohydrolase II	*I. lacteus*	B2ZZ24	47.2	5.3	**20.6**	4
2	14			Cellulase	*I. lacteus*	Q9Y724	55.8	4.6	**13.9**	3
3	7	x		Rhamnogalacturonan-hydrolase	*I. lacteus*	B6E8Y7	46.7	6.9	**17.4**	3
4	7			Cellobiohydrolase	*I. lacteus*	Q75NB5	54.8	5.3	**15.4**	4
5	14	x		Cellulase	*I. lacteus*	Q9Y724	55.8	4.6	**215.8**	10
6	14			Cellulase	*I. lacteus*	Q9Y724	55.8	4.6	**85.3**	7
7	7	x	x	Cellulase	*I. lacteus*	Q9Y724	55.8	4.6	**139.4**	11
8	7			Cellobiohydrolase	*I. lacteus*	Q75NB5	54.8	5.3	**66.7**	8
9	14	x	x	Cellobiohydrolase II	*I. lacteus*	B2ZZ24	47.2	5.3	**90.9**	7
10	7			Cellobiohydrolase II	*I. lacteus*	B2ZZ24	47.2	5.3	**46.0**	7
11	7			Cellobiohydrolase II	*I. lacteus*	B2ZZ24	47.2	5.3	**25.2**	5
12	7	x		Endoglucanase	*I. lacteus*	Q5W7K4	42.2	4.9	**15.4**	3
13	7			Acetyl xylan esterase	*P. chrysosporium*	H2ESB9	38.9	6.5	**12.9**	2
14	7			Acetyl xylan esterase	*P. chrysosporium*	H2ESB9	38.9	6.5	**15.5**	2
15	7			Polyporopepsin	*I. lacteus*	P17576	35.0	4.7	**20.0**	5
16	7			Aspartic protease	*Pholiota nameko*	G3XKT3	42.8	5.5	**70.0**	2
17	14	x		Rhamnogalacturonan-hydrolase	*I. lacteus*	B6E8Y7	46.7	6.9	**27.3**	6
18	7	x		Acetyl xylan esterase	*P. chrysosporium*	H2ESB9	38.9	6.5	**27.9**	2
19	7	x		Cellobiohydrolase II	*I. lacteus*	B2ZZ24	47.2	5.3	**4.1**	2
20	7	x		Endo-1,4-β-xylanase A (*)	*P.chrysosporium*	Q9HEZ1	43.5	5.4	**3.1**	1
21	14	x		Putative protein hypP2 (*)	*Moniliophthora perniciosa*	Q6U7U4	47.9	8.7	**6.1**	1
22	14	x		Putative uncharacterized protein hypP2 (*)	*Moniliophthora perniciosa*	Q6U7U4	47.9	8.7	**6.0**	1
23	14			Aspartic protease (*)	*Pholiota nameko*	G3XKT3	42.8	5.5	**3.9**	1
24	14		x	Aspartic protease (*)	*Pholiota nameko*	G3XKT3	42.8	5.5	**3.7**	1
25	14		x	Putative protein (*)	*Puccinia graminis*	E3JYE0	21.2	6.3	**2.7**	1
26	7	x		Aspartic protease (*)	*Pholiota nameko*	G3XKT3	42.8	5.5	**3.9**	1
27	7	x		Serine-type peptidase(*)(**)	*Punctularia strigosozonata*	Punst1 106327	59.2	4.9	**53.1**	1
28	7	x		Putative protein hypP2 (*)	*Moniliophthora perniciosa*	Q6U7U4	47.9	8.7	**5.6**	1
29	7	x		Cellulase	*I. lacteus*	Q9Y724	55.8	4.6	**9.1**	2
30	7	x		Cellobiohydrolase (*)	*I. lacteus*	Q75NB5	54.8	5.3	**2.7**	1
31	7		x	Cellobiohydrolase	*I. lacteus*	Q75NB5	54.8	5.3	**12.9**	2
32	7		x	Cellobiohydrolase	*I. lacteus*	Q75NB5	54.8	5.3	**6.3**	2
33	7			Cellobiohydrolase II	*I. lacteus*	B2ZZ24	47.2	5.3	**14.2**	3
34	7	x		Cellobiohydrolase II (*)	*I. lacteus*	B2ZZ24	47.2	5.3	**8.5**	1
35	7	x		Histone H4 (Fragment) (*)	*Moniliophthora perniciosa*	E2LLY3	8.8	11.6	**5.1**	1
36	21	x	x	Cellobiohydrolase II	*I. lacteus*	B2ZZ24	47.2	5.3	**37.1**	6
37	21		x	Endoglucanase	*I. lacteus*	Q5W7K4	42.2	4.9	**63.1**	3
38	L		x	GH3/ β-glucosidase	*Serpula lacrymans*	F8PMW3	78.3	4.7	**63.3**	4
39	L		x	Putative protein (*)	*Moniliophthora perniciosa*	E2M3P0	13.2	4.7	**3.4**	1
40	L		x	Glyoxal oxidase* (*)	*Punctularia strigosozonata*	Punst1 68820	59.6	5.2	**1.9**	1
41	L		x	Polyporopepsin	*I. lacteus*	P17576	35.0	4.7	**25.6**	2
42	L		x	Exo-β-(1→3)-galactanase	*I. lacteus*	B9ZZS1	16.8	47.8	**6.7**	4
43	L		x	Mannose-6-phosphatase	*P. chrysosporium*	Q281W3	38.4	6.6	**71.6**	4

(1) Incubation time in which the spot was first detected. L=differential spots for SmF cultures.
(2) The cross indicates the absence of the spot in SmF cultures.
(3) The cross indicates the absence of the spot in SSF cultures on wheat straw supplemented with a manganese salt.
(*) Proteins identified from a single peptide matching.
(**) Proteins identified only using the JGI database.

After the second SSF week, almost all spots from the major proteins detected at the final incubation period were visualized (Fig. 1b). Rhamnogalacturonan-hydrolase (spot 17) and different isoforms of cellulases (spots 2, 5, 6, 9) were produced. A very faint spot from pectinase was first observed in 7-d gels (spot 3), but an intense secretion of this protein was detected from two incubation weeks onwards. Pectin content in lignocellulosic materials is low (Sato et al., 2007), but the increased expression of this enzyme suggests some relevant role during *I. lacteus* colonization and degradation. No other pectinases were identified in the samples, which is in good agreement with the fact that this fungus is adapted to degrade decaying biomass (Ravalason et al., 2012). In parallel, many small-sized proteins came into view. The JGI database matched some of them (spots 21, 22, 25, and 28) to cerato-platanin or Barwin-related endoglucanases. These proteins, secreted by a number of non-pathogenic and pathogenic fungal species when interacting with plant or animal cells, are involved in cell wall biogenesis or degradation (de Oliveira et al., 2011).

In the 21-d secretome, two new spots (36, 37) were observed, matching respectively with CBHII and endoglucanase (Table 2). A total of 37 spots and 18 different proteins were identified. The protein spot intensity of some cellulases (spots 2, 5, 6, 7, 8, 9, and 11) and an aspartic proteinase (spot 16), probably similar to the polyporopepsin and other aspartic proteases were already detected in the 14-d SSF samples, were much more intense in the older 21-d sample.

The proteins identified using both databases (Table S1) are in good agreement in most cases, and the presence of several proteins in some spots insufficiently separated in the gel can be inferred from the data displayed in this table. For example, spot 10, heavily stained in all gels (Fig. 1a-c) probably contains a mixture of proteins. The hits returned with maximal scores from JGI and Uniprot corresponded to MnP and CBHII, respectively, suggesting that both proteins are present in the crude and migrate together. MnP catalyzes the cleavage of C-C and C-O bonds of the lignin polymer (Sánchez, 2009) and this enzyme activity is frequently found in lignocellulose-degradation processes by *I. lacteus* (Novotny et al., 2009).

3.1.2. Analysis of the 21-d I. lacteus *EPP*

The analysis of the secretome released after growing *I. lacteus* on wheat straw for 21-d using a shotgun proteomics approach was an excellent complement to confirm the data from 2D-gels and disclose the presence of extracellular proteins virtually undetectable by other techniques. The results from the search against the basidiomycota database of Uniprot

(Table S2) identified 37 proteins, of which 11 hits corresponding to *I. lacteus* enzymes. Most of them are involved in lignocellulose degradation and were functionally classified, according to their biological role, such as glycoside hydrolases (GHs), oxidoreductases, esterases, proteases, phosphatases, and proteins with other or unknown functions (Fig. 2). The 45 hits identified from the search using the JGI database (Table S3) corresponded to enzymes from related basidiomycetes, with similar functionalities to those returned by Uniprot.

Table 3 summarizes the ten extracellular proteins (Top-10) identified with maximal scores from Uniprot database. This set of proteins rather agree with the most intense spots in 2D-gels (e.g. CBHII, cellulases, and proteases had the highest scores and spot intensities, respectively) and was in accordance with previous reports comparing both methodologies (Espino et al., 2010). However, some new proteins were identified that may be relevant in the application of enzymatic decay of wheat straw. Among them, a melanin-decolorizing enzyme, whose role in fungal plant infection (Butler and Day, 1998b) and in resistance to environmental and chemical agents (Butler and Day, 1998a) were reported, an exo-β-1→3 galactanase, implicated in hemicellulose degradation and isolated by Tsumuraya et al. (1990) from this fungus, and a hypothetical peroxidase (cpop21) from the Polyporaceae family, can be highlighted. A recent report from Salvachúa et al. (2013a) described the isolation from *I. lacteus* liquid cultures of a dye-decolorizing peroxidase (DyP), able to degrade azo- and antroquinone-dyes and phenolic and non-phenolic compounds. The protein was purified and analyzed by MALDI-TOF-MS/MS, giving 95% homology with cpop21. Our results here show for the first time its production during SSF on wheat straw, a natural lignocellulosic environment.

Several minor proteins were also detected when the EPP was analyzed by nanoLC-MS/MS. The most significant were glyoxal oxidase (which is a copper radical oxidase) and CDH (Tables S2 and S3). These two enzymes are oxidoreductases able to produce the H_2O_2 required for the action of extracellular peroxidases (Vanden Wymelenberg et al., 2005; Zorn et al., 2005). Moreover, CDH has also been implicated in: generating Fe^{2+} *via* Fenton chemistry, thus producing highly reactive hydroxyl radicals (Vanden Wymelenberg et al., 2005), binding cellulose, which probably enhances cellulase activities by relieving product inhibition (Kersten, 2007), and preventing phenoxy radical-dependent re-polymerization of lignin (Abbas et al., 2005). Finally, other hits corresponded to putative uncharacterized proteins whose functions, still unknown, could be assumed to be related to lignocellulose degradation.

Table 3. Summary of the ten extracellular proteins (Top-10) identified with maximal scores, from the shotgun analysis of the secretomes investigated in the present work, using the Uniprot database. UP= unique peptides.

EPP[1]	Predicted protein function	Species [2]	Uniprot ID	MM (kDa)	pI	Score	UP	Spots [3]
IL SSF	Cellobiohydrolase II	IL	B2ZZ24	47.2	5.3	606.0	13	1,9,10,11,19,33,34
	Polyporopepsin	IL	P17576	35.0	4.7	307.2	8	15,16
	Cellulase	IL	Q9Y724	55.8	4.6	193.3	9	2,5,6,7,29
	Acetyl xylan esterase	PC	H2ESB9	38.9	6.5	142.2	2	13,14,18
	Melanin-decolorizing enzyme	Ce	B3IWB3	38.3	5.1	142.1	10	10
	Peroxidase cpop21 (DyP) *	IL	P87212	53.9	5.0	122.2	8	6
	Endoglucanase	IL	Q5W7K4	42.2	4.9	118.3	3	12
	Cellobiohydrolase	IL	Q75NB5	54.8	5.3	106.0	11	4,8,30,31,32
	Exo-β-(1→3)-galactanase	IL	B9ZZS1	47.8	6.7	99.8	8	10
	Rhamnogalacturonan-hydrolase	IL	B6E8Y7	46.7	6.9	84.5	10	3,17
IL SmF	Polyporopepsin	IL	P17576	35.0	4.7	4867.5	13	15
	Peroxidase cpop21*	IL	P87212	53.9	5.0	684.8	13	6
	Melanin-decolorizing enzyme	Ce	B3IWB3	38.3	5.1	368.6	11	10
	Exo-β-(1→3)-galactanase	IL	B9ZZS1	47.8	6.7	202.2	11	10,42
	Ribonuclease T2	IL	Q8LW55	41.8	5.1	137.4	4	--
	Glycoside hydrolase family 3	SL	F8NLG7	89.6	5.0	130.3	1	38
	Glycoside hydrolase family 3	SL	F8PMW3	78.3	4.7	111.6	2	38
	Mannose-6-phosphatase	PC	Q281W3	38.4	6.6	87.5	3	43
	Aspartic protease	PN	G3XKT3	42.8	5.5	63.7	3	16,23,24,26
	Manganese peroxidase 3	LG	H2D7E4	38.6	4.5	56.7	3	10
PC SSF	Manganese peroxidase isozyme 3	PC	Q1K9D0	39.8	4.6	348.7	8	a
	Glucan 1,3-β-glucosidase	PC	Q2Z1W1	82.0	5.8	327.6	8	b
	Cellulase	PC	Q7LIJ0	53.8	4.9	286.6	13	c
	Copper radical oxidase	PC	Q0ZKA8	67.8	5.5	265.8	11	d
	Endo-1,4-β-xylanase A	PC	Q9HEZ1	43.5	5.4	209.8	4	e
	Cellobiohydrolase II (Fragment)	PC	H3K419	46.3	5.1	189.6	6	f
	Endo-1,4-β-xylanase C	PC	B7SIW2	42.3	4.9	151.9	6	g
	Family S53 protease	PC	Q281W2	58.4	4.9	133.8	3	h
	Exoglucanase 1	PC	P13860	54.8	5.5	117.1	7	i
	Endo-β-glucanase	PC	C6H0M6	33.6	5.4	113.8	6	j
PO SSF	Manganese peroxidase	PO	G8FPZ2	38.5	4.7	629.7	8	k
	Subtilisin-like protease	PO	Q6ZYK6	93.2	5.3	330.3	11	l
	Laccase	PO	Q96TR4	57.4	6.1	284.1	9	m
	Putative uncharacterized protein	PO	D2JY75	27.8	6.6	162.8	7	n
	Peptidyl-Lys metalloendopeptidase	PO	P81055	17.9	6.2	118.5	5	o
	Ribonuclease T2	PO	Q75NB1	41.5	6.4	65.1	4	p
	α-L-arabinofuranosidase	PO	G0TES6	68.9	8.1	52.2	3	q
	Putative aspartyl-proteinase (Fragment)	PO	Q96TV7	18.5	6.2	51.8	3	r
	Cellulose 1,4-β-cellobiosidase	PO	A5AA53	49.3	5.6	50.6	4	s
	Peptidase 1	PO	C4PFY6	38.7	8.2	42.4	2	t

(1) IL= *I. lacteus;* PC= *P. chrysosporium;* PO= *P. ostreatus*; SSF= solid-state fermentation; SmF= submerged cultures

(2) Abbreviation for other species: Ce= *Ceriporiopsis* sp.; SL= *Serpula lacrymans;* PN= *Pholiota nameko;* LG= *Lenzites gibbosa.*

(3) Spot numbers where the protein was detected with maximal score (Table S1). In PC and PO, proteins were traced in the gel on the basis of their theoretical pI and MM, and marked by letters.

***** This protein was recently isolated from *I. lacteus* and characterized as DyP (Salvachúa et al., 2013a).

3.2. Secretome of *I. lacteus* growing on different culture conditions

3.2.1. Secretome of I. lacteus *growing on Mn^{2+}-supplemented wheat straw*

The supplementation with Mn^{2+} during *I. lacteus* pretreatment is known to improve the enzymatic hydrolysis yields of different lignocellulosic substrates, such as wheat straw (Table 1) and corn stover (Salvachúa et al., 2013b; Song et al., 2012). In this study, a 2D-PAGE differential analysis of the enzymes secreted by *I. lacteus,* growing for 21-d on wheat straw supplemented or not with a Mn^{2+} salt, was performed (Fig. 1d and 1c). The enzymatic profiles were similar in both cases, and new spots were not observed. However, some proteins were missing in cultures with added Mn^{2+}. Most of them (spots 7, 9, 31, 32, 36, 37) corresponded to cellulose-degrading enzymes. In parallel, spot 15 which was identified as polyporopepsin in 2D-gels of 21-d SSF basal cultures was intensely stained indicating either an increased secretion of this protein or the release of a different enzyme that co-migrated with the peptidase. In addition, the MM and pI of the overexpressed protein coincided with those reported for a MnP from *I. lacteus* (Shin et al., 2005). This spot was excised from the gel of the Mn^{2+}-supplemented culture, digested, and analyzed. A mixture of polyporopepsin and a MnP were identified, both with scores around 50, indicating that, as expected, this enzyme was induced by Mn^{2+} (Bonnarme and Jeffries, 1990).

3.2.2. Secretome of I. lacteus *growing in submerged cultures*

The enzyme production in a non-lignocellulosic medium mimicking N- and C-deficient culture conditions was studied in SmF cultures with CSS medium at long incubation times (21-d). Moreover, higher amount of *I. lacteus* biomass was produced in CSS when compared to other synthetic media (Salvachúa et al., 2013b). The extracellular enzymatic pattern was examined using the same proteomic tools previously applied for SSF secretomes: 2D-gels, followed by tryptic in-gel digestion and MS/MS identification of the differential spots, and direct LC-MS/MS analysis of the tryptic peptides mixture from the whole EPP.

The enzyme pattern in SmF (Fig. 1e) was not very different from that observed on SSF (Fig. 1c). Whereas many cellulases, CBHs, and proteases were produced under both culture conditions, six new intense spots emerged in SmF (spots 38-43), whose identities are given in Table 2. Among them, the most heavily stained (spot 38) matched with a β-glucosidase. As previously described, this enzyme is involved in the complete hydrolysis of cellulose to glucose and was not detected when the fungus was grown under SSF conditions. Mannose-6-phosphatase (spot

43), which has been shown to be involved in the extracellular dephosphorylation of LiP isozymes from *P. chrysosporium* in carbon-starved cultures (Vanden Wymelenberg et al., 2006), was also produced. In contrast, the spots corresponding to rhamnogalacturonan-hydrolases, endo-1,4-β-glucanases, endo-1,4-β-xylanases, some cellulases, and CBHII were missing in SmF cultures (Table 2). Obviously, the production of such a wide battery of cellulases and hemicellulases is not required in a medium without lignocellulose. As expected, spots 21, 22, and 28 from ceratoplatanins neither appeared. LC-MS/MS identification of the proteins from the whole EPP (Tables S4 and S5), revealed the secretion of minor amounts of rhamnogalacturonase, exo-β-1,3-glucanase and subtilisin-like protease. In general, there was a good agreement between the results obtained from 2D-gels and those found by EPP shotgun analysis. The ten extracellular proteins (Top-10) identified with maximal scores using Uniprot database are presented in Table 3. Three enzymes were strongly induced in SmF cultures: (1) polyporopepsin, which can be implicated in protein degradation, supplying nitrogen for fungal growth, (2) the ribonuclease T2, that can be excreted in response to phosphate starvation and consequently for phosphate scavenging from RNA (MacIntosh, 2011), and (3) the peroxidase cpop21 (currently identified as DyP), which can be produced to oxidize more complex molecules to be used as energy/nutrient source. All of these enzymes have probably been secreted as a fungal response to survive in a medium poor in essential nutrients. A similar behavior has been previously reported for *Pleurotus sapidus* in SmF cultures, being peptidolytic and ligninolytic enzymes the major components of its secretome (Zorn et al., 2005).

The relative representation of each enzyme family (%) in SSF and SmF cultures (Fig. 2) was not very dissimilar, although the former contained a few more GHs and less oxidoreductases than the latter. In fact, the diversity of oxidoreductases was identical in both cases (Tables S2-S4). Comparable expression patterns were also described (Sato et al., 2007) for *P. chrysosporium* growing in SmF (containing cellulose) and SSF cultures on wood. In contrast, Zorn et al. (2005) reported that the production of ligninolytic enzymes by *P. sapidus* was really influenced by the presence of some lignocellulosic inductors.

3.3. Comparative study of the *I. lacteus*, *P. ostreatus*, and *P. chrysosporium* secretomes growing on wheat straw

3.3.1. Fungi, databases, and degradation patterns

The secretome from 21-d *I. lacteus* SSF cultures was compared to those from two white-rot fungi, *P. chrysosporium* and *P. ostreatus*. The growth of these species on wheat straw produced different degradation patterns,

and the biotreated material gave sugar yields lower than those attained for *I. lacteus* after enzymatic hydrolysis (Table 1). As in the previous experiments, the extracellular proteins were separated by 2D-PAGE or directly digested and analyzed by LC-MS/MS without prior fractionation. The genomes of these species have been sequenced and are fully available from the JGI database. Then, proteins were identified from the shotgun analyses.

The MS/MS data were searched against the two databases, and each protein list was organized in order to classify the enzymes in different functional groups (Tables S6-S9). In all cases, the JGI database returned more hits than Uniprot (Fig. 2). This is because many hypothetical proteins, deduced from genomic sequences already available, are deposited in that database. Moreover, the percentages yielded for some protein groups were quite different when the inputs from both databases were compared. This is probably due to the fact that many proteins from the JGI have not been annotated yet, and may need to be corrected.

Even higher differences were found when the number of proteins identified was compared to those predicted from genomes. A total of 769 proteins have been predicted to be part of *P. chrysosporium* secretome (Vanden Wymelenberg et al., 2006). However, in the current work, 4-fold fewer proteins were detected (around 191). This highlights the need of studying secretomes from cultures and not by computational predictions, since the protein set released to the extracellular medium is variable and depends on the environment.

The percentages for the diverse functional groups returned by Uniprot (Fig. 2) moderately correlated with the different fungal degradation patterns. *P. chrysosporium*, which showed a preferential consumption of carbohydrates during biopretreatment of wheat straw (Table 1), mostly produced GHs (enzymes involved in cellulose and xylan degradation). Actually, the secretome from *P. chrysosporium* showed to be more similar to those typical of ascomycetes (e.g. *Fusarium verticilloides* and *Ustilago maydis*) than to those from the basidiomycetes included in this study, suggesting that it could be used for improving enzymatic saccharification of wheat straw (Couturier et al., 2012; Ravalason et al., 2012).

On the contrary, *P. ostreatus* produced less GHs than oxidoreductases (Fig. 2h), what can be related to the selectivity towards lignin degradation of *Pleurotus* species (Salvachúa et al., 2011). Among its Top-10 proteins, an α-L-arabinofuranosidase was identified. The action of this enzyme could be crucial to improve hemicellulose and lignin removal since in wheat straw most lignin is directly linked through ether linkages to arabinosyl side chains of xylans (Ren and Sun, 2010). The lignin, once released from

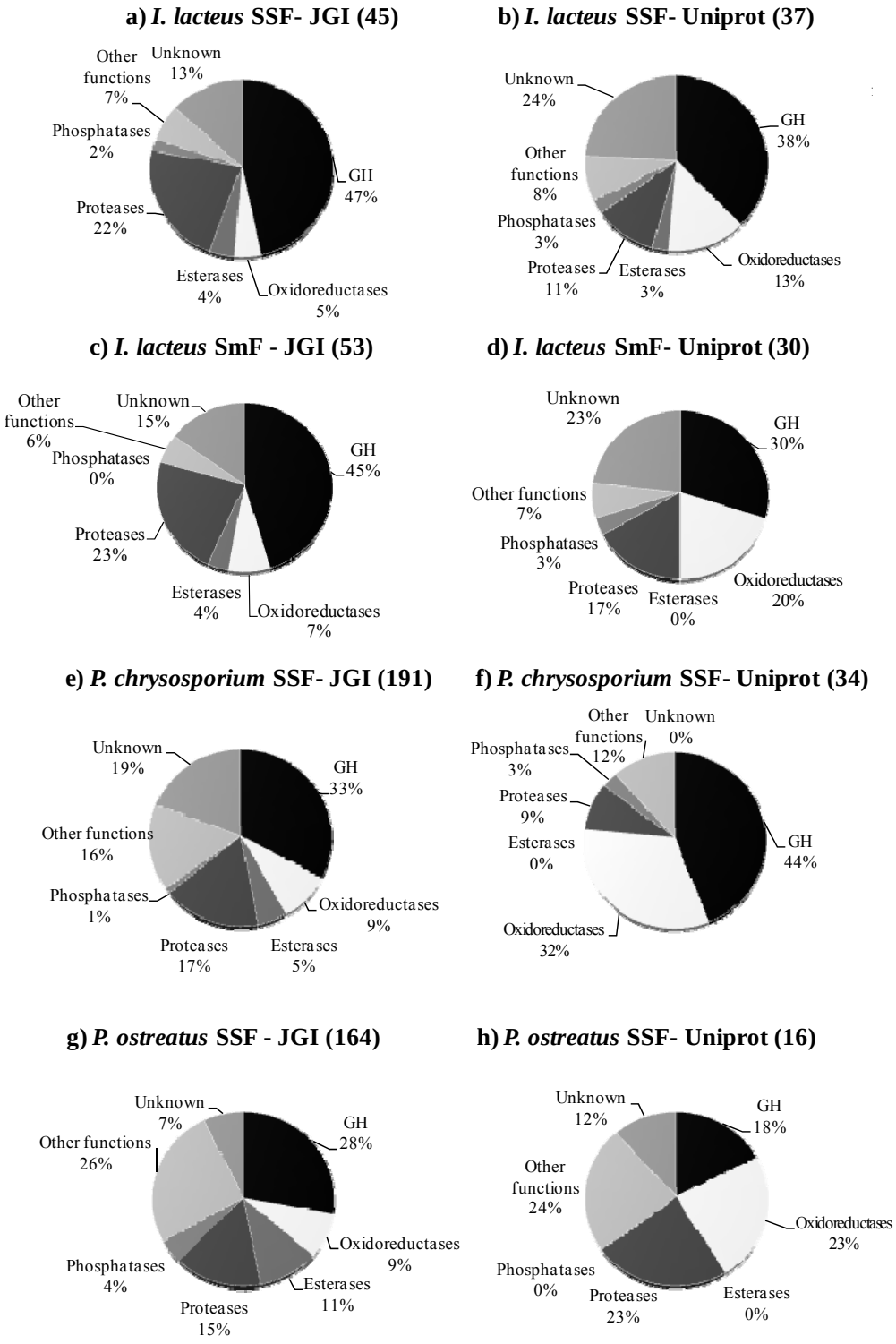

Fig. 2. Functional classification of the lignocellulose-degrading enzymes found in the secretomes analyzed. The total number of protein matches from JGI and Uniprot databases (Tables S2-S9) is shown in parenthesis. Basidiomycota databases were used for *I. lacteus* secretome searches. The results from *P. chrysosporium* and *P. ostreatus* were searched against their own databases. SSF= solid state fermentation on wheat straw; SmF= submerged cultures in CSS; GH= glycosyl hydrolases.

the hemicellulose anchor, would be more accessible for the extracellular oxidoreductases.

Finally, although *I. lacteus* released a percentage of GHs similar to *P. chrysosporium,* the amount of extracellular oxidoreductases was lower, inducing the simultaneous degradation of all lignocellulosic components (Table 1). Nevertheless, some proteins were detected in the secretomes from the three fungi such as esterases, proteases, and phosphatases. Proteases, whose role has usually been neglected when studying the decay of lignocellulosic substrates, have been found among the Top-10 proteins of all fungi, seeming to have a great significance for the wheat straw deconstruction. Moreover, plant proteins have an incredibly diversity and may need a diverse pool of proteases for its degradation (Espino et al., 2010). Nitrogen is the limiting nutrient in woody biomass and thus the acquisition of nitrogen through the action of proteases may be central toward growth.

The Top-10 proteins (Table 3) from *P. chrysosporium* and *P. ostreatus* were directly traced on their respective 2D-gels according to MM and pI (Fig. 1f and 1g). A similar protein distribution has been described from these white-rot fungi growing in minimal medium (Fragner et al., 2013). As measured by the spots intensity, MnPs (spots a, k) and cellulases (spots c, s) were the major protein types secreted by *P. chrysosporium* and *P. ostreatus.* In contrast, *I. lacteus* released more CBHs (spots 10, 11) and polyporopepsine (spots 15, 16). Comparison of the two techniques applied to analyze fungal secretomes showed that direct analysis of the unfractionated EPP by nanoLC-MS/MS provided much more information and allowed a better description of the different fungal degradation patterns. Moreover, in view of all these results, it can be concluded that the knowledge on the relative proportions of the different enzyme groups is insufficient to discern the mechanisms implicated in fungal degradation. Detailed information on the identity of the main enzymes belonging to each group is required to elucidate these mechanisms.

3.3.2. Oxidoreductases and lignin degradation in wheat straw

As mentioned above, *I. lacteus* secreted DyPs, MnP, CDHs, and glyoxal oxidases (Tables S2, S3). *P. chrysosporium* released the same enzymes, excluding DyP, but also some others such as lignin peroxidases (LiP), pyranose 2-oxidase, and GMC oxidoreductases (both producing H_2O_2) (Tables S6-S7). MnPs from *P. chrysosporium* were identified with high scores and in considerable amounts (spot a). In previous works, this enzyme activity was not detected by colorimetric methods in the soluble fraction from cultures on wheat straw (Salvachúa et al., 2011), although it had been reported in *P. chrysosporium* cultures on spruce (Ravalason et al.,

2008). Maybe, under SSF on wheat straw the protein is being secreted but it is not active, which agrees with the deficient lignin loss quantified at 21-d (Table 1). In contrast, *P. ostreatus* secretome contained mostly MnPs, laccases, and glyoxal oxidases, a profile really similar to that found in *Ganorderma lucidum* (Manavalan et al., 2012) (Table S8-S9). The detection of MnP and laccase activities in the extracellular medium of this fungus, growing on wheat straw, had also been previously described (Salvachúa et al., 2011). Cytochrome P450 and some mono-oxygenases were also identified. These enzymes, whose production has been reported in *Phanerochaete carnosa* growing on spruce and cellulose, participate in the bioconversion of exogenous aromatic compounds (Mahajan and Master, 2010).

These results suggest that the diversity of lignin-degrading enzymes available in the extracellular matrix does not always run in parallel with the extent of lignin degradation and/or an improvement of the accessibility to carbohydrates in lignocellulose (see Table 1). Considering the results obtained for *I. lacteus*, the combination of MnP and DyP activities together with glyoxal oxidases and CDHs, which produce H_2O_2 for those peroxidases, seems to be a very effective cocktail for biopretreatment of wheat straw.

3.3.3. GHs produced by fungi for wheat straw degradation

Among the carbohydrate active enzymes (CAZY), the GHs (EC 3.2.1.) are the most widespread group and their classification is currently based on sequence similarities. GHs hydrolyze the glycosidic bonds between two or more carbohydrates or between a carbohydrate and a non-carbohydrate moiety (http://www.cazy.org/Glycoside-Hydrolases.html). Their accurate identification is sometimes difficult since many families of GHs do not have functional annotations and contain multiple enzymes.

The secretomes from *P. chrysosporium*, *P. ostreatus*, and *I. lacteus* growing on wheat straw contained enzymes classified into 24, 30, and 11 GH different families, respectively (Table 4). The GHs secreted by *I. lacteus* SmF cultures cluster into 10 different families. Proteins from some groups, such as GH3, GH5, and GH35 were represented in all of the conditions tested in the present study, regardless of the fungal species or the type of culture. These include a variety of enzymes involved in cellulose and hemicellulose degradation. In contrast, hydrolases from families GH6, GH7, GH10, and GH74 were detected only from SSF cultures. Only these four GH families contain CBHs, suggesting that this type of exocellulases is really induced by lignocellulose.

Many other families of GHs containing starch-degrading enzymes (GH13, GH15, GH31) and pectinases (GH2, GH28) were found in *P. ostreatus*, and several families were only represented in this species. Some of them are GH16, GH55, GH72, GH76, GH78, and GH105, which are mostly implied in fungal metabolism, as for example α-mannosidases (Ravalason et al., 2008), and GH4, GH51, GH79, and GH115, which include enzymes such as α-arabinofuranosidases and α-glucuronidases implicated in the complete hydrolysis of hemicellulose (van den Brink and de Vries, 2011).

Similarly, proteins from some GH families were represented in *P. chrysosporium* (11, 17, 18, 25, 30, 71), but did not appear in the two other species. Enzymes from the family GH30 are involved in the complete hydrolysis of cellulose and xylan by β-glucosidases and β-xylosidases, what implies the extensive/complete degradation of both polymers and thus, increased sugar consumption during biopretreatment (Table 1).

The GH families detected only in *I. lacteus* were GH74 in SSF and GH125 in SmF cultures. The family GH74 contains xyloglucanases, that have been reported to enhance the performance of complex cell-wall digesting cocktails (Jovanovic et al., 2009). The only protein in family GH125 is an exo-α-1,6-mannosidase, a type of enzyme barely described to date (Gregg et al., 2011). The number of GH families represented in SmF and SSF *I. lacteus* cultures was similar, although they were quite different from a qualitative point of view. It is worth to emphasize that proteins from family GH30, involved in the complete hydrolysis of cellulose and hemicelluloses, were detected only in SmF cultures, not in SSF.

The detection of the called "enigmatic" family GH61 in *P. chrysosporium* and *I. lacteus* should also be pointed out, since proteins from this group have been implicated in the initial steps of lignocelluloses breakdown by white-rot fungi, disrupting the cellulose structure and enhancing its digestibility by cellulases in lignocelluloses, although not in pure cellulose (Harris et al., 2010).

3.4. Why *I. lacteus* is so efficient pretreating wheat straw for 2G-ethanol production?

Based on the results presented here, we propose that *I. lacteus* degrades cellulose, using a large machinery of exocellulases and endoglucanases (as per results from the first week of SSF). Simultaneously, hemicellulose and pectins are mainly being broken down via acetyl xylan esterase and rhamnogalacturonan hydrolase, respectively. Due to the specific hydrolytic action of these enzymes, large polysaccharide fragments are mostly released. Our results also suggest that the enzymatic action of lignin-

degrader oxidoreductases such as MnP and DyP, and proteases such as polyporopepsin, enhance wheat straw deconstruction by facilitating the action of the carbohydrate-degrading enzymes. This enzyme profile yielded easily hydrolysable products with high sugar content. The key of that sugar enrichment is that the extracellular enzymatic pool is deficient in those proteins that catalyze the complete hydrolysis of cellulose and hemicelluloses to their monomeric units, hampering extensive sugar consumption for fungal growth. As an example, β-glucosidases, β-xylosidases, and α-glucuronidases, or proteins included in their GHs families (such as GH1, GH3, GH4, GH30, GH43, GH51, and GH115) were not detected in the secretome of *I. lacteus* from SSF cultures, or were detected as minor proteins. The positive effect on glucose yields of adding Mn^{2+} to the cultures could be explained from two findings: the release of several isoforms of cellulase showed some degree of inhibition, which probably caused a decrease in cellulose degradation and consumption, and the induction of a MnP that presumably produced an enhancement in cellulose accessibility during the enzymatic hydrolysis.

4. CONCLUSIONS

The current work describes for the first time the composition of the secretome of *I. lacteus* growing on wheat straw. The protein pattern secreted during SSF fungal growth justifies the fitness of this species for biopretreatment processes in 2G-ethanol production. Our comprehensive analysis of enzymes released through proteomic tools and comparison with other fungi provides insight into these biological processes. The secretome of *I. lacteus* can be of interest to be used for pretreatment of lignocellulosic material or enzymatic hydrolysis improvement through the preparation of optimized enzyme–cocktails. Due to the potential of *I. lacteus* in these processes, this fungus may warrant consideration in future genome projects.

Table 4. Diversity of the GH families detected in the secretomes from *P. chrysoporium*, *P. ostreatus*, and *I. lacteus* growing on wheat straw (SSF) and *I. lacteus* growing in submerged cultures (SmF), returned by JGI and Uniprot databases. Crosses (X) show the GH family to which the listed proteins belong, according to http://www.cazy.org/Glycoside-Hydrolases.html data.

Organism	**Culture**	**Glycoside hydrolase family**																																							
P. chrysosporium	SSF			3		5	6	7	8	10	11	12		15		17	18	20	25	27	28	30	31	35	37	43	47			61	71						88				
P. ostreatus	SSF	1	2	3	4	5	6	7	8	10		12	13	15	16			20		27	28		31	35	37		47	51	55			72		76	78	79	88	92	105	115	
I. lacteus	SSF		2	3*		5	6	7		10														35		43*				61			74					92*			
I. lacteus	SmF		2	3		5								15								30	31	35		43*												92*			125
Type of enzymes (1)																																									
Cellulose degrading enzymes																																									
Cellulases									X																																
Endo-1,4-β-glucanases				X		X		X				X			X													X					X								
Cellobiohydrolases							X	X		X																							X								
Exo-1,4-β-glucanases		X		X			X																																		
β-Glucosidases		X		X																		X																			
Hemicellulose degrading enzymes																																									
Xylanases and xyloglucanases						X				X	X	X				X										X							X	X							
Endo-1,4-β-xylanases				X		X			X						X																										
Endo-1,3-β-xylanases										X																X															
β-Xylosidases																						X				X															
Arabinofuranosidases				X																						X		X													
α- Glucuronidases					X																															X				X	
Pectin degrading enzymes																																									
β-Galactosidases		X	X																					X																	
β-Mannosidases		X	X			X																																			
Starch degrading enzymes													X	X									X				X														
Other GHs (2)		X	X	X	X	X	X	X	X			X				X	X	X	X	X	X	X		X	X	X		X	X	X	X	X		X	X	X	X	X	X	X	X

(1) Each functional group contains the most representative enzymes.
(2) This group contains activities different than those detailed in the Table (http://www.cazy.org/Glycoside-Hydrolases.html)
* These GH families were not detected in *I. lacteus´* spots, but were identified from EPP analyses.

ACKNOWLEDGMENTS

This work has been carried out with funding from the Spanish project PRI-PIBAR-2011-1402. D. Salvachúa thanks the Spanish Ministry of Economy for a FPU fellowship and to Prashanti Iyer and the Proteomics Facility in Penn State University for their assistance during her pre-doctoral stay.

REFERENCES

Abbas, A., Koc, H., Liu, F., Tien, M., 2005. Fungal degradation of wood: initial proteomic analysis of extracellular proteins of *Phanerochaete chrysosporium* grown on oak substrate. Curr. Genetics 47, 49-56.

Adav, S.S., Ravindran, A., Sze, S.K., 2012. Quantitative proteomic analysis of lignocellulolytic enzymes by *Phanerochaete chrysosporium* on different lignocellulosic biomass. J. Proteomics 75, 1493-1504.

Barr, B.K., Hsieh, Y.L., Ganem, B., Wilson, D.B., 1996. Identification of two functionally different classes of exocellulases. Biochemistry 35, 586-592.

Bonnarme, P., Jeffries, T.W. 1990. Mn(II) regulation of lignin peroxidases and manganese-dependent peroxidases from lignin-degrading white rot fungi. Appl. Environ. Microbiol. 56, 210-217.

Bouws, H., Wattenberg, A., Zorn, H., 2008. Fungal secretomes - nature's toolbox for white biotechnology. Appl. Microbiol. Biotechnol. 80, 381-388.

Butler, M.J. Day, A.W., 1998a. Destruction of fungal melanins by ligninases of *Phanerochaete chrysosporium* and other white rot fungi. Int. J. Plant Sci. 159, 989-995.

Butler, M.J. Day, A.W., 1998b. Fungal melanins: a review. Can. J. Microbiol. 44, 1115-1136.

Couturier, M., Navarro, D., Olive, C., Chevret, D., Haon, M., Favel, A., Lesage-Meessen, L., Henrissat, B. et al., 2012. Post-genomic analyses of fungal lignocellulosic biomass degradation reveal the unexpected potential of the plant pathogen *Ustilago maydis*. Bmc Genomics 13.

de Oliveira, A.L., Gallo, M., Pazzagli, L., Benedetti, C.E., Cappugi, G., Scala, A., Pantera, B., Spisni, A. et al., 2011. The structure of the elicitor cerato-platanin (CP), the first member of the CP fungal protein family, reveals a double psi b-barrel fold and carbohydrate binding. J. Biol. Chem. 286, 17560-17568.

Du, W., Yu, H., Song, L., Zhang, J., Weng, C., Ma, F., Zhang, X., 2011. The promoting effect of byproducts from *Irpex lacteus* on subsequent enzymatic hydrolysis of bio-pretreated cornstalks. Biotech. Biofuels 4, 37.

Espino, J.J., Gutierrez-Sanchez, G., Brito, N., Shah, P., Orlando, R., Gonzalez, C., 2010. The *Botrytis cinerea* early secretome. Proteomics 10, 3020-3034.

Fragner, D., Zomorrodi, M., Kues, U., Majcherczyk, A., 2013. Optimized protocol for the 2-DE of extracellular proteins from higher basidiomycetes inhabiting lignocellulose. Electrophoresis 30, 2431-2441.

Gregg, K.J., Zandberg, W.F., Hehemann, J.H., Whitworth, G.E., Deng, L., Vocadlo, D.J., Boraston, A.B., 2011. Analysis of a new family of widely distributed metal-independent α-mannosidases provides unique insight into the processing of N-linked glycans. J. Biol. Chem. 286, 15586-15596.

Harris, P.V., Welner, D., McFarland, K., Re, E., Poulsen, J.C.N., Brown, K., Salbo, R., Ding, H. et al., 2010. Stimulation of lignocellulosic biomass hydrolysis by proteins of glycoside hydrolase family 61: structure and function of a large, enigmatic family. Biochem. 49, 3305-3316.

Ji, X.L., Zhang, W.T., Gai, Y.P., Lu, B.Y., Yuan, C.Z., Liu, Q.X., Mu, Z.M., 2012. Patterns of lignocellulose degradation and secretome analysis of *Trametes trogii* MT. Int. Biodeter. Biodegr. 75, 55-62.

Jovanovic, I., Magnuson, J.K., Collart, F., Robbertse, B., Adney, W.S., Himmel, M.E., Baker, S.E., 2009. Fungal glycoside hydrolases for saccharification of lignocellulose: outlook for new discoveries fueled by genomics and functional studies. Cellulose 16, 687-697.

Kersten, P. Cullen, D., 2007. Extracellular oxidative systems of the lignin-degrading Basidiomycete *Phanerochaete chrysosporium*. Fungal Genet. Biol. 44, 77-87.

Kuhar, S., Nair, L.M., Kuhad, R.C., 2008. Pretreatment of lignocellulosic material with fungi capable of higher lignin degradation and lower carbohydrate degradation improves substrate acid hydrolysis and the eventual conversion to ethanol. Can. J. Microbiol. 54, 305-313.

Lee, J. 1997. Biological conversion of lignocellulosic biomass to ethanol. J. Biotechnol. 56, 1-24.

MacIntosh, G.C., 2011. RNase T2 Family: Enzymatic Properties, Functional Diversity, and Evolution of Ancient Ribonucleases, in: A.W.Nicholson (Ed.), Ribonucleases, Nucleic Acids and Molecular Biology. pp. 89-114.

Mahajan, S. Master, E.R., 2010. Proteomic characterization of lignocellulose-degrading enzymes secreted by *Phanerochaete carnosa* grown on spruce and microcrystalline cellulose. Appl. Microbiol. Biotechnol. 86, 1903-1914.

Manavalan, T., Manavalan, A., Thangavelu, K.P., Heese, K., 2012. Secretome analysis of *Ganoderma lucidum* cultivated in sugarcane bagasse. J. Proteomics 77, 298-309.

Martínez, A.T., Speranza, M., Ruiz-Dueñas, F.J., Ferreira, P., Camarero, S., Guillén, F., Martínez, M.J., Gutiérrez, A. et al., 2005. Biodegradation of lignocellulosics: Microbiological, chemical and enzymatic aspects of fungal attack to lignin. IBBS-13 (Proc. 13th Intern. Biodeter. Biodegr. Symp., 4-9 September).

Martínez, D., Larrondo, L.F., Putnam, N., Gelpke, M.D., Huang, K., Chapman, J., Helfenbein, K.G., Ramaiya, P. et al., 2004. Genome sequence of the lignocellulose

degrading fungus *Phanerochaete chrysosporium* strain RP78. Nat. Biotechnol. 22, 695-700.

Novotny, C., Cajthaml, T., Svobodova, K., Susla, M., Sasek, V., 2009. *Irpex lacteus*, a white-rot fungus with biotechnological potential - review. Folia Microbiologica 54, 375-390.

Pinto, P.A., Dias, A.A., Fraga, I., Marques, G., Rodrigues, M.A.M., Colaco, J., Sampaio, A., Bezerra, R.M.F., 2012. Influence of ligninolytic enzymes on straw saccharification during fungal pretreatment. Bioresour. Technol. 111, 261-267.

Ravalason, H., Grisel, S., Chevret, D., Favel, A., Berrin, J.G., Sigoillot, J.C., Herpoel-Gimbert, I., 2012. *Fusarium verticillioides* secretome as a source of auxiliary enzymes to enhance saccharification of wheat straw. Bioresour. Technol. 114, 589-596.

Ravalason, H., Jan, G., Molle, D., Pasco, M., Coutinho, P.M., Lapierre, C., Pollet, B., Bertaud, F. et al., 2008. Secretome analysis of *Phanerochaete chrysosporium* strain CIRM-BRFM41 grown on softwood. Appl. Microbiol. Biotechnol. 80, 719-733.

Ren, J-L, Sun, R-C, 2010. Hemicelluloses, in: Sun, R-C (Ed.), Cereal straw as a a resource for sustainable biomaterials and biofuels. Chemistry, extractives, lignins, hemicelluloses and cellulose. Elsevier, Amsterdam, pp. 73-130.

Ribeiro, D.A., Cota, J., Alvarez, T.M., Bruechli, F., Bragato, J., Pereira, B.M., Pauletti, B.A., Jackson, G. et al., 2012. The *Penicillium echinulatum* secretome on sugar cane bagasse. Plos One 7.

Salvachúa, D., Prieto, A., López-Abelairas, M., Lu-Chau, T., Martínez, A.T., Martínez, M.J., 2011. Fungal pretreatment: An alternative in second-generation ethanol from wheat straw. Bioresour. Technol. 102, 7500-7506.

Salvachúa, D., Prieto, A., Martinez, A.T., Martinez, M.J., 2013a. Characterization of a novel DyP-type peroxidase from *Irpex lacteus* and its application in the enzymatic hydrolysis of wheat straw. Appl. Environ. Microb. doi:10.1128/AEM.00699-13

Salvachúa, D., Prieto, A., Vaquero, M.E., Martinez, A.T., Martínez, M.J., 2013b. Sugar recoveries from wheat straw following treatments with the fungus *Irpex lacteus*. Bioresour. Technol. 131, 218-225.

Sánchez, C. 2009. Lignocellulosic residues: Biodegradation and bioconversion by fungi. Biotechnol. Advances 27, 185-194.

Sato, S., Liu, F., Koc, H., Tien, M., 2007. Expression analysis of extracellular proteins from *Phanerochaete chrysosporium* grown on different liquid and solid substrates. Microbiology-Sgm 153, 3023-3033.

Saykhedkar, S., Ray, A., Ayoubi-Canaan, P., Hartson, S.D., Prade, R., Mort, A.J., 2012. A time course analysis of the extracellular proteome of *Aspergillus nidulans* growing on sorghum stover. Biotech. Biofuels 5.

Shin, K.S., Kim, Y.H., Lim, J.S., 2005. Purification and characterization of manganese peroxidase of the white-rot fungus *Irpex lacteus*. J. Microbiol. 43, 503-509.

Song, L., Ma, F., Zeng, Y., Zhang, X., Yu, H., 2012. The promoting effects of manganese on biological pretreatment with *Irpex lacteus* and enzymatic hydrolysis of corn stover. Bioresour. Technol. http://dx.doi.org/10.1016/j.biortech.2012.09.004.

Tsumuraya, Y., Mochizuki, N., Hashimoto, Y., Kovac, P., 1990. Purification of an Exo-Beta-(1→3)-D-galactanase of *Irpex lacteus* (*Polyporus tulipiferae*) and its action on arabinogalactan proteins. J. Biol. Chem. 265, 7207-7215.

Van den Brink, J. de Vries, R.P., 2011. Fungal enzyme sets for plant polysaccharide degradation. Appl. Microbiol. Biotechnol. 91, 1477-1492.

Vanden Wymelenberg, A., Minges, P., Sabat, G., Martínez, D., Aerts, A., Salamov, A., Grigoriev, I., Shapiro, H. et al., 2006. Computational analysis of the *Phanerochaete chrysosporium* v2.0 genome database and mass spectrometry identification of peptides in ligninolytic cultures reveal complex mixtures of secreted proteins. Fungal Genet. Biol. 43, 343-356.

Vanden Wymelenberg, A., Sabat, G., Martínez, D., Rajangam, A.S., Teeri, T.T., Gaskell, J., Kersten, P.J., Cullen, D., 2005. The *Phanerochaete chrysosporium* secretome: Database predictions and initial mass spectrometry peptide identifications in cellulose-grown medium. J. Biotechnol. 118, 17-34.

Vinzant, T.B., Adney, W.S., Decker, S.R., Baker, J.O., Kinter, M.T., Sherman, N.E., Fox, J.W., Himmel, M.E., 2001. Fingerprinting *Trichoderma reesei* hydrolases in a commerical cellulase preparation. Appl. Biochem. Biotechnol. 91-3, 99-107.

Wessel, D. Flugge, U.I., 1984. A method for the quantitative recovery of protein in dilute-solution in the presence of detergents and lipids. Anal. Biochem. 138, 141-143.

Xu, C., Ma, F., Zhang, X., Chen, S., 2010. Biological pretreatment of corn stover by *Irpex lacteus* for enzymatic hydrolysis. J. Agric. Food Chem. 58, 10893-10898.

Yang, F., Jensen, J.D., Svensson, B., Jorgensen, H.J., Collinge, D.B., Finnie, C., 2012. Secretomics identifies *Fusarium graminearum* proteins involved in the interaction with barley and wheat. Mol. Plant Pathol. 13, 445-453.

Zorn, H., Peters, T., Nimtz, M., Berger, R.G., 2005. The secretome of *Pleurotus sapidus*. Proteomics 5, 4832-4838.

Supplementary Tables

Table S1. Protein identification from 2D-gels (Fig. 1) of the secretome from *I. lacteus* growing under **SSF** on wheat straw and in **SmF** cultures in CSS. All matches returned by JGI and Uniprot, ordered according to maximal score in each database, are given. UP= Unique peptides; CBM= carbohydrate-binding module. *Proteins already annotated in JGI. **DyP from *Irpex lacteus*.

Homologous to proteins		Database	Species	Accession number	MM (kDa)	pI	Score	Proteins	UP	Peptides	Coverage (%)
Spot 1	GH10*	JGI	*Bjerkandera adusta*	Bjead1_1 24950	40.2	6.5	**5.3**	4	2	2	5.6
	Aspartic-type endopeptidase	JGI	*Sphaerobolus stellatus*	Sphst1 174318	35.0	4.8	**5.0**	5	2	2	3.3
	Cellobiohydrolase II	Uniprot	*Irpex lacteus*	B2ZZ24	47.2	5.3	**20.6**	1	4	4	12.6
	Endoglucanase	Uniprot	*Irpex lacteus*	Q5W7K4	42.2	4.9	**19.0**	1	3	3	11.0
	Polyporopepsin	Uniprot	*Irpex lacteus*	P17576	35.0	4.7	**14.1**	1	5	5	13.8
	Cellulase	Uniprot	*Irpex lacteus*	Q9Y724	55.8	4.6	**12.1**	1	4	4	9.1
	Cellobiohydrolase	Uniprot	*Irpex lacteus*	Q75NB5	54.8	5.3	**11.8**	2	3	3	8.3
Spot 2	Cellulase	Uniprot	*Irpex lacteus*	Q9Y724	55.8	4.6	**13.9**	1	3	3	6.3
	Cellobiohydrolase	Uniprot	*Irpex lacteus*	Q75NB5	54.8	5.3	**8.9**	2	3	3	5.6
	Cellobiohydrolase II	Uniprot	*Irpex lacteus*	B2ZZ24	47.2	5.3	**7.8**	1	3	3	7.3
Spot 3	Protein binding. ATP binding (actin)	JGI	*Paxillus involutus*	Paxin1 20222	30.8	5.1	**2.6**	65	1	1	4.0
	Rhamnogalacturonan-hydrolase	Uniprot	*Irpex lacteus*	B6E8Y7	46.7	6.9	**17.4**	1	3	3	9.3
Spot 4	β-1.6-N-acetylglucosaminyltransferase	JGI	*Phanerochaete chrysosporium*	Phchr1 121730	89.5	4.6	**30.7**	2	1	1	2.2
	Cellobiohydrolase	Uniprot	*Irpex lacteus*	Q75NB5	54.8	5.3	**15.4**	2	4	4	9.4
Spot 5	GH7*	JGI	*Phanerochaete carnosa*	Phaca1 264060	53.8	4.3	**50.1**	6	2	2	4.9
	Cellulase	Uniprot	*Irpex lacteus*	Q9Y724	55.8	4.6	**215.8**	1	10	10	33.1
Spot 6	GH7*	JGI	*Phanerochaete carnosa*	Phaca1 264060	53.8	4.3	**17.9**	1	1	1	2.9
	Cellulase	Uniprot	*Irpex lacteus*	Q9Y724	55.8	4.6	**85.3**	1	7	7	23.8
	Peroxidase**	Uniprot	Polyporaceae	P87212	53.9	5.0	**12.1**	1	1	1	3
Spot 7	GH7	JGI	*Sphaerobolus stellatus*	Sphst1 205747	35.8	4.6	**16.7**	48	1	2	8.5
	Cellulase OS	Uniprot	*Irpex lacteus*	Q9Y724	55.8	4.6	**139.4**	1	11	11	34.8
Spot 8	GH7	JGI	*Sphaerobolus stellatus*	Sphst1 54354	53.3	5.1	**21.3**	50	2	2	5.6
	GH7*	JGI	*Pleurotus ostreatus*	PleosPC9_1 100231	47.9	4.5	**6.4**	30	2	2	5.3
	Cellobiohydrolase	Uniprot	*Irpex lacteus*	Q75NB5	54.8	5.3	**66.7**	1	5	8	17.9
	Exocellulase	Uniprot	*Irpex lacteus*	Q9Y723	55.0	4.8	**52.0**	1	1	4	10.3
	Cellulase	Uniprot	*Irpex lacteus*	Q9Y724	55.8	4.6	**43.4**	1	6	6	16.2
	Cellulase	Uniprot	*Irpex lacteus*	Q9Y722	54.5	4.9	**41.7**	1	6	6	14.7
Spot 9	1. 4-beta cellobiohydrolase. GH6. CBM*	JGI	*Punctularia strigosozonata*	Punst1 89180	47.1	4.9	**36.3**	6	1	1	4.7
	Cellobiohydrolase II	Uniprot	*Irpex lacteus*	B2ZZ24	47.2	5.3	**90.9**	1	7	7	19.9
	Cellobiohydrolase	Uniprot	*Irpex lacteus*	Q75NB5	54.8	5.3	**60.4**	2	6	6	18.0
	Peroxidase**	Uniprot	Polyporaceae	P87212	53.9	5.0	**3.0**	1	1	1	3.0

Table S1. Continued

Homologous to proteins		Database	Species	Accession number	MM (kDa)	pI	Score	Proteins	UP	Peptides	Coverage (%)
Spot 10	MnP9-short*	JGI	*Phlebia brevispora*	Phlbr1 147108	38.3	4.6	**21.1**	26	2	4	16.4
	MnP2s*	JGI	*Trametes versicolor*	Trave1 112835	38.3	4.5	**19.0**	24	1	3	11.6
	CBM1-GH10*/CBM1	JGI	*Phlebiopsis gigantea*	Phlgi1 85016	43.1	4.9	**13.8**	8	2	2	6.7
	GH7	JGI	*Bjerkandera adusta*	Bjead1_1 207890	22.4	6.3	**9.1**	54	1	2	10.6
	GH7*	JGI	*Pleurotus ostreatus*	PleosPC9_1 100231	47.9	4.5	**6.1**	29	2	2	5.3
	GH7*	JGI	*Phanerochaete carnosa*	Phaca1 264060	53.8	4.3	**5.6**	5	1	2	4.9
	Cellobiohydrolase II	Uniprot	*Irpex lacteus*	B2ZZ24	47.2	5.3	**46.0**	1	7	7	19.9
	Endoglucanase	Uniprot	*Irpex lacteus*	Q5W7K4	42.2	4.9	**32.5**	1	3	3	11.0
	Cellobiohydrolase	Uniprot	*Irpex lacteus*	Q75NB5	54.8	5.3	**29.6**	2	6	6	15.0
	Rhamnogalacturonan-hydrolase	Uniprot	*Irpex lacteus*	B6E8Y7	46.7	6.9	**25.6**	1	7	7	21.7
	Cellulase	Uniprot	*Irpex lacteus*	Q9Y724	55.8	4.6	**20.0**	1	5	5	14.5
	Melanin-decolorizing enzyme	Uniprot	*Ceriporiopsis sp.*	B3IWB3	38.3	5.1	**18.3**	13	4	5	22.3
	Manganese peroxidase 1	Uniprot	*Spongipellis sp.*	Q2HWK0	37.8	4.5	**12.1**	1	2	2	9.8
	Mn peroxidase MNP3	Uniprot	*Polyporus brumalis*	G0Z9F2	38.1	4.6	**10.9**	20	1	2	9.1
	Endo-1.4-β-xylanase A	Uniprot	*Phanerochaete chrysosporium*	Q9HEZ1	43.5	5.4	**10.1**	2	2	2	6.6
	Cellulase	Uniprot	*Irpex lacteus*	Q9Y722	54.5	4.9	**8.4**	1	2	2	4.6
	Polyporopepsin	Uniprot	*Irpex lacteus*	P17576	35.0	4.7	**5.4**	1	2	2	6.5
	Exo-β-(1→3)-galactanase	Uniprot	*Irpex lacteus*	B9ZZS1	47.8	6.7	**4.4**	1	2	2	7.6
	Peroxidase**	Uniprot	Polyporaceae	P87212	53.9	5.0	**3.0**	1	1	1	3.0
Spot 11	CBM1-GH10*	JGI	*Phlebiopsis gigantea*	Phlgi1 85016	43.1	4.9	**9.2**	8	2	2	6.7
	Cellobiohydrolase II	Uniprot	*Irpex lacteus*	B2ZZ24	47.2	5.3	**25.2**	1	5	5	14.8
	Endoglucanase	Uniprot	*Irpex lacteus*	Q5W7K4	42.2	4.9	**17.7**	1	2	2	7.5
	Cellulase	Uniprot	*Irpex lacteus*	Q9Y724	55.8	4.6	**14.6**	1	4	4	10.5
	Melanin-decolorizing enzyme	Uniprot	*Irpex lacteus*	B3IWB3	38.3	5.1	**13.2**	1	4	4	18.4
	Polyporopepsin	Uniprot	*Irpex lacteus*	P17576	35.0	4.7	**11.1**	1	3	3	10.6
	Cellobiohydrolase	Uniprot	*Irpex lacteus*	Q75NB5	54.8	5.3	**10.2**	2	2	2	5.6
Spot 12	Peptidase S41	JGI	*Bjerkandera adusta*	Bjead1_1 256345	74.1	5.6	**13.3**	4	1	2	4.3
	Esterase/lipase/thioesterase	JGI	*Phanerochaete chrysosporium*	Phchr1 129015	30.5	6.7	**9.0**	5	2	2	13.2
	Endoglucanase	Uniprot	*Irpex lacteus*	Q5W7K4	42.2	4.9	**15.4**	1	3	3	11.0
	Cellobiohydrolase	Uniprot	*Irpex lacteus*	Q75NB5	54.8	5.3	**11.9**	2	2	2	5.0
	Melanin-decolorizing enzyme	Uniprot	*Ceriporiopsis sp.*	B3IWB3	38.3	5.1	**8.7**	1	2	2	9.5
	Cellobiohydrolase II	Uniprot	*Irpex lacteus*	B2ZZ24	47.2	5.3	**8.2**	1	3	3	7.3
	Acetyl xylan esterase	Uniprot	*Phanerochaete chrysosporium*	H2ESB9	38.9	6.5	**9.0**	1	2	2	10.1
Spot 13	Esterase/lipase/thioesterase	JGI	*Phanerochaete chrysosporium*	Phchr1 129015	30.5	6.7	**12.9**	5	2	2	13.2
	Acetyl xylan esterase	Uniprot	*Phanerochaete chrysosporium*	H2ESB9	38.9	6.5	**12.9**	1	2	2	10.1
	Endoglucanase	Uniprot	*Irpex lacteus*	Q5W7K4	42.2	4.9	**11.0**	1	3	3	11.0
	Cellobiohydrolase II	Uniprot	*Irpex lacteus*	B2ZZ24	47.2	5.3	**8.3**	1	3	3	7.3
	Melanin-decolorizing enzyme	Uniprot	*Ceriporiopsis sp.*	B3IWB3	38.3	5.1	**6.9**	1	2	2	9.5
Spot 14	Peptidase S41	JGI	*Bjerkandera adusta*	Bjead1_1 256345	74.1	5.6	**20.2**	5	2	2	4.3
	Esterase/lipase/thioesterase	JGI	*Phanerochaete chrysosporium*	Phchr1 129015	30.5	6.7	**15.5**	5	2	2	13.2
	Acetyl xylan esterase	Uniprot	*Phanerochaete chrysosporium*	H2ESB9	38.9	6.5	**15.5**	1	2	2	10.1
	Endoglucanase	Uniprot	*Irpex lacteus*	Q5W7K4	42.2	4.9	**12.4**	1	2	2	8.8
	Cellobiohydrolase II	Uniprot	*Irpex lacteus*	B2ZZ24	47.2	5.3	**11.2**	1	3	3	7.3
	Melanin-decolorizing enzyme	Uniprot	*Ceriporiopsis sp.*	B3IWB3	38.3	5.1	**7.2**	1	2	2	9.5

Table S1. Continued

Homologous to proteins		Database	Species	Accession number	MM (kDa)	pI	Score	Proteins	UP	Peptides (%)	Coverage
Spot 15	Aspartic-type endopeptidase activity	JGI	*Sphaerobolus stellatus*	Sphst1 264141	33.9	5.2	**10.9**	7	2	2	6.1
	GH7*	JGI	*Phanerochaete carnosa*	Phaca1 264060	53.8	4.3	**8.7**	12	2	2	4.9
	Polyporopepsin	Uniprot	*Irpex lacteus*	P17576	35.0	4.7	**20.0**	1	5	5	14.1
	Endoglucanase	Uniprot	*Irpex lacteus*	Q5W7K4	42.2	4.9	**17.7**	1	4	4	12.8
	Cellulase	Uniprot	*Irpex lacteus*	Q9Y724	55.8	4.6	**15.8**	1	4	4	9.1
	Cellobiohydrolase II	Uniprot	*Irpex lacteus*	B2ZZ24	47.2	5.3	**13.7**	1	4	4	12.0
	Cellobiohydrolase	Uniprot	*Irpex lacteus*	Q75NB5	54.8	5.3	**10.3**	2	3	3	7.1
Spot 16	Aspartic-type endopeptidase activity	JGI	*Sphaerobolus stellatus*	Sphst1 264141	33.9	5.2	**65.8**	3	1	2	6.1
	Aspartic protease	Uniprot	*Pholiota nameko*	G3XKT3	42.8	5.5	**70.0**	1	2	2	6.1
	Endoglucanase	Uniprot	*Irpex lacteus*	Q5W7K4	42.2	4.9	**30.1**	1	3	3	11.0
	Cellobiohydrolase II	Uniprot	*Irpex lacteus*	B2ZZ24	47.2	5.3	**25.5**	1	4	4	13.5
	Polyporopepsin	Uniprot	*Irpex lacteus*	P17576	35.0	4.7	**17.8**	1	4	4	19.7
Spot 17	Rhamnogalacturonan-hydrolase	Uniprot	*Irpex lacteus*	B6E8Y7	46.7	6.9	**27.3**	1	6	6	23.7
Spot 18	Esterase/lipase/thioesterase	JGI	*Phanerochaete chrysosporium*	Phchr1 129015	30.5	6.7	**19.8**	5	2	2	13.2
	Acetyl xylan esterase	Uniprot	*Phanerochaete chrysosporium*	H2ESB9	38.9	6.5	**27.9**	1	2	2	10.1
	Cellobiohydrolase II	Uniprot	*Irpex lacteus*	B2ZZ24	47.2	5.3	**5.8**	1	2	2	5.1
Spot 19	Esterase/lipase/thioesterase	JGI	*Phanerochaete chrysosporium*	Phchr1 129015	30.5	6.7	**5.9**	4	1	1	8.9
	Cellobiohydrolase II	Uniprot	*Irpex lacteus*	B2ZZ24	47.2	5.3	**4.1**	1	2	2	4.7
Spot 20	Endo-1.4-β-xylanase A	Uniprot	*Phanerochaete chrysosporium*	Q9HEZ1	43.5	5.4	**3.1**	2	1	1	3.4
Spot 21	Cerato-platanin/ Barwin-related endoglucanase	JGI	*Pleurotus ostreatus*	PleosPC9_1 102212	14.8	5.2	**3.3**	1	1	1	10.5
	Putative uncharacterized protein hypP2	Uniprot	*Moniliophthora perniciosa*	Q6U7U4	47.9	8.7	**6.1**	1	1	1	4.7
Spot 22	Cerato-platanin/ Barwin-related endoglucanase	JGI	*Pleurotus ostreatus*	PleosPC9_1 102212	14.8	5.2	**10.9**	1	1	1	10.5
	Putative uncharacterized protein	Uniprot	*Melampsora larici-populina*	F4R4N7	28.1	9.9	**6.0**	1	1	1	8.1
Spot 23	Cerato-platanin/ Barwin-related endoglucanase	JGI	*Pleurotus ostreatus*	PleosPC9_1 102212	14.8	5.2	**3.2**	1	1	1	10.5
	Aspartic protease	Uniprot	*Pholiota nameko*	G3XKT3	42.8	5.5	**3.9**	1	1	1	3.7
Spot 24	Aspartic-type endopeptidase activity	JGI	*Phlebia brevispora*	Phlbr1 115558	43.4	4.9	**2.9**	1	1	1	3.4
	Aspartic protease	Uniprot	*Pholiota nameko*	G3XKT3	42.8	5.5	**3.7**	1	1	1	3.7
Spot 25	Cerato-platanin/ Barwin-related endoglucanase	JGI	*Pleurotus ostreatus*	PleosPC9_1 102212	14.8	5.2	**3.1**	1	1	1	10.5
	Putative uncharacterized protein	Uniprot	*Puccinia graminis*	E3JYE0	21.2	6.3	**2.7**	1	1	1	6.4
Spot 26	Splicing coactivator SRm160/300	JGI	*Hydnomerulius pinastri*	Hydpi2 28112	79.5	10.4	**1.9**	1	1	1	1.9
	Aspartic protease	Uniprot	*Pholiota nameko*	G3XKT3	42.8	5.5	**3.9**	1	1	1	3.7
Spot 27	Serine-type peptidase activity/ subtilase activity	JGI	*Punctularia strigosozonata*	Punst1 106327	59.2	4.9	**53.1**	1	1	1	4.1
Spot 28	Cerato-platanin/ Barwin-like endoglucanases	JGI	*Pleurotus ostreatus*	PleosPC9_1 102212	14.8	5.2	**3.4**	1	1	1	10.5
	Putative uncharacterized protein hypP2	Uniprot	*Moniliophthora perniciosa*	Q6U7U4	47.9	8.7	**5.6**	1	1	1	4.7
Spot 29	α-N-arabinofuranosidase activity	JGI	*Galerina marginata*	Galma1 227157	66.6	8.0	**4.9**	1	1	1	1.6
	Cellulase	Uniprot	*Irpex lacteus*	Q9Y724	55.8	4.6	**9.1**	1	2	2	3.6
	Cellobiohydrolase	Uniprot	*Irpex lacteus*	Q75NB5	54.8	5.3	**8.9**	2	3	3	7.3
	Cellobiose dehydrogenase	Uniprot	*Irpex lacteus*	Q6AW20	82.1	5.5	**7.2**	1	3	3	4.1
Spot 30	Cellobiohydrolase	Uniprot	*Irpex lacteus*	Q75NB5	54.8	5.3	**2.7**	2	1	1	1.7
Spot 31	Esterase/lipase/thioesterase	JGI	*Phanerochaete chrysosporium*	Phchr1 7398	54.0	5.2	**8.1**	3	1	1	2.8
	Cellobiohydrolase	Uniprot	*Irpex lacteus*	Q75NB5	54.8	5.3	**12.9**	2	2	2	5.0
Spot 32	Catalytic activity/ Esterase/lipase/thioesterase	JGI	*Phanerochaete chrysosporium*	Phchr1 7398	54.0	5.2	**19.4**	3	1	1	2.8
	Cellobiohydrolase	Uniprot	*Irpex lacteus*	Q75NB5	54.8	5.3	**6.3**	2	2	2	4.6

Table S1. Continued

Homologous to proteins		Database	Species	Accession number	MM (kDa)	pI	Score	Proteins	UP	Peptides (%)	Coverage
Spot 33	1. 4-β cellobiohydrolase. GH6/ 'CAZy_ID 260597*	JGI	*Punctularia strigosozonata*	Punst1 89180	47.1	4.9	**5.3**	6	1	1	4.7
	Cellobiohydrolase II	Uniprot	*Irpex lacteus*	B2ZZ24	47.2	5.3	**14.2**	1	3	3	9.7
Spot 34	Cellobiohydrolase II	Uniprot	*Irpex lacteus*	B2ZZ24	47.2	5.3	**8.5**	1	1	1	4.7
Spot 35	Histone H4 (Fragment)	Uniprot	*Moniliophthora perniciosa*	E2LLY3	8.8	11.6	**5.1**	14	1	1	12.7
Spot 36	Cellobiohydrolase II	Uniprot	*Irpex lacteus*	B2ZZ24	47.2	5.3	**37.1**	4	6	6	18.8
Spot 37	Peptidase S41	JGI	*Bjerkandera adusta*	Bjead1_1 256345	74.1	5.6	**7.3**	5	2	2	4.3
	Endoglucanase	Uniprot	*Irpex lacteus*	Q5W7K4	42.2	4.9	**63.1**	1	3	3	11.0
	Cellobiohydrolase II	Uniprot	*Irpex lacteus*	B2ZZ24	47.2	5.3	**16.7**	3	4	4	13.7
Differential spots in submerged cultures of *I. lacteus*											
Spot 38	GH3*	JGI	*Phlebiopsis gigantea*	Phlgi1 81135	99.0	5.1	**152.4**	23	3	7	6.2
	GH3	JGI	*Pisolithus microcarpus*	Pismi1 463669	78.0	4.7	**111.1**	13	2	4	4.6
	GH3*/ β-glucosidase*	JGI	*Coniophora puteana*	Conpu1 112748	95.6	4.9	**87.3**	14	1	4	4.5
	GH3*	JGI	*Laccaria bicolor*	Lacbi2 178737	80.9	5.2	**31.8**	5	1	2	3.0
	GH2*	JGI	*Bjerkandera adusta*	Bjead1_1 463744	103.5	5.4	**23.0**	7	1	3	4.7
	GH2	JGI	*Phlebiopsis gigantea*	Phlgi1 94774	104.0	4.9	**19.5**	7	1	3	4.6
	GH3	Uniprot	*Serpula lacrymans*	F8PMW3	78.3	4.7	**63.3**	8	2	4	4.4
	β-glucosidase	Uniprot	*Postia placenta*	B8P3C1	84.6	4.7	**47.1**	1	1	2	3.1
	Polyporopepsin	Uniprot	*Irpex lacteus*	P17576	35.0	4.7	**28.1**	1	3	3	17.4
	GH3	Uniprot	*Laccaria bicolor*	B0D734	80.9	5.2	**22.6**	7	3	4	6.1
Spot 39	Six-hairpin glycosidase-like	JGI	*Trametes versicolor*	Trave1 35444	74.4	5.8	**46.4**	4	2	2	6.1
	GH3*	JGI	*Phlebiopsis gigantea*	Phlgi1 81135	99.0	5.1	**10.0**	29	4	4	4.8
	Putative uncharacterized protein	Uniprot	*Moniliophthora perniciosa*	E2M3P0	13.2	4.7	**3.4**	1	1	1	13.0
Spot 40	candidate glyoxal oxidase*	JGI	*Punctularia strigosozonata*	Punst1 68820	59.6	5.2	**1.9**	1	1	1	3.4
Spot 41	Peptidase S8 and S53	JGI	*Punctularia strigosozonata*	Punst1 106327	59.2	4.9	**64.4**	1	1	1	4.1
	Polyporopepsin	Uniprot	*Irpex lacteus*	P17576	35.0	4.7	**25.6**	1	2	2	13.2
Spot 42	GH15/glucan 1.4-α-glucosidase	JGI	*Trametes versicolor*	Trave1 28580	60.9	5.4	**58.4**	1	1	1	2.1
	Six-hairpin glycosidase-like	JGI	*Trametes versicolor*	Trave1 35444	74.4	5.8	**9.9**	4	2	2	6.1
	Exo-β-(1→3)-galactanase	Uniprot	*Irpex lacteus*	B9ZZS1	16.8	47.8	**6.7**	1	4	4	19.0
	Putative uncharacterized protein	Uniprot	*Coprinopsis cinerea*	A8NY20	7.2	57.0	**5.7**	3	2	2	5.2
Spot 43	Endonuclease/exonuclease/phosphatase family	JGI	*Phanerochaete chrysosporium*	Phchr1 3383	39.0	8.6	**24.8**	4	2	2	5.6
	Mannose-6-phosphatase	Uniprot	*Phanerochaete chrysosporium*	Q281W3	38.4	6.6	**71.6**	2	4	4	8.2

Table S2. Functional classification of proteins from ***I. lacteus*** **secretome growing on wheat straw**. Proteins were identified from the LC-MS/MS data from the entire secretome (EPP), searching against the Basidiomycota database of **Uniprot**. Different groups are ordered from the highest to the lowest score in each functional group.GH= glycoside hydrolase family. **Identified as *Irpex lacteus* proteins.

Homologous to predicted proteins (Uniprot)	Uniprot ID	MM (kDa)	pI	Score	Proteins	Unique peptides	Peptides	Coverage (%)
Glycoside hydrolases								
Cellobiohydrolase II**	B2ZZ24	47.2	5.3	606.0	1	13	14	37.4
Cellulase**	Q9Y724	55.8	4.6	193.3	1	9	9	28.5
Endoglucanase**	Q5W7K4	42.2	4.9	118.3	1	3	3	11.0
Cellobiohydrolase**	Q75NB5	54.8	5.3	106.0	1	11	11	29.4
Exo-β-(1-->3)-galactanase**	B9ZZS1	47.8	6.7	99.8	1	8	8	32.4
Rhamnogalacturonan-hydrolase**	B6E8Y7	46.7	6.9	84.5	1	10	10	33.9
Endo-1.4-β-xylanase A	Q9HEZ1	43.5	5.4	57.7	2	3	3	15.7
GH3	F8NLG7	89.6	5.0	47.2	2	1	2	3.1
Cellulase**	Q9Y722	54.5	4.9	45.0	1	6	6	14.9
GH3	F8PMW3	78.3	4.7	36.5	2	2	3	4.3
CellobiohydrolaseII	A8CED8	47.3	5.1	19.4	1	2	3	8.4
GH74	A9CSH7	88.3	5.3	15.3	1	3	3	4.9
GH35	B0DSN5	119.6	6.0	11.5	1	2	2	2.2
GH61	D8PNG1	23.9	5.7	11.3	1	2	2	8.7
Oxidoreductases								
Peroxidase cpop21	P87212	53.9	5.0	122.2	1	8	8	26.9
Manganese peroxidase 3	H2D7E4	38.6	4.5	80.5	1	3	4	15.6
Cellobiose dehydrogenase**	Q6AW20	82.1	5.5	65.6	1	9	9	14.9
Copper radical oxidase	Q0ZKA4	108.3	4.7	49.7	1	2	2	2.8
Manganese peroxidase 1	Q2HWK0	37.8	4.5	19.6	1	2	3	14.0
Esterases								
Acetyl xylan esterase	H2E9	38.9	6.5	142.2	1	2	2	10.1
Proteases								
Polyporopepsin**	P17576	35.0	4.7	307.2	1	8	9	48.5
Aspartic protease	G3XKT3	42.8	5.5	35.6	1	3	4	8.3
Aspartic peptidase A1	B0CYE2	44.1	5.1	32.7	1	3	5	11.5
Family A1 protease	Q281W1	41.9	5.9	15.1	2	2	2	2.7
Phosphatases								
Mannose-6-phosphatase	Q281W3	38.4	6.6	21.3	1	3	3	5.9
Other functions								
Melanin-decolorizing enzyme	B3IWB3	38.3	5.1	142.1	1	10	11	41.5
Ribonuclease T2**	Q8LW55	41.8	5.1	30.9	1	2	2	6.8
Ubiquitin (Fragment)	Q01868	6.2	8.6	5.3	48	2	2	32.7
Unknown functions								
Putative uncharacterized protein	E2LEF2	19.0	5.9	30.8	2	2	2	13.8
Putative uncharacterized protein	D8PQ40	44.1	4.9	28.4	1	2	4	4.9
Putative uncharacterized protein	A8NY20	57.0	5.7	19.5	1	3	3	6.7
Putative uncharacterized protein	B8PLG1	59.0	5.0	12.7	1	2	3	5.2
Putative uncharacterized protein	B8P882	71.2	6.9	12.0	1	2	2	4.0
Putative uncharacterized protein	F8NRS6	55.4	5.1	7.8	2	1	2	3.8

Table S3. Functional classification of proteins from ***I. lacteus*** **secretome growing on wheat straw**. Proteins were identified from the LC-MS/MS data from the entire secretome (EPP), searching against the Basidiomycota database from **JGI.** Different groups are ordered from the highest to the lowest score in each functional group. GH= glycoside hydrolase family; CBM= carbohydrate-binding module. *Annotated protein.

Homologous to predicted proteins (JGI)	JGI ID	MM (kDa)	pI	Score	Proteins	Unique peptides	Peptides	Coverage (%)
Glycoside hydrolases								
GH6/ CBM	Phchr1 133052	48.4	5.3	293.0	2	4	4	10.7
GH2*	Phlgi1 94774	104.0	4.9	96.9	1	3	3	4.6
GH3*	Phlgi1 81135	99.0	5.1	81.9	1	4	6	5.9
GH10/ CBM	Phchr1 138345	43.5	5.4	79.5	1	3	3	15.7
GH3*/ β-glucosidase*	Conpu1 112748	95.6	4.9	77.4	1	2	4	4.9
GH35/ β-galactosidase	Gansp1 116588	108.8	5.1	69.4	1	3	3	3.5
Six-hairpin glycosidase-like	Hetan2 48511	54.4	5.4	31.7	5	2	2	6.8
GH10*	Bjead1 24950	40.2	6.5	43.6	1	2	3	9.4
CBM*	Phlgi1 31010	35.1	4.6	34.6	1	2	2	7.0
α-1.2-mannosidase	Phchr1 133585	90.5	4.9	31.1	2	2	2	3.0
GH92*	Phaca1 255063	91.9	4.9	31.1	1	2	2	3.2
GH35*/ β-galactosidase	Phlgi1 129018	108.7	5.2	27.4	2	2	2	1.5
GH5/ CBM/ CAZy_ID 259705*	Dicsq1 65561	41.0	4.8	27.3	1	2	2	5.9
GH43*/ CBM35*	Bjead1 424941	47.5	6.1	25.6	1	3	3	8.5
GH7*	PleosPC9 100231	47.9	4.5	25.2	13	2	2	5.3
GH5*	Bjead1 100935	43.7	6.1	24.5	1	3	3	11.1
GH74*/ CBM1*	Phlgi1 98770	87.0	5.0	22.0	1	2	2	3.1
GH7/ CBM	Phchr1 127029	54.9	5.3	21.9	1	2	2	4.1
GH7*/ CBM	Phaca1 264060	53.8	4.3	19.7	1	2	2	4.9
GH61*	Dicsq1 102981	22.9	5.7	18.3	3	2	2	10.1
GH5*	Trave1 33056	38.1	4.7	16.7	2	2	2	4.7
Oxidorreductases								
Manganese peroxidase 9 short*	Phlbr1 147108	38.3	4.6	105.4	1	4	4	16.4
Glyoxal oxidase*	Punst1 68820	59.6	5.2	18.2	1	2	2	5.9
Esterases								
Esterase/lipase/thioesterase	Phchr1 129015	30.5	6.7	188.5	1	2	2	13.2
Carboxylesterase. type B	Phchr1 7398	54.0	5.2	69.3	3	2	2	5.2
Proteases								
Peptidase S53	Punst1 106327	59.2	4.9	109.5	1	2	2	6.1
Peptidase A1*	Lacbi2 292906	44.1	5.1	47.3	3	2	5	11.5
Peptidase A1	Hebcy1 58903	44.4	5.2	43.7	1	2	5	11.5
Peptidase A1	Phlgi1 460435	40.4	5.0	34.6	1	2	2	3.1
Peptidase A1	Sphst1 264141	33.9	5.2	29.6	1	2	2	6.1
Peptidase S10/ serine carboxypeptidase	Bjead1 39510	70.6	4.9	27.8	1	1	2	4.6
Amidase signature enzyme	Hetan2 10776	50.0	5.0	16.9	13	1	2	4.1
Peptidase S53	PleosPC15 1077652	63.4	5.6	16.3	2	2	2	4.1
Amidase signature enzyme	Dacsp1 53351	46.5	4.7	15.9	1	1	2	4.8
Peptidase A1	Plicr1 701179	43.3	5.1	15.6	1	3	3	4.5
Phosphatases								
Histidine acid phosphatase	Wolco1 27937	49.5	5.9	7.8	1	2	2	5.2

Table S3. Continued

Homologous to predicted proteins (JGI)	JGI ID	MM (kDa)	pI	Score	Proteins	Unique peptides	Peptides	Coverage (%)
Other functions								
Ferritin/ribonucleotide reductase-like	Hetan2 431223	91.2	4.8	40.5	1	1	3	3.8
β-1.6-N-acetylglucosaminyltransferase	Phchr1 121730	89.5	4.6	82.2	1	3	3	4.9
Neutral/alkaline nonlysosomal ceramidase	Phchr1 3167	72.5	6.3	13.5	1	2	2	4.8
Unknown functions								
Putative uncharacterized protein	Bjead 424391	61.1	5.2	49.5	1	3	3	5.6
Putative uncharacterized protein	Phaca1 204873	96.1	5.1	35.2	1	2	4	5.8
Putative uncharacterized protein	Phaca1 247599	33.3	4.6	34.6	1	2	2	10.8
Hypothetical protein*	Cersu1 119820	71.2	4.8	28.8	1	1	2	4.6
Putative uncharacterized protein	Phchr1 3383	39.0	8.6	22.5	1	3	3	5.9
Hypothetical protein*	Cersu1 155413	71.3	4.7	14.0	1	2	2	3.1

Table S4. Functional classification of proteins from ***I. lacteus*** **secretome growing on submerged cultures** in CSS. Proteins were identified from the LC-MS/MS data from the entire secretome (EPP), searching against the Basidiomycota database of **Uniprot**. Different groups are ordered from the highest to the lowest score in each functional group.GH= glycoside hydrolase family. **Identified as *Irpex lacteus* proteins.

Homologous to predicted proteins (Uniprot)	Uniprot ID	MM (kDa)	pI	Score	Proteins	Unique peptides	Peptides	Coverage (%)
Glycoside hydrolases								
Exo-β-(1->3)-galactanase**	B9ZZS1	47.8	6.7	202.2	1	11	11	50.5
GH3	F8NLG7	89.6	5.0	130.3	2	1	2	3.1
GH3	F8PMW3	78.3	4.7	111.6	2	2	3	4.3
Cellobiohydrolase**	Q75NB5	54.8	5.3	54.4	1	6	6	11.3
Endoglucanase**	Q5W7K4	42.2	4.9	51.7	1	3	3	11.0
Rhamnogalacturonan-hydrolase**	B6E8Y7	46.7	6.9	41.3	1	5	5	13.1
GH35	B0DSN5	119.6	6.0	34.6	1	2	2	2.2
Cellobiohydrolase II**	B2ZZ24	47.2	5.3	32.7	1	4	4	12.6
Exo-beta-1.3-glucanase	Q53UH0	46.1	4.7	29.3	1	2	2	8.8
Oxidoreductases								
Peroxidase cpop21	P87212	53.9	5.0	684.8	1	13	13	47.1
Manganese peroxidase 3	H2D7E4	38.6	4.5	56.7	1	3	4	15.6
Cellobiose dehydrogenase**	Q6AW20	82.1	5.5	33.4	1	5	5	5.5
Copper radical oxidase	Q0ZKA4	108.3	4.7	27.0	1	2	2	2.8
Glyoxal oxidase (Fragment)	Q7LIJ2	56.0	5.6	25.5	3	2	2	5.5
Peroxidase 1	B0BK71	54.9	5.5	10.5	1	2	2	3.1
Proteases								
Polyporopepsin**	P17576	35.0	4.7	4867.5	1	13	14	60.6
Aspartic protease	G3XKT3	42.8	5.5	63.7	1	3	4	8.3
Aspartic peptidase A1	B0CYE2	44.1	5.1	52.0	1	3	5	11.5
Family A1 protease	Q281W1	41.9	5.9	11.6	2	2	2	2.7
Subtilisin-like protease (Fragment)	Q6H8Q3	86.9	4.8	6.7	1	2	2	1.8
Phosphatases								
Mannose-6-phosphatase	Q281W3	38.4	6.6	87.5	1	3	3	5.9
Other functions								
Melanin-decolorizing enzyme	B3IWB3	38.3	5.1	368.6	1	11	12	41.8
Ribonuclease T2**	Q8LW55	41.8	5.1	137.4	1	4	4	14.4
Unknown function								
Putative uncharacterized protein	D8PJY8	56.5	4.7	59.6	1	1	2	7.3
Putative uncharacterized protein	D8PQ40	44.1	4.9	53.2	1	2	4	4.9
Putative uncharacterized protein	A8NY20	57.0	5.7	46.1	1	2	3	6.7
Putative uncharacterized protein	B8PLG1	59.0	5.0	29.8	1	2	3	5.2
Putative uncharacterized protein	F8NRS6	55.4	5.1	27.6	2	1	2	3.8
Putative uncharacterized protein	E2LEF2	19.0	5.9	19.2	2	2	2	13.8
Putative uncharacterized protein	B8P882	71.2	6.9	19.0	1	2	2	4.0

Table S5. Functional classification of proteins from ***I. lacteus*** **secretome growing on submerged cultures** in CSS. Proteins were identified from the LC-MS/MS data from the entire secretome (EPP), searching against the Basidiomycota database from **JGI.** Different groups are ordered from the highest to the lowest score in each functional group. GH= glycoside hydrolase family; CBM= carbohydrate-binding module. *Annotated protein.

Homologous to predicted proteins (JGI)	JGI ID	MM (kDa)	pI	Score	Proteins	Unique peptides	Peptides	Coverage (%)
Glycoside hydrolases								
GH15*/ Glucan 1.4-α-glucosidase	Trave1 28580	60.9	5.4	1093.7	1	2	2	9.0
GH15/ Six-hairpin glycosidase-like/CAZy_ID 263180*	Hetan2 44412	56.4	4.7	262.0	1	2	2	9.8
GH3*	Phlgi1 81135	99.0	5.1	203.9	1	4	6	5.9
GH2*	Phlgi1 94774	104.0	4.9	161.2	1	1	3	4.6
GH3	Serla 133022	95.7	5.0	136.5	1	2	3	6.6
GH2*/ Galactose-binding like/Predicted β-mannosidase	Bjead 463744	103.5	5.4	128.8	1	2	4	5.8
GH125*/ Six-hairpin glycosidase-like	Phlgi1 97503	55.8	5.2	88.8	1	4	4	9.9
GH35/ Beta-galactosidase	Gansp1 116588	108.8	5.1	85.3	1	3	3	3.5
GH3	Phlbr1 29514	100.1	5.0	58.4	1	2	3	5.3
Six-hairpin glycosidase-like	Schco2 1185226	56.5	4.7	47.0	1	1	2	7.3
GH92*	Bjead 365447	90.2	5.2	40.5	1	3	4	5.7
GH92*	Phaca1 255063	91.9	4.9	39.7	1	2	2	3.2
GH5*	Phlgi1 100064	46.3	5.3	37.9	1	2	3	11.1
GH92*	Phaca1 123038	90.2	4.8	37.9	1	2	3	4.2
Six-hairpin glycosidase-like	Bjead 149865	79.0	5.4	37.8	1	2	2	4.5
GH43*/ CBM35*	Bjead 424941	47.5	6.1	32.3	2	2	2	4.7
GH35*/ β-galactosidase	Phlgi1 129018	108.7	5.2	32.1	2	2	2	1.5
Amidase signature	Gymlu1 179802	58.8	4.8	31.9	2	2	4	6.5
GH5*	Bjead 100935	43.7	6.1	30.1	1	3	4	13.9
GH7/CBM	Phchr1 127029	54.9	5.3	22.3	1	2	2	4.1
GH31*	Phlgi1 127611	98.1	5.3	20.2	3	2	2	1.6
GH30/ β-glucocerebrosidase	Phchr1 9011	58.8	6.0	18.4	1	2	2	3.9
GH31/ Maltase glucoamylase and related hydrolases	Bjead 214996	20.1	8.7	17.6	3	2	2	5.5
GH35/ β-galactosidase	Galma1 275642	109.3	8.5	16.6	1	2	2	2.3
Oxidoreductases								
Glyoxal oxidase/ Coper radical oxidase*	Trave1 117805	59.9	5.5	53.3	2	2	2	5.4
Haem peroxidase/ MnP2s*	Trave1 112835	38.3	4.5	46.1	1	3	3	11.6
Glyoxal oxidase*	Punst1 68820	59.6	5.2	32.1	1	2	2	5.9
Glyoxal oxidase	Dicsq1 104366	59.7	5.4	28.4	1	2	2	4.0
Esterases								
Carboxylesterase. type B	Phchr1 7398	54.0	5.2	1157.1	3	2	2	5.2
Carbohydrate Esterase Family 15 protein*	Punst1 122520	42.0	4.8	19.0	1	1	2	6.7

Table S5. Continued

Homologous to predicted proteins (JGI)	JGI ID	MM (kDa)	pI	Score	Proteins	Unique peptides	Peptides	Coverage (%)
Proteases								
Peptidase S53	Punst1 106327	59.2	4.9	2983.0	1	2	2	6.1
Peptidase S10. serine carboxypeptidase	Bjead 157470	51.8	5.4	79.1	1	2	2	6.6
Peptidase A1	Phlgi1 460435	40.4	5.0	58.6	1	2	2	3.1
Peptidase A1	Hebcy1 58903	44.4	5.2	53.6	1	2	5	11.5
Peptidase A1*	Lacbi2 292906	44.1	5.1	53.5	3	2	5	11.5
Peptidase S10. serine carboxypeptidase	Bjead 39510	70.6	4.9	37.9	2	2	2	4.6
Peptidase A1	Sphst1 264141	33.9	5.2	25.6	1	2	2	6.1
Amidase signature enzyme	Bjead 41819	57.7	5.1	24.7	4	1	3	5.4
Peptidase A1	Bjead 33438	42.0	8.6	24.7	1	2	2	2.7
Amidase signature enzyme	Dacsp1 53351	46.5	4.7	22.2	1	1	3	6.6
Peptidase A1	Phchr1 40125	41.8	5.2	20.5	1	2	2	3.3
Peptidase A1	Plicr1 701179	43.3	5.1	13.0	1	3	3	4.5
Other functions								
β-1.6-N-acetylglucosaminyltransferase	Phchr1 121730	89.5	4.6	38.6	1	3	3	4.9
Flagellar basal body rod protein	PleosPC9 87860	42.4	5.1	34.6	1	3	3	7.7
Ferritin/ribonucleotide reductase-like	Hetan2 431223	91.2	4.8	11.7	1	2	2	2.6
Unknown function								
DUF1793	Trave1 35444	74.4	5.8	71.2	1	2	2	6.1
Putative uncharacterized protein	Phchr1 3383	39.0	8.6	68.7	1	3	3	5.9
Putative uncharacterized protein	Bjead 424391	61.1	5.2	27.3	1	3	3	5.6
Putative uncharacterized protein	Fompi1 128275	42.7	4.3	26.3	1	1	2	4.8
Hypothetical protein*	Cersu1 155413	71.3	4.7	23.0	1	2	2	3.1
Putative uncharacterized protein	Phaca1 247599	33.3	4.6	15.8	1	2	2	10.8
DUF1793	Punst1 132507	74.4	4.8	14.4	1	2	2	6.4
Putative uncharacterized protein	Sphst1 194507	29.2	5.8	5.2	2	2	2	6.0

Table S6. Functional classification of proteins from ***P. chrysosporium*** **secretome growing on wheat straw**. Proteins were identified from the LC-MS/MS data from the entire secretome (EPP), searching against the *P. chrysosporium* database of **Uniprot**. Different groups are ordered from the highest to the lowest score in each functional group.GH= glycoside hydrolase family; CBM= carbohydrate-binding module.

Predicted proteins (Uniprot)	Uniprot ID	MM (kDa)	pI	Score	Proteins	Unique peptides	Peptides	Coverage (%)
Glycoside hydrolases								
Glucan 1.3-β-glucosidase	Q2Z1W1	82.0	5.8	327.6	1	8	8	15.2
Cellulase	Q7LIJ0	53.8	4.9	286.6	2	13	13	35.7
Endo-1.4-β-xylanase A	Q9HEZ1	43.5	5.4	209.8	2	4	6	23.3
Cellobiohydrolase II (Fragment)	H3K419	46.3	5.1	189.6	2	6	6	20.1
Endo-1.4-β-xylanase C	B7SIW2	42.3	4.9	151.9	2	6	8	29.6
Exoglucanase 1	P13860	54.8	5.5	117.1	1	7	7	16.5
Endo-β-glucanase	C6H0M6	33.6	5.4	113.8	1	6	6	20.0
β-glucosidase (Fragment)	Q8TGC6	83.4	5.7	62.9	1	5	5	8.2
Mannan endo-1.4-beta-mannosidase activity/CBM	Q0PQY7	48.7	4.4	56.8	1	2	2	6.8
Galactan 1.3-β-galactosidase	Q50KB2	47.8	5.9	51.3	1	5	5	16.3
Mannan endo-1.4-beta-mannosidase activity/CBM	Q0PQY8	49.0	5.0	49.4	1	2	2	6.7
Endo-1.4-beta-xylanase B	B7SIW1	30.4	6.1	47.9	3	2	2	11.0
Endoglucanase	Q66NB7	40.4	5.3	41.5	1	3	3	17.6
α-galactosidase	Q9HFZ9	48.5	4.8	20.9	1	3	3	7.8
Oxidoreductases								
Manganese peroxidase isozyme 3	Q1K9D0	39.8	4.6	348.7	1	8	8	33.8
Copper radical oxidase	Q0ZKA8	67.8	5.5	265.8	1	11	11	26.9
Cellobiose dehydrogenase	Q12661	81.9	5.3	113.5	2	10	10	15.8
Glyoxal oxidase	Q01773	59.1	5.2	78.7	1	9	9	18.3
Lignin peroxidase isozyme H8 (Fragment)	D1M7B6	35.1	4.7	52.3	5	1	3	11.5
Ligninase LG5	P11543	39.4	4.6	45.0	1	2	4	13.2
Copper radical oxidase	Q0ZKA7	70.3	4.8	35.0	2	2	2	5.4
Manganese peroxidase MnP1 (Fragment)	Q6T246	20.3	4.6	30.1	4	2	2	15.6
Copper radical oxidase	Q0ZKA5	107.9	4.9	16.3	1	3	3	4.4
Pyranose 2-oxidase	Q6QWR1	69.3	6.5	14.3	1	2	2	2.9
1.4-benzoquinone reductase	Q9Y763	21.4	6.2	12.9	1	2	2	15.4
Proteases								
Family S53 protease	Q281W2	58.4	4.9	133.8	1	3	3	9.9
Family A1 protease	Q281W1	41.9	5.9	53.0	1	4	4	12.6
Subtilisin-like protease (Fragment)	Q6H8Q3	86.9	4.8	37.8	1	5	5	5.2
Phosphatase enzymes								
Mannose-6-phosphatase	Q281W3	38.4	6.6	85.3	1	9	9	30.5
Other functions								
Putative laminarinase	Q874E3	33.9	5.2	88.0	1	3	3	12.0
Actin (Fragment)	Q7Z8L2	39.5	5.7	19.6	1	4	4	14.0
Translation elongation factor EF1-alpha (Fragment)	Q5EG85	34.1	8.4	18.8	1	3	3	8.3
14-3-3 1 protein	Q562H7	28.8	4.9	10.2	1	2	2	6.7

Table S7. Functional classification of proteins from ***P. chrysosporium*** **secretome growing on wheat straw**. Proteins were identified from the LC-MS/MS data from the entire secretome (EPP), searching against the *P. chrysosporium* database of **JGI**. Different groups are ordered from the highest to the lowest score in each functional group. GH= glycoside hydrolase family; CBM= carbohydrate-binding module. *Annotated protein.

Predicted proteins (JGI)	JGI ID (Phchr1)	MM (kDa)	pI	Score	Proteins	Unique peptides	Peptides	Coverage (%)
Glycoside hydrolases								
GH10	125669	35.2	5.6	454.7	1	9	9	32.8
Glucan 1.3-β-glucosidase	8072	84.4	5.8	296.7	1	7	7	11.9
GH7/CBM	137372	58.1	5.2	284.5	1	11	13	33.0
GH28/ polygalacturonase	3805	39.8	5.3	239.5	1	8	8	29.1
GH10	7045	31.0	7.4	217.8	1	4	8	43.5
GH6/CBM	133052	48.4	5.3	189.6	1	6	6	19.1
GH10/CBM	138345	43.5	5.4	183.6	1	4	6	23.3
GH7/CBM	129072	53.9	4.8	155.8	2	5	8	23.4
GH155/Glucan 1.4-α-glucosidase	138813	60.8	5.4	153.7	1	10	10	26.1
GH10/CBM	138715	42.3	4.9	151.9	1	6	8	29.6
α-1.2. mannosidase	133585	90.5	4.9	147.3	1	11	11	17.2
CBM	3097	42.8	5.3	137.7	1	3	3	13.5
CBM	130517	49.2	5.9	137.0	1	4	6	17.0
GH18/ chitinase active site / CBM	6412	49.2	5.1	130.7	1	6	6	23.7
GH47	4550	59.5	4.9	122.0	1	10	10	23.6
GH18/ chitinase active site / CBM	134311	54.9	6.2	117.4	1	7	7	16.7
GH7/CBM	127029	54.9	5.3	117.1	2	4	7	16.5
GH/ BNR repeat	28013	66.6	4.8	107.0	3	7	8	18.1
GH13/α- amylase	38357	52.1	4.9	103.3	1	7	7	14.9
GH7/CBM	137216	53.8	4.5	102.4	2	2	5	14.7
GH10/CBM	139732	37.7	5.4	101.7	1	2	6	22.7
GH3	9257	83.8	5.7	94.1	1	11	11	17.4
Glucan 1.3-β-glucosidase	135724	46.5	5.9	92.3	1	8	8	32.0
Putative glucanase precursor	10833	33.3	5.2	88.0	1	3	3	12.2
GH/ chitinase active site	137237	30.4	6.8	88.0	1	4	4	20.0
GH35/ β-galactosidase	9466	113.3	6.0	87.4	1	8	8	9.5
GH5*	6433	58.0	4.5	85.4	1	5	5	17.9
GH30	9011	58.8	6.0	80.2	1	5	5	9.5
Endoglucanase-4	138739	33.6	5.5	78.9	1	3	3	15.7
GH71	134357	48.4	7.4	73.9	1	4	4	11.3
GH88	840	49.7	5.2	73.4	1	3	3	7.8
GH61/CBM	31049	34.5	5.4	71.5	1	2	2	11.0
GH18/ chitinase active site	39872	42.8	4.5	68.8	1	4	4	12.9
GH28	29397	44.3	5.5	67.8	1	5	5	12.0
GH5/CBM	4361	49.2	6.7	67.4	1	3	3	11.0
GH3/CBM	134658	85.4	5.7	62.9	1	5	5	8.0
GH3	36045	90.8	6.2	62.4	5	8	8	10.2
GH3	139063	88.0	5.4	60.3	1	8	8	8.6
GH12	7048	27.0	4.9	57.9	1	2	2	10.0

Table S7. Continued

Predicted proteins (JGI)	JGI ID (Phchr1)	MM (kDa)	pI	Score	Proteins	Unique peptides	Peptides	Coverage (%)
α-N-arabinofuranosidase A	3651	55.3	5.4	57.3	1	2	2	4.5
GH5/CBM	5115	40.8	4.5	56.8	1	2	2	8.2
GH5/CBM	140501	47.7	4.9	49.4	1	2	2	7.0
GH11/CBM	133788	30.4	6.1	47.9	1	2	2	11.0
GH13/starch-binding/ α-amylase	7087	61.1	5.6	47.8	1	4	4	9.0
Glucan 1.3-β-glucosidase	132568	76.5	6.2	47.7	1	3	3	5.2
GH18/chitinase active site	128098	45.3	4.2	47.1	1	2	2	5.3
β-mannosidase	135385	100.6	5.1	45.4	1	4	4	5.8
α-1.2.mannosidase	1930	93.1	5.2	43.7	1	4	4	6.4
GH31	125462	103.6	5.5	43.2	2	7	7	11.5
GH. clan GH-D	4422	30.3	4.7	43.1	1	4	4	14.7
GH43	4822	32.9	5.1	35.8	1	2	2	9.1
GH37	140627	72.7	4.8	32.7	1	4	4	6.6
GH. BNR repeat	138266	77.7	5.0	32.2	1	4	5	7.1
GH18/ chitinase active site	2991	48.9	6.5	32.2	1	3	3	14.3
GH61	41123	23.6	7.1	31.1	1	3	3	16.3
GH27. clan GH-D	125033	47.7	4.9	29.6	1	4	4	11.6
GH43	297	49.1	9.3	26.2	1	2	2	5.9
GH43	133070	33.8	5.4	24.2	1	3	3	12.6
GH3	129849	86.8	4.9	19.7	1	5	5	6.7
GH20	37522	46.9	5.1	18.9	1	2	2	5.5
Endo-1.4-β-galactosidase	138710	36.7	6.0	14.7	1	2	2	12.6
GH5	5773	74.2	5.0	12.7	1	4	4	7.1
GH28	140428	87.3	5.2	12.6	1	2	2	3.1
Oxidoreductasas								
Haem peroxidase/ Fungal lignin peroxidase	878	39.9	4.6	342.0	2	7	8	33.8
Glyoxal oxidase	124009	67.8	5.5	262.2	1	10	10	23.6
GMC oxidoreductase/ Pyridine nucleotide-disulphide oxidoreductase	11098	82.0	5.5	113.5	1	10	10	15.8
Haem peroxidase/ Fungal lignin peroxidase	3589	40.1	4.7	105.7	2	1	2	4.5
Glyoxal oxidase	11068	59.1	5.3	69.4	1	8	8	16.6
Haem peroxidase/ Fungal lignin peroxidase	10957	39.6	4.6	50.2	4	1	3	10.2
Haem peroxidase/ Fungal lignin peroxidase	131738	39.3	4.6	43.0	4	2	4	13.2
Glyoxal oxidase	134241	80.8	5.1	35.0	1	2	2	4.7
FAD-dependent pyridine nucleotide-disulphide oxidoreductase	135167	51.1	6.9	30.4	2	4	4	9.8
Haem peroxidase/ Fungal lignin peroxidase	140708	39.5	5.0	30.1	2	2	2	7.9
GMC oxidoreductase	6270	66.6	5.7	23.8	1	3	3	6.3
Aldo/keto reductase	125914	40.6	7.0	8.7	2	2	2	4.4
Aldo/keto reductase family proteins	7571	35.5	6.8	21.2	1	2	2	6.3
FAD linked oxidase	3896	65.1	6.0	15.4	1	3	3	6.7
Haem peroxidase/ Fungal lignin peroxidase	8895	39.4	4.7	11.3	2	1	2	8.1
GMC oxidoreductase	126879	73.1	6.7	4.8	1	2	2	3.2
Alkyl hydroperoxide reductase. thiol specific antioxidant and related enzymes*	10009	25.0	6.3	4.6	1	2	2	9.5
Esterases								
Esterase/lipase/thioesterase	126075	35.6	6.4	81.2	2	3	3	15.1
Lipolytic enzyme. G-D-S-L	10607	41.2	5.6	54.0	1	4	4	10.7
Esterase/lipase/thioesterase	126191	56.0	5.5	49.1	1	6	6	14.2
Pectinesterase	132137	36.0	6.2	42.0	1	4	4	12.1
Esterase/lipase/thioesterase	7398	54.0	5.2	29.2	1	3	3	8.4

Table S7. Continued

Predicted proteins (JGI)	JGI ID (Phchr1)	MM (kDa)	pI	Score	Proteins	Unique peptides	Peptides	Coverage (%)
Esterase/lipase/thioesterase / Peptidase S28	37642	50.5	5.4	28.6	1	2	2	6.2
Phosphoesterase	30283	36.1	4.4	15.4	1	2	2	7.1
Esterase/lipase/thioesterase	3761	54.6	6.3	13.1	1	2	2	4.7
Pectinesterase	8580	45.3	5.9	9.2	1	3	3	6.7
Proteases								
Peptidase S8 and S53. subtilisin. kexin. sedolisin	26825	59.1	5.2	219.0	1	6	6	22.7
Peptidase aspartic. active site/ Peptidase A1. pepsin	8470	44.2	5.0	194.1	1	4	5	20.2
Peptidase aspartic. active site/ Peptidase A1. pepsin	8469	44.8	5.0	187.1	1	6	7	19.9
Amidase	3346	55.2	5.5	136.3	1	9	9	21.1
Peptidase S10. serine carboxypeptidase	8913	97.3	8.5	134.7	2	4	4	6.2
Tripeptidyl aminopeptidase	133020	59.0	4.9	133.8	1	3	3	9.8
Peptidase S10. serine carboxypeptidase	3855	51.6	5.4	100.1	1	4	4	14.9
Peptidase A4. scytalidopepsin B	43144	21.7	4.5	93.8	2	2	5	29.9
Peptidase aspartic. active site/ Peptidase A1	138924	41.2	5.7	93.0	1	6	6	18.6
Peptidase aspartic. active site/ Peptidase A1	129956	38.6	4.6	92.1	1	5	5	14.9
Peptidase A4. scytalidopepsin B/ Aspartic-type endopeptidase activity	121400	27.2	5.2	77.9	1	2	3	19.4
Peptidase aspartic. active site/ Peptidase A1	128676	39.6	4.6	67.7	2	2	2	6.8
Peptidase aspartic. active site/ Peptidase A1	29558	33.4	4.4	67.1	1	2	2	9.2
Peptidase aspartic. active site/ Peptidase A1	135608	41.9	5.9	53.0	1	4	4	12.6
Peptidase A4. scytalidopepsin B/ Aspartic-type endopeptidase activity	120995	26.8	6.2	51.6	1	1	3	9.4
Peptidase A4. scytalidopepsin B/ Aspartic-type endopeptidase activity	8468	44.2	5.4	48.0	1	3	3	7.9
Peptidase aspartic. active site/ Peptidase A1	8008	42.9	6.6	41.6	2	3	3	8.1
Protease-associated PA/ Peptidase S8 and S53. subtilisin. kexin. sedolisin	133799	93.3	5.0	37.8	1	5	5	4.8
Peptidase A4. scytalidopepsin B	7318	28.6	4.5	31.9	1	3	3	18.1
Amidase	140657	68.8	6.5	22.9	1	3	3	7.1
Protease-associated PA/ Peptidase S8 and S53. subtilisin. kexin. sedolisin	133613	87.5	5.4	20.4	1	3	3	3.7
Peptidase S8 and S53. subtilisin. kexin. sedolisin	1483	61.1	5.9	18.5	1	2	2	3.9
Peptidase S8 and S53. subtilisin. kexin. sedolisin	129261	64.1	5.9	15.8	1	2	2	3.7
Amidase	3719	55.1	5.4	14.2	1	2	2	3.5
Peptidase aspartic. active site/ Peptidase A1	126189	36.9	4.2	14.1	1	2	2	6.4
Peptidase S10. serine carboxypeptidase	2656	67.9	5.5	14.1	2	3	3	4.9
Peptidase. eukaryotic cysteine peptidase active site	123502	70.6	5.2	11.5	2	2	2	5.9
Peptidase aspartic. active site/ Peptidase A1	138453	33.5	4.2	10.5	1	2	2	6.1
Peptidase aspartic. active site/ Peptidase A1	7917	44.9	6.2	9.4	1	2	2	4.0
Peptidase aspartic. active site/ Peptidase A1	131827	34.9	4.6	4.7	1	2	2	7.2
Peptidase A1. pepsin	8365	62.4	4.9	4.2	1	2	2	2.5
Phosphatase enzymes								
Histidine acid phosphatase	137138	60.4	6.2	282.1	2	9	9	17.8
Endonuclease/exonuclease/phosphatase	138954	64.8	5.9	55.8	1	1	3	4.9
Other functions								
Aminotransferase	138738	65.4	4.7	156.6	1	10	12	24.5
Lipocalin-related protein and Bos/Can/Equ allergen	123909	33.8	5.5	109.3	1	6	6	19.9
Survival protein SurE	5655	31.5	4.7	92.7	1	4	4	12.5
Polysaccharide deacetylase	124827	37.5	4.8	80.2	1	4	4	17.4
Pectin lyase-like	8645	23.0	6.0	76.9	1	6	6	24.6
Thaumatin. pathogenesis-related	3280	26.8	5.0	66.3	1	1	2	12.9
Thaumatin. pathogenesis-related	5297	28.4	5.3	62.4	1	1	2	12.3
Ribonuclease T2	126123	41.4	5.2	43.3	1	3	3	11.8

Table S7. Continued

Predicted proteins (JGI)	JGI ID (Phchr1)	MM (kDa)	pI	Score	Proteins	Unique peptides	Peptides	Coverage (%)
Protein prenyltransferase	6458	39.6	5.3	41.5	1	3	3	18.0
Polysaccharide lyase family 8	6736	92.3	4.8	39.2	1	3	3	4.7
Porin. eukaryotic type	138775	31.4	8.9	38.2	1	5	5	20.1
Glutathione S-transferase	140259	25.4	7.1	30.1	1	5	5	18.0
Parallel beta-helix repeat	1249	51.1	5.4	29.4	1	3	3	6.8
Aldehyde dehydrogenase	8882	109.0	5.0	25.7	2	4	4	6.1
Aldehyde dehydrogenase*	137014	55.4	6.6	25.6	1	4	4	8.8
Polysaccharide deacetylase/ tubulin	132376	54.5	4.8	23.3	1	3	3	7.0
Stomatin	40896	29.7	8.1	20.3	1	3	3	11.0
Actin/actin-like	139298	52.5	6.7	19.6	1	4	4	10.6
Glycosyl transferase. family 35	5751	98.2	6.4	19.1	1	3	3	3.1
Translation elongation factor EF-1/ Protein synthesis factor. GTP-binding*	134660	50.1	9.1	16.8	1	3	3	5.7
Zinc-containing alcohol dehydrogenase superfamily*	1675	40.4	6.1	15.6	1	2	2	5.3
Glycosyl transferase. group 1	122462	81.6	6.5	15.1	1	2	2	2.9
Cys/Met metabolism pyridoxal-phosphate-dependent enzymes	10555	45.6	6.8	14.4	2	2	2	5.4
N-6 Adenine-specific DNA methylase	137275	69.3	6.5	14.3	1	2	2	2.9
Flavodoxin/nitric oxide synthase*	10307	21.4	6.2	12.9	1	2	2	15.4
14-3-3 protein (putative ortholog to S. cerevisiae Protein BMH2*)	139500	27.3	5.1	10.2	1	2	2	7.1
Proteasome α-subunit	133187	29.4	7.5	9.7	1	2	2	8.2
D-isomer specific 2-hydroxyacid dehydrogenase. NAD-binding	140211	39.2	6.9	9.3	2	2	2	5.3
E1 protein and Def2/Der2 allergen	6572	18.3	4.9	4.7	1	2	2	16.1
Unknown function								
Putative uncharacterized protein	130748	57.6	4.8	295.7	1	2	2	6.7
Putative uncharacterized protein	964	32.8	5.6	193.2	1	7	7	28.1
Putative uncharacterized protein	140079	75.3	5.9	186.7	1	10	10	22.7
Putative uncharacterized protein	5607	48.9	5.7	132.5	1	6	6	23.1
Putative uncharacterized protein	8738	11.9	7.1	102.8	3	4	5	75.7
Putative uncharacterized protein	6991	51.3	4.7	87.3	1	7	7	23.7
Putative uncharacterized protein	3383	39.0	8.6	85.3	1	9	9	30.3
Putative uncharacterized protein	6482	44.3	5.0	65.7	1	4	6	17.2
Putative uncharacterized protein	3328	78.4	6.1	59.6	1	7	7	10.2
Putative uncharacterized protein	6450	83.1	5.0	57.4	1	5	5	8.5
Putative uncharacterized protein	6069	65.7	4.9	47.9	1	4	4	9.4
Putative uncharacterized protein	7029	37.1	5.2	46.4	1	4	4	13.2
Putative uncharacterized protein	7437	47.1	7.0	46.1	1	4	4	10.5
Putative uncharacterized protein	3431	67.6	4.8	43.2	1	4	4	8.5
Uncharacterised conserved protein UCP028846	139777	53.8	5.6	41.9	1	6	6	11.6
Putative uncharacterized protein	123916	37.0	4.9	41.1	1	4	4	12.1
Putative uncharacterized protein	122884	73.0	5.3	40.5	1	4	4	7.7
Putative uncharacterized protein	3168	49.8	6.5	39.0	1	5	5	13.4
Putative uncharacterized protein	2035	28.8	4.4	36.1	1	3	3	17.1
Protein DUF338*	138982	58.7	4.7	30.3	1	4	4	11.7
Putative uncharacterized protein	5774	59.6	5.2	26.6	1	3	3	6.0
Putative uncharacterized protein	125335	68.0	5.7	26.1	1	2	2	3.9
Putative uncharacterized protein	3653	42.2	5.0	24.8	1	2	2	6.1
Putative uncharacterized protein	4912	76.8	10.5	23.9	1	2	2	4.2
Putative uncharacterized protein	8737	11.5	5.9	23.7	3	1	2	24.8
Protein DUF338	7122	57.5	4.5	22.3	1	3	3	8.3
Putative uncharacterized protein	2256	72.3	5.6	22.2	1	4	4	5.9

Table S7. Continued

Predicted proteins (JGI)	JGI ID (Phchr1)	MM (kDa)	pI	Score	Proteins	Unique peptides	Peptides	Coverage (%)
Putative uncharacterized protein	122292	66.2	5.8	19.2	1	3	3	5.4
Putative uncharacterized protein	6997	83.8	5.7	14.2	1	2	2	3.8
Putative uncharacterized protein	134621	33.1	4.5	14.2	2	2	2	9.9
Putative uncharacterized protein	1999	63.5	5.2	12.0	1	2	2	3.9
Putative uncharacterized protein	2037	30.4	5.5	11.2	1	2	2	10.8
Putative uncharacterized protein	2163	15.2	6.3	10.9	1	2	2	15.7
Putative uncharacterized protein	7809	45.7	6.4	9.1	1	2	2	4.2
Putative uncharacterized protein	280	101.0	5.1	7.6	1	2	2	2.5
Putative uncharacterized protein	4690	79.3	7.1	5.6	1	2	2	4.1

Table S8. Functional classification of proteins from ***P. ostreatus*** **secretome growing on wheat straw**. Proteins were identified from the LC-MS/MS data from the entire secretome (EPP), searching against the *P. ostreatus* database of **Uniprot.** Different groups are ordered from the highest to the lowest score in each functional group.

Predicted proteins (Uniprot)	Uniprot ID	MM (kDa)	pI	Score	Proteins	Unique peptides	Peptides	Coverage (%)
Glycoside hydrolases								
α-L-arabinofuranosidase	G0TES6	68.9	8.1	52.2	1	3	3	6.4
Cellulose 1.4-β-cellobiosidase	A5AA53	49.3	5.6	50.6	1	4	4	9.4
Cellulose 1.4-β-cellobiosidase	A5AA50	55.6	5.0	37.0	3	2	2	3.4
Oxidoreductases								
Manganese peroxidase	G8FPZ2	38.5	4.7	629.7	3	8	8	35.8
Laccase	Q96TR4	57.4	6.1	284.1	1	9	9	20.9
Manganese peroxidase	O74179	36.9	4.8	24.4	3	2	2	4.8
Laccase	D4AIA5	56.1	6.8	11.4	3	3	3	7.4
Proteases								
Subtilisin-like protease	Q6ZYK6	93.2	5.3	330.3	2	11	11	21.1
Peptidyl-Lys metalloendopeptidase	P81055	17.9	6.2	118.5	1	5	5	46.4
Putative aspartyl-proteinase (Fragment)	Q96TV7	18.5	6.2	51.8	1	3	3	21.4
Peptidase 1	C4PFY6	38.7	8.2	42.4	1	2	2	13.0
Other functions								
Ribonuclease T2	Q75NB1	41.5	6.4	65.1	1	4	4	14.2
Bilirubin oxidase	Q9UVY4	56.8	4.9	33.3	7	3	3	9.9
Putative ubiquitin (Fragment)	Q96TW1	27.3	8.9	28.3	1	3	3	33.3
Glyceraldehyde-3-phosphate dehydrogenase	D0VBH9	36.0	7.2	10.7	4	2	2	6.3
Unknown function								
Putative uncharacterized protein	D2JY75	27.8	6.6	162.8	2	7	7	42.8
Putative uncharacterized protein	D2JY77	26.4	10.0	6.4	1	2	2	7.9

Table S9. Functional classification of proteins from ***P. ostreatus*** **secretome growing on wheat straw**. Proteins were identified from the LC-MS/MS data from the entire secretome (EPP), searching against the *P. ostreatus* database of **JGI**. Different groups are ordered from the highest to the lowest score in each functional group.GH= glycoside hydrolase family; CBM= carbohydrate-binding module. *Annotated protein.

Predicted proteins (JGI)	JGI ID (PleosPC15)	MM (kDa)	pI	Score	Proteins	Unique peptides	Peptides	Coverage (%)
Glycoside hydrolases								
GH7/ CBM	1092970	55.9	4.8	981.9	1	10	22	61.2
GH47	1053206	58.7	5.2	699.4	1	10	13	35.9
GH47	1104326	60.5	5.5	602.8	1	9	9	22.0
GH7/ Concanavalin A-like lectin/ Glucanase	1039666	52.8	5.1	503.4	1	6	18	48.1
GH3	1035754	82.8	6.0	295.2	1	13	13	23.8
GH47*	1035282	58.8	5.2	251.2	1	4	7	17.9
GH28*	39721	41.7	5.8	244.5	1	5	5	11.5
GH79*	62138	55.8	5.9	227.8	1	11	11	28.3
GH3*	41613	76.5	5.9	209.5	1	10	11	17.5
GH5*/ CBM	1067505	40.9	5.1	176.3	1	9	9	40.8
GH6*/ CBM	48333	47.2	5.3	169.9	1	7	7	20.7
GH7*	1038048	48.8	4.6	161.7	1	8	10	24.3
GH16*/ Concanavalin A-like lectin/ Glucanase	1040267	34.9	4.8	161.4	1	7	7	31.8
GH37* / Six-hairpin glycosidase-like	1046178	72.6	5.4	141.0	1	7	7	15.4
GH35*	1066752	113.2	6.5	134.0	1	14	14	17.5
GH72*	1062416	58.3	4.7	112.1	1	4	4	9.3
GH10*	1078540	35.7	6.8	93.1	1	6	6	21.5
GH15*/ Glucan 1.4-alpha-glucosidase	29106	61.4	5.4	84.4	1	5	5	16.4
GH2*	61779	106.7	5.6	73.4	1	7	7	8.5
GH76*/ Six-hairpin glycosidase-like	1064904	38.3	6.2	68.2	1	4	4	16.3
GH5*/ CBM	1101955	41.8	5.1	68.1	1	4	4	24.0
GH115*	1045181	16.4	9.6	65.9	1	4	4	30.9
GH115*	162095	109.5	5.4	64.4	1	10	10	13.1
GH12*	50765	26.1	5.8	62.0	1	4	4	25.3
GH3*	1049518	83.6	5.7	38.8	1	2	2	3.5
GH35*	1113377	82.2	6.4	38.4	1	5	5	8.1
GH31*	1061735	106.4	6.1	32.1	1	4	4	4.0
GH20*	1094009	59.5	6.3	30.3	1	3	3	8.7
GH	1036297	77.0	6.5	27.6	1	1	3	6.3
GH1	153105	69.1	6.5	26.1	1	3	3	4.8
α-L-rhamnosidase	1108884	41.2	7.6	26.0	1	2	2	9.5
GH20*/ GH-D	1064686	64.3	5.9	21.1	1	4	4	10.9
GH27*/ GH-D	51341	42.7	6.9	20.6	1	2	2	7.4
GH13*/ Carbohydrate-binding-like fold/ α-amylase	1095839	61.7	5.4	20.4	1	3	3	4.9
GH55*	37178	82.8	6.0	18.5	1	3	3	5.9
GH51*/ α-L-arabinofuranosidase*	1042120	65.0	9.3	16.9	1	2	2	4.3
GH88*/ GH105*	154213	44.7	6.8	16.8	1	2	2	4.5
GH5*	49423	46.2	6.7	16.2	1	2	2	6.1
GH105*	1063776	41.7	5.3	16.0	1	2	2	5.2
GH27*/ GH-D	1035175	43.6	5.0	15.8	1	2	2	8.0
GH3*	1074900	164.0	6.3	15.5	1	1	2	1.1

Table S9. Continued

Predicted proteins (JGI)	JGI ID (PleosPC15)	MM (kDa)	pI	Score	Proteins	Unique peptides	Peptides	Coverage (%)
Six-hairpin glycosidase-like	159035	41.6	7.9	13.2	1	2	2	6.5
GH92*/ Six-hairpin glycosidase-like	1110177	87.8	6.3	12.3	1	3	3	6.1
GH88*/ Six-hairpin glycosidase-like	1031712	43.6	8.2	11.7	1	2	2	5.3
Gh35*/ Glycogen/starch/alpha-glucan phosphorylase	1058949	97.9	6.3	11.6	1	3	3	3.5
GH78*/ α-L-rhamnosidase/ Six-hairpin glycosidase-like	13903	65.7	5.7	10.1	1	2	2	4.3
Oxidoreductases								
Haem peroxidase/ Fungal lignin peroxidase	199491	38.3	4.7	436.1	1	4	5	14.8
Multi-copper-oxidase Laccase2/ Similar to POXA3*	1067328	57.4	6.1	282.1	1	9	9	20.9
Manganese peroxidase 2*	199510	37.9	5.2	194.0	1	3	4	10.3
Manganese peroxidase 5*	199511	37.7	4.7	91.5	1	5	5	17.5
Glyoxal oxidase / Galactose oxidase	1065295	59.6	5.7	89.1	1	5	5	13.0
Glyoxal oxidase	1078518	58.7	6.9	77.6	1	9	9	21.3
Glyoxal oxidase	1109338	61.7	6.8	61.4	1	7	7	16.6
Manganese peroxidase 1*	1041740	38.1	5.1	24.5	1	3	3	10.0
Aldo/keto reductase	1102061	35.2	6.3	24.1	1	5	5	12.6
Manganese peroxidase 3*	1089546	37.3	4.8	22.5	1	2	2	4.8
Aldo/keto reductase	1075590	39.9	7.1	16.8	1	2	2	5.6
Haem peroxidase. animal/ Cytochrome P450	1065994	111.6	6.5	13.1	1	2	2	2.4
Multicopper oxidase. type 1.2.3/ Laccase*	1113032	57.9	6.8	9.4	1	2	2	4.5
Aldo/keto reductase	1090974	37.1	5.9	8.3	1	3	3	7.7
Esterases								
Carboxylesterase. type B	1091241	59.3	7.0	1157.1	1	17	17	45.2
Carboxylesterase. type B	1047807	56.3	7.4	418.3	1	14	14	33.2
Lipase. GDSL / Esterase. SGNH hydrolase-type	1102068	26.5	7.5	129.1	1	7	7	44.9
Carboxylesterase. type B	1040351	56.7	8.5	110.8	1	8	8	18.0
Carboxylesterase. type B / C-type lectin fold	33340	76.1	6.1	82.6	1	7	7	12.9
Carboxylesterase. type B	1078816	54.4	7.6	51.7	1	7	7	21.0
Pectinesterase/ Carbohydrate Esterase Family 8 protein*	1044335	42.2	5.0	50.8	1	3	3	11.0
Carbohydrate Esterase Family 1*	1114413	38.9	6.2	38.7	1	2	2	6.0
Carbohydrate Esterase Family 15*	1086797	46.5	7.7	28.3	1	2	2	7.9
Glycerophosphoryl diester phosphodiesterase	1074827	39.9	6.9	24.2	1	2	2	5.5
Pectinesterase/ Carbohydrate Esterase Family 8*	1061918	35.6	8.6	20.0	1	3	3	17.7
Lipase. GDSL	1078000	45.6	6.0	17.5	1	3	3	8.1
Lipase. class 3	1044280	31.9	6.9	16.0	1	2	2	7.6
Carbohydrate Esterase Family 4*	1111329	48.4	4.8	13.3	1	2	2	5.1
Metallophosphoesterase	157761	112.6	5.1	12.9	1	2	2	1.8
Esterase. SGNH hydrolase-type/ Carbohydrate Esterase Family 16*	1075485	17.6	5.5	10.1	1	2	2	17.9
Carboxylesterase. type B/ Carboxylesterase and related proteins*	1051283	48.7	8.2	10.1	1	2	2	5.3
Proteases								
Peptidase S8 and S53	1077652	63.4	5.6	4612.3	1	10	10	24.3
Peptidase aspartic	1064571	37.5	6.2	2037.5	1	6	6	26.2
Peptidase aspartic/ Similar to Merops A01A peptidase*	1040870	42.2	5.7	438.8	1	5	5	17.4
Peptidase aspartic. catalytic/ Similar to Merops A10A protease*	26137	32.1	5.0	369.4	1	5	5	38.7
Amidase signature enzyme	1046424	43.0	5.0	337.1	1	6	8	26.5
Peptidase S10. serine carboxypeptidase	175915	57.8	5.1	323.6	1	9	9	25.8
Peptidase S8 and S53	1112600	93.3	5.3	312.3	1	10	10	20.0
Peptidase S8 and S53	1039782	62.6	5.8	287.9	1	5	5	8.3

Table S9. Continued

Predicted proteins (JGI)	JGI ID (PleosPC15)	MM (kDa)	pI	Score	Proteins	Unique peptides	Peptides	Coverage (%)
Peptidase S10/ Serine carboxypeptidase	1073281	49.5	4.7	260.0	1	8	8	31.5
Peptidase S41	1111045	74.2	6.0	215.8	1	12	12	21.3
Peptidase M36	62198	62.9	6.1	209.7	1	5	5	11.9
Amidase signature enzyme	1032663	32.7	5.1	181.0	1	5	9	28.9
Metalloprotease	1037634	33.9	5.7	116.6	1	5	5	24.4
Amidase signature enzyme	20196	51.9	5.2	100.0	1	2	5	8.9
Peptidase A1/ Peptidase aspartic*	1055405	43.3	5.1		1	5	5	14.6
Peptidase S10/ Serine carboxypeptidase	1078405	51.7	5.8	74.4	1	6	6	19.0
Peptidase S8 and S53	1088548	38.7	8.2	40.1	1	2	2	13.0
Peptidase M28	1079957	48.8	5.7	39.3	1	2	2	5.8
Peptidase C19/	1031730	26.2	4.6	38.4	1	3	3	19.8
Peptidase S41	1060558	70.8	5.3	30.3	1	5	5	9.4
Amine oxidase	1064593	71.1	6.3	29.1	1	2	2	4.6
Peptidase	10257	42.4	5.3	27.7	1	2	2	5.1
Peptidase A1/ Peptidase aspartic*	1089322	59.9	7.0	24.9	1	3	3	7.5
Peptidase S28	1045574	60.6	5.2	20.6	1	2	2	5.3
Protease-associated PA/ ABC transporter-like	157203	93.6	6.9	13.1	1	3	3	4.8
Phosphatases								
Phosphatase	1095212	34.7	5.5	167.0	1	8	8	33.1
Survival protein SurE-like phosphatase	162185	31.4	4.8	108.3	1	4	4	18.7
Histidine acid phosphatase	1110233	41.1	5.4	98.2	1	3	3	11.4
Histidine acid phosphatase	185948	47.7	6.5	51.8	1	4	4	10.6
Histidine acid phosphatase	1101887	60.7	6.2	34.0	1	4	4	8.0
Alkaline phosphatase	1099298	59.6	6.5	20.6	1	2	2	4.4
Histidine acid phosphatase	1035741	49.7	6.5	10.2	1	2	2	6.0
Other functions								
Thaumatin. pathogenesis-related	1081316	26.6	4.4	577.3	1	3	3	27.0
β-1.6-N-acetylglucosaminyltransferase. contains WSC domain	1114640	109.8	4.9	566.2	1	11	14	21.6
β-1.6-N-acetylglucosaminyltransferase. contains WSC domain	1081617	80.3	5.1	544.0	1	9	12	28.1
Phosphatidylserine decarboxylase-related	1062065	49.6	4.9	241.0	1	9	9	25.0
Site-specific DNA-methyltransferase (cytosine-N4-specific)*	1045048	33.0	7.0	231.0	1	6	6	25.9
Membrane attack complex component/perforin/complement C9	1086943	102.7	5.5	223.7	1	15	15	19.9
Amidohydrolase 2	1049583	19.7	4.5	139.9	1	2	2	11.5
α/β hydrolase fold-1	3428	29.9	6.7	137.3	1	5	5	22.9
Cerato-platanin / Barwin-related endoglucanase	1088025	14.4	7.7	136.0	1	2	2	18.9
Short-chain dehydrogenase/reductase SDR/ NAD(P)-binding / Glucose/ribitol dehydrogenase	1114616	26.0	9.2	133.7	1	8	8	32.8
Short-chain dehydrogenase/reductase SDR / Glucose/ribitol dehydrogenase/ NAD(P)-binding	1069103	28.2	7.6	115.2	1	8	8	36.2
Flavodoxin/nitric oxide synthase / Flavoprotein WrbA	41896	21.5	6.5	106.8	1	4	4	32.2
NmrA-like/ NAD(P)-binding/ Polysaccharide Lyase Family1*	53399	31.8	6.4	69.5	1	5	5	19.9
Pectate lyase/Amb allergen/ Polysaccharide Lyase Family1*	1054721	32.5	6.8	68.4	1	5	5	23.6
Aldehyde dehydrogenase	1090768	54.6	6.4	63.1	1	6	6	14.2
Fumarylacetoacetase	1032901	33.1	7.0	62.5	1	6	6	15.1
Macrophage migration inhibitory factor	21661	13.3	7.2	50.3	1	3	3	27.5
Short-chain dehydrogenase/reductase SDR / NAD(P)-binding / Glucose/ribitol dehydrogenase	1033771	28.9	7.9	49.0	1	5	5	22.0
Polysaccharide lyase family 8*	1101738	81.0	5.4	44.8	1	2	4	7.0
Ribonuclease T2	185836	40.8	6.3	44.7	1	3	3	9.6

Table S9. Continued

Predicted proteins (JGI)	JGI ID (PleosPC15)	MM (kDa)	pI	Score	Proteins	Unique peptides	Peptides	Coverage (%)
Transketolase	1113999	69.3	6.1	44.3	1	7	7	14.8
Hemopexin	1113759	26.2	5.1	42.2	1	5	5	25.3
Neutral/ Alkaline nonlysosomal ceramidase	1065698	69.4	6.9	34.4	1	5	5	7.5
SMP-30/ Gluconolaconase/ LRE-like region	169186	42.5	6.7	33.9	1	3	3	6.3
Cupin 2. conserved barrel / Bicupin. oxalate decarboxylase/oxidase	1078793	48.5	4.7	29.3	1	2	2	5.3
Ferritin/ Ribonucleotide reductase-like	1096735	44.8	5.7	26.9	1	4	4	11.5
Dienelactone hydrolase	1088515	30.3	5.9	25.0	1	2	2	10.3
Ubiquitin	1088454	42.7	8.1	24.4	6	2	2	23.6
YD repeat	1114460	218.4	6.2	23.5	1	3	3	1.6
Acetamidase/Formamidase	52279	43.0	5.5	23.4	1	2	2	7.0
Short-chain dehydrogenase/reductase SDR / Glucose ribitol dehydrogenase	162527	26.3	6.0	15.4	1	2	2	10.4
Ribosomal protein L18e	1063630	20.9	11.3	14.2	1	3	3	20.4
Thaumatin. pathogenesis-related	21503	26.9	4.8	14.1	1	2	2	11.4
Thiolase/ Ribosomal protein S3. C-terminal	1062741	72.3	8.3	13.8	1	2	2	2.8
SMP-30/ Gluconolaconase/ LRE-like region	1109731	40.9	6.2	10.1	1	2	2	5.3
SMP-30/ Gluconolaconase/ LRE-like region	1042025	78.1	5.2	10.1	1	2	2	3.3
6-phosphogluconate dehydrogenase. NAD-binding	1037028	26.6	7.5	10.1	1	2	2	9.4
Amidohydrolase 2	53363	35.2	4.8	8.6	1	2	2	5.4
Ribosomal protein S4	1054562	22.3	10.7	8.6	1	2	2	7.8
Short-chain dehydrogenase/reductase SDR / Glucose/ribitol dehydrogenase/ NAD(P)-binding	1090751	31.0	8.4	5.6	1	2	2	10.2
Membrane attack complex component/perforin/complement C9	163136	55.0	5.3	4.9	1	2	2	4.7
Ribosomal protein S3Ae	1089059	29.5	9.9	4.4	1	2	2	7.0
Homogentisate 1.2-dioxygenase / Cupin. RmlC-type	1107843	53.1	6.2	4.0	1	2	2	3.6
Unknown function								
Putative uncharacterized protein	1079640	19.0	4.8	399.8	1	2	2	16.6
Putative uncharacterized protein	1080147	37.9	7.4	273.4	1	1	3	10.2
Putative uncharacterized protein	1080163	37.7	5.6	244.9	1	5	7	38.5
Putative uncharacterized protein	1066218	47.8	4.9	122.0	1	6	6	17.9
Putative uncharacterized protein	1032791	51.4	5.8	91.3	1	5	5	13.8
Putative uncharacterized protein	1076067	43.9	6.4	89.3	1	5	5	17.8
Putative uncharacterized protein	1049780	38.4	6.1	76.7	1	5	5	18.3
Putative uncharacterized protein	1111275	21.8	9.0	70.8	1	3	3	14.8
DUF427	1046408	28.6	7.1	37.7	1	4	4	13.3
Putative uncharacterized protein	1078081	31.5	7.2	22.7	1	2	2	11.9
Putative uncharacterized protein	161080	26.2	5.5	13.0	1	3	3	18.9
Putative uncharacterized protein	1113075	53.5	5.6	11.2	1	2	2	4.8

Chapter 4

Characterization of a novel DyP-type peroxidase from *Irpex lacteus* and its application in the enzymatic hydrolysis of wheat straw

Davinia Salvachúa, Alicia Prieto, Ángel T. Martínez, María Jesús Martínez

Applied and Environmental Microbiology (2013)
doi:10.1128/AEM.00699-13

ABSTRACT

Irpex lacteus is a white-rot basidiomycete proposed for a wide spectrum of biotechnological applications which presents an interesting, but still scarcely known, enzymatic oxidative system. Among these enzymes, the production, purification, and identification of a new dye-decolorizing peroxidase (DyP)-type enzyme, as well as its physico-chemical, spectroscopic, and catalytic properties, are described in the current work. According to its N-terminal sequence and peptide mass fingerprinting analyses, *I. lacteus* DyP showed high homology (>95%) with the hypothetical (nor isolated nor characterized) protein cpop21, from an unidentified species of the family Polyporaceae. The enzyme had a low optimal pH (2-4), was very stable to acid pH and temperature, and showed improved activity and stability at high H_2O_2 concentrations compared to other peroxidases. Other attractive features of *I. lacteus* DyP were its high catalytic efficiency oxidizing the recalcitrant anthraquinone and azo- dyes assayed (k_{cat}/K_m = 1.6 x 10^6 s^{-1} M^{-1}), and its ability of oxidizing non-phenolic aromatic compounds like veratryl alcohol. In addition, the effect of this DyP during the enzymatic hydrolysis of wheat straw was checked. The results suggest that *I. lacteus* DyP displayed a synergistic action with cellulases during the hydrolysis of wheat straw, increasing significantly the fermentable glucose recoveries from this substrate. These results show a promising biotechnological potential for this enzyme.

1. INTRODUCTION

Irpex lacteus is a basidiomycete with a noteworthy biotechnological potential. This white-rot fungus has been applied in biodegradation of toxic compounds (Moon and Song, 2012), dye-decolorization (Kalpana et al., 2012), water and soil bioremediation (Novotny et al., 2000), and biopretreatment of lignocellulosic substrates to improve sugar recoveries for bioethanol production (Pinto et al., 2012; Salvachúa et al., 2011). Its efficiency in these processes has been mainly attributed to the release of a battery of ligninolytic enzymes, namely Mn^{2+}-oxidizing peroxidases (MnP), lignin peroxidases (LiP), and laccases (Novotny et al., 2009). However, some reports have also described the production of another type of peroxidases, designated as non-specific (Shin, 2004) or Mn^{2+}-independent peroxidases (Cajthaml et al., 2008; Salvachúa et al., 2013), which could have an important implication in these processes and have not been isolated and/or characterized up to date.

According to Welinder et al. (Welinder, 1992), heme peroxidases are classified into two superfamiles, animal and plant peroxidases, and the latter is further divided into three categories according to their origin. Class I peroxidases come from the prokaryotic lineage and class II and III peroxidases are secreted by fungi and plants, respectively. In the fungal kingdom, MnP, LiP, and versatile peroxidases (VP) are the main representatives of the group and the most studied so far (Martínez et al., 2009). Nevertheless, a new family of heme peroxidases, known as DyP-type peroxidases (EC 1.11.1.19), has been described in the last years (Hofrichter et al., 2010; Ruiz-Dueñas and Martínez, 2010; Sugano et al., 2007; Sugano, 2009). These enzymes constitute an independent group of heme-peroxidases and seem to offer attractive catalytic properties for biotechnological purposes (Liers et al., 2010; Zelena et al., 2009; Zorn et al., 2011).

DyPs show no sequence homology to other fungal peroxidases, presenting structural divergence from them, low sequence similarity with disparity in heme pocket residues, and singular catalytic properties such as very low optimal pHs and high apparent affinity for substituted anthraquinones (Faraco et al., 2007; Sugano, 2009). In addition to typical peroxidase activity, a hydrolase or oxygenase activity has been suggested for DyP (Sugano et al., 2009). The physiological role of DyPs is still controversial but it has been suggested that they are a part of the catalytic system secreted by fungi for oxidizing non-phenolic substrates, such as lignin and/or toxic aromatic products, or acting as a defense mechanism against oxidative stress (Liers et al., 2012). There are hundreds of putative DyP sequences in genomes (Floudas et al., 2012) and 222 members have

been registered in PeroxiBase (http://peroxibase.toulouse.inra.fr/), however only 8 proteins have been characterized so far, and 6 belong to fungal DyPs (Liers et al., 2012). On the basis of sequence homologies, phylogenetic, and tertiary structure analyses, a peroxidase from *Termitomyces albuminosus*, and one hypothetical peroxidase (cpop21) from an unidentified Polyporaceae species have also been included in this group (Sugano et al., 2007; Sugano, 2009).

In the current work, a novel DyP from *I. lacteus*, related to the putative cpop21 enzyme, has been isolated and characterized. In addition, the catalytic properties of the enzyme, as well as its application as a supplement for the enzymatic hydrolysis of wheat straw are discussed.

2. MATERIALS AND METHODS

2.1. Microorganism, culture conditions, and enzyme production

The basidiomycete *I. lacteus*, deposited in Centro de Investigaciones Biológicas (Madrid, Spain) as IJFM A792 (CCBAS 238 617/93), was maintained on 2% malt extract agar (w/v) at 4ºC and pre-cultured on the same medium at 28ºC. After 1 week, four 1-cm^2 agar plugs were cut and used to inoculate 250 mL flasks with 30 mL of a corn steep solid based medium (CSS) at 28ºC and 180 rpm (Salvachúa et al., 2011). The growth medium contained corn steep solids (26.3 g), glucose (40 g), $FeSO_4$ x $7H_2O$ (0.4 g), $(NH_4)_2SO_4$ (9 g), KH_2PO_4 (4 g), and $CaCO_3$ (7 g). After 7 days, the cultures were homogenized (Omnimixer, Sorvall) and 2.5 mL were transferred to 250 mL flasks containing 30 mL of the same medium and incubated under identical conditions. Samples were taken periodically to follow the enzyme secretion, as described below, and remaining glucose was measured with the "Glucose-TR" kit (Spinreact).

2.2. Enzymatic assays

Mn-oxidizing peroxidase activity (MnP) was measured by the formation of Mn^{+3}-tartrate complex (ε_{238}= 6,500 cm^{-1} M^{-1}) during the oxidation of 0.1 mM $MnSO_4$ in 100 mM tartrate buffer at pH 5. DyP-like activity was followed by the oxidation of 2.5 mM 2,2´-azino-bis(3-ethylthiazoline-6-sulfonate) (ABTS) to its cation radical (ε_{418}= 36,000 cm^{-1} M^{-1}) in 100 mM tartrate buffer at pH 5 (standard conditions) and the decolorization of an anthraquinone-dye, 50 μM Reactive Blue 19 (RBlue19) (ε_{595}= 10,000 cm^{-1} M^{-1}) in the same buffer at pH 4. In all cases, peroxidase activity assays were carried out in the presence of 0.1 mM H_2O_2. Laccase activity was also determined following ABTS and RBlue19 oxidation in the absence of H_2O_2.

An additional battery of substrates was used to check the effect of pH on *I. lacteus* DyP activity and to study its kinetic parameters. The selected substrates were 2,6-dimethoxyphenol (DMP) and veratryl alcohol (VA), as representatives of phenolic and non-phenolic compounds, respectively, and Reactive Black 5 (RBlack5), as an azo-dye. Enzyme activities were followed by the increase in absorbance at 469 nm for DMP (ε_{469}= 27,500 cm^{-1} M^{-1}) and 310 nm for VA (ε_{310}= 9,300 cm^{-1} M^{-1}) and the decrease of absorbance at 598 nm for RBlack5 (ε_{598}= 30,000 cm^{-1} M^{-1}). These reactions were performed in the presence of 0.1 mM H_2O_2.

All measurements were carried out at room temperature. Control treatments, without H_2O_2 and/or without enzyme were performed. One unit of activity (1 U) is defined as the amount of enzyme releasing 1 μmol of product per minute under the defined reaction conditions.

2.3. Enzyme purification

When maximal DyP-like activity was detected, cultures were harvested and filtered to separate the mycelium. Then the culture broth was vacuum-filtered through 0.22 μM membranes (Millipore Corporation), concentrated 30-fold and dialyzed against 10 mM sodium tartrate buffer (pH 5) under continuous stirring at 4ºC in a tangential ultra-filtration system (Amicon, Millipore Corporation) using a 10-kDa cutoff membrane. This enzymatic crude was used for further purification studies and enzymatic hydrolysis assays of wheat straw.

The enzyme was purified using an ÄKTA HPLC system (GE Healthcare), using columns from the same provider, in three consecutive steps. The eluted fractions were monitored at 280 nm and 410 nm to detect total and heme-containing proteins, respectively. In anion-exchange chromatography, columns were equilibrated with 10 mM sodium phosphate buffer at pH 7. The first separation step was performed on a Hi-Trap Q FF 5 mL cartridge at a flow rate of 1 mL min^{-1}. After 12 mL, the retained proteins were eluted with a linear NaCl gradient from 0 to 20% in 50 mL and then from 20 to 100% in 13 mL. 100% NaCl was maintained for 11 mL. Peroxidase activity was measured by ABTS and Mn^{2+} oxidation at standard conditions and the appropriate fractions were pooled, concentrated, dialyzed against 10 mM sodium phosphate buffer at pH 7 and loaded into a Mono-Q™ column HR 5/5 at a flow rate of 0.8 mL min^{-1}. A NaCl lineal gradient from 0 to 16% in 33 mL was applied, raising to 100% NaCl in 3 mL. Fractions with DyP-like activity were again pooled, concentrated and the mixture proteins separated by size-exclusion chromatography (SEC) in Superdex-75 HR 10/30 with 10 mM sodium phosphate buffer (pH7) plus 150 mM NaCl at 0.3 mL min^{-1}. The purified

DyP was dialyzed against 10 mM sodium tartrate buffer at pH 5. The homogeneity of the protein was confirmed by sodium dodecyl sulfate-polyacrylamide gel electrophoresis (SDS-PAGE) in 12% gels stained with Coomassie Brilliant Blue R-250 (Sigma). The purification yield was calculated from total protein quantification in a NanoDrop 2000 spectrophotometer (Thermo Fischer Scientific) taking into account the peroxidase activity against ABTS.

2.4. Enzyme characterization

The molecular mass of *I. lacteus* DyP was estimated by SDS-PAGE (12% polyacrylamide gel) by using pre-stained standard proteins (Bio-Rad) and confirmed by MALDI-TOF mass spectrometry (Autoflex III, Bruker Daltonics), calibrated with the protein calibration standard II from Bruker. The isoelectric point (pI) of the desalted protein was determined by isoelectrofocusing (IEF) in gels with 5% polyacrylamide and a mixture of ampholines to obtain a pH range of 2.5-5 (mixing 85% from pH 2.5-5 and 15% from pH 3-10, from GE healthcare), with 1 M H_3PO_4, and 1 M NaOH in anode and cathode, respectively. After IEF, the pH values were directly measured from the gel to obtain a pI calibration line. Proteins were stained with Coomassie Brilliant Blue R-250 and for peroxidase activity (zymogram) with ABTS and H_2O_2 at standard conditions, after washing the gels for 10 min with 100 mM sodium tartrate buffer at pH 5.

To determine its glycosylation degree, the protein was deglycosylated with Endoglycosidase H (Roche) in 10 mM tartrate sodium buffer (pH 5) at 37ºC overnight. The molecular mass and pI of the deglycosylated DyP were examined as previously described for the native enzyme. The amount of N-linked carbohydrates was determined by the difference in molecular mass of the native and the deglycosylated protein obtained by MALDI-TOF, and expressed as weight percentage.

The UV-visible spectrum of the enzyme at resting state, in 10 mM sodium tartrate buffer, pH 5, was recorded in the range from 800 to 300 nm (UV 160 Spectrophotometer, Shimadzu).

2.5. Effect of pH and temperature on *I. lacteus* DyP activity and stability

To study the effect of pH on enzyme activity, the substrates ABTS (2.5 mM), DMP (2.5 mM), VA (10 mM), RBlue19 (50 μM), and RBlack5 (25 μM) were prepared in Sorensen's glycine buffer (100 mM) from pH 1.5 to 2, and Britton & Robinson buffer (100 mM) from pH 2 to 9. The percent of oxidation or decolorization for each substrate was calculated considering the pH of maximum activity as 100%.

To determine the effect of pH and temperature on DyP stability, the enzyme was incubated in 100 mM Britton & Robinson buffer from pH 2 to 9 at 4, 25, and 50ºC. Samples were withdrawn at 0, 0.25, 1, 6, 24, 48, and 168 h to calculate the residual activity by using the standard ABTS assay at pH 3 described above. The initial activity of the enzyme was taken as 100%.

The T_{50} value, defined as the temperature at which 50% of activity is lost in a 10 min-incubation, was also checked. To determine this thermostability index, the protein was incubated in 10 mM sodium tartrate buffer (pH 5) at various temperatures from 25 to 80ºC during 10 min, cooled on ice, and rewarmed to room temperature for 5 minutes prior to residual activity determination by the standard assay at pH 3. The temperature at which the enzyme retained the maximum residual activity was taken as 100%.

2.6. Enzyme kinetics

The Michaelis-Menten and catalytic constants (K_m, $k_{cat,}$ and k_{cat}/K_m) were determined incubating the enzyme (~1.5 nM) with varying concentrations of: i) ABTS, DMP, VA, RBlue19, and RBlack5 with a constant H_2O_2 concentration (0.1 mM), and ii) H_2O_2 in the presence of a constant ABTS concentration (2.5 mM). The values for the kinetic parameters and their correspondent errors were calculated with Sigma Plot v.12. The kinetics and the specificity of *I. lacteus* DyP towards each of these substrates were measured at the optimum pH of the enzyme: ABTS, DMP, and RBlack5 substrates were prepared in 100 mM sodium tartrate buffer at pH 3, RBlue19 in the same buffer at pH 4, and VA in 100 mM Britton & Robinson buffer at pH 2.

2.7. Enzyme activation/inactivation assays

All following DyP activity measurements were performed at standard assay conditions at pH 3 with some modifications. First of all, enzyme inactivation by its own co-susbstrate (H_2O_2), at concentrations from 50 mM to 0.3 μM (two-fold serial dilutions), was tested at short reaction times (1 min) in the presence of 2.5 mM ABTS. The enzyme concentration used for this assay was 1.5 nM.

DyP inactivation was also followed over the time using different [H_2O_2]/ [enzyme] molar ratios, maintaining constant the enzyme (50 nM) and varying H_2O_2 concentration from 12.8 mM to 6.25 μM in 10 mM tartrate buffer pH 5 at 25 ºC, in the absence of reducing substrate. Samples were taken at different times and residual activity was measured.

Additionally, standard assays at pH 3 were carried out in the presence and absence of two different concentrations (0.2 and 2 mM) of different cations (Mn^{2+}, Co^{2+}, Ni^{2+}, Cu^{2+}, Fe^{3+}, Ca^{2+}, Mg^{2+}, K^{+}, Li^{+}, Ba^{2+}, Zn^{2+}, Pb^{2+}, Hg^{2+}, and Ag^{1+}), EDTA, and N_3Na. DyP was incubated with these compounds for 10 min prior to the activity measurement.

2.8. N-terminal sequence and peptide mass fingerprinting analyses

The N-terminal amino acid sequence was analyzed by Edman's sequential degradation in a protein sequencer Procise 494 (Perkin Elmer). Homology searches were performed using the BLAST program from the National Center for Biotechnology Information (NCBI, Bethesda, USA) database.

For peptide mass fingerprinting, the purified protein was analyzed by SDS-PAGE in a 7.5% polyacrylamide gel and stained with SYPRO Ruby (Bio-Rad). The band was excised and subjected to tryptic in-gel digestion in a DigestPro MS digestor (Intavis AG). MS analyses of the tryptic peptides were performed in an Autoflex III MALDI-TOF/TOF mass spectrometer (Bruker Daltonics, Bremen, Germany) controlled by the flexControl 3.0 software (Bruker Daltonics). Three of the tryptic peptides were chosen to carry out fragmentation and sequencing. MALDI-MS and MS/MS data were combined through the BioTools 3.0 program (Bruker Daltonics) to search against the non-redundant protein database from the NCBI using the MASCOT 2.3 search engine (Matrix Science). Scores greater than 86 are considered significant ($p<0.05$).

2.9. Enzymatic hydrolysis of wheat straw

The effectiveness of different enzyme mixtures in wheat straw hydrolysis was checked by measuring the cellulose and hemicellulose digestibility yields. Prior to the enzymatic hydrolysis, wheat straw was subjected or not to biopretreatment with *I. lacteus* during 21 days in basal conditions, combined or not with a mild alkali treatment (0.1% sodium hydroxide), as previously reported (Salvachúa et al., 2013). Hydrolysis of the different substrates was performed in duplicate at 5% (w/v) in 100 mM sodium citrate buffer (pH 4.8) at 50 ºC and 165 rpm for 60 h using the following enzymatic mixtures: i) commercial cellulases, such as Celluclast (15 U global cellulase) and NS50010 (15 U of β-glucosidase), and xylanases, as NS50013 (30 U of global xylanase) and NS50030 (30 U of β-xylosidase), all provided by Novozymes, ii) the previous commercial cocktails plus the enzymatic crude of *I. lacteus* containing 30 U of DyP, iii) only the enzymatic crude of *I. lacteus* (30 U of DyP), and iv) the previous commercial cocktails plus the purified DyP (30 U of DyP which corresponded to 150 μg of protein). Global cellulose activity was determined as filter paper units, β-glucosidase against *p*-nitrophenyl

glucopyranoside, global xylanases against birch xylan, β-xylosidase against *p*-nitrophenyl xylopyranoside, and DyP against RBlue19 in the presence of 0.1 mM H_2O_2 in sodium tartrate buffer pH 4. Units of commercial cellulases and xylanases are referred to gram of cellulose or xylan, respectively, and DyP units are referred to gram of wheat straw. The residual activity of DyP was also checked at the end of enzymatic hydrolysis. After having proved the stability of the enzyme against H_2O_2, an aliquot of 0.8 mM H_2O_2 was added to all samples at 0, 24, and 48 h. Controls consisted of substrates plus buffer without any enzyme supplementation and were incubated under the same conditions. Substrate characterization (percentage of cellulose and hemicellulose before and after biopretreatment), fermentable sugar release quantification, and digestibility estimations were performed as detailed by Salvachúa et al. (Salvachúa et al., 2013).

3. RESULTS

3.1. Production and purification

The secretion of peroxidases by *I. lacteus*, detected by H_2O_2-dependent oxidation of ABTS (to colored cation radical) and RBlue19 decolorization, started at day 4 and 12, respectively. A first activity peak against Mn^{2+} and ABTS, which corresponded to MnP, was detected at 7 days. This activity decreased over the time but a second MnP peak appeared at 21 days, coinciding with a maximum activity against RBlue19 (Fig. 1). Laccase activity was not detected during the whole growing period.

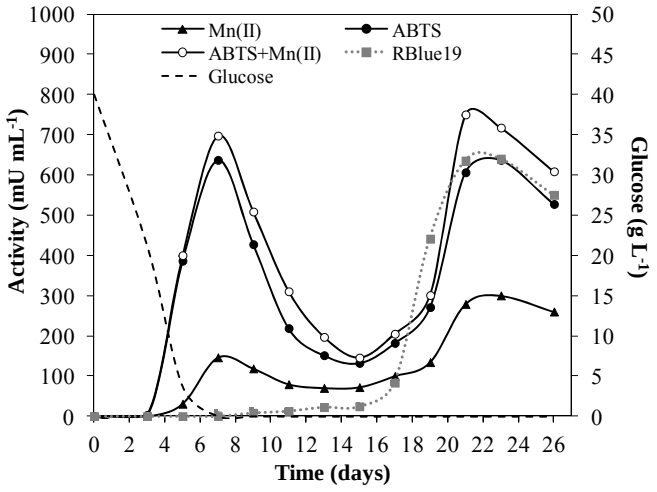

Fig. 1. Peroxidase activities and residual glucose in *I. lacteus* cultures incubated in CSS during 26 days. The oxidation of Mn^{2+}, ABTS, and ABTS plus 0.1mM Mn^{2+} were followed at pH 5 and the oxidation of Reactive Blue 19 at pH 4. Standard deviations from triplicate cultures were less than 10%.

After the first purification chromatographic step (Table 1), DyP was fully separated from the other peroxidases released to the medium. The chromatogram profile showed 3 peaks at 410 nm (Fig. 2A), with relative ABTS activity representing 6%, 80% and 14% of total activity, respectively. The second fraction, eluting at a NaCl concentration of 0.1 mM, was the only one without MnP activity and was selected to continue the purification process. After three chromatographic steps (Fig. 2A, B, C) an electrophoretically homogeneous enzyme preparation was achieved (Fig. 2D), reaching a 32-fold purification factor with a yield of 18.6 % (Table 1).

Table 1. Purification of DyP from the enzymatic crude of *I. lacteus* growing in CSS liquid medium.

Step	Activity* (U)	Protein (mg)	Specific activity (U mg^{-1})	Yield (%)	Purification (fold)
Culture filtrate	117.0**	9.69	1.2	100.0	1.0
HiTrap-Q	90.7	1.39	6.5	77.5	5.7
Mono-Q	45.0	0.22	13.8	49.6	12.0
Superdex-75	8.4	0.05	37.8	18.6	32.3

* Activity was measured with 2.5 mM ABTS in 100 mM sodium tartrate buffer (pH 5) and 0.1 mM H_2O_2.
** This value could be over-estimated due to the presence of ABTS-oxidizing MnPs in the *I. lacteus* culture.

3.2. Characterization of *I. lacteus* DyP

The exact molecular mass of the purified native enzyme, glycosylated and N-deglycosylated, was 57,125 and 51,108 Da, respectively, as determined by MALDI-TOF (Fig. 3A and 3B). These data indicate that DyP contains about 10.5% of N-linked carbohydrate. Concerning pI, both forms of the enzyme appeared as single bands in IEF with pI values of 3.85 and 3.75, respectively (Fig. 3D). DyP zymograms revealed that the deglycosylated protein was fully active (data not shown).

The UV-visible spectrum of DyP at resting-state showed the main Soret band at 406 nm and two charge transfer bands at 505 and 636 nm (Fig. 3C), as well as a Reinheitszahl ratio (A_{406}/A_{280}) of 1.59. The molar absorption coefficient of *I. lacteus* DyP was ε_{406}=140,527 M^{-1} cm^{-1}, similar to those found in other peroxidases and DyPs (Kim and Shoda, 1999).

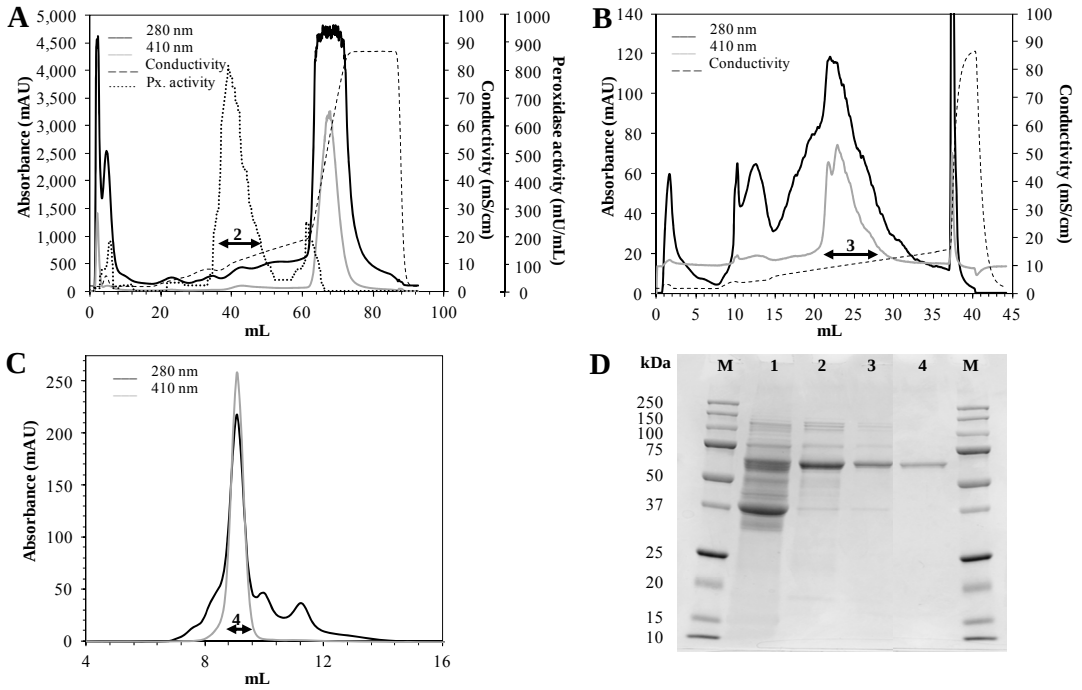

Fig. 2. Purification and SDS-PAGE of DyP from the enzymatic crude of *I. lacteus*. Anion exchange chromatography in (A) HiTrap-Q FF and (B) Mono-Q, and (C) SEC in a Superdex-75 column. Each collected fraction, used for the subsequent chromatographic step, is signaled with an arrow. (D) SDS-PAGE (12%) gel from the culture filtrate (lane 1) and the fractions collected after aech purification step (lanes 2, 3,and 4). M corresponds to the molecular mass markers.

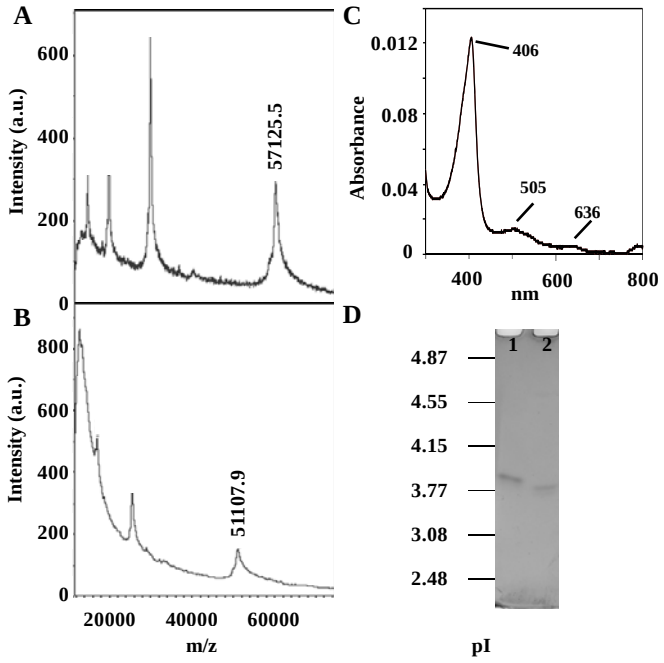

Fig. 3. Characterization of *I. lacteus* DyP. Molecular mass estimation of the purified DyP by MALDI-TOF of the (A) glycosylated and (B) deglycosylated form; (C) spectrum from 300 to 800 nm; (D) IEF gel from pI 2.5 to 5 of the glycosylated (lane 1) and deglycosylated (lane 2) DyP, stained with Coommasie Blue R-250.

3.3. Effect of pH and temperature on *I. lacteus* DyP activity and stability

The effect of pH on DyP activity was initially examined with different substrates at pH ranging from 1.5 to 9. As shown in Figure 4, DyP was active in a pH range between 1.5 and 6, although relative activities and optimum pH differed among the tested substrates. VA oxidation was optimal at pH 2, but the residual activity decreased to 40% at pH 1.75 and 3. In contrast, the highest optimal pH was observed at pH 4 for RBlue19 decolorization. The oxidation of ABTS and DMP showed similar pH profiles, with pH 3 as the optimum value and 20% residual activity at pH 2. The optimum pH for RBlack5 oxidation was also pH 3, but in this case the enzyme retained a 60% of residual activity at pH 2.

Additionally, the stability of *I. lacteus* DyP was checked at three different temperatures and pH range between 2 to 9. When maintained at 4ºC for 1 week, the residual activity was higher than 70% at all pH tested excluding pH 9, where the activity loss was around 80% (Fig. 5A). After 1 week incubation at 25ºC, the enzyme was also quite stable, with residual activities superior than 50% at pH values comprised between 3 and 7 (Fig. 5B) and even retaining 15% activity at pH 2. In view of this result, some activity loss during the purification process (at pH 7 and 25ºC) may occur during the first hours but, after 24 h, that loss is insignificant. At 50 ºC, DyP displayed the highest activity at pH 4 and 5 (Fig. 5C), with a half-life (50% of the activity) of 8 h, keeping some activity after 48 h of incubation. When the pH was set at 3 and 6, the half-life of DyP was around 2 h. Regarding the T_{50} index, the calculated value was 63ºC at pH 5 (Fig. 5D). The maximum activities, taken as the 100%, were detected at 25 and 30ºC.

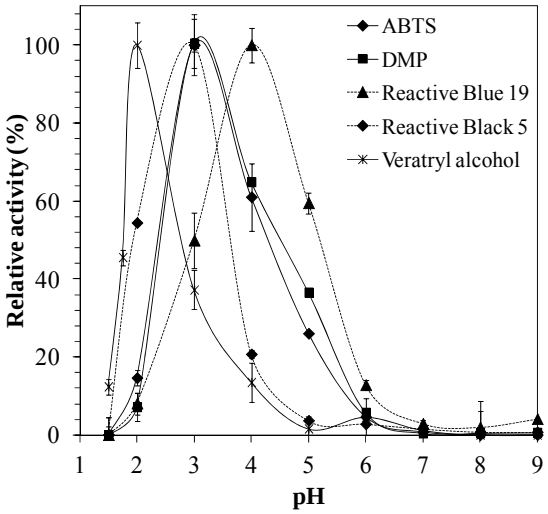

Fig. 4. Optimum pH of the purified *I. lacteus* DyP oxidizing different substrates.

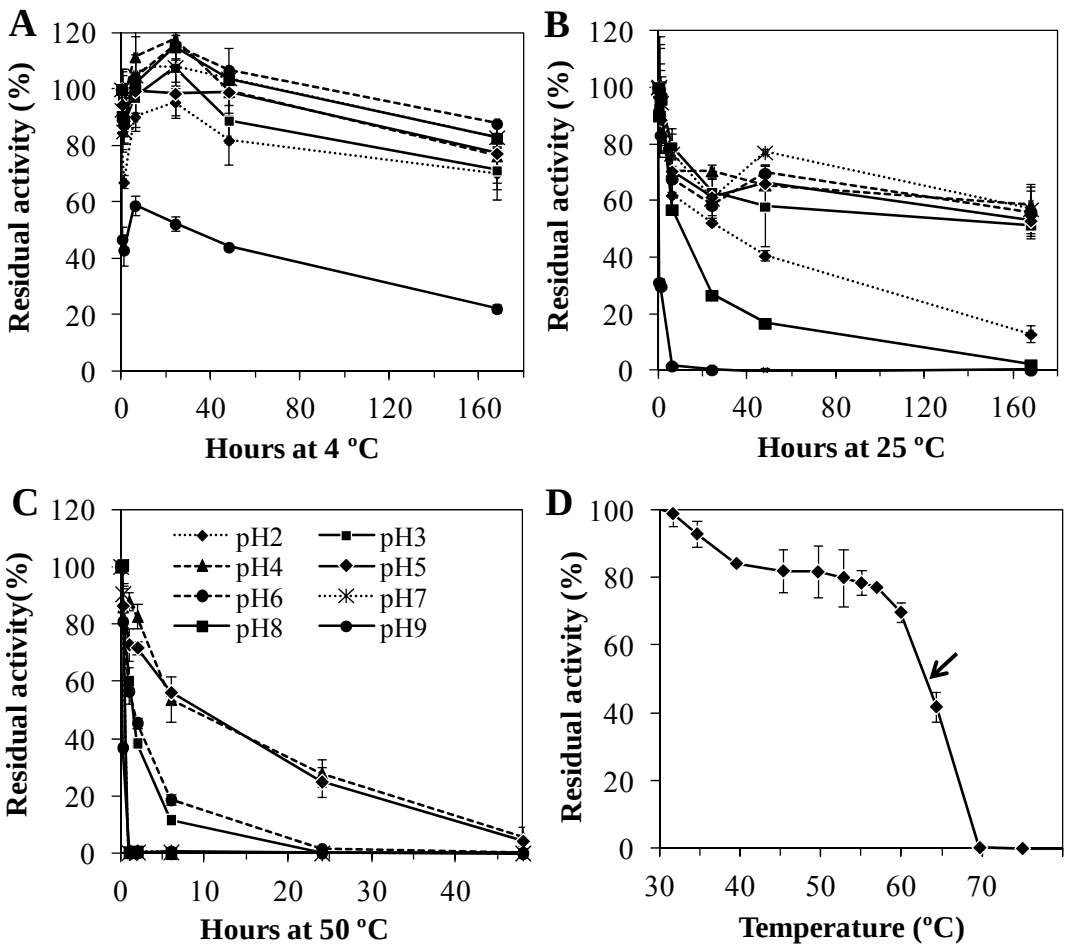

Fig. 5. Thermo-stability of the purified *I. lacteus* DyP at (A) 4 ºC, (B) 24 ºC, and (C) 50 ºC at different pHs and (D) T_{50} estimation (at pH 5).

3.4. Catalytic properties

Diverse substrates were oxidized by DyP in the presence of H_2O_2, and the kinetic parameters of the enzyme were calculated for each of them being summarized in Table 2. The highest activity was found for ABTS (k_{cat} = 224 s^{-1}), followed by similar values with DMP and RBlue19 (k_{cat} = 70 s^{-1}). The enzyme showed the lowest activities for VA and RBlack5.

The Michaelis constant (K_m) for dyes was lower than for DMP and ABTS, and the catalytic efficiency (k_{cat}/K_m) was significantly superior for the anthraquinone-type dye RBlue19 (5.9 x 10^6 s^{-1} M^{-1}), but it was even higher for the synthetic substrate ABTS (7.97 x 10^6 s^{-1} M^{-1}). The highest K_m (> 3,600 µM) was found towards VA. The apparent affinity for H_2O_2 was lower than that reported for other DyPs (Liers et al., 2010; Ogola et al., 2010).

Table 2. Kinetic parameters of *I. lacteus* DyP and pH at which they were evaluated. Substrates oxidation was measured using 0.1 mM H_2O_2.

	pH	K_m (μM)	k_{cat} (s^{-1})	k_{cat}/K_m ($s^{-1} M^{-1}$)
ABTS	3	28.0 ± 2.6	224.0 ± 4.0	8.0 ± 0.7 x 10^6
DMP	3	72.6 ± 9.5	70.9 ± 2.1	9.7 ± 0.1 x 10^5
Veratryl alcohol	2	3610.0 ± 211.0	2.70 ± 0.1	8.3 ± 0.0 x 10^2
Reactive Blue 19	4	13.5 ± 1.6	79.9 ± 3.2	5.9 ± 0.5 x 10^6
Reactive Black 5	3	11.2 ± 0.9	11.9 ± 0.4	1.1 ± 0.05 x 10^6
H_2O_2 *	3	79.5 ± 11.7	419.0 ± 18.8	5.3 ± 0.6 x 10^6

* Measured with 2.5 mM ABTS

3.5. Inactivation of *I. lacteus* DyP

Firstly, the enzyme inactivation by its own co-substrate, H_2O_2, was checked at 1 min reaction time in the presence of ABTS. The maximum relative activity was reached at final H_2O_2 concentrations between 0.4 and 0.8 mM, which corresponds to a [H_2O_2]/ [DyP] molar ratio of 250,000 and 500,000 respectively, and then gradually dropped off (data not shown). A residual activity of 30% still remained at 12.5 mM H_2O_2 and the enzyme was completely inactivated in the presence of 50 mM H_2O_2.

DyP inactivation by H_2O_2, in the absence of reducing substrate, was also assayed at different times and concentrations, (Fig. 6). When a [H_2O_2]/ [DyP] molar ratio of 250,000 was used, the enzyme was completely inactivated in 20 min of incubation. In contrast, a residual activity of 40% was observed in the treatment with 128,000 equivalents. DyP was inactivated progressively and similarly over the time between molar ratios of 128 and 8,000 in 5 hours of incubation.

The effect of two concentrations of several cations on DyP activity was also assayed, and any of them activated the enzyme (data not shown). In most cases, a residual activity higher than 60% was retained, but 80% of the enzyme's activity was lost in reactions with Fe^{3+} and Hg^{2+}, and disappeared completely in the presence of 2 mM Pb^{2+}, as well as 2 mM NaN_3. The addition of 0.2 mM EDTA did not inhibit the enzyme, and 2 mM of the same reagent caused only a slight inactivation, what suggests that there are not essential ions in the reaction mixture for the enzyme activity.

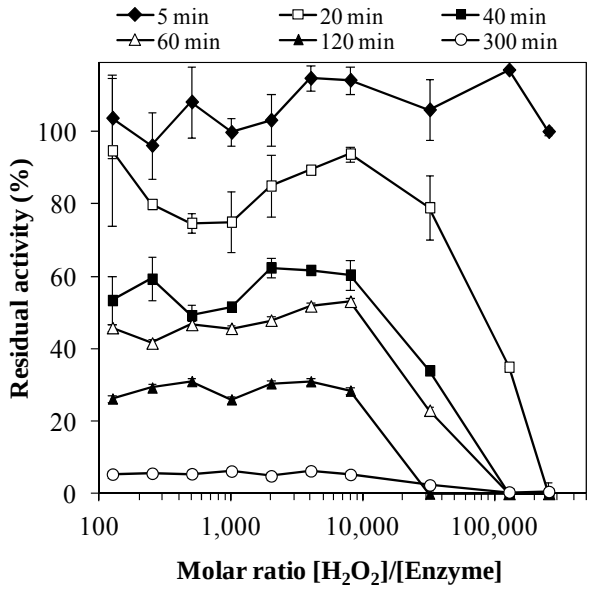

Fig. 6. H_2O_2 stability of the purified *I. lacteus* DyP at different times. DyP (50 nM) was incubated at 25 ºC in 10 mM tartrate buffer (pH 5) containing different H_2O_2 concentrations (from 6.25 uM to 12.8 mM). The residual activity (measured with ABTS) was referred to DyP activity incubated in the absence of H_2O_2 (100%). Error bars are means of duplicated treatments.

3.6. N-terminal sequencing and peptide mass fingerprinting of *I. lacteus* DyP

The N-terminal region of the purified enzyme was sequenced (Table 3). Data bank homology searches (NCBI) returned the hypothetical peroxidase cpop21 from an unidentified species in the family Polyporaceae as the best hit (>95% identity), followed by the DyP from *T. albuminosus* (>85% identity). Lower identities and/or shorter alignments were found with the DyP from *Bjerkandera adusta* strain Dec1, formerly classified as *Thanatephorus cucumeris* (Yoshida et al., 2011), and the *Auricularia delicata* DyP. The combined search of the protein fingerprint and the MS/MS spectrum of three of the tryptic peptides (selected for fragmentation and sequencing) rendered a maximum score of 332 for the 499 amino acids hypothetical peroxidase cpop21 (accession numbers AAB58908 (NCBI), U77073 (GenBank), and 5097 (Peroxibase)). Table 4 shows the peptides from DyP which match with cpop21.

Table 3. Alignment of *I. lacteus* DyP N-terminal sequence with other DyP sequences returned by NCBI with significant scores (E-value <0.05). X indicates an unidentified residue. Conserved residues are in black. Lacking residues are represented as dashes.

Microorganism	Accession number	Amino terminus	Identity (%)
I. lacteus	---	SAGXDS-LPFENIQGDILVGM	
Unidentified Polyporaceae*	AAB58908	SAGNDS-LPFENIQGDILVGM	>95
T. albuminosus*	AAM21606	DDSI-PFENIQADILVGM	>70
B. adusta*	BAA77283	A-NDTILPLNNIQGDILVGM	>70
A. delicata*	EJD38892	AANDAALPFNDIQGDILAGM	>65

* The hypothetical protein sequence includes part of the signal peptide.
** The amino-terminus sequence corresponds to the mature protein.

Table 4. Matching peptides with cpop21, after DyP trypsin digestion and PMF analysis.

Peptide sequence	Observed mass (*m/z*)	Expected mass (*m/z*)	cpop21 position (aa)**
QTFGLDPR	933.48	932.47	458-465
CPFTAHVR	987.49	986.48	359-366
QLVPEFHK	997.55	996.54	278-285
SEPLGLDPVIGQGTR*	1538.83	1537.82	443-457
NNDFNYIHPGEDLTTDETR*	2250.99	2249.99	340-358
GTNVDGVFLIGSDDVTTTNQYR*	2372.15	2371.14	167-188

*Peptides chosen for fragmentation and sequencing.
** Starting and ending amino acid (aa) positions.

3.7. Enzymatic hydrolysis of wheat straw

Untreated wheat straw is composed of cellulose (37%), hemicellulose (23%) and lignin (24%). After 21-days of treatment with *I. lacteus* the above amounts decreased in 8%, 3%, and 9%, respectively, while a mild alkali treatment did not change sugar percentages significantly. The enzymatic hydrolysis of biopretreated wheat straw showed enhanced yields respect to the non-biopretreated controls (Fig. 7). In addition, the mild alkali washing also produced a considerable increase in cellulose digestibility, being more remarkable in the biopretreated wheat straw. As expected, the addition of commercial cellulase and xylanase formulations strongly improved the free sugar content with respect to the control. In contrast, the hydrolysis of the lignocellulosic material using the enzymatic crude from *I. lacteus* either as the unique enzyme source, or added as a supplement of the commercial cocktails, dropped drastically. Nevertheless, supplementation with purified DyP improved significantly the cellulose digestibility. In non-biopretreated wheat straw, with and without alkali

washing, this value lifted from 27 to 38% and from 24 to 30%, respectively, but the effect was more evident on biopretreated wheat straw with a rise from 71 to 89% in NaOH-treated samples and from 43 to 50% in those not subjected to alkali pretreatment. A parallel decrease in hemicellulose digestibility was observed in some cases (data not shown). Furthermore, the residual DyP activity at the end of the treatment (60 h) was around 5-10% which means that the peroxidase retains activity.

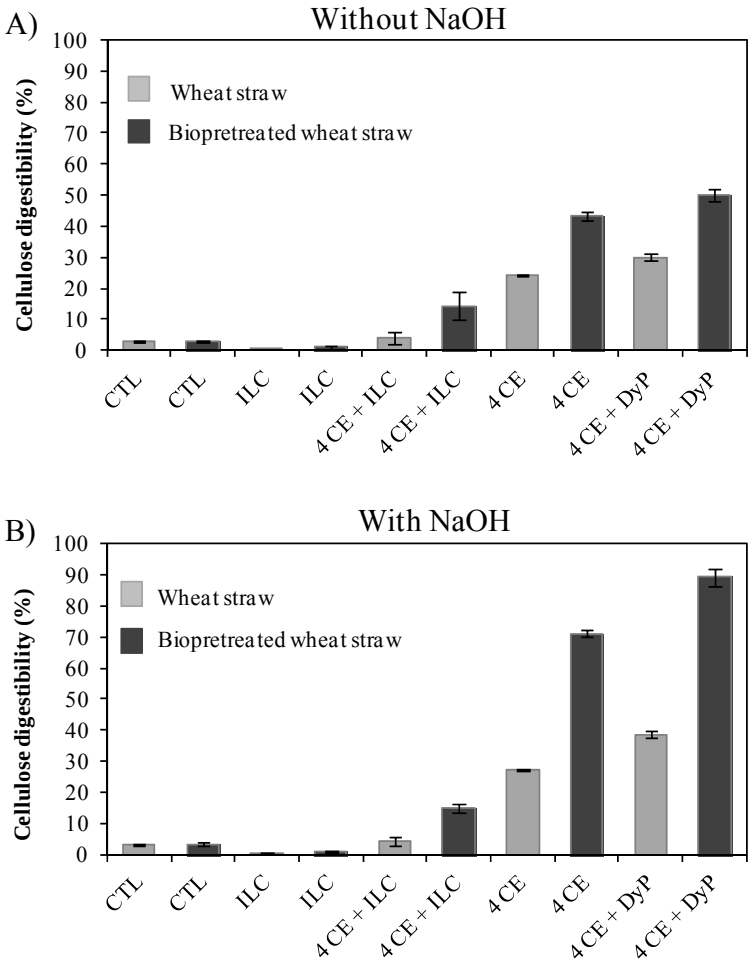

Fig. 7. Cellulose digestibility from wheat straw (A) without additional alkali washing pretreatment and (B) with NaOH pretreatment, complemented or not with a biological pretreatment by *I. lacteus* during 21 days. Diverse hydrolysis treatments were applied using four enzymatic commercial cocktails (4 CE), the enzymatic crude of *I. lacteus* (ILC), and the purified peroxidase from *I. lacteus* (DyP). Substrates without any enzymatic supplementation were incubated in the same conditions (CTL).

4. DISCUSSION

I. lacteus and its extracellular oxidative enzymatic system offer a great potential for different biotechnological applications. The detection of Mn-independent peroxidase in *I. lacteus* growing on wheat straw has been recently described (Salvachúa et al., 2013). With the aim of producing and

purifying it, peroxidase production was followed in a liquid medium (CSS) known to produce high *I. lacteus* biomass in comparison with other media (Salvachúa et al., 2013). According to the peroxidases production profile found in the present study, it can be suggested that the fungus starts producing MnPs when glucose is almost consumed. These MnPs, apparently showing both Mn-dependent and independent activity, would belong to a recently described subfamily of short MnPs (Floudas et al., 2012; Hilden et al., 2006) whose components, in addition to primary activity on Mn^{2+}, are able to oxidize phenols and ABTS in the absence of Mn^{2+}, as described in *Pleurotus ostreatus* (Giardina et al., 2000) and *Agrocybe praecox* (Steffen et al., 2002). *I. lacteus* reduced the peroxidase production until the third week of incubation, when MnP production increased again, together with a peak of DyP, which was able to oxidize high redox-potential substrates such as anthraquinones. DyP appeared when the carbon:nitrogen ratio in the cultures was very low, which is in accordance with the production profile reported by Cajthaml et al. (Cajthaml et al., 2008) in *I. lacteus* liquid cultures spiked with polycyclic aromatic hydrocarbons (PAHs). Laccase was not detected what suggest that both DyP and MnP are the main oxidative enzymes secreted by *I. lacteus* in these culture conditions. At the time of culture harvesting, the major peroxidase in the enzymatic crude of *I. lacteus* was a DyP-like peroxidase, as brought out after the first chromatographic step, where 80% of the total peroxidase activity against ABTS was found. The above data suggest that the production of DyP by *I. lacteus* under different environmental or experimental conditions should be studied by using specific substrates to get a deeper understanding of the presence of this enzyme and to avoid imprecise enzyme identifications as Mn-independent peroxidase.

In order to confirm the *I. lacteus* peroxidase identification as a member of the DyP superfamily, comparison of its N-terminal sequence and peptide mass fingerprint with those from other proteins was performed. Both analyses returned, with maximal identity and score, the hypothetical cpop21 peroxidase from Polyporaceae which belongs to the DyP-type peroxidase family. The N-terminus of *I. lacteus* DyP matched with the amino acidic sequence starting at the position 53 of cpop21, suggesting that a ~50 amino-acid signal peptide exists in the latter hypothetical protein as found in *T. albuminosus* DyP (Johjima et al., 2003). The fourth amino acid was not identified by Edman degradation. One of the reasons to explain this fact could be the existence of an N-glycosylated asparagine residue hindering its identification. Taking into account that the sixth position is occupied by a serine residue, it suggests the existence of a consensus sequence for N-glycosylation (N-X-S/T) (Shimokawa et al., 2009; Sugano

et al., 1999) which in addition coincides with the sequence in analogous position 56-58 (N-D-S) in cpop21.

Concerning the physical properties of the purified enzyme, SDS-PAGE disclosed that, similarly to most fungal DyPs, *I. lacteus* DyP is a monomeric protein, while most bacterial DyPs form oligomeric species (Ogola et al., 2009). The molecular mass was 57.1 kDa, higher than that reported for all LiPs and MnPs from *I. lacteus* (Novotny et al., 2009) but similar to DyPs from other microorganisms (Faraco et al., 2007; Kim and Shoda, 1999; Liers et al., 2012). The protein contained around 10.5% of N-linked carbohydrate chains, lower than the 17% found in the native DyP from *B. adusta* (Kim and Shoda, 1999). Independently if *I. lacteus* DyP is glycosylated or not, the protein's pI was acidic, a usual feature among fungal peroxidases (Shin et al., 2005) and DyP-like peroxidases whose pI range is between 3.7 and 4.3. The A_{406}/A_{280} ratio (1.59) and absorption peaks in the UV-visible spectrum of the heme-protein were similar to those found for other native DyPs (Kim and Shoda, 1999; Ogola et al., 2009; Sugano, 2009).

On the basis of its substrate specificity and catalytic properties, *I. lacteus* DyP can be considered a high-redox potential enzyme and be classified into the DyP-like peroxidase family (Sugano et al., 2007). As previously mentioned this DyP did not oxidize Mn^{2+} and exhibited higher decolorizing activity and catalytic efficiency toward anthraquinone- than azo-dyes, although the K_m for both was similar. It has been reported that hydroxyl-free anthraquinones are not usually a substrate for non DyP-type peroxidases and if they are, the oxidation is very low (Liers et al., 2012; Sugano et al., 2007). Furthermore, the specificity and catalytic efficiency for RBlack5 was superior to that reported for other DyPs (Liers et al., 2012), other high-redox potential enzymes as VP (Banci et al., 2003), or the classical HRP (Ogola et al., 2009). The activity against the phenolic compound DMP reached higher values than those reported for other phenol peroxidases as soybean peroxidase (Liers et al., 2012), although the catalytic efficiency for this substrate was poorer compared to the dyes. *I. lacteus* DyP was also able to oxidize VA (Kim and Shoda, 1999), although the K_m for this substrate was quite high, in the range found for other DyPs (Liers et al., 2010) and VP (Martínez et al., 1996) (although the latter enzyme has much higher k_{cat}). The K_m for H_2O_2 in the presence of ABTS (the substrate for which the highest activity and catalytic efficiency were obtained) was in the magnitude of other fungal and plant peroxidases (with K_m values from 5 μM in *Auricularia auricula-judae* DyP to 152 μM in *Coprinopsis cinerea* peroxidase) (Liers et al., 2012). The catalytic efficiency for H_2O_2 was slightly lower than the reported in other DyPs but superior to those found in HRP and LiP from *Phanerochaete*

chrysosporium (Liers et al., 2012). The maximum activities with the co-substrate H_2O_2 were found between 0.4 to 0.8 mM, what suggests that an increase of this co-substrate´s concentration (from 0.1 mM to 0.4-0.8 mM) should be used to measure the enzyme activity in future works.

The optimal pHs for the enzyme activity were acidic specially for VA, which was better oxidized at pH 2, a value slightly higher than the reported for the isoforms of *A. auricula-judae* (Liers et al., 2012). In contrast, the optimum pH oxidizing DMP was more acid than those found for other DyPs, but similar to VP from *P. eryngii* (Martínez et al., 1996), and VP and LiP from *B. adusta* and *P. chrysosporium* (Liers et al., 2012). The optimal pH for RBlue19 was one point higher than for the other substrates, including the azo-dye RBlack5. Similar pH variations between dyes was observed with the bacterial DyP from *Anabaena* sp. (Ogola et al., 2009).

Taking into consideration its feasible biotechnological applications, the stability of *I. lacteus* DyP was evaluated at different pHs and temperatures. The enzyme showed to be very stable at 4ºC and 25ºC in a wide range of pHs, excluding those more basic (8 and 9). In fact, at pH 2 and 25ºC the enzyme still retained 62% of activity after 6 h, similar to that found in the isoform AjII of *A. auricula-judae* after 4h at 20ºC, pH 2.5 (Liers et al., 2010). The ability to work efficiently under such low pH environments is a characteristic that distinguish DyPs from most peroxidases (Sugano et al., 2007). This enzyme also showed to be active at pH 4 and 5 during 48 h at 50ºC, which is required for its use in enzymatic hydrolysis of lignocellulosic substrates. It was more stable than AjII (Liers et al., 2010) and the DyP from *Anabaena* sp. (Ogola et al., 2009) which had an activity loss of 90% at 50ºC in 3 h. The thermal index T_{50} was 63ºC and the most severe drop was produced from 60ºC, keeping still 70% of the activity at that temperature. The *B. adusta* DyP isoenzymes lost their activity completely at 55ºC, even without previous incubation (Kim and Shoda, 1999; Shimokawa et al., 2009). Keeping in mind the fungal origin of *I. lacteus* DyP, the habitat of *I. lacteus* in the northern temperature zone (Novotny et al., 2009), and its natural environment, wood and litter decay, the obtained data (high activity and stability at acid pHs and promoted at low temperatures) fits with a potential physiological role in nature during lignocellulose degradation.

Concerning enzyme inactivation, the first compound tested was its own co-sustrate, H_2O_2. The enzyme showed increased activity to high H_2O_2 concentrations at reaction times compared to other DyPs (Kim and Shoda, 1999; Ogola et al., 2009).That enhanced activity could be explained by the higher turnover rate (k_{cat}=419 s^{-1}) (Table 3), compared to usual values in fungal peroxidases (k_{cat}=240-270 s^{-1}) (Kim and Shoda, 1999; Liers et al.,

2012). In general, it is very difficult to contrast the stability against H_2O_2 among peroxidases because many factors, such as pH, time, and temperature during the incubation, have a great influence (Böckle et al., 1999). However, in view of these results and considering the [H_2O_2]/[enzyme] molar ratio and the incubation time, *I. lacteus* DyP seems to be even more resistant than other improved peroxidases for H_2O_2 stability, such as *Pleurotus eryngii* VP (García-Ruiz et al., 2012) and *Anabaena* sp. DyP (Ogola et al., 2010). On the other hand, an excess of the tested ions (2 mM) produced a slight decrease in the enzyme activity, and only Fe^{3+}, Hg^{2+}, Pb^{2+}, as well as NaN_3, affected severely the enzyme performance. In particular, Pb^{2+} has been demonstrated to be an important MnP inhibitor (Tuomela et al., 2005). Mn^{2+} did not enhance DyP activity, which agrees with findings from fungal (Kim and Shoda, 1999; Ogola et al., 2009) but no bacterial DyPs (Ahmad et al., 2011), where some activation has been described.

The applicability of *I. lacteus* DyP in second-generation ethanol production from wheat straw, a process of high biotechnological interest (Salvachúa et al., 2013), was checked including this enzyme in the enzymatic hydrolysis step. In the current work, it has been re-asserted that (i) the type of pretreatment, used to remove and/or deconstruct lignin, a heteropolymer of phenolic and non-phenolic residues and the main barrier to get high fermentable sugar yields, and (ii) the enzyme mixture used to further hydrolyze cellulose and hemicellulose, were essential for sugar recoveries improvement from wheat straw (Talebnia et al., 2010). The addition of the whole enzymatic crude of *I. lacteus* influenced negatively the hydrolysis yields. This can be due to the presence, in the extracellular material secreted by this microorganism, of a heterogeneous mixture of enzymes including some proteases (data not shown), which could have hydrolyzed the commercial enzymes added. In contrast, Du et al. (Du et al., 2011) reported that by-products from *I. lacteus* cultures improved the enzymatic hydrolysis of biotreated cornstalks. Nevertheless, the purified DyP increased cellulose digestibility (fermentable glucose recovery) in all cases, especially in the biologically or alkali-washed pretreated substrate. Briefly, these results suggest that DyP and cellulases exhibit a synergistic action during cellulose degradation of wheat straw through the oxidation of lignin´s phenolic- and non-phenolic compounds, thus making the cellulose polymers more accessible to cellulase attack. Similar results have been described in a patent after treating non starch-carbohydrates with a peroxidase of *Marasmius scorodonius* (Zorn et al., 2009), which seems to be a DyP-type peroxidase. However, very few investigations have been included peroxidases in this type of application what enhances the novelty of these results.

To summarize, in the current work a novel high redox-potential DyP has been isolated and characterized from *I. lacteus*. Despite its classification as a DyP-type peroxidase, this enzyme presents some advantageous features, such as high stability to pH and temperature and increased resistance to H_2O_2, which turns it into a really interesting enzyme to be applied in biotechnological processes such as enzymatic deconstruction of lignocellulose for bioethanol production or dye-decolorization. Future work is focused on cloning, sequence analysis, and heterologous expression of *I. lacteus* DyP, for further application and structure-function studies.

ACKNOWLEDGMENTS

This work has been carried out with funding from the Spanish project PRI-PIBAR-2011-1402 and EU FP7 project "Peroxicats" (KBBE-2010-4-265397). D. Salvachúa thanks the Spanish Ministry of Economy for a FPU fellowship. The authors thank the "Proteomics and Genomics" and "Protein Chemistry" Facilities at CIB.

REFERENCES

Ahmad, M., Roberts, J.N., Hardiman, E.M., Singh, R., Eltis, L.D., Bugg, T.D., 2011. Identification of DypB from *Rhodococcus jostii* RHA1 as a lignin peroxidase. Biochem. 50, 5096-5107.

Banci, L., Camarero, S., Martínez, A.T., Martínez, M.J., Pérez-Boada, M., Pierattelli, R., Ruiz-Dueñas, F.J., 2003. NMR study of Mn(II) binding by the new versatile peroxidase from the white-rot fungus *Pleurotus eryngii*. J. Biol. Inorg. Chem. 8, 751-760.

Böckle, B., Martínez, M.J., Guillén, F., Martínez, A.T., 1999. Mechanism of peroxidase inactivation in liquid cultures of the ligninolytic fungus *Pleurotus pulmonarius*. Appl. Environ. Microbiol. 65, 923-928.

Cajthaml, T., Erbanova, P., Kollmann, A., Novotny, C., Sasek, V., Mougin, C., 2008. Degradation of PAHs by ligninolytic enzymes of *Irpex lacteus*. Folia Microbiologica 53, 289-294.

Du, W., Yu, H., Song, L., Zhang, J., Weng, C., Ma, F., Zhang, X., 2011. The promoting effect of byproducts from *Irpex lacteus* on subsequent enzymatic hydrolysis of bio-pretreated cornstalks. Biotech. Biofuels 4, 37.

Faraco, V., Piscitelli, A., Sannia, G., Giardina, P., 2007. Identification of a new member of the dye-decolorizing peroxidase family from *Pleurotus ostreatus*. World J. Microbiol. Biotechnol. 23, 889-893.

Floudas, D., Binder, M., Riley, R., Barry, K., Blanchette, R.A., Henrissat, B., Martinez, A.T., Otillar, R. et al., 2012. The paleozoic origin of enzymatic lignin decomposition reconstructed from 31 fungal genomes. Science 336, 1715-1719.

García-Ruiz, E., Gonzalez-Perez, D., Ruiz-Dueñas, F.J., Martinez, A.T., Alcalde, M., 2012. Directed evolution of a temperature-, peroxide- and alkaline pH-tolerant versatile peroxidase. Biochem. J. 441, 487-498.

Giardina, P., Palmieri, G., Fontanella, B., Rivieccio, V., Sannia, G., 2000. Manganese peroxidase isoenzymes produced by *Pleurotus ostreatus* grown on wood sawdust. Arch. Biochem. Biophys. 376, 171-179.

Hilden, K.S., Makela, M.R., Hakala, T.K., Hatakka, A., Lundell, T., 2006. Expression on wood, molecular cloning and characterization of three lignin peroxidase (LiP) encoding genes of the white rot fungus *Phlebia radiata*. Curr. Genetics 49, 97-105.

Hofrichter, M., Ullrich, R., Pecyna, M.J., Liers, C., Lundell, T., 2010. New and classic families of secreted fungal heme peroxidases. Appl. Microbiol. Biotechnol. 87, 871-897.

Johjima, T., Ohkuma, M., Kudo, T., 2003. Isolation and cDNA cloning of novel hydrogen peroxide-dependent phenol oxidase from the basidiomycete *Termitomyces albuminosus*. Appl. Microbiol. Biotechnol. 61, 220-225.

Kalpana, D., Velmurugan, N., Shim, J.H., Oh, B.T., Senthil, K.i., Lee, Y.S., 2012. Biodecolorization and biodegradation of reactive Levafix Blue E-RA granulate dye by the white rot fungus *Irpex lacteus*. J. Environ. Manag. 111, 142-149.

Kim, S.J. Shoda, M., 1999. Purification and characterization of a novel peroxidase from *Geotrichum candidum* Dec 1 involved in decolorization of dyes. Appl. Environ. Microbiol. 65, 1029-1035.

Liers, C., Bobeth, C., Pecyna, M., Ullrich, M., Hofrichter, M., 2010. DyP-like peroxidases of the jelly fungus *Auricularia auricula-judae* oxidizing nonphenolic lignin model compounds and high redox potential dyes. Appl. Microbiol. Biotechnol. 85, 1869-1879.

Liers, C., Pecyna, M.J., Kellner, H., Worrich, A., Zorn, H., Steffen, K.T., Hofrichter, M., Ullrich, R., 2012. Substrate oxidation by dye-decolorizing peroxidases (DyPs) from wood- and litter-degrading agaricomycetes compared to other fungal and plant heme-peroxidases. Appl. Microbiol. Biotechnol. doi:10.1007/s00253-012-4521-2.

Martínez, A.T., Ruiz-Dueñas, F.J., Martínez, M.J., del Río, J.C., Gutiérrez, A., 2009. Enzymatic delignification of plant cell wall: from nature to mill. Curr. Opin. Biotechnol. 20, 348-357.

Martínez, M.J., Ruiz-Dueñas, F.J., Guillén, F., Martínez, A.T., 1996. Purification and catalytic properties of two manganese-peroxidase isoenzymes from *Pleurotus eryngii*. Eur. J. Biochem. 237, 424-432.

Moon, D.S. Song, H.G., 2012. Degradation of alkylphenols by white rot fungus *Irpex lacteus* and its manganese peroxidase. Appl. Biochem. Biotechnol. 168, 542-549.

Novotny, C., Cajthaml, T., Svobodova, K., Susla, M., Sasek, V., 2009. *Irpex lacteus*, a white-rot fungus with biotechnological potential - review. Folia Microbiologica 54, 375-390.

Novotny, C., Erbanova, P., Cajthaml, T., Rothschild, N., Dosoretz, C., Sasek, V., 2000. *Irpex lacteus*, a white rot fungus applicable to water and soil bioremediation. Appl. Microbiol. Biotechnol. 54, 850-853.

Ogola, H.J.O., Kamiike, T., Hashimoto, N., Ashida, H., Ishikawa, T., Shibata, H., Sawa, Y., 2009. Molecular Characterization of a Novel Peroxidase from the Cyanobacterium *Anabaena* sp Strain PCC 7120. Appl. Environ. Microbiol. 75, 7509-7518.

Ogola, H.J.O., Hashimoto, N., Miyabe, S., Ashida, H., Ishikawa, T., Shibata, H., Sawa, Y., 2010. Enhancement of hydrogen peroxide stability of a novel *Anabaena* sp. DyP-type peroxidase by site-directed mutagenesis of methionine residues. Appl. Microbiol. Biotechnol. 87, 1727-1736.

Pinto, P.A., Dias, A.A., Fraga, I., Marques, G., Rodrigues, M.A.M., Colaco, J., Sampaio, A., Bezerra, R.M.F., 2012. Influence of ligninolytic enzymes on straw saccharification during fungal pretreatment. Bioresour. Technol. 111, 261-267.

Ruiz-Dueñas, F.J. Martínez, A.T., 2010. Structural and functional features of peroxidases with a potential as industrial biocatalysts, in: Torres, E., Ayala, M. (Eds.), Biocatalysts based on heme peroxidases. Springer, Berlin, pp. 37-59.

Salvachúa, D., Prieto, A., López-Abelairas, M., Lu-Chau, T., Martínez, A.T., Martínez, M.J., 2011. Fungal pretreatment: An alternative in second-generation ethanol from wheat straw. Bioresour. Technol. 102, 7500-7506.

Salvachúa, D., Prieto, A., Vaquero, M.E., Martinez, A.T., Martínez, M.J., 2013. Sugar recoveries from wheat straw following treatments with the fungus *Irpex lacteus*. Bioresour. Technol. 131, 218-225.

Shimokawa, T., Shoda, M., Sugano, Y., 2009. Purification and characterization of two DyP isozymes from *Thanatephorus cucumeris* Dec 1 specifically expressed in an air-membrane surface bioreactor. J. Biosci. Bioeng. 107, 113-115.

Shin, K.S., Kim, Y.H., Lim, J.S., 2005. Purification and characterization of manganese peroxidase of the white-rot fungus *Irpex lacteus*. J. Microbiol. 43, 503-509.

Shin, K.W., 2004. The role of enzymes produced by white-rot fungus *Irpex lacteus* in the decolorization of the textile industry effluent. J. Microbiol. 42, 37-41.

Steffen, K.T., Hofrichter, M., Hatakka, A., 2002. Purification and characterization of manganese peroxidases from the litter-decomposing basidiomycetes *Agrocybe praecox* and *Stropharia coronilla*. Enzyme Microb. Technol. 30, 550-555.

Sugano, Y., 2009. DyP-type peroxidases comprise a novel heme peroxidase family. Cell Mol. Life Sci. 66, 1387-1403.

Sugano, Y., Matsushima, Y., Tsuchiya, K., Aoki, H., Hirai, M., Shoda, M., 2009. Degradation pathway of an anthraquinone dye catalyzed by a unique peroxidase DyP from *Thanatephorus cucumeris* Dec 1. Biodegradation 20, 433-440.

Sugano, Y., Muramatsu, R., Ichiyanagi, A., Sato, T., Shoda, M., 2007. DyP, a unique dye-decolorizing peroxidase, represents a novel heme peroxidase family. J. Biol. Chem. 282, 36652-36658.

Sugano, Y., Sasaki, K., Shoda, M., 1999. cDNA cloning and genetic analysis of a novel decolorizing enzyme, peroxidase gene *dyp* from *Geotrichum candidum* Dec 1. J. Biosci. Bioeng. 87, 411-417.

Talebnia, F., Karakashev, D., Angelidaki, I., 2010. Production of bioethanol from wheat straw: An overview on pretreatment, hydrolysis and fermentation. Bioresour. Technol. 101, 4744-4753.

Tuomela, M., Steffen, K.T., Kerko, E., Hartikainen, H., Hofrichter, M., Hatakka, A., 2005. Influence of Pb contamination in boreal forest soil on the growth and ligninolytic activity of litter-decomposing fungi. FEMS Microbiol. Ecol. 53, 179-186.

Welinder, K.G., 1992. Superfamily of plant, fungal and bacterial peroxidases. Curr. Opin. Struct. Biol. 2, 388-393.

Yoshida, T., Tsuge, H., Konno, H., Hisabori, T., Sugano, Y., 2011. The catalytic mechanism of dye-decolorizing peroxidase DyP may require the swinging movement of an aspartic acid residue. FEBS J 278, 2387-2394.

Zelena, K., Hardebusch, B., Huelsdau, B., Berger, R.G., Zorn, H., 2009. Generation of norisoprenoid flavors from carotenoids by fungal peroxidases. J. Agric. Food Chem. 57, 9951-9955.

Zorn, H., Scheibner, M., Hulsdau, B., Berger, R.G., de Boer, L., Meima, R.B,. 2011. Novel enzymes for use in enzymatic bleaching of food products. Patent [US 7,981,636 B2.]. United States.

Zorn, H., Szweda, R., Kumar, M., Wilms, J., 2009. Method for modifying non-starch carbohydrate material using peroxidase enzyme. Patent [US200913054178]. United States.

Chapter 5

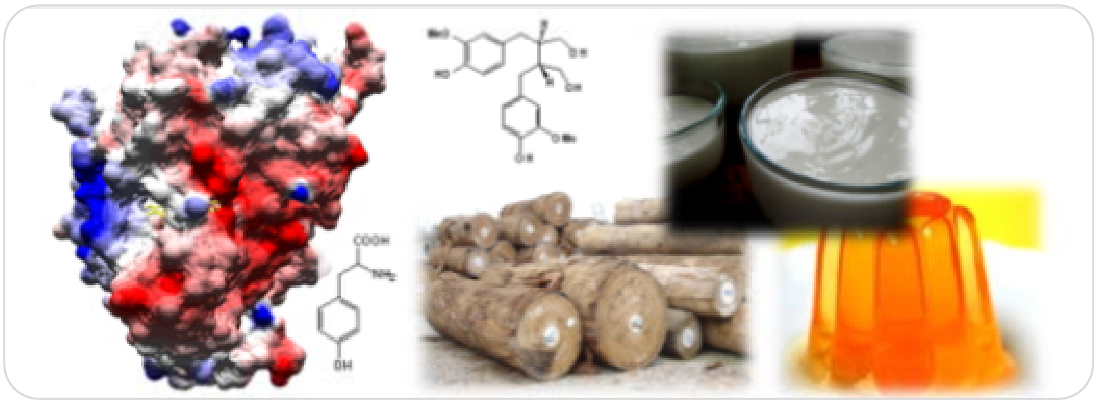

Versatile peroxidase as a valuable tool for generating new biomolecules by homogeneous and heterogeneous cross-linking

Davinia Salvachúa, Alicia Prieto, Maija-Liisa Mattinen, Tarja Tamminen, Tiina Liitiä, Martina Lille, Stefan Willför, Angel T. Martínez, María Jesús Martínez, Craig B. Faulds.

Enzyme and Microbial Technology (2013) 52, 303–311.

ABSTRACT*

The modification and generation of new biomolecules intended to give higher molecular- mass species for biotechnological purposes, can be achieved by enzymatic cross-linking. The versatile peroxidase (VP) from *Pleurotus eryngii* is a high redox-potential enzyme with oxidative activity on a wide variety of substrates. In this study, VP was successfully used to catalyse the polymerization of low molecular mass compounds, such as lignans and peptides, as well as larger macromolecules, such as protein and complex polysaccharides. Different analytical, spectroscopic, and rheological techniques were used to determine structural changes and/or variations of the physicochemical properties of the reaction products. The lignans secoisolariciresinol and hydroxymatairesinol were condensed by VP forming up to 8 unit polymers in the presence of organic co-solvents and Mn^{2+}. Moreover, 11 units of the peptides YIGSR and VYV were homogeneously cross-linked. The heterogeneous cross-linking of one unit of the peptide YIGSR and several lignan units was also achieved. VP could also induce gelation of feruloylated arabinoxylan and the polymerization of β-casein. These results demonstrate the efficacy of VP to catalyze homo- and hetero-condensation reactions, and reveal its potential exploitation for polymerizing different types of compounds.

Keywords: Enzymatic polymerization, organic co-solvent, lignan, peptide, β-casein, feruloylated arabinoxylan.

*** Addenda to the original manuscript.** Previously to the experiments included in the paper, the efficiency of the *I. lacteus* crude, which contained among others low- and high-redox potential peroxidases as manganese dependent peroxidases (MnP) and dye decolorizing peroxidases (DyP), respectively (Chapter 3), was checked in lignan polymerization assays and compared with a versatile peroxidase (VP) from *Pleurotus eryngii* catalyzing the same reaction. VP produced higher molecular mass species, indicating that this enzyme was more efficient than the enzymes of the *I. lacteus* crude polymerizing lignans, especially in reactions in the presence of Mn^{2+}. Thus, the complete study was carried out with VP.

1. INTRODUCTION

Biotransformation is a useful way for modifying or producing novel structures and materials, which can then be exploited in a broad range of applications. The enzymatic polymerization and hetero-conjugation of various substrates is a method of primary interest to reach that goal. Biocatalysis is advantageous over chemical procedures, since: (i) it is an environmentally friendly alternative that uses milder and less contaminant reactions (Kobayashi et al., 2001) and (ii) it can produce more specific cross-links, as many enzymes have high chemo-, regio-, and enantio-selectivity (Walde and Guo, 2011). The use of oxidoreductases, as radical-forming enzyme systems, to render homo or hetero-polymers of very diverse molecules is an attractive example of this, and the enzymatically synthesized polymers may exhibit new or improved properties in comparison with their respective precursors (Miletic et al., 2012).

Versatile peroxidases (VP) are an interesting group of oxidoreductases (EC 1.11.1.16; described as a Reactive Black 5:hydrogen peroxide oxidoreductase) whose activity in these polymerization reactions has not been previously explored at the molecular level. These enzymes are secreted by fungi and included in the class II of the superfamily of plant-fungal-bacterial heme-peroxidases, together with manganese peroxidases (MnP), lignin peroxidases (LiP), generic peroxidases (GP) as *Coprinopsis cinerea* (synonym *Coprinus cinereus*) peroxidase (CiP) (Hofrichter et al., 2010). To date, these enzymes and their encoding genes have been found and characterized only in white rot, wood-decaying Basidiomycota belonging to the class Agaricomycetes, as described in the comparative genomic research recently published by Floudas et al. (Floudas et al., 2012). VPs constitute an example of enzyme multifunctionality, combining the catalytic properties of MnP, LiP, and low redox-potential peroxidases. Therefore, VP displays a wide oxidative activity on substrates having different chemical structures and redox-potentials, including compounds that cannot be oxidized by low redox-potential peroxidases, such as fungal GP, horseradish peroxidase (HRP) and other plant peroxidases (Banci et al., 2003; Heinfling et al., 1998; Pérez-Boada et al., 2005; Rodríguez et al., 2004). Recent research efforts of VPs have focused on the understanding of their reaction mechanisms and structure-function relationships (Ruiz-Dueñas et al., 1999; Ruiz-Dueñas et al., 2009), in the search of adequate systems for the expression of VP (Lú-Chau et al., 2004), and in enzyme improvement through directed evolution (García-Ruiz et al., 2012). Nevertheless, the potential applications of VPs have not yet been fully exploited, in spite of being a very promising group of enzymes from a biotechnological point of view (Hamid and Khalil, 2009).

Different substrates previously used in enzymatic polymerization reactions (Martínez-López et al., 2011; Matheis and Whitaker, 1984; Mattinen et al., 2011; Steffensen et al., 2008), representing low-molecular mass, oligomeric, and polymeric substrates, were chosen to evaluate the polymerizing ability of VP. Lignans are diphenolic compounds found in the cell wall of higher plants, formed by β-β coupling of two cinnamyl precursors (Saleem et al., 2005), and their chemical structure depends especially on the plant species from which they are isolated. These compounds can appear in side-streams from industrial processing of lignocellulosic material, *e.g.* mechanical pulping and paper processing, and should be removed to avoid undesirable effects, such as interferences with process chemicals (Buchert et al., 2002). Polymerization of lignans into larger molecules is one way to eliminate these unwanted effects. Lignans may also serve as precursors for the enzymatic production of value-added polymers or materials with improved functional properties (Mattinen et al., 2009). These synthetic reactions are challenging, since most of them may only be performed in the presence of organic solvents, jeopardizing the stability of the enzyme catalyst. On the other hand, the enzymatic polymerization of bioactive peptides, proteins as β-casein, or feruloylated arabinoxylans (FAX), which have well-known functional properties (Arihara, 2006; Niño-Medina et al., 2010; Saleem et al., 2005; Stanic et al., 2010), could lead to tailored products with improved/modified organoleptic or functional properties such as reduced fat content, texture, solubility, mouth feel, better digestibility, emulsification, viscosity, gelling, or resistance to heat or proteolytic attack during enzyme digestion (Boeriu, 2008; Buchert et al., 2010).

Therefore, the aim of the present study was to determine if the VP from *Pleurotus eryngii* is able to catalyze the covalent homogeneous and/or heterogeneous cross-linking of selected small and large molecules, in the presence and absence of organic solvents, thus producing novel biocompounds. The extent of the condensation reactions was also evaluated.

2. MATERIALS AND METHODS

2.1. Substrates

The lignans used in this study (Fig. 1), namely secoisolariciresinol (SECO), hydroxymatairesinol (HMR), matairesinol (MR), cyclolariciresinol (CYCLO), and 7-hydroxy-secoisolariciresinol (7-HSECO) were prepared as described earlier (Anderegg and Rowe, 1974; Eklund et al., 2002; Smeds et al., 2007)**.** The bioactive peptides EPPGGSKVILF, RKRSRKE, VEPIPY, YIGSR, and VYV were obtained from Sigma (St Louis, MO, USA). YST was bought from Biokemis (Saint Petersburg, Russia). GLY

was obtained from Fluka (Buchs, Switzerland). The bovine β-casein protein (24 kDa, 85% purity) was purchased from Sigma-Aldrich (Taufkirchen, Germany). FAX from maize bran, containing an alkali-extractable ferulic acid content of 6.2 mg g^{-1}, was kindly given to CBF by Cambridge Biopolymers Ltd. (Cambridge, UK).

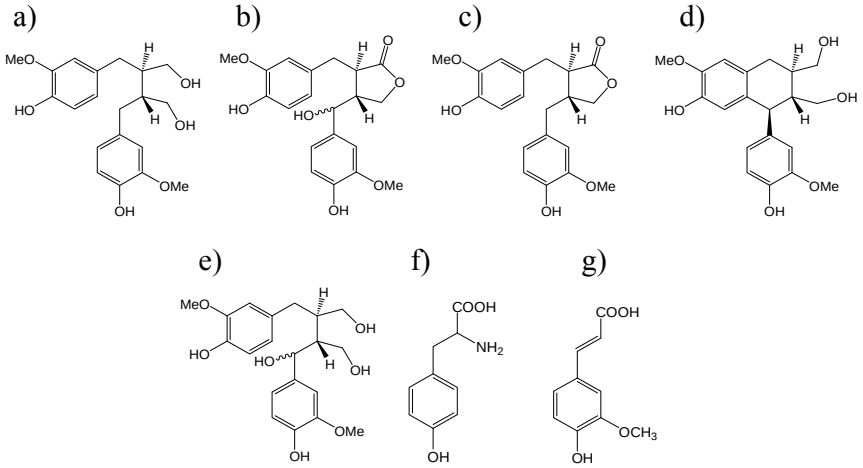

Fig. 1. Chemical structures of phenolic model compounds: (a) SECO, (b) HMR, (c) MR, (d) CYCLO, (e) and 7-HSECO lignans, (f) tyrosine, and (g) trans-ferulic acid.

2.2. Enzyme activity

VP was isolated and purified from *P. eryngii* cultures as previously described (Martínez et al., 1996). Its Mn^{2+}-oxidizing activity was determined spectrophotometrically at 238 nm through the formation of the Mn^{3+}·tartrate complex (ε_{238}= 6500 $M^{-1}cm^{-1}$) in a reaction mixture containing 0.1 mM $MnSO_4$ (Mn^{2+}) in 25 mM sodium tartrate buffer (pH 5.0), with the addition of 0.1 mM H_2O_2 to start the reaction. The effect of two organic solvents on VP activity was also checked through the evaluation of Mn^{2+}-independent activities following the oxidation of 1 mM 2,6-dimethoxyphenol (DMP) to dimeric coerulignone (ε_{469}=55000 $M^{-1}cm^{-1}$) and 1 mM 2,2'-azino-bis(3-ethylbenzothiazoline-6-sulphonic acid) (ABTS) to $ABTS^{+}$· (ε_{436}=29300 $M^{-1}cm^{-1}$) in 25 mM sodium tartrate buffer (pH 5.0). Solutions containing from 0% to 50% (v/v) of either ethanol or 1,2-propanediol in 25 mM sodium tartrate buffer (pH 5.0), in the presence or absence of 0.1 mM Mn^{2+} and 0.1 mM H_2O_2, were prepared as solvents for the substrates. The VP stability during 24 h-reactions was also checked in 25 mM sodium tartrate buffer (pH 5.0), 20%, and 50% ethanol (dissolved in the same buffer at equal final concentration), with and without Mn^{2+}. The percentage of residual activity was calculated at 0, 0.5, 2, and 24 h using Mn^{2+} /H_2O_2 as substrates and taking the initial activity in buffer as 100%. Measurements were carried out in triplicate at room temperature.

One unit of activity (1 U) is defined as the amount of enzyme releasing 1 μmol of product per minute under the defined reaction conditions.

2.3. Substrate solutions

The lignan SECO (3 mM), all peptides (3 mM), β-casein (1 mg mL^{-1}), and FAX (30 mg mL^{-1}) were prepared in 25 mM sodium tartrate buffer (pH 5.0). The remaining lignans were dissolved in 20% ethanol in the same buffer at a 3 mM final concentration, except 7-HSECO, which was dissolved in 50% ethanol buffer. All solutions were left standing for at least 30 min to be stabilized before commencing the enzymatic treatments.

2.4. Cross-linking assays

The enzyme reactions detailed below were initiated by addition of 0.1 mM H_2O_2, supplementing with a second dosage after 1 h of incubation and briefly agitated after each H_2O_2 supplementation. As an exception, the FAX assays were performed with a single dosage of 0.2 mM H_2O_2 at the beginning of the treatment. Unless otherwise stated, these treatments were performed in the presence of Mn^{2+} (0.1 mM), in duplicate, at room temperature. Negative controls consisted of reactions lacking VP or H_2O_2 incubated under the same conditions than the test reactions (with and without Mn^{2+}).

2.4.1. Homogeneous cross-linking of lignans and peptides

The polymerization of different substrates was performed in 1.5 mL Eppendorf tubes with a 1.5 U mL^{-1} VP in a final volume of 200 μL. Aliquots (3 μL) of each reaction mixture were removed after 0.5 and 2 h of incubation for subsequent analysis by matrix-assisted laser desorption/ionisation-time of flight-mass spectroscopy (MALDI-TOF MS). Lignan treatments were also performed during 24 h, in the absence of Mn^{2+}. To stop these reactions 0.05% (w/v) NaN_3 was added and samples from lignan treatments were lyophilized for further size exclusion chromatography (SEC) analysis. The effect on the polymerization efficiency of a lower enzymatic dose (0.15 U mL^{-1}) and a higher H_2O_2 concentration (0.5 mM), during 0.5, 2 and 24 h, was studied and separately assayed using HMR lignan as substrate.

2.4.2. Heterogeneous cross-linking of lignans with peptides

Reactions containing equal volumes (85 μL) of the 3 mM solutions of the SECO or HMR lignans and of the tyrosine-containing peptides were mixed with 1.5 U mL^{-1} VP, in a final volume of 200 μL. Aliquots (3 μL) were withdrawn after 0.5 and 2 h reaction and analyzed by MALDI-TOF MS.

2.4.3. Homogeneous cross-linking of β-casein

Three VP doses (0.015, 0.15, and 1.5 U mL^{-1}) were assayed in 1 mL reactions for β-casein polymerization, incubating separately for 2, 6, and 24 h with continuous stirring at 300 rpm. Aliquots (30 μL) from each treatment were separated and immediately mixed with loading buffer (10 μL), boiled for 10 min and analyzed by sodium dodecyl sulphate-polyacrylamide gel electrophoresis (SDS-PAGE). The remaining enzymatic reactions were stopped with NaN_3 (0.05%, w/v) and samples were lyophilized for further transmission electron microscopy (TEM) analysis.

2.4.4. Homogeneous cross-linking of FAX

The ability of VP to cross-link FAX, inducing gel formation, was investigated in reactions containing VP doses of 0.015, 0.15, 1.5 U mL^{-1} in a total volume of 1.5 mL. Mixtures were briefly vortexed and 1.3 mL was immediately removed and placed on the rheometer plate. Rheological analysis started 3 min after H_2O_2 activation. For swelling experiments, reactions were prepared with the same enzyme doses, in 2 mL syringes (diameter 1.5 cm), in a final volume of 1 mL. Reactions were allowed to gel for 15 h before analyzing the swelling degree.

2.5. MALDI-TOF MS analyses

MALDI-TOF MS spectra of VP-treated lignans and peptides were recorded on a Bruker Autoflex II instrument equipped with a N_2-laser (337 nm, 100 μJ) and previously calibrated with peptide and protein standard solutions from same distributor (Bremen, Germany). For the analyses, 3 μL of the reaction solution were mixed 1:1 (v:v) with saturated α-cyano-4-hydroxycinnamic acid matrix from Sigma-Aldrich (St Louis, MO, USA) dissolved in 0.1% trifluoroacetic acid from Fluka (Buchs, Switzerland) containing 50% acetonitrile. 1 μL of the sample-matrix solution was spotted onto the stainless steel target plate and allowed to dry at room temperature. Positive ion mass spectra were recorded in reflector mode (m/z range 500-3500) and linear mode (m/z range 3500-10000). FlexAnalysis (version 2.4) was used for data analysis (Bruker, Bremen, Germany). Lignans were detected as their sodium adducts.

2.6. SEC analyses

Samples from lignan treatments were dissolved in 0.1 M NaOH and analyzed by high performance SEC eluting with the same solvent (0.5 mL min^{-1} flow rate) at 25 °C, in MCX 1000 and 100000 Å columns connected in tandem and coupled to a precolumn (all from PSS Mainz, Germany). The elution profiles were followed at 280 nm with a Waters UV detector.

The molar mass distributions (MMD), and weight average molar masses (M_w) were calculated against polystyrene sulphonate (Na-PSS) standards, using the Waters Empower 2 software.

2.7. SDS-PAGE analysis

SDS-PAGE was used to analyze the formation of β-casein polymers smaller than 250 kDa. Samples were loaded onto Criterion TGX Stain-Free™ precast gels (4-20%) and visualized on the Criterion Stain Free™ Imager System. Precision Plus Protein™ Standards (10-250 kDa) were used for molecular weight estimations. All instruments and reagents were purchased to Bio-Rad (Hercules, CA, USA).

2.8. Microscopy analysis

Lyophilized β-casein samples, subjected or not to a 24 h VP treatment, were dissolved in distilled water or 6 M urea to observe non-enzymatic aggregates and enzymatic cross-links, respectively. Glow-discharged carbon-coated formvar grids were placed face-down over a droplet of sample. After 1 min, the grid was removed, blotted briefly with filter paper and negatively stained with 2 % uranyl acetate for 40 s, blotted quickly and air-dried. Samples were observed by TEM in a JEOL 1230 instrument (Tokyo, Japan) operated at 100 kV.

2.9. Rheological measurements and gel swelling analysis

The gelation of the cross-linked FAX was monitored by using an AR-G2 rheometer (TA Instruments, Crawley, UK) in oscillatory mode at a constant temperature of 22ºC. A plate-plate geometry with a diameter of 40 mm and a gap of 1 mm was used for the measurements, with a solvent trap to prevent sample drying during analysis. Gel formation was followed during 4 h, by monitoring the storage modulus (G´), the loss modulus (G´´) and the phase angle at a constant frequency of 0.1 Hz and a strain of 0.01 %.

To evaluate the gel swelling properties, cross-linked FAXs were allowed to swell in 10 mL of a 0.02 % (w/v) NaN_3 solution. After 32 h, samples were blotted, weighted, and subsequently added to new NaN_3 solutions at room temperature. The equilibrium swelling was reached when the weight of the samples did not change more than 3%. The swelling ratio (q) is calculated according to the equation: $q= (W_s – W_i)/ W_i$, where W_s is the weight of the swollen gel at each measured time and W_i is the weight of the gel before swelling.

3. RESULTS AND DISCUSSION

3.1. Influence of organic co-solvents and Mn^{2+} on VP activity and stability

The lignans included in the present study were selected for their different structures and the degree of solubility in aqueous solutions or organic co-solvents. Enzymes can be severely affected by the presence of organic solvents, which generally cause a sharp activity drop due to modification of the protein conformation (Faulds et al., 2011). For this reason, VP activity was first established in the presence of different concentrations of ethanol and 1,2-propanediol, two solvents chosen for their ability to solubilize softwood and hardwood lignins and for being completely water-miscible.

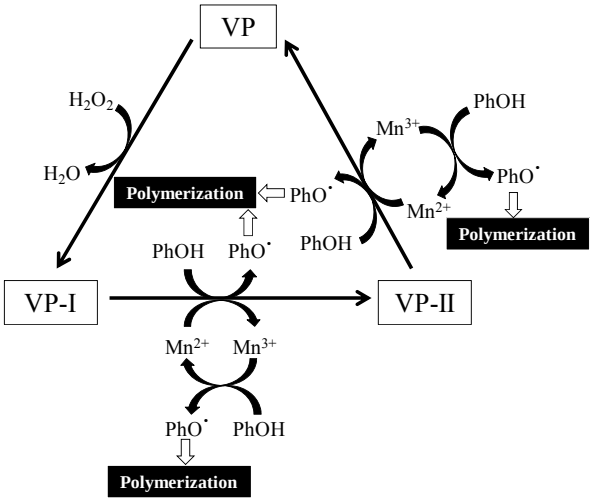

Fig. 2. Scheme of the versatile peroxidase (VP) catalytic cycle adapted from Ruiz-Dueñas et al. (1999). As shown, VP can oxidize, among others: (i) phenolic substrates (PhOH), such as lignans and tyrosine, to the corresponding phenoxy radicals (PhO·) which are able to polymerize; and (ii) Mn^{2+} to Mn^{3+}, the latter acting as a diffusible oxidizer of different compounds including phenols.

Initial activities in aqueous buffers were determined to be 15 U mL^{-1} for Mn^{2+}, 1 U mL^{-1} with ABTS, and 0.4 U mL^{-1} for DMP. VP-activity against ABTS and DMP increased in the presence of Mn^{2+}, reaching 1.6 U mL^{-1} and 3.6 U mL^{-1}, respectively. This enhanced activity on phenols and dyes in Mn^{2+}-containing reactions has been previously reported (Martínez et al., 1996), and it is related to the catalytic versatility of VP, oxidizing them in both Mn^{2+}-independent and Mn^{2+}-mediated reactions (Fig. 2).

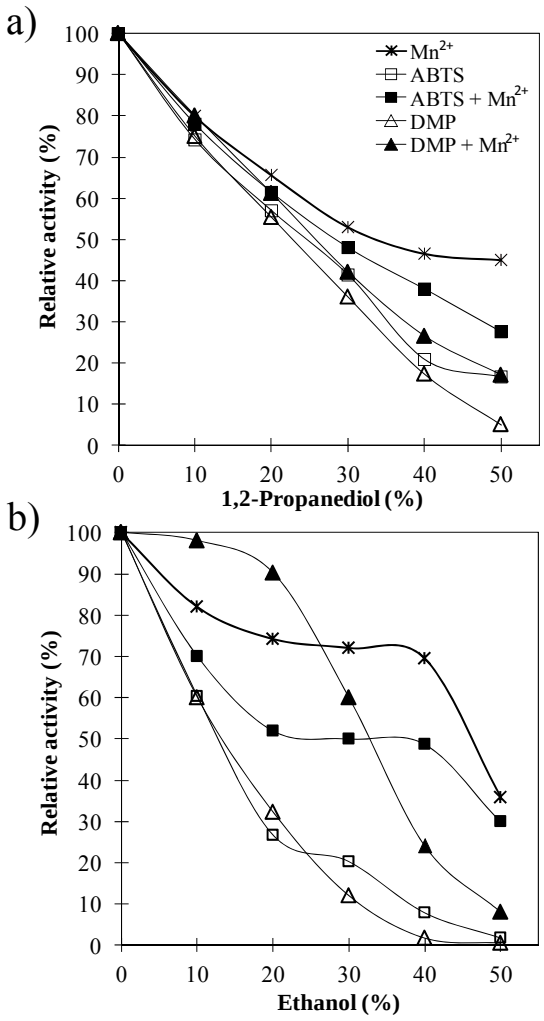

Fig. 3. Effect of (a) 1,2-propanediol and (b) ethanol on VP activity against three different substrates (Mn^{2+}, ABTS and DMP). ABTS and DMP reactions were followed in the presence and absence of 0.1 mM Mn^{2+}. All reactions were initiated with 0.1 mM H_2O_2. 100% corresponded to the enzymatic activity in the absence of those organic solvents, and values are expressed as the percentage of residual activity. Standard deviations from triplicates were less than 5% of the average value in all cases.

Figure 3 shows the effect of the two solvents on Mn^{2+}, DMP, and ABTS oxidation. As 1,2-propanediol concentration increased (Fig. 3a), a concurrent decrease in VP residual activity was observed. The decrease was significantly lower in reactions with Mn^{2+}, especially at high solvent concentrations, although some activity was retained in all reactions even with 50% of this organic solvent**.** On the other hand, the effect of ethanol on VP activity (Fig. 3b) was diverse. With Mn^{2+} as the substrate, VP was quite stable in up to 40% ethanol, with only a 30% decrease in activity. The oxidation of DMP in the presence of Mn^{2+} appeared not to be affected by the use of ethanol concentrations ≤ 20%. The activity of a *B. adusta* VP at low ethanol concentrations has also been described (Rodakiewicz-Nowak et al., 2006) although, according to our data, the VP from *P. eryngii* seems to be more resistant. However, a high activity loss was observed in DMP

reactions without Mn^{2+} that could be explained by reduced accessibility of ethanol through the narrow Mn-oxidation channel, compared with the main heme access-channel where DMP is oxidized (Morales et al., 2012). From the above results, and taking into account that most of the lignans used in this study are soluble at low ethanol concentrations (20%), this solvent was selected for further enzyme stability assays. The enzyme in buffer, as well as in the presence or absence of Mn^{2+}, retained the initial activity during the 24 h of incubation. With 20% ethanol in the absence of Mn^{2+}, the residual activity was 84 and 43% at 0.5 and 24 h, respectively, while in the presence of the ion was 87 and 82% (with 50% ethanol the enzyme lost its activity quickly, retaining 2.1% and 3.4% activity after 0.5 h with and without Mn^{+2}, respectively). It can thus be concluded that the presence of Mn^{2+} exerts a stimulating and stabilizing effect on the oxidation reactions and VP respectively. The former effect is due to Mn^{3+}-mediated oxidation of DMP and ABTS, while the stabilizing effect indicates lower inhibition when the VP Mn^{2+}-oxidation site is occupied by the ion during incubation with ethanol.

3.2. Small molecules cross-linking by VP

3.2.1. Lignan cross-linking analysis

Several parameters, such as the degree of polymerization (DP), the molecular mass (MM), and molar mass distribution (MMD) of the polymers enzymatically synthesized, should be analysed to compare the efficiency of VP in lignans polymerization with that reported for other oxidative enzymes (Mattinen et al., 2008). The polymerization of the substrates (DP and MM) was followed by MALDI-TOF MS. Control treatments, in the presence and absence of Mn^{2+}, containing lignans and H_2O_2 but lacking enzyme were conducted to check for substrates self-polymerization, revealing the presence of dimers and trimers of lignans (Table 1).

These non-enzymatic cross-links could arise from oxidation reactions, involving O_2 or H_2O_2, mediated by traces of metal ions (Eklund et al., 2005; Gómez-Toribio et al., 2001). Despite of these unspecific links, the VP/H_2O_2 system was capable of synthesizing molecules of much higher DP compared to the controls. Table 1 shows that most cross-linking occurred during the first 30 min of reaction and that the presence of Mn^{2+} enhanced the polymerization efficiency, raising both the reaction rate and the maximum DP of the products over the reaction time at all solvent concentrations. Table 2 depicts the predicted and experimental MM (accuracy $\leq \pm$ 1 Da) of the longest lignan homopolymers synthesized by VP, and the spectra of the reaction products are represented in Figure 4.

Table 1. Effect of 0.1 mM Mn^{2+} and incubation time on the VP-catalyzed polymerization of five different lignans. The control (CTL) was a VP-untreated sample incubated during 24 h, adding two dosages of 0.1 mM H_2O_2 at the beginning of the reaction and after 1 h, similarly to the VP-treatments. Analyses were performed on duplicates of two independent reactions, showing identical spectra.

Lignan	Solvent	Maximal degree of polymerization*							
		- Mn^{2+}				+ Mn^{2+}			
		CTL	30 min	2 h	24h	CTL	30 min	2 h	24h
SECO	Buffer	2	5	7	8	2	8	8	9
HMR	20% Ethanol	3	5	7	6	3	8	8	7
MR	20% Ethanol	2	4	5	5	2	5	6	7
CYCLO	20% Ethanol	2	5	6	6	2	6	7	7
7-HSECO	50% Ethanol	2	3	3	3	2	6	7	7

* Values represent the maximum number of lignan units cross-linked as detected by MALDI-TOF MS.

The assembly of lignan monomers is produced through an ether or carbon-carbon linkage that causes the elimination of two hydrogen atoms per cross-link (Mattinen et al., 2011). The theoretical mass of the products can be calculated according to the equation [[nMM-(n-1)2H] + Na^+], where n is the number of monomers and MM is the molecular mass of lignan. The water-soluble SECO was the most efficiently polymerized substrate, forming nonamers and octamers in the presence and absence of Mn^{2+}, respectively, after 24 h incubation. This value was similar or slightly higher than those reported for the cross-linking of SECO catalyzed by fungal (Mattinen et al., 2009) or bacterial laccases (Moya et al., 2011). Over the first 2 h of reaction, polymerization of both SECO and HMR progressed at similar rates, but after 24 h the maximum DP of the later decreased in one unit while the SECO polymer reached its highest length (Table 1). Buchert et al. (2002), reported the synthesis of HMR oligomers after 2 h incubation with a fungal laccase, but the products were 3-4 units smaller than those found in the present study at the same reaction time. Regarding 7-HSECO, the lignan dissolved in 50% ethanol, it is remarkable that the addition of Mn^{+2} produced two-fold larger oligomers as compared to the reaction without the cation, which could be due to an increased VP catalytic efficiency and stability, as described in the previous section.

SEC analysis of the VP-untreated and treated lignans, in the presence of Mn^{2+}, showed the reduction of the low MM peak from the substrates along the incubation time, and a parallel increase of the M_w of the products. Figure 5 illustrates the MMD profiles of SECO and HMR, the two lignans that reached the highest DP. A single peak, corresponding to substrates, was observed after SEC of control samples without peroxidase. The appearance of oligomers along the reaction time is detected as new

shoulders or peaks at the right of the substrates peak. The small increase in the low MM fraction from 24 h HMR reactions could be explained by the coexistence of polymerization and degradation activities in the reaction mixture, as previously reported for soluble-lignin samples treated with VP (Moreira et al., 2007) and MnP (Hofrichter et al., 2001). This finding is in accordance with the fading of the signal from HMR octamers detected by MALDI-TOF analysis of this sample (Table 1). However, the global M_w of the reaction components raised approximately 100 Da from 2 h to 24 h, suggesting that polymerization predominated over depolymerization during this period.

Table 2. Assignment of masses (m/z) of the longest lignan and peptide polymers detected by MALDI-TOF MS in VP-catalysed reactions. Homopolymerization and heteropolymerization experiments were performed in the presence of 0.1 mM Mn^{2+}, adding two dosages of 0.1 mM H_2O_2 at the beginning of the reaction and after 1 h. All reactions were incubated during 2 h excluding the homopolymerization of lignans which was carried out for 24 h. HMR polymerization was accomplished with 0.5 mM H_2O_2 during 2 h.

Substrate	Monomer (Da)	DP*	Predicted m/z (Da)	Experimental ** m/z (Da)
Homopolymers				
Lignans				
SECO	362.1	9	3264.9	3264.1 (-0.8)
HMR	374.1	9	3372.9	3372.8 (-0.1)
MR	358.1	7	2516.7	2517.6 (0.9)
CYCLO	360.1	7	2530.7	2531.5 (0.8)
7-HSECO	378.1	7	2656.7	2656.4 (-0.3)
Peptides				
RKRSRKE	959.1	1	959.1	959.6 (0.5)
EPPGGSKVILF	1125.3	1	1125.3	1125.5 (0.2)
GLY	351.4	8	2797.2	2796.9 (-0.3)
YST	369.2	8	2939.0	2939.6 (0.6)
VYV	379.5	11	4154.5	4155.0 (0.5)
YIGSR	594.7	11	6521.7	6522.6 (0.9)
VEPIPY	716.8	7	5027.6	5028.2 (0.6)
Heteropolymers				
YIGSR/SECO	594.7/ 362.1	1/5	2394.2	2393.7 (-0.5)
YIGSR/HMR	594.7/374.1	1/4	2082.1	2082.6 (0.5)

* DP= maximal degree of polymerization.
** The m/z differences between the theoretical and the detected masses, shown in parentheses, are within the experimental error of the technique.

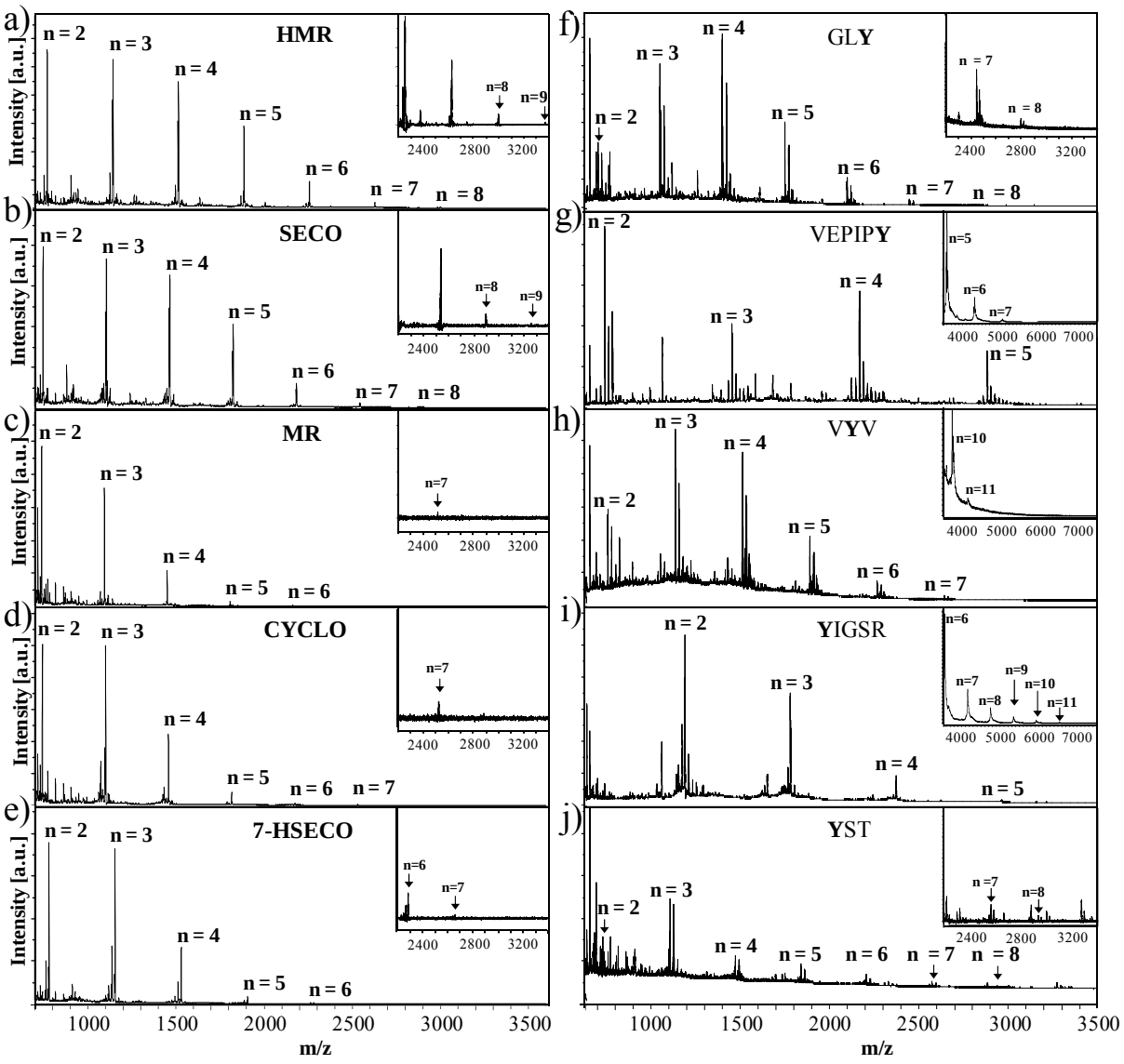

Fig. 4. MALDI-TOF mass spectra (reflector mode) of polymerized lignans and peptides. VP-treated lignans were incubated during 24 h with 0.1 mM Mn^{2+} and two dosages of 0.1 mM H_2O_2 at 0 and 1 h (excluding HMR whose incubation was carried out during 2 h with 0.1 mM Mn^{2+} and two dosages of 0.5 mM H_2O_2 at 0 and 1 h): (a) HMR, (b) SECO, (c) MR, (d) CYCLO, and (e) 7-HSECO. Peptides were incubated for 2 h with 0.1 mM Mn^{2+} and two dosages of 0.1 mM H_2O_2 at 0 and 1 h: (f) GLY, (g) YST, (h) VYV, (i) YIGSR, and (j) VEPIPY. The number of monomers (n) of each lignan or peptide is shown above the corresponding peak. An enlargement of m/z 2200-3400 region of all substrates is framed excluding VEPIPY, VYV, and YIGSR whose enlargements correspond to the m/z 3500-7000 Da (lineal mode) since they form oligomers larger than 3500 Da. All the analyses were performed on duplicate (two independent reactions), showing identical spectra.

As in the case for all peroxidases, H_2O_2 is essential for VP activity and its eventual depletion stops the reaction. The effect of different VP/H_2O_2 ratios on HMR cross-linking was assayed for 24 h treatments, either increasing 5-fold the peroxide concentration or decreasing 10-fold VP dosage (from 1.5 to 0.15 U mL^{-1}), and samples were analyzed at different

reaction times. Enzyme-free controls demonstrated that HMR treatment with 0.5 mM H_2O_2 did not induce any additional polymerization. In contrast, HMR polymers only one DP larger in molecular size than those detected in low-peroxide reactions were detected in the VP dosed with 5-fold more H_2O_2 system. The M_w values increased around 200 and 300 Da in 2 h and 24 h-reactions, compared to the equivalent products obtained with 0.1 mM H_2O_2. SEC profiles (Fig. 5b) showed that the low MM peak decreased around 50% in height, while a high-MM fraction of almost the same intensity appeared. Thus, higher doses of peroxide did not cause inhibition of VP, but rather improved its polymerization capacity. On the other hand, a reduced VP dosage resulted in the production of HMR oligomers of 5, 6 and 7 monomers after 0.5, 2, and 24 h, respectively, demonstrating that the amount of enzyme affected only the initial reaction rate, reaching the same DP values obtained at higher VP doses in 24 h (Table 1).

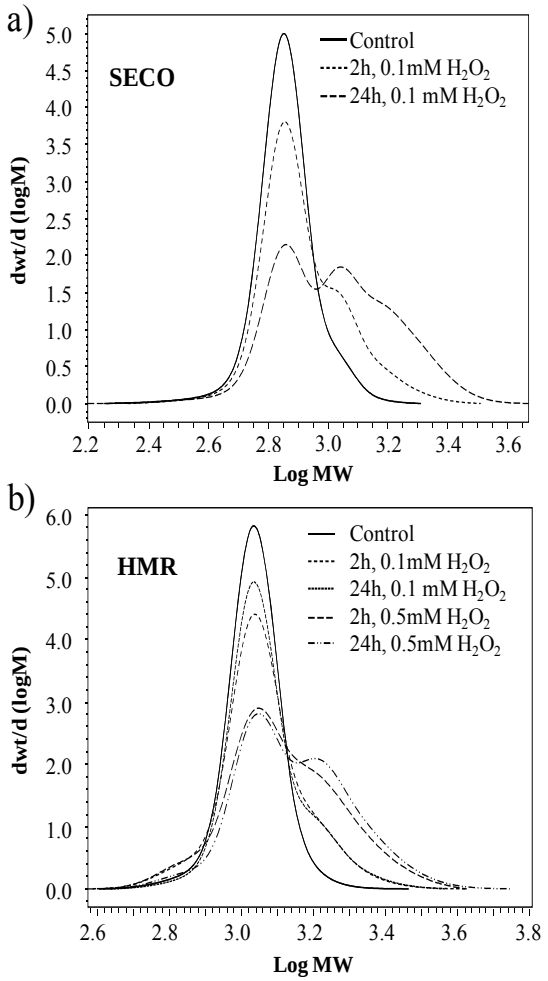

Fig. 5. Molar mass increase after VP treatment in the presence of 0.1 mM Mn^{2+} of: a) SECO and b) HMR. Controls correspond to VP-untreated SECO or HMR with 0.1mM H_2O_2 at 24 h of incubation. Controls corresponding to VP-untreated HMR with 0.5 mM H_2O_2 were similar to the previous control and are not represented in Fig. 5b.

3.2.2. Peptide cross-linking analysis

The positive effect of Mn^{2+} in VP-catalyzed polymerization reactions has already been deduced from the previous experiments. The VP treatment of peptides, of different length and amino acid sequence, was performed in the presence of this cation. No peptide cross-linking occurred in the absence of VP or H_2O_2, as well as in peptides lacking tyrosine residues (Table 2) such as RKRSRKE and EPPGGSKVILF. In contrast, the VP/H_2O_2 system was highly efficient polymerizing tyrosine-containing peptides, being as previously described for other oxidoreductases (Mattinen et al., 2005; Michon et al., 1997; Steffensen et al., 2008). Polypeptides were formed through the loss of two hydrogen atoms, probably due to the formation of dityrosine or isodityrosine bonds, resulting in monoisotopic masses whose theoretical value can be calculated according to the equation: [nMM-(n-1)2H], where n is the number of monomers and MM is the molecular mass of each peptide. As an exception, the polymers from VEPIPY were detected as their sodium adduct. Table 2 shows the experimental and predicted MM from the highest DP molecules synthesized upon VP-treatment, and Figure 4 depicts the spectra of the reaction products.

The peptide length and the position of tyrosine in the sequence had no effect on the DP of the products formed by the action of VP. This finding contrasts with the results obtained in similar reactions performed with HRP (Michon et al., 1997) or CiP (Steffensen et al., 2008), in which a strong effect of these two parameters on cross-linking has been reported. VP has several catalytic sites, one for (low efficiency) oxidation of phenols and dyes at the main heme access channel, a second one for Mn^{2+} oxidation at a (small) second heme access channel, and the third site for (high efficiency) oxidation of phenolic and nonphenolic aromatic substrates, located at the protein surface (Ruiz-Dueñas et al., 2009). These features, which are not observed in other peroxidases (such as HRP) that only present the "classical" oxidation site at the main heme channel, can facilitate substrate oxidation even if the reactive moiety, such as the tyrosine, is placed in the middle of the sequence. Therefore, the cross-linking of tyrosine-containing peptides by HRP may be very restricted by steric hindrances and enzyme inhibition (Michon et al., 1997). In contrast, VP can also oxidize its substrates at a second exposed catalytic site and via Mn^{2+} diffusion (Fig. 2), bypassing these problems.

In addition, VP-induced polymerization of peptides was very fast, reaching the maximum DP after 30 min in all cases. Regardless the reaction time, the predominant signals in most spectra corresponded to dimers, although tetramers and trimers were the main peaks detected after 2 h of reaction using GLY or VYV as the substrates, respectively (Fig. 4). The

MMD of the products, derived from MALDI-TOF MS spectra, changed while the reaction proceeded due to the production of larger species. The production of pentamers of GLY, using a laccase from *Trametes hirsuta* (Mattinen et al., 2005) and hexamers of VYV with the *C. cinerea* peroxidase (Steffensen et al., 2008) in 24 h, are poor values when compared to the nonamers of GLY and the undecamers of VYV obtained in VP-reactions of 30 min (Table 2). The results suggest that beyond a certain DP range, peptides polymerization is not favored under the reaction conditions used in this study or by other steric factors. Despite this limitation, our results show that, even at short reaction times, the polymerization degree was higher using VP, even though this enzyme has a more restricted activity compared to laccases, especially due to the low H_2O_2 concentration tested in this study.

3.2.3. Heterogeneous cross-linking of lignans with peptides

VP reactions containing SECO or HMR and each of the tyrosine-containing peptides were incubated for 30 min and 2 h and analyzed to test the ability of the enzyme to catalyze the synthesis of heteropolymers. The MALDI-TOF spectra of the reaction products for each peptide-containing reaction showed that in most cases only lignan homopolymers were formed, detecting up to nonamers of SECO and octamers of HMR. Steffensen and co-workers (Steffensen et al., 2009) suggested that monolignols can have antioxidant effects, avoiding tyrosine oxidation in peptides when they are added to the reaction at the same concentration. Moreover, although the molar concentration of both substrates in the reaction mixture was the same and the MM of the tripeptides (GLY, VYV, YST) and the lignans is also similar, the later contain two-fold more reactive sites than the peptides (two phenols per one tyrosine, respectively). The probability for heterocomplex formation appears to increase with the number of reactive sites in the biopolymer. This proposition contrasts with the results obtained with VEPIPY. In this last case, and taking into account the gravimetric amount of the compound in the final reaction mixture, polymerization was not observed even though this peptide and the lignans contained a similar number of reactive sites.

Hetero-oligomers were only formed in reactions containing the peptide YIGSR with both lignans (Fig. 6), although lignan homo-oligomers were also detected. These heterogeneous cross-linking reactions took place through the elimination of two hydrogen atoms according to the equation: $[nMM(YIGSR)+[nMM(lignan)-(n-1)2H^+]-2H^+]$.

Peaks corresponding to peptide homo-oligomers were not found, contrasting with the high DP of the YIGSR units produced when incubated alone with VP (Table 2). YIGSR is a peptide derived from laminin and it is

considered as an adhesive ligand, what can possibly facilitate its attachment and linking to other molecules (Zustiak et al., 2010). These results indicate that, in the presence of both substrates, VP has a preference for lignans and if a hetero-crosslinking occurs, only the lignan chain is further elongated.

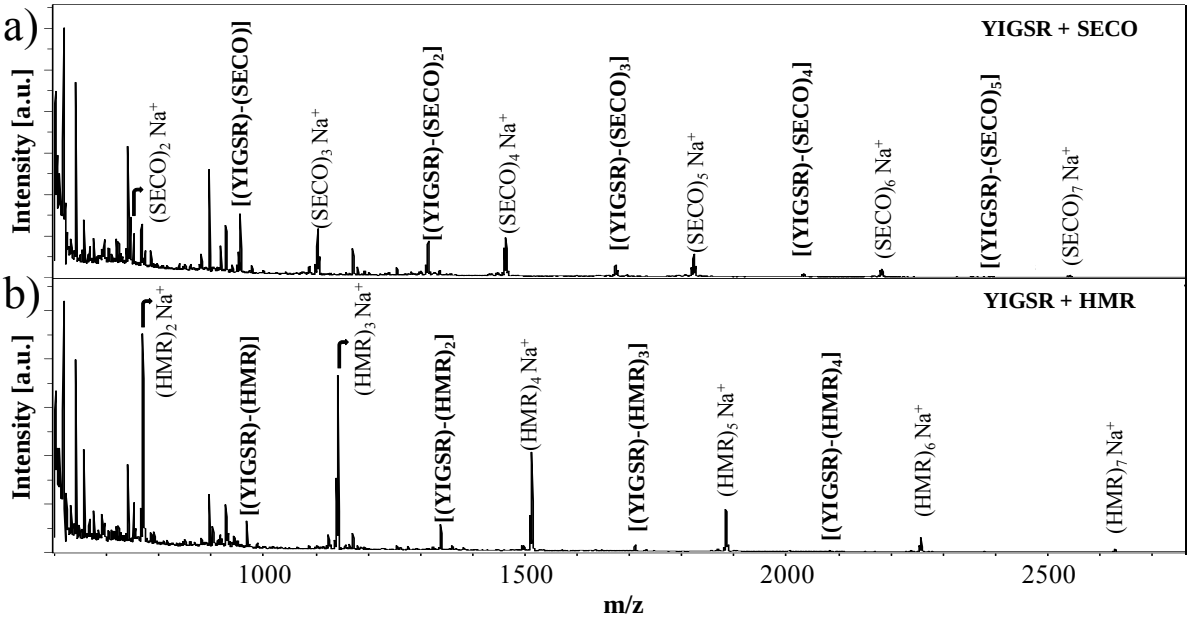

Fig. 6. MALDI-TOF mass spectra from VP-heteropolymerization of YIGSR peptide with (a) SECO lignan and (b) HMR lignan during 2 hours in the presence of 0.1 mM Mn^{2+} and H_2O_2. A second dosage of 0.1 mM peroxide was added after 1h incubation. The units' number of the homo- and the hetero-polymers is shown above the corresponding peak. Analyses were performed on duplicates of two independent reactions, showing identical spectra.

3.3. Large molecules cross-linking by VP

3.3.1. β-Casein cross-linking

As VP was shown to efficiently cross-link small tyrosine-containing peptides, the milk protein β-casein, consisting of 209 amino acids, four of which are tyrosines (Monogioudi et al., 2009), was selected to determine if VP could cross-link larger proteins. The products were analyzed under dissociating and reducing conditions by SDS-PAGE, confirming that the complexes observed were due to the formation of covalent bonds and not by molecular aggregation. Large-size molecular species (approximately 150 kDa) appeared even at the lowest enzyme dosage and the band corresponding to the β-casein monomer slightly decreased over the reaction time, suggesting that a low percentage of protein was modified (Fig. 7, lane 6). In contrast, medium and high doses of VP resulted in an almost total fading of the β-casein monomer after 24 h (Fig. 7, lanes 7 and 10). Moreover, bands higher than 250 kDa were observed at the top of the

running gel, corresponding to polymers of at least 10-11 β-casein monomers.

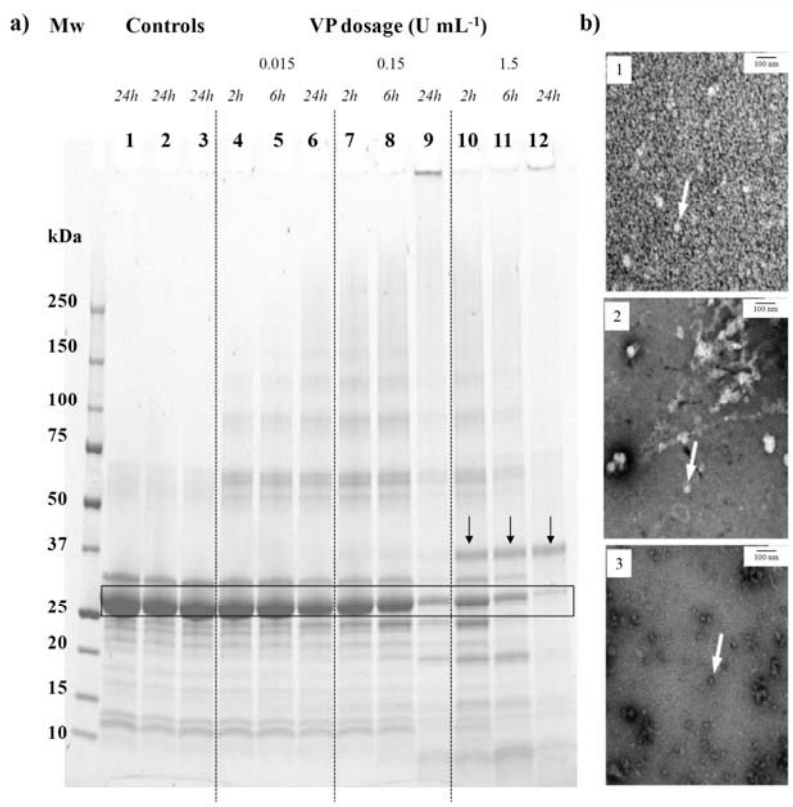

Fig. 7. Cross-linking of β-casein analysed by SDS-PAGE and TEM. a) SDS-PAGE of β-casein (Lane 1); β-casein plus H_2O_2 (Lane 2); β-casein plus VP (Lane 3); VP/H_2O_2-treated β-casein with 0.015 U mL^{-1} of VP (Lanes 4-6); VP/H_2O_2-treated β-casein with 0.15 U mL^{-1} (Lanes 7-9); VP/H_2O_2-treated β-casein with 1.5 U mL^{-1} (Lanes 10-12). Arrows are signaling the VP band (~43 kDa). The β-casein monomer is framed along the gel. b) TEM photomicrographs of untreated β-casein (1), and VP-treated β-casein during 24 h of incubation with an enzyme dosage of 1.5 U mL^{-1} dissolved in water (2) or in urea 6 M (3). Arrows are signaling β-casein monomers.

The polymerization of casein has been previously reported using HRP (Matheis and Whitaker, 1984) and HRP plus ferulic acid (Li et al., 2009) with similar results to those reported in the present study. Bands with a lower mass than β-casein appeared after long incubation times and in reactions with high VP doses. As previously discussed, the peroxidase can simultaneously catalyze polymerization and degradation at extended reaction times (Fig. 7, lanes 7 to 10). After 24 h of incubation, a slight aggregation was detected in all samples, which could be produced by the intra- and intermolecular transference of radicals formed from proteins during the reaction (Dauphas et al., 2005; Monogioudi et al., 2011). TEM images (Fig. 7) from water solutions of VP-treated casein allowed the observation of the protein as fibers, representing a typical product structure upon molecular aggregation (Werning et al., 2008). When VP-treated β-

casein was dissolved in urea to disrupt aggregates, polymers were observed as irregular and compact structures with a broad range of sizes.

3.3.2. FAX cross-linking

Small deformation oscillatory rheology was used to follow gel formation caused by the oxidative cross-linking of feruloylated arabinoxylan. Control treatments lacking VP or H_2O_2 did not produce gels during 4 h reactions, and the same result was obtained with the lowest VP dosage (0.015 U mL^{-1}). Neither the use of 1.5 U mL^{-1} of VP was useful for this monitoring since it produced an immediate gelation after H_2O_2 addition. A dosage of 0.15 U mL^{-1} VP was selected for further experiments. The profile obtained with 3% FAX fitted the typical kinetic behavior displayed in enzymatic systems containing laccases (Carvajal-Millan et al., 2005) or other peroxidases (Martínez-López et al., 2011). Figure 8 shows an initial increase of both G´ and G´´ followed by a plateau region. That plateau reached G´ values of around 90 Pa and G´´ values of 0.5 Pa in 10 and 7 min respectively, indicating that the sample had gel-like properties. The final phase angle was very low (below 0.5 degrees), highlighting the high elasticity of the gel.

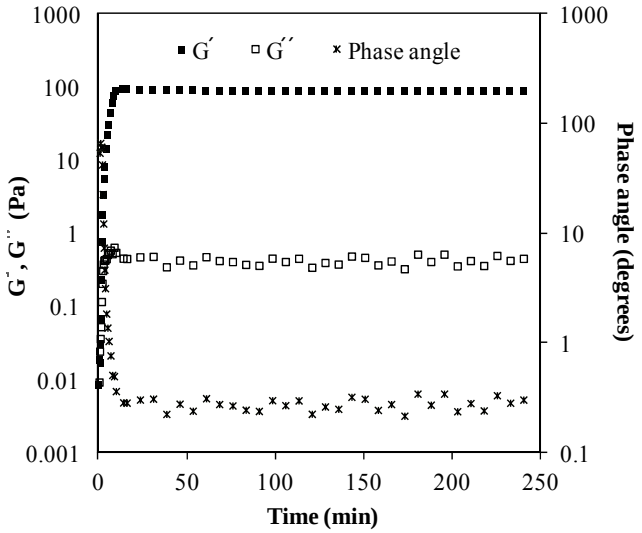

Fig. 8. The effects of VP-treatment on the rheological properties of FAX gels. Samples were analyzed in duplicate, showing coefficients of variation lower than 5%.

The gelation point, calculated from the crossover point of G' and G'', took place in about 2 min. Apart from the diferulic covalent bonds, non-covalent links between arabinoxylans might also occur (Berlanga-Reyes et al., 2011; Niño-Medina et al., 2010) and therefore the measured rheological properties depend on the arabinoxylan structural characteristics and the ferulic acid concentration.

Gels were generated only in reactions with 0.15 and 1.5 U mL^{-1} VP, reaching the swelling equilibrium between 4 and 6 h, with swelling ratio values (q) of 53.4 ± 0.4 and 65.4 ± 1.1 g water/g FAX, respectively. These values were higher than those reported in other enzyme-catalysed FAX gelation studies (Meyvis et al., 2000). The fast reaction rate achieved with VP could cause the trapping of uncrosslinked FAX molecules inside the gel structure. These molecules would expand quickly in contact with water, leading to its increased intake in the resultant FAX networks (Martínez-López et al., 2011).

4. CONCLUSIONS

The modification by enzymatic cross-linking of biomolecules using the VP from *P. eryngii* has been achieved. The reaction conditions during VP treatments had a great influence in the reaction yields. In general, Mn^{2+} seemed to improve the VP stability and/or its catalytic efficiency even in the presence of organic co-solvents, which are essential in most reactions involving lignans. Only peptides containing tyrosine residues, regardless of their position in the sequence, are capable of forming a covalent bond through this kind of reactions, and heteropolymerization of lignans with a peptide resulted to be feasible. Moreover, VP-catalyzed cross-linking produced high mass macromolecules from β-casein and FAX. In view of these results, the application of VP for efficient polymerization of oxidizable compounds is suggested. Further screening of other potential substrates for VP and studies on the optimization of the polymerization reaction will be designed in the future. The *P. eryngii* VP used in this work is currently being subjected to structural-functional studies enabling rational design, as well as to directed molecular evolution, to improve its resistance to pH and H_2O_2, two important challenges for its application in biotechnological processes.

ACKNOWLEDGEMENTS

D. Salvachúa thanks the Spanish Ministry of Economy and Competitiveness for a FPU fellowship, P. Matikainen and B. Hillebrandt for technical assistance and Dr. K. Viljanen for the phenolic acids analysis (VTT, Espoo, Finland). We also thank Fernando Escolar for its help in TEM and J. Gil (CIB, Madrid, Spain). This work has been carried out with funding from the EU FP7 project "Peroxicats" (KBBE-2010-4-265397), the Spanish Ministry of Science and Innovation (BIO2009-08446, PRI-PIBAR-2011-1402), and the project "Lignin Fibre" financed by the Academy of Finland (Grant number 133091).

REFERENCES

Anderegg, R.J. Rowe, J.W., 1974. Lignans, the major component of resin from *Araucaria angustifolia* knots. Holzforschung 28, 171.

Arihara, K., 2006. Functional properties of bioactive peptides derived from meat proteins, in: Nollet, L.M.L., Toldrá, F. (Eds.), Advanced technologies for meat processing. CRC Press, Boca Raton, FL, pp. 254-273.

Banci, L., Camarero, S., Martínez, A.T., Martínez, M.J., Pérez-Boada, M., Pierattelli, R., Ruiz-Dueñas, F.J., 2003. NMR study of Mn(II) binding by the new versatile peroxidase from the white-rot fungus *Pleurotus eryngii*. J. Biol. Inorg. Chem. 8, 751-760.

Berlanga-Reyes, C.M., Carvajal-Millan, E., Lizardi-Mendoza, J., Islas-Rubio, A.R., Rascón-Chu, A., 2011. Enzymatic cross-linking of alkali extracted arabinoxylans: gel rheological and structural characteristics. Int. J. Mol. Sci. 12, 5853-5861.

Boeriu, C. 2008. Peroxidases in food industry: crosslinking of proteins and polysaccharides to impart novel functional properties. Romanian Biotech. Lett. 13, 81-86.

Buchert, J., Cura, D.E., Ma, H., Gasparetti, C., Monogioudi, E., Faccio, G., Mattinen, M., Boer, H. et al., 2010. Crosslinking food proteins for improved functionality. Annu. Rev. Food Sci. Technol. 113-138.

Buchert, J., Mustranta, A., Tamminen, T., Spetz, P., Holmbom, B., 2002. Modification of spruce lignans with *Trametes hirsuta* laccase. Holzforschung 56, 579-584.

Carvajal-Millan, E., Landillon, V., Morel, M.H., Rouau, X., Doublier, J.L., Micard, V., 2005. Arabinoxylan gels: Impact of the feruloylation degree on their structure and properties. Biomacromol. 6, 309-317.

Dauphas, S., Mouhous-Riou, N., Metro, B., Mackie, A.R., Wilde, P.J., Anton, M., Riaublanc, A., 2005. The supramolecular organisation of +¦-casein: effect on interfacial properties. Food Hydrocol 19, 387-393.

Eklund, P., Sillanpää, R., Sjöholm, R., 2002. Synthetic transformation of hydroxymatairesinol from Norway spruce (*Picea abies*) to 7-hydroxysecoisolariciresinol, (+)-lariciresinol and (+)-cyclolariciresinol. J. Chem. Soc. Perk. T. 1 1906-1910.

Eklund, P.C., Långvik, O.K., Wärnå, J.P., Salmi, T.O., Willför, S.M., Sjöholm, R.E., 2005. Chemical studies on antioxidant mechanisms and free radical scavenging properties of lignans. Org. &Biomol. Chem. 3, 3336-3347.

Faulds, C.B., Pérez-Boada, M., Martínez, A.T., 2011. Influence of organic co-solvents on the activity and substrate specificity of feruloyl esterases. Bioresour. Technol. 102, 4962-4967.

Floudas, D., Binder, M., Riley, R., Barry, K., Blanchette, R.A., Henrissat, B., Martinez, A.T., Otillar, R. et al., 2012. The paleozoic origin of enzymatic lignin decomposition reconstructed from 31 fungal genomes. Science 336, 1715-1719.

García-Ruiz, E., González-Pérez, D., Ruiz-Dueñas, F.J., Martinez, A.T., Alcalde, M., 2012. Directed evolution of a temperature-, peroxide- and alkaline pH-tolerant versatile peroxidase. Biochem. J. 441, 487-498.

Gómez-Toribio, V., Martínez, A.T., Martínez, M.J., Guillén, F., 2001. Oxidation of hydroquinones by the versatile ligninolytic peroxidase from *Pleurotus eryngii*: H_2O_2 generation and the influence of Mn^{2+}. Eur. J. Biochem. 268, 4787-4793.

Hamid, M. Khalil, U.R., 2009. Potential applications of peroxidases. Food Chem. 115, 1177-1186.

Heinfling, A., Ruiz-Dueñas, F.J., Martínez, M.J., Bergbauer, M., Szewzyk, U., Martínez, A.T., 1998. A study on reducing substrates of manganese-oxidizing peroxidases from *Pleurotus eryngii* and *Bjerkandera adusta*. FEBS Lett. 428, 141-146.

Hofrichter, M., Lundell, T., Hatakka, A., 2001. Conversion of milled pine wood by manganese peroxidase from *Phlebia radiata*. Appl. Environ. Microbiol. 67, 4588-4593.

Hofrichter, M., Ullrich, R., Pecyna, M.J., Liers, C., Lundell, T., 2010. New and classic families of secreted fungal heme peroxidases. Appl. Microbiol. Biotechnol. 87, 871-897.

Kobayashi, S., Uyama, H., Kimura, S., 2001. Enzymatic polymerization. Chem. Rev. 101, 3793-3818.

Li, J., Li, T., Zhao, X., 2009. Hydrogen peroxide and ferulic acid-mediated oxidative cross-linking of casein catalyzed by horseradish peroxidase and the impacts on emulsifying property and microstructure of acidified gel. African J. Biotechnol. 8, 6993-6999.

Lú-Chau, T.A., Ruiz-Dueñas, F.J., Camarero, S., Feijoo, G., Martínez, M.J., Lema, J.M., Martínez, A.T., 2004. Effect of pH on the stability of *Pleurotus eryngii* versatile peroxidase during heterologous production in *Emericella nidulans*. Bioprocess Biosyst. Eng. 26, 287-293.

Martínez, M.J., Ruiz-Dueñas, F.J., Guillén, F., Martínez, A.T., 1996. Purification and catalytic properties of two manganese-peroxidase isoenzymes from *Pleurotus eryngii*. Eur. J. Biochem. 237, 424-432.

Martínez-López, A.L., Carvajal-Millan, E., Lizardi-Mendoza, J., López-Franco, Y.L., Rascón-Chu, A., Salas-Muñoz, E., Barron, C., Micard, V., 2011. The peroxidase/H_2O_2 system as a free radical-generating agent for gelling maize bran arabinoxylans: rheological and structural properties. Molecules 16, 8410-8418.

Matheis, G. Whitaker, J.R., 1984. Peroxidase-Catalyzed Cross Linking of Proteins. J. Prot. Chem. 3, 35-48.

Mattinen, M.L., Kruus, K., Buchert, J., Nielsen, J.H., Andersen, H.J., Steffensen, C.L., 2005. Laccase-catalyzed polymerization of tyrosine-containing peptides. FEBS J 272, 3640-3650.

Mattinen, M.L., Maijala, P., Nousiainen, P., Smeds, A., Kontro, J., Sipila, J., Tamminen, T., Willför, S. et al., 2011. Oxidation of lignans and lignin model compounds by laccase in aqueous solvent systems. J. Mol. Catal. B-Enzym. 72, 122-129.

Mattinen, M.L., Struijs, K., Suortti, T., Mattila, I., Kruus, K., Willför, S., Tamminen, T., Vincken, J.P., 2009. Modification of lignans by *Trametes hirsuta* laccase. Bioresources 4, 482-496.

Mattinen, M.L., Suortti, T., Gosselink, R., Argyropoulus, D.S., Evtuguin, D., Suurnäkki, A., de Jong, E., Tamminen, T., 2008. Polymerization of different lignins by laccase. Bioresources 3, 549-565.

Meyvis, T.K.L., De Smedt, S.C., Demeester, J., Hennink, W.E., 2000. Influence of the degradation mechanism of hydrogels on their elastic and swelling properties during degradation. Macromolecules 33, 4717-4725.

Michon, T., Chenu, M., Kellershon, N., Desmadril, M., Gueguen, J., 1997. Horseradish peroxidase oxidation of tyrosine-containing peptides and their subsequent polymerization: A kinetic study. Biochemistry 36, 8504-8513.

Miletic, N., Nastasovic, A., Loos, K., 2012. Immobilization of biocatalysts for enzymatic polymerizations: Possibilities, advantages, applications. Bioresour. Technol. 115, 126-135.

Monogioudi, E., Creusot, N., Kruus, K., Gruppen, H., Buchert, J., Mattinen, M.L., 2009. Cross-linking of β-casein by *Trichoderma reesei* tyrosinase and *Streptoverticillium mobaraense* transglutaminase followed by SEC-MALLS. Food Hydrocol. 23, 2008-2015.

Monogioudi, E., Permi, P., Filpponen, I., Lienemann, M., Li, B., Argyropoulos, D., Buchert, J., Mattinen, M.L., 2011. Protein analysis by P-31 NMR spectroscopy in ionic liquid: quantitative determination of enzymatically created cross-links. J. Agric. Food Chem. 59, 1352-1362.

Morales, M., Mate, M.J., Romero, A., Martinez, M.J., Martinez, A.T., Ruiz-Dueñas, F.J., 2012. Two oxidation sites for low redox potential substrates: A directed mutagenesis, kinetic,and crystallographic study on *Pleurotus eryngii* versatile peroxidase. J. Biol. Chem. 287, 41053-41067.

Moreira, P.R., Almeida-Vara, E., Malcata, F.X., Duarte, J.C., 2007. Lignin transformation by a versatile peroxidase from a novel *Bjerkandera* sp strain. Intern. Biodeterior. Biodegrad. 59, 234-238.

Moya, R., Saastamoinen, P., Hernandez, M., Suurnäkki, A., Arias, E., Mattinen, M.L., 2011. Reactivity of bacterial and fungal laccases with lignin under alkaline conditions. Bioresour. Technol. 102, 10006-10012.

Niño-Medina, G., Carvajal-Millan, E., Rascón-Chu, A., Marquez-Escalante, J.A., Guerrero, V., Salas-Munoz, E., 2010. Feruloylated arabinoxylans and arabinoxylan gels: structure, sources and applications. Phytochem. Rev. 9, 111-120.

Pérez-Boada, M., Ruiz-Dueñas, F.J., Pogni, R., Basosi, R., Choinowski, T., Martínez, M.J., Piontek, K., Martínez, A.T., 2005. Versatile peroxidase oxidation of high redox potential aromatic compounds: Site-directed mutagenesis, spectroscopic and crystallographic investigations of three long-range electron transfer pathways. J. Mol. Biol. 354, 385-402.

Rodakiewicz-Nowak, J., Jarosz-Wilkolazka, A., Luterek, J., 2006. Catalytic activity of versatile peroxidase from *Bjerkandera fumosa* in aqueous solutions of water-miscible organic solvents. Appl. Cat. A:General 308, 56-61.

Rodríguez, E., Nuero, O., Guillén, F., Martínez, A.T., Martínez, M.J., 2004. Degradation of phenolic and non-phenolic aromatic pollutants by four *Pleurotus* species: the role of laccase and versatile peroxidase. Soil Biol. Biochem. 36, 909-916.

Ruiz-Dueñas, F.J., Martínez, M.J., Martínez, A.T., 1999. Molecular characterization of a novel peroxidase isolated from the ligninolytic fungus *Pleurotus eryngii*. Mol. Microbiol. 31, 223-236.

Ruiz-Dueñas, F.J., Morales, M., García, E., Miki, Y., Martínez, M.J., Martínez, A.T., 2009. Substrate oxidation sites in versatile peroxidase and other basidiomycete peroxidases. J. Exp. Bot. 60, 441-452.

Saleem, M., Kim, H.J., Ali, M.S., Lee, Y.S., 2005. An update on bioactive plant lignans. Nat. Prod. Rep. 22, 696-716.

Smeds, A.I., Eklund, P.C., Sjöholm, R.E., Willför, S.M., Nishibe, S., Deyama, T., Holmbom, B.R., 2007. Quantification of a broad spectrum of lignans in cereals, oilseeds, and nuts. J. Agric. Food Chem. 55, 1337-1346.

Stanic, D., Monogioudi, E., Dilek, E., Radosavljevic, J., Atanaskovic-Markovic, M., Vuckovic, O., Raija, L., Mattinen, M. et al., 2010. Digestibility and allergenicity assessment of enzymatically crosslinked beta-casein. Mol. Nutr. Food. Res. 54, 1273-1284.

Steffensen, C.L., Mattinen, M.L., Andersen, H.J., Kruus, K., Buchert, J., Nielsen, J.H., 2008. Cross-linking of tyrosine-containing peptides by hydrogen peroxide-activated *Coprinus Cinereus* peroxidase. Eur. Food. Res. Technol. 227, 57-67.

Steffensen, C.L., Stensballe, A., Kidmose, U., Degn, P.E., Andersen, M.L., Nielsen, J.H., 2009. Modifications of amino acids during ferulic acid-mediated, laccase-catalysed cross-linking of peptides. Free Radical Research 43, 1167-1178.

Walde, P. Guo, Z., 2011. Enzyme-catalyzed chemical structure-controlling template polymerization. Soft Matter 7, 316-331.

Werning, M.L., Corrales, M.A., Prieto, A., Fernández de Palencia, P., Navas, J., López, P., 2008. Heterologous expression of a position 2-substituted (1-3)-β-D-glucan in *Lactococcus lactis*. Appl. Environ. Microbiol. 74, 5259-5262.

Zustiak, S.P., Durbal, R., Leach, J.B., 2010. Influence of cell-adhesive peptide ligands on poly(ethylene glycol) hydrogel physical, mechanical and transport properties. Acta Biomaterialia 6, 3404-3414.

Discusión general



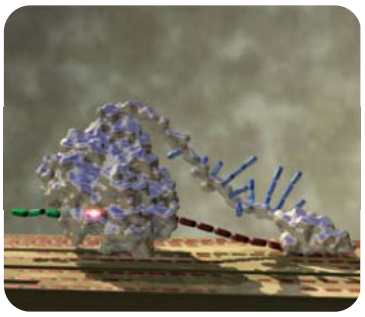

DISCUSIÓN GENERAL

Como se ha explicado anteriormente, el bioetanol 2G es un tipo de combustible, producido a partir de materiales lignocelulósicos, que constituye en la actualidad una de las alternativas más atractivas para disminuir el consumo de gasolina en automoción. Sin embargo, como se ha podido deducir del presente trabajo, para poder aprovechar los carbohidratos que contiene una estructura tan compleja como la lignocelulosa, es imprescindible someter la materia prima a procesos de pretratamiento e hidrólisis enzimática antes de poder llevar a cabo la fermentación (Talebnia et al., 2010). Estas dos etapas suponen el mayor costo del proceso de producción, por lo que toda investigación dirigida a su mejora conlleva un avance en la generación de biocombustibles avanzados. En esta Tesis se han abordado varios aspectos relacionados con este tema: la investigación de la efectividad de un método limpio de pretratamiento, utilizando microorganismos degradadores de la lignocelulosa, el estudio pormenorizado del sistema enzimático secretado por el hongo más eficiente en la degradación de paja de trigo y la caracterización de una nueva enzima implicada en el proceso y con características prometedoras de cara a su explotación.

1. BIOPRETRATAMIENTO DE LA PAJA DE TRIGO

En primer lugar, se analizó la eficiencia de un pretratamiento biológico como alternativa a los métodos físico-químicos comúnmente usados que, aunque efectivos, son poco respetuosos con el medio ambiente y suelen generar inhibidores que perjudican el proceso de fermentación. Se realizó un experimento con 21 hongos basidiomicetos, que fueron inoculados sobre paja de trigo en condiciones de fermentación en estado sólido y cultivados durante 7, 14 y 21 días. El efecto de los tratamientos fúngicos se evaluó en cada uno de los cultivos estudiando: (i) las modificaciones del sustrato durante el biopretratamiento (degradación de celulosa, hemicelulosa y lignina), (ii) su digestibilidad después de la hidrólisis enzimática y (iii) el rendimiento final de recuperación de azúcares. Además, se valoró en los cultivos la presencia de algunas enzimas extracelulares implicadas en la degradación de la lignina.

El tratamiento con 8 de las 21 cepas de basidiomicetos ensayadas mejoró la digestibilidad de la paja de trigo respecto del control no biopretratado, llegando a máximos de digestibilidad en la celulosa del 82% y en la hemicelulosa del 78% tras 21 días de incubación (Salvachúa et al., 2011). Estos valores son atractivos a primera vista, pero si el incremento de digestibilidad del sustrato va ligado a un alto consumo de carbohidratos, el balance final de azúcares potencialmente fermentables puede no resultar rentable de cara a la producción de etanol. De hecho, de los 8 hongos, sólo

5 incrementaron la proporción de azúcares fermentables, recuperándose hasta el 70% de la glucosa a los 21 días y el 62% de la xilosa tras 14 días de biopretratamiento.

Una de las principales desventajas del biopretratamiento es que se requieren tiempos largos de incubación para obtener buenos niveles de digestibilidad, lo que ralentiza y encarece el proceso de producción y, en muchos casos, incrementa el consumo de azúcares durante el crecimiento del hongo (Galbe y Zacchi, 2007). Con el objetivo de acelerar el proceso, la paja de trigo, ya alterada por el crecimiento de los microorganismos, se sometió a un tratamiento químico suave consistente en un lavado con NaOH muy diluida, tras el cual la digestibilidad de la celulosa mejoró significativamente debido a la solubilización de la lignina con el álcali (Kumar et al., 2009). Estos sustratos pretratados se hidrolizaron con cócteles enzimáticos comerciales ricos en actividad celulasa y hemicelulasa y la glucosa liberada se fermentó con una cepa industrial de *S. cerevisiae*, valorando el etanol producido. Con la metodología empleada en este trabajo, se alcanzaron rendimientos finales de producción de etanol del 62% con dos de los hongos estudiados, tras 21 días de biopretratamiento. Además, los resultados obtenidos mostraron que las conversiones de glucosa a etanol eran en algunos casos mayores del 90%, lo que sugiere que, como consecuencia de la combinación de ambos tipos de pretratamiento, no se produjeron compuestos que perjudicaran significativamente ni la hidrólisis enzimática ni la capacidad de la levadura para llevar a cabo la fermentación.

De entre todas las cepas evaluadas, el microorganismo que proporcionó los mejores resultados a los 14 días de tratamiento fue *Irpex lacteus* y por esta razón fue elegido como el candidato más apropiado para continuar el estudio. Con el fin de tratar de optimizar los rendimientos finales del proceso, el hongo seleccionado se incubó sobre paja de trigo en 9 condiciones de cultivo diferentes, en cada una de las cuales se alteró un solo parámetro con respecto a las condiciones previamente utilizadas en el muestreo (Salvachúa et al., 2013d). La mayoría de las variaciones introducidas en los cultivos no produjo ningún efecto positivo. Solamente la reducción del tamaño de la paja y la adición de Mn^{2+} mejoraron significativamente la digestibilidad de la materia prima respecto de las condiciones iniciales, llegando al 100% de digestibilidad de la hemicelulosa. Sin embargo, la recuperación final de azúcares, y en concreto la de la glucosa, únicamente mejoró alrededor de un 6%, en el medio suplementado con sales de Mn^{2+}. Esto puede explicarse tanto por la inducción por este ion de actividades ligninolíticas como MnP, como por la disminución de la producción de celulasas, tal y como se comprobó en los experimentos de proteómica de la presente Tesis (Salvachúa et al., 2013a).

En muchas ocasiones, la comparación de los resultados descritos por diferentes grupos de trabajo es complicada, ya que pocas publicaciones aportan datos para el proceso global, desde el biopretratamiento hasta la producción de etanol. A pesar de las dificultades y los numerosos factores a tener en cuenta durante el pretratamiento de paja de trigo con hongos, los rendimientos obtenidos, hasta el momento, han sido prometedores y mejores que los descritos por otros grupos de investigación para tratamientos similares del mismo sustrato con *I. lacteus* u otros organismos (Dias et al., 2010; Pinto et al., 2012; Wan y Li, 2011). Por otra parte, los resultados del biopretratamiento con *I. lacteus* son comparables o mejores que los publicados utilizando algunos procedimientos no biológicos. Así, Koullas et al. (1992) solo obtuvieron valores de digestibilidad del 61% con paja de trigo tras un drástico pretratamiento de pulverización del sustrato. Con tratamientos físico-químicos, como explosión por vapor (EV), agua caliente en fase líquida (ACL) y explosión por vapor con amoniaco (AFEX), se han alcanzado valores de digestibilidad de la celulosa de alrededor de un 93% (Talebnia et al., 2010) y hasta del 98% en tratamientos con ácido diluido (Kootstra et al., 2009). Sin embargo, hay que tener en cuenta que el empleo de estos enérgicos tratamientos suele conllevar una pérdida de azúcares fermentables ya que, en cierta proporción, los monosacáridos se degradan a furfural o hidroximetilfurfural. Además, se sabe que estos compuestos, y otros como ácidos y sustancias de naturaleza fenólica derivados de la degradación/transformación de la lignina tras la aplicación de métodos físico-químicos, son fuertemente tóxicos y pueden afectar negativamente a la etapa de hidrólisis enzimática y al crecimiento de la levadura fermentadora, y por tanto, a la conversión de los azúcares a etanol (Alvira et al., 2010). Este efecto fue descrito claramente por Chen et al. (2007), ya que la aplicación de tratamientos ácidos y alcalinos liberó un 10% más de glucosa que el máximo obtenido con nuestro pretratamiento combinado, pero a pesar de este resultado, la producción de etanol superó los valores obtenidos en el presente trabajo en tan solo un 3%. Estos resultados convierten al pretratamiento biológico en una alternativa/herramienta interesante para su futura aplicación en procesos de producción de etanol 2G. Ciertamente, algunos aspectos para su utilización a gran escala deben ser solventados. Las primeras aproximaciones se encaminan al uso de biorreactores especialmente diseñados para esta etapa, que facilitarían el mantenimiento de las condiciones ambientales óptimas y de la esterilidad de la materia prima (Mitchell et al., 2006).

Parece lógico pensar que la degradación preferencial de la lignina, que es la barrera física para la acción de las enzimas hidrolíticas, debería mejorar el rendimiento de la recuperación de azúcares (Keller et al., 2003).

Sin embargo, los resultados de nuestro trabajo indicaron que no siempre las mayores tasas de deslignificación o una degradación selectiva de la lignina mejoran la digestibilidad y mucho menos el rendimiento de recuperación de azúcares. Del mismo modo, se observó que una mayor secreción de enzimas ligninolíticas tampoco se correlacionaba significativamente con el rendimiento del proceso. Una explicación a estos fenómenos puede ser que la degradación extensiva de la lignina facilite la disponibilidad y consumo de los carbohidratos para el crecimiento del hongo, lo que disminuiría la recuperación final de azúcares fermentables (Capelari y Tomás-Pejó, 1997). Como norma general, la mayor degradación de lignina tuvo lugar en aquellos cultivos que produjeron más cantidad de peroxidasas (dependientes y no-dependientes de Mn). Durante el desarrollo de la Tesis, se comprobó que esta última actividad estaba relacionada con la presencia de una nueva enzima identificada como una peroxidasa decoloradora de tintes (DyP) (Salvachúa et al., 2013b; Salvachúa et al., 2013a). Sin embargo, hay que tener en cuenta que la degradación de la lignocelulosa por hongos no se debe exclusivamente a la acción de las enzimas extracelulares. Esta degradación también puede estar promovida por mecanismos de oxidación avanzada, en los que juegan además un papel importante las enzimas, mediados por radicales libres y metabolitos oxidantes de bajo peso molecular, muy inespecíficos, muy eficientes y difíciles de controlar (Gómez-Toribio et al., 2001). Como consecuencia de lo mencionado anteriormente, se puede concluir que es no es fácil correlacionar el nivel de enzimas extracelulares, el grado de deslignificación del sustrato y el rendimiento del proceso. Además, estos resultados muestran una vez más que los hongos de podredumbre blanca, incluso creciendo sobre un mismo sustrato y en idénticas condiciones de cultivo, producen patrones de degradación muy diferentes.

En conjunto, estos hallazgos demuestran que, en relación con la producción de bioetanol, (i) muy pocos hongos son adecuados para el biopretratamiento y que (ii) al evaluar un hongo o unas condiciones de cultivo para este fin no basta con analizar parámetros aislados (por ej. degradación de lignina, digestibilidad o producción enzimática) sino que hay que estudiar la eficiencia del proceso completo.

2. PROTEÍNAS SECRETADAS POR *I. lacteus* DURANTE EL BIOPRETRATAMIENTO DE LA PAJA DE TRIGO

Los resultados del biopretratamiento dejaron claro que es muy difícil correlacionar la liberación de algunas enzimas ligninolíticas con el rendimiento del proceso. Como ya hemos comentado, la degradación de la lignocelulosa tiene lugar por la labor conjunta de complejos procesos oxidativos, cuya acción es difícil de evaluar, y de una extensa batería de

enzimas, que no siempre se detectan con facilidad mediante simples estudios de actividad enzimática. En esta dirección, y para conocer más a fondo el sistema enzimático implicado en la degradación de paja de trigo por *I. lacteus*, se recurrió al empleo de herramientas proteómicas para analizar el secretoma de este hongo, ya que estas técnicas son idóneas para analizar todas las proteínas secretadas por el hongo (Bouws et al., 2008). El secretoma fúngico no tiene una composición constante sino que, por el contrario, es altamente flexible y se adapta a su entorno (Girard et al., 2013). Por ello, es de esperar que la composición del secretoma de *I. lacteus* varíe a lo largo del biopretratamiento o al cambiar las condiciones de cultivo. En nuestro caso, se investigó la evolución del patrón de proteínas extracelulares en distintos momentos del biopretratamiento de la paja de trigo. Además, el secretoma del hongo tras 21 días de incubación, se estudió en las mismas condiciones de cultivo pero en presencia de Mn^{2+}, variación con la que se había obtenido la máxima recuperación de glucosa (Salvachúa et al., 2013d). Asimismo, se prepararon cultivos líquidos de *I. lacteus* con el fin de comparar el perfil de proteínas secretadas con el observado en condiciones de fermentación en estado sólido sobre paja de trigo. Las proteínas contenidas en cada uno de los secretomas fueron separadas mediante electroforesis bidimensional, y a continuación los *spots* seleccionados fueron picados y digeridos con tripsina, analizando los péptidos trípticos mediante nanoLC-MS/MS.

Desde la primera semana de cultivo, *I. lacteus* secretó enzimas que degradan la celulosa y la hemicelulosa, como celobiohidrolasas y acetil-xilano esterasas. Sin embargo, las enzimas implicadas en la hidrólisis total de ambos polímeros, como son las β-glucosidasas y las β-xilosidasas (Abbas et al., 2005), no se detectaron en ningún momento del biopretratamiento. Por esta razón, aunque los polisacáridos están degradados tras el biopretratamiento, el hongo no es capaz de metabolizarlos para su propio crecimiento, ya que no llegan a producirse azúcares libres, dejando un residuo enriquecido en carbohidratos. La degradación de la lignina de la paja de trigo por *I. lacteus* tuvo lugar simultáneamente a la de los polisacáridos (capítulos 1 y 2), detectando también algunas enzimas ligninolíticas o relacionadas con este proceso en su secretoma. Destacaremos las peroxidasas dependientes de Mn^{2+} (MnP), una peroxidasa que posteriormente fue descrita como DyP (Salvachúa et al., 2013b) y enzimas tales como la glioxal oxidasa y la celobiosa deshidrogenasa (CDH) que intervienen en el ciclo de producción del peróxido de hidrógeno, necesario para el ciclo catalítico de las peroxidasas (Vanden Wymelenberg et al., 2005).

Al analizar el perfil enzimático liberado en los cultivos con Mn^{2+}, se observó un perfil proteico similar, aunque el hongo produjo menos

diversidad de celulasas y, como cabía esperar, la actividad MnP estaba inducida en presencia de este ión. Por último, comentar que muchas de las enzimas liberadas por *I. lacteus* en cultivos sumergidos, libres de paja de trigo, fueron las mismas que se habían detectado en los experimentos de fermentación en estado sólido. Aún así, las diferencias detectadas entre ambos secretomas resultaron muy interesantes. De entre los 6 *spots* expresados diferencialmente en cultivos sumergidos destacaremos uno, muy intenso, que corresponde a la β-glucosidasa. Otras proteínas inducidas en estos cultivos fueron poliporopepsina, ribonucleasa T2 y DyP, todas ellas probablemente producidas para sobrevivir en un medio pobre en nutrientes esenciales (MacIntosh, 2011; Zorn et al., 2005).

Entre los hongos ensayados en el muestreo inicial habíamos observado diferentes patrones de degradación de la paja de trigo. Como hemos descrito, el inducido por *I. lacteus* se caracterizó por una transformación simultánea de los polisacáridos y la lignina. De entre los restantes microorganismos seleccionamos dos, con patrones de degradación diferentes, cuyos genomas estaban disponibles, para estudiar más en detalle sus secretomas. Los elegidos fueron *P. chrysosporium,* que degrada preferentemente la celulosa, y *P. ostreatus*, que normalmente degrada selectivamente la lignina (Salvachúa et al., 2011; Valmaseda et al. 1991). Para realizar la comparación del perfil de proteínas extracelulares producidas por los tres hongos, tras 21 días de incubación sobre paja de trigo, recurrimos al análisis del conjunto de péptidos trípticos, obtenido a partir de secretomas completos, mediante nanoLC-MS/MS. Esta técnica, extraordinariamente sensible, permite identificar proteínas minoritarias, que no son detectables por otros procedimientos. Como era de esperar, ambos hongos produjeron perfiles enzimáticos muy diferentes entre sí y también distintos del encontrado en *I. lacteus*. *P. chrysosporium* liberó más enzimas implicadas en la degradación completa de la celulosa mientras que *P. ostreatus* secretó una mayor diversidad de enzimas oxidorreductasas, relacionadas con la degradación de la lignina.

Como puede deducirse de los resultados expuestos hasta el momento, la degradación biológica con *I. lacteus* es una herramienta excelente para generar un sustrato enriquecido en azúcares y fácilmente accesible para las enzimas hidrolíticas. Además, el conjunto de proteínas secretadas por estos hongos podría ser dirigido hacia la expresión o no de determinadas enzimas según las condiciones de cultivo, lo que puede resultar muy interesante para ser utilizado como cóctel enzimático en distintas etapas del proceso de producción de bioetanol 2G (Ravalason et al., 2012). Por ejemplo, el secretoma de *I. lacteus* podría contribuir a la mejora del biopretratamiento, mientras que el de *P. chrysosporium* sería probablemente adecuado para

mejorar la digestibilidad de la celulosa y la hemicelulosa durante la hidrólisis enzimática.

3. PRODUCCIÓN, PURIFICACIÓN Y CARACTERIZACIÓN DE UNA NUEVA DyP DE *I. lacteus* Y SU APLICACIÓN EN LA MEJORA DE LA SACARIFICACIÓN DURANTE LA PRODUCCIÓN DE ETANOL 2G

El estudio del secretoma fúngico mediante técnicas proteómicas permitió profundizar en los mecanismos de degradación de la lignocelulosa y desveló mezclas enzimáticas que pueden ser atractivas para diferentes aplicaciones. Pero otro aspecto muy interesante de estas investigaciones es la posibilidad de descubrir nuevas enzimas (Bouws et al., 2008). Al analizar el secretoma de *I. lacteus* se detectó una proteína que, por la combinación de su huella peptídica y de la secuencia de varios péptidos internos, mostró una alta identidad con una peroxidasa hipotética, de un hongo de la familia Polyporaceae, denominada cpop21. Mediante estudios de homología de secuencia, esta proteína encajaba en una clase de enzimas recientemente descrita, las peroxidasas decoloradoras de tintes (DyP). El papel en la naturaleza de estas enzimas de alto potencial redox es desconocido, aunque se ha sugerido que intervienen en la oxidación de la lignina y de otros compuestos aromáticos recalcitrantes, y que se liberan como mecanismo de defensa en condiciones de stress oxidativo (Liers et al., 2012). En la actualidad, sólo seis enzimas de este tipo han sido aisladas y purificadas a partir de hongos (Liers et al., 2012). Por esta razón, se decidió abordar el estudio de esta nueva proteína.

Con el objetivo de producir la enzima más fácilmente y proceder a su purificación, se cultivó *I. lacteus* en medio líquido, puesto que la proteína se producía también en estas condiciones. Durante el transcurso del cultivo, se sondeó su liberación a través de ensayos de actividad colorimétricos empleando sustratos específicos de la DyP, como son los colorantes de tipo antraquinona. A los 21 días de cultivo, la DyP fue una de las enzimas mayoritarias en el sobrenadante de *I. lacteus*. Su producción en medio líquido fue muy tardía (alrededor de 20 días), lo que sugiere que su liberación tiene lugar durante el metabolismo secundario, en condiciones de cultivo altamente deficientes en N y C.

Una vez purificada, la DyP de *I. lacteus* demostró ser una hemo-glicoproteína monomérica de masa molecular 57,1 kDa y pI 3,85. Estos resultados concuerdan con los descritos para otras DyP de origen fúngico (Liers et al., 2012). Su secuencia N-terminal, presentó un 95% de homología con la de la peroxidasa hipotética cpop21 y más de un 85% con las de las DyP de otros hongos. En cuanto a sus características funcionales, la enzima presentó rasgos típicos de las DyP, como pH óptimos de actividad muy bajos (de 2 a 4) y actividad frente a compuestos fenólicos,

no fenólicos y colorantes de tipo antraquinona y tipo azo (Hofrichter et al., 2010). Sin embargo, la DyP de *I. lacteus* fue muy estable a pH ácidos, altas temperaturas y peróxido de hidrógeno, co-sustrato necesario para la actividad de estas enzimas. Esa estabilidad al peróxido de hidrógeno fue incluso mejor que la de algunas variantes de peroxidasas mejoradas por evolución o mutagénesis dirigida (García-Ruiz et al., 2012; Ogola et al., 2010). Todas estas propiedades convierten a esta DyP en una herramienta muy interesante de cara a sus posibles aplicaciones biotecnológicas.

El papel de las DyP durante la degradación de la lignocelulosa es controvertido (Liers et al., 2012). Sin embargo, a la vista de los resultados del presente estudio, podemos sugerir que esta proteína tiene una relación directa con la degradación de la lignina. Por una parte, su presencia favorece la hidrólisis enzimática de la paja de trigo y por otra, su producción está moderadamente correlacionada (r = 0,62) con la degradación de lignina durante el biopretratamiento de la paja de trigo por *I. lacteus* (Salvachúa et al., 2013d).

Teniendo en cuenta nuestro interés en la mejora de la producción de bioetanol 2G, se estudió el potencial de la DyP de *I. lacteus* para mejorar la digestibilidad de la paja de trigo, pretratada o no, durante el proceso de hidrólisis enzimática, añadiendo la enzima pura como suplemento a los cócteles con celulasas y hemicelulasas comerciales. En ambos casos, la adición de DyP incrementó la digestibilidad de la celulosa, aunque el efecto fue más significativo en el caso de la paja biopretratada. La DyP pareció actuar sinérgicamente con las celulasas, mejorando la accesibilidad de los azúcares por una continua oxidación de la lignina. Muy pocos estudios, casi todos publicados como patentes, plantean suplementar con peroxidasas los cócteles de hidrólisis enzimática para incrementar la digestibilidad de residuos lignocelulósicos (Zorn et al., 2009). Por tanto, este estudio puede ser el germen de una vía de investigación para la mejora de cócteles enzimáticos.

4. SÍNTESIS DE NUEVOS COMPUESTOS CATALIZADA POR PEROXIDASAS FÚNGICAS DE ALTO POTENCIAL REDOX

Entre los objetivos iniciales de este trabajo se planteó investigar otros posibles ámbitos de aplicación de las enzimas estudiadas. Hasta este momento, todos nuestros experimentos se habían dirigido hacia la degradación de material lignocelulósico, pero en la naturaleza, muchas de las enzimas implicadas en este complejo proceso son capaces de catalizar también reacciones de síntesis. Como ya hemos comentado, la biosíntesis de lignina, catalizada por lacasas y peroxidasas vegetales, se produce mediante el acoplamiento de radicales libres de tipo fenoxilo (Adler, 1977).

Por esta razón, enzimas como la peroxidasa de rábano o la de soja son las más utilizadas cuando se trata de llevar a cabo la polimerización *in vitro* de sustratos muy variados (Hollmann y Arends, 2012; Kobayashi et al., 2001). Muy pocos estudios han empleado peroxidasas fúngicas en este ámbito aunque la acción de las lacasas fúngicas en estas reacciones ha sido exhaustivamente detallada (Buchert et al., 2002; Mattinen et al., 2005; Mattinen et al., 2009; Steffensen et al., 2008). La transformación de dichos compuestos en moléculas de mayor tamaño tiene como finalidad principal la producción de homo- o heteropolímeros, con propiedades funcionales nuevas o diferentes y de alto valor añadido (Saleem et al., 2005; Niño-Medina et al., 2010; Arihara et al., 2006; Stanic et al., 2010; Boeriu, 2008).

Como ya hemos visto, el secretoma de *I. lacteus* contiene, entre otras muchas enzimas, peroxidasas de alto y bajo potencial redox (DyP y MnP). Por esta razón, se decidió ensayar la capacidad del crudo obtenido tras 21 días de fermentación en estado sumergido, para polimerizar lignanos y compararla con la de la peroxidasa versátil de *Pleurotus eryngii* (VP), una peroxidasa fúngica muy estudiada en nuestro laboratorio y que nunca se había ensayado en este tipo de reacciones. Los lignanos son compuestos difenólicos formados por unión β-β de dos precursores cinamílicos que se encuentran en la pared celular de las plantas (Saleem et al., 2005). Las reacciones se llevaron a cabo en etanol, ya que los lignanos no son solubles en agua, y en presencia o ausencia de Mn^{2+}. Tanto el crudo de *I. lacteus* como la VP de *P. eryngii* indujeron la polimerización de los cinco lignanos ensayados. Dado que los productos de mayor grado de polimerización se detectaron en las reacciones con Mn^{2+} catalizadas por la VP, los estudios se continuaron con esta enzima y en presencia de Mn^{2+}.

Los ensayos de polimerización se realizaron utilizando sustratos de diferente naturaleza y tamaño molecular como péptidos, proteínas y arabinoxilanos feruloilados (Salvachúa et al., 2013c). En algunos de los casos, la VP fue incluso más eficiente que otras oxidorreductasas procedentes de hongos (Butcher et al., 2002; Mattinen et al., 2005; Steffensen et al., 2008) o actuó de una manera muy similar a las de plantas (Michon et al., 1997). Estos resultados abren una nueva vía de aplicación para las peroxidasas fúngicas, en concreto para la peroxidasa versátil, que ha demostrado ser altamente eficaz. Además, sugieren que los procesos de polimerización y degradación a través de oxidorreductasas son inevitablemente simultáneos, ya sea en procesos de biodegradación y/o biopolimerización.

BIBLIOGRAFÍA

Abbas, A., Koc, H., Liu, F., Tien, M., 2005. Fungal degradation of wood: initial proteomic analysis of extracellular proteins of *Phanerochaete chrysosporium* grown on oak substrate. Curr. Genetics 47, 49-56.

Adler, E., 1977. Lignin chemistry - Past, present and future. Wood Sci. Technol. 11, 169-218.

Alvira, P., Tomás-Pejó, E., Ballesteros, M., Negro, M.J., 2010. Pretreatment technologies for an efficient bioethanol production process based on enzymatic hydrolysis: A review. Bioresour. Technol. 101, 4851-4861.

Bouws, H., Wattenberg, A., Zorn, H., 2008. Fungal secretomes - nature's toolbox for white biotechnology. Appl. Microbiol. Biotechnol. 80, 381-388.

Buchert, J., Mustranta, A., Tamminen, T., Spetz, P., Holmbom, B., 2002. Modification of spruce lignans with *Trametes hirsuta* laccase. Holzforschung 56, 579-584.

Capelari, M. Tomás-Pejó, E., 1997. Lignin degradation and in vitro digestibility of wheat straw treated with Brazilian Tropical species of white-rot fungi. Folia Microbiologica 42, 481-487.

Chen, Y., Sharma-Shivappa, R., Keshwani, D., Chen, C., 2007. Potential of agricultural residues and hay for bioethanol production. Appl. Biochem. Biotechnol. 142, 276-290.

Dias, A.A., Freitas, G.S., Marques, G.S.M., Sampaio, A., Fraga, I.S., Rodrigues, M.A.M., Evtuguin, D.V., Bezerra, R.M.F., 2010. Enzymatic saccharification of biologically pre-treated wheat straw with white-rot fungi. Bioresour. Technol. 101, 6045-6050.

Galbe, M. Zacchi, G., 2007. Pretreatment of lignocellulosic materials for efficient bioethanol production. Adv. Biochem. Eng. Biotechnol. 108, 41-65.

García-Ruiz, E., González-Pérez, D., Ruiz-Dueñas, F.J., Martínez, A.T., Alcalde, M., 2012. Directed evolution of a temperature-, peroxide- and alkaline pH-tolerant versatile peroxidase. Biochem. J. 441, 487-498.

Girard, V., Dieryckx, C., Job, C., Job, D., 2013. Secretomes: The fungal strike force. Proteomics 13, 597–608.

Gómez-Toribio, V., Martínez, M.J., Martínez, A.T., Guillén, F., 2001. Quinone redox cycling as a mechanism for extracellular hydroxyl radical production by white-rot fungi. Abs. 8th Intern. Conf. Biotechnology in the Pulp and Paper Industry, Helsinki, 4-8 June.

Hofrichter, M., Ullrich, R., Pecyna, M.J., Liers, C., Lundell, T., 2010. New and classic families of secreted fungal heme peroxidases. Appl. Microbiol. Biotechnol. 87, 871-897.

Hollmann, F. Arends, I.W., 2012. Enzyme initiated radical polymerizations. Polymers 4, 759-793.

Keller, F.A., Hamilton, J.E., Nguyen, Q.A., 2003. Microbial pretreatment of biomass. Appl. Biochem. Biotechnol. 105 -108, 27-41.

Kobayashi, S., Uyama, H., Kimura, S., 2001. Enzymatic polymerization. Chem. Rev. 101, 3793-3818.

Kootstra, A., Beeftink, H.H., Scott, E.L., Sanders, J.P., 2009. Comparison of dilute mineral and organic acid pretreatment for enzymatic hydrolysis of wheat straw. Biochem. Engineer. J. 46, 126-131.

Koullas, D.P., Christakopoulos, P., Kekos, D., Macris, B.J., Koukios, E.G., 1992. Correlating the effect of pretreatment on the enzymatic-hydrolysis of straw. Biotechnol. Bioeng. 39, 113-116.

Kumar, P., Barrett, D., Delwiche, M., Stroeve, P., 2009. Methods for pretreatment of lignocellulosic biomass for efficient hydrolysis and biofuel production. Ind. Eng. Chem. Res. 48, 3713-3729.

Liers, C., Pecyna, M.J., Kellner, H., Worrich, A., Zorn, H., Steffen, K.T., Hofrichter, M., Ullrich, R., 2012. Substrate oxidation by dye-decolorizing peroxidases (DyPs) from wood- and litter-degrading agaricomycetes compared to other fungal and plant heme-peroxidases. Appl. Microbiol. Biotechnol. doi:10.1007/s00253-012-4521-2.

MacIntosh, G.C., 2011. RNase T2 family: enzymatic properties, functional diversity, and evolution of ancient ribonucleases, in: A.W.Nicholson (Ed.), Ribonucleases, Nucleic Acids and Molecular Biology. pp. 89-114.

Mattinen, M.L., Kruus, K., Buchert, J., Nielsen, J.H., Andersen, H.J., Steffensen, C.L., 2005. Laccase-catalyzed polymerization of tyrosine-containing peptides. FEBS J 272, 3640-3650.

Mattinen, M.L., Struijs, K., Suortti, T., Mattila, I., Kruus, K., Willför, S., Tamminen, T., Vincken, J.P., 2009. Modification of lignans by *Trametes hirsuta* laccase. Bioresources 4, 482-496.

Michon, T., Chenu, M., Kellershon, N., Desmadril, M., Gueguen, J., 1997. Horseradish peroxidase oxidation of tyrosine-containing peptides and their subsequent polymerization: A kinetic study. Biochemistry 36, 8504-8513.

Mitchell, A.D., Krieger, N., Berovic, M., 2006. Solid-state fermentation bioreactors: fundamentals of design and operations. Springer-Verlag Berlin Heidelberg: Springer.

Ogola, H.J., Hashimoto, N., Miyabe, S., Ashida, H., Ishikawa, T., Shibata, H., Sawa, Y., 2010. Enhancement of hydrogen peroxide stability of a novel *Anabaena* sp. DyP-type peroxidase by site-directed mutagenesis of methionine residues. Appl. Microbiol. Biotechnol. 87, 1727-1736.

Pinto, P.A., Dias, A.A., Fraga, I., Marques, G., Rodrigues, M.A.M., Colaco, J., Sampaio, A., Bezerra, R.M.F., 2012. Influence of ligninolytic enzymes on straw saccharification during fungal pretreatment. Bioresour. Technol. 111, 261-267.

Ravalason, H., Grisel, S., Chevret, D., Favel, A., Berrin, J.G., Sigoillot, J.C., Herpoel-Gimbert, I., 2012. *Fusarium verticillioides* secretome as a source of auxiliary

enzymes to enhance saccharification of wheat straw. Bioresour. Technol. 114, 589-596.

Saleem, M., Kim, H.J., Ali, M.S., Lee, Y.S., 2005. An update on bioactive plant lignans. Nat. Prod. Rep. 22, 696-716.

Salvachúa, D., Tien, M., Fernández, M., García-Tabares, F., de los Ríos, V., Martínez, A.T., Martínez, M.J., Prieto, A., 2013a. Differential proteomic analysis of the secretome of *Irpex lacteus* and other white-rot fungi growing on wheat straw. Manuscript in preparation.

Salvachúa, D., Prieto, A., López-Abelairas, M., Lu-Chau, T., Martínez, A.T., Martínez, M.J., 2011. Fungal pretreatment: An alternative in second-generation ethanol from wheat straw. Bioresour. Technol. 102, 7500-7506.

Salvachúa, D., Prieto, A., Martínez, A.T., Martínez, M.J., 2013b. Characterization of a novel DyP-type peroxidase from *Irpex lacteus* and its application in the enzymatic hydrolysis of wheat straw . Appl. Environ. Microb. doi:10.1128/AEM.00699-13.

Salvachúa, D., Prieto, A., Mattinen, M.L., Tamminen, T., Liitia, T., Lille, M., Willfor, S., Martínez, A.T. et al., 2013c. Versatile peroxidase as a valuable tool for generating new biomolecules by homogeneous and heterogeneous cross-linking. Enzyme Microb. Technol. 52, 303-311.

Salvachúa, D., Prieto, A., Vaquero, M.E., Martínez, A.T., Martínez, M.J., 2013d. Sugar recoveries from wheat straw following treatments with the fungus *Irpex lacteus*. Bioresour. Technol. 131, 218-225.

Steffensen, C.L., Mattinen, M.L., Andersen, H.J., Kruus, K., Buchert, J., Nielsen, J.H., 2008. Cross-linking of tyrosine-containing peptides by hydrogen peroxide-activated *Coprinus cinereus* peroxidase. Eur. Food. Res. Technol. 227, 57-67.

Talebnia, F., Karakashev, D., Angelidaki, I., 2010. Production of bioethanol from wheat straw: An overview on pretreatment, hydrolysis and fermentation. Bioresour. Technol. 101, 4744-4753.

Valmaseda, M., Martínez, M.J., Martínez, A.T., 1991. Kinetics of wheat straw solid state fermentation with *Trametes versicolor* and *Pleurotus ostreatus*: lignin and polysaccharide alteration and production of related enzymatic activities. Appl. Microbiol. Biotechnol. 35, 817–823.

Vanden Wymelenberg, A., Sabat, G., Martínez, D., Rajangam, A.S., Teeri, T.T., Gaskell, J., Kersten, P.J., Cullen, D., 2005. The *Phanerochaete chrysosporium* secretome: Database predictions and initial mass spectrometry peptide identifications in cellulose-grown medium. J. Biotechnol. 118, 17-34.

Wan, C., Li, Y., 2011. Effectiveness of microbial pretreatment by *Ceriporiopsis subvermispora* on different biomass feedstocks. Bioresour. Technol. 102, 7507-7512.

Zorn, H., Peters, T., Nimtz, M., Berger, R.G., 2005. The secretome of *Pleurotus sapidus*. Proteomics 5, 4832-4838.

Zorn, H., Szweda,R., Kumar,M., Wilms,J. 2009. Method for modifying non-starch carbohydrate material using peroxidase enzyme. Patent [US200913054178]. United States.

Conclusiones / Conclusions

CONCLUSIONES

1. Muy pocos basidiomicetos son adecuados para el biopretratamiento de la paja de trigo en el proceso de producción de bioetanol 2G, ya que la mayoría producen un consumo excesivo de azúcares o no dejan suficientemente accesibles los polisacáridos de la pared celular vegetal para que las enzimas hidrolíticas actúen sobre ellos.

2. La combinación de un pretratamiento biológico de la paja de trigo, utilizando los hongos *Irpex lacteus* y *Poria subvermispora*, con otro alcalino, muy suave, incrementó significativamente el rendimiento del proceso y no generó compuestos que afectaran negativamente las subsecuentes etapas de producción de bioetanol 2G.

3. Utilizando *I. lacteus*, el hongo que produjo mayor liberación de azúcares fermentables a los 14 días de incubación, se comprobó que la adición de Mn^{2+} a la paja de trigo durante el biopretratamiento, mejora significativamente la recuperación de glucosa.

4. No se ha encontrado una correlación clara entre la producción de enzimas ligninolíticas y la degradación de la lignina con un aumento en el rendimiento global del proceso.

5. El estudio del secretoma de *I. lacteus* en diferentes condiciones de cultivo, reveló la presencia de enzimas relacionadas con la degradación de la lignocelulosa como peroxidasas, oxidasas, celulasas y hemicelulasas. En condiciones de fermentación en estado sólido, no se detectaron las enzimas que hidrolizan los polisacáridos hasta sus monómeros (como β-glucosidasas o β-xilosidasas). Este hecho explicaría por qué este hongo consume pocos carbohidratos de la paja de trigo y mejora los rendimientos de azúcares fermentables en comparación con los obtenidos con los otros hongos estudiados.

6. Una nueva peroxidasa secretada por *I. lacteus* durante el biopretratamiento de paja de trigo se produjo también en medio líquido, lo que facilitó su purificación y caracterización. Esta proteína se identificó como una enzima de alto potencial redox perteneciente a la familia de las peroxidasas decoloradoras de tintes (DyP). Es muy estable a pH ácido, altas temperaturas y elevadas concentraciones de peróxido de hidrógeno. Es la primera vez que se describe en este hongo y sus propiedades la convierten en una herramienta de gran interés para diferentes aplicaciones biotecnológicas.

7. Se ha comprobado que la adición de la DyP de *I. lacteus* junto con celulasas y hemicelulasas comerciales durante la etapa de hidrólisis enzimática de paja de trigo, mejora significativamente la digestibilidad de la celulosa. Esto sugiere que podría ser de gran interés para aumentar el rendimiento en la producción de etanol 2G a partir de este material lignocelulósico.

8. Se ha descrito una nueva aplicación para algunas peroxidasas fúngicas de alto potencial redox. En concreto, la peroxidasa versátil de *Pleurotus eryngii* cataliza eficientemente la polimerización de compuestos fenólicos de baja masa molecular, como lignanos y péptidos, o de macromoléculas, como proteínas o arabinoxilanos feruloilados, para generar productos con propiedades nuevas o diferentes.

CONCLUSIONS

1. Very few basidiomycetes are suitable for wheat straw biopretreatment in the 2G bioethanol production process, since most of them consume sugars extensively or do not make plant cell-wall polysaccharides accessible for hydrolytic enzymes.

2. The combination of a biological pretreatment of wheat straw, using the fungi *Irpex lacteus* and *Poria subvermispora*, with a mild alkali pretreatment, renders a significant increase of process yields, without generating by-products which negatively affect down-stream steps in 2G bioethanol production.

3. Employing *I. lacteus*, the fungus which produced the highest fermentable sugar release at 14 days of incubation, it was demonstrated that the addition of Mn^{2+} to wheat straw during the biopretreatment significantly improves glucose recoveries.

4. There is not a clear correlation between ligninolytic enzymes production and lignin degradation levels with an improvement of the global process yield.

5. The study of the *I. lacteus* secretome in different culture conditions, revealed the presence of enzymes related with lignocellulose degradation, such as peroxidases, oxidases, cellulases, and hemicellulases. The enzymes involved in the complete hydrolysis of the cellulose and hemicellulose to their monosaccharides (such as β-glucosidases or β-xylosidases) were not detected in solid-state fermentation cultures. This finding would explain why this fungus consumes few carbohydrates from wheat straw and improves the yields of fermentable sugars compared to the other fungi tested.

6. A new peroxidase secreted by *I. lacteus* during the biopreatment was also produced in liquid medium, facilitating its purification and characterization as a high-redox potential enzyme of the dye-decolorizing peroxidases family (DyP). This enzyme is very stable to acidic pH, and high temperatures and H_2O_2 concentrations. DyP production has been described for the first time in this fungus and its excellent properties turn this enzyme into an interesting tool for different biotechnological applications.

7. It has been proved that the addition of *I. lacteus* DyP together with commercial cellulases and hemicellulases during the enzymatic hydrolysis of wheat straw, significantly improves the cellulose digestibility. This fact suggests that the use of DyP could be attractive for enhancing 2G bioethanol production yield from this lignocellulosic material.

8. A new application for some high-redox potential enzymes has been described. In particular, the versatile peroxidase of *Pleurotus eryngii* efficiently catalyzes the polymerization of low-molecular mass phenolic compounds, such as lignans and peptides, and macromolecules, such as proteins and feruloylated arabinoxylans, generating products with new or different properties.